

Catalytic synthesis of higher alcohols

Zur Erlangung des akademischen Grades eines

DOKTORS DER NATURWISSENSCHAFTEN

(Dr. rer. nat.)

von der KIT-Fakultät für Chemie und Biowissenschaften

des Karlsruher Instituts für Technologie (KIT)

genehmigte

DISSERTATION

von

Ing. Civ. Quim. Karin Marcela Walter Bahamondes

aus

Concepción, Chile

KIT-Dekan : Prof. Dr. Willem Klopper
Referent : Prof. Dr. Jan-Dierk Grunwaldt
Korreferent : Prof. Dr.-Ing. Jörg Sauer
Tag der mündlichen Prüfung : 21.10.2016



This document is licensed under the Creative Commons Attribution – Share Alike 3.0 DE License
(CC BY-SA 3.0 DE): <http://creativecommons.org/licenses/by-sa/3.0/de/>

Acknowledgments

There are many persons whom I like to thank for helping me to finish my PhD thesis.

Firstly, I want to thank to my supervisor Prof. Dr. J.-D. Grunwaldt for allowing me to do my thesis in his working group. I appreciate that he trusted me and allowed me to develop a topic which is currently relevant. All together this has been a gratifying experience which has helped me to grow both in a professional and a personal way. I would like to thank Prof. Dr.-Ing. Jörg Sauer for being the co-referee for my thesis.

I am grateful to PD Dr. Wolfgang Kleist for his support during this thesis, especially for his critical corrections of the many posters, presentations, papers, and finally this thesis. These corrections allowed me to learn how to communicate in a scientifically appropriate way. Personally, I am thankful for understanding me when I needed it the most and for motivating me to keep going despite the frustrations along the way.

I am especially grateful to Dr. Martin Schubert for his support at the beginning of my PhD, for teaching me how to work both independently and in groups, for his infinite patience in teaching me until I understood, for helping me discuss my results, but above all for never stopping to support me, even though he stopped working at KIT.

My work would not have been complete without the assistance of many other persons. I want to thank Angela Beilmann (ITCP, KIT) for the BET measurements and also for nice conversations together, Hermann Köhler (IKFT, KIT) for the ICP-OES, Joachim Haertle, Dr. Thomas Otto and Doreen Neumann-Walter (IKFT, KIT) for the H₂-TPR, Dr. Sina Baier (ITCP, KIT), Xiaoke Mu (INT, KIT) and Dr. Di Wang (INT, KIT) for the HRTEM, Marion Lenzner (IKFT, KIT) for the TGA, Paul Sprenger (ITCP/KIT) for the flame spray pyrolysis, and finally all you who have spent a beamtime with me (Dr. Maria Casapu, Dr. Dmitry Doronkin, Dr. Ana Zimina, Dr. Thomas Sheppard, Dr. Tobias Günter, Chiara Boscagli, and many others ...), especially Dr. Hudson Wallace Pereira de Carvalho and Dr. Abhijeet Gaur (ITCP, KIT) for helping me with the data evaluation. I would like to thank ANKA at KIT for granting beamtime at the XAS-beamline.

I would like to thank the mechanical workshop (Herr Kehrwecker, Herr Eberle and Herr Raft) for their good disposition, especially for helping while I was constructing the continuous-flow reactor and for teaching me everything that is related to tools, screws and pipes. I am grateful

to the glass-blowers (Giovani, Klaus, Daniela and Jasmin) for designing all the glassware that I required. I would also like to thank Herr Mainzer and Herr Kahrau from the electrical workshop. Especially, I have to mention Herr Weiss for always receiving us with a smile and taking care of me.

In general, I want to thank all the colleagues at IKFT for making me part of their institute, the nice talks and events and for helping me whenever I needed it. I am grateful to all my colleagues at ITCP for the support during my thesis, the discussion and the more relaxing moments. I am happy to have met each of you. Particularly, I would like to thank Dr. Thomas Sheppard for taking the time to proof read my thesis.

I would like to thank DAAD for the financial support during my thesis and KIT, in particular the programs EE and SCI, for financial support for the construction of the setups. I am thankful to the Helmholtz Research School Energy Related Catalysis for the financial support, the courses and summer and winter schools. I would also like to thank each member of this school who have become my friends. I am thankful to have met you.

Thank you to my colleagues, ex-colleagues and friends from the office in Campus North (Konstantin, Chiara, Martin, Benjamin, Kai, Melanie, Marc and Oliver), the girls from Campus North (Karla, Ewelina, Julia, Sophia and Christine), my friends from Campus South (Thomas, Gülperi and Paul) and my friends who already finished the PhD and are distributed all over Germany (Kirsten, Marina, Meike and Denise) for their support and company, which helped me to make an enjoyable and fulfilling PhD experience. With you I have shared many scientific discussions, trips, laughter and times that I will never forget. I have to mention also my friends from the bus and the latino lunches, that have made more than one afternoon more pleasant (making lunch time particularly long) and have joined me in numerous bus rides to and from Campus North.

In general, I want to thank my friends inside and outside KIT for always supporting me unconditionally and making me feel a bit more like in a family. Each of you made my stay in Karlsruhe happier. Thanks to my friends from all my life, that are in Chile or somewhere else. Your phone calls and messages made my day happier and helped me to keep going.

Finally, I would like to thank my family for listening to me, supporting me and loving me from a distance. Without you none of this would have been possible.

Abstract

The current interest in renewable energy sources is a response to both scarcity and increasing prices of current energy sources, as well as to stricter environmental policies. In this context, biomass processing techniques appear to be a very interesting field since they ensure a CO₂ neutral cycle. Particularly, generation of synthesis gas from biomass sources is of great importance for the future energy market and chemical industry. Synthesis gas reactions using different catalysts lead to a great variety of fuels and chemicals. Among these products, alcohols are very attractive since they offer advantages when used as fuels or fuel additives for example. Current transportation systems are, for example, already operated with ethanol or mixtures of ethanol with traditional fuels. Nevertheless, methanol and ethanol exhibit some disadvantages in comparison to higher alcohols (HA, C₃₊ alcohols). HA are less miscible with water, less corrosive and blend better with gasoline. HA production from synthesis gas is currently being studied over several catalyst systems without reaching adequate selectivities and yields necessary to consider further scale up. Modified methanol synthesis catalysts are the focus of this thesis, they constitute well-known catalysts and modified with promoters, leading to increased yields of higher alcohols. The rate-limiting step for this type of catalyst is regarded as C₁ to C₂ chain growth step. Therefore the strategy applied in the present thesis was to mix ethanol with the synthesis gas, in order to propagate the chain growth from this step.

Firstly, doped CuO/ZnO catalysts were prepared and screened in the HA synthesis using a batch reactor. CuO/ZnO catalysts were doped either with Ru or Cs. Cs proved to be a better dopant, since the presence of Ru favored particularly the production of alkanes under the conditions applied. The catalyst was then doped with Cs contents between 0.3 and 3.0 mol.% and tested in the traditional HA synthesis. An optimal Cs concentration corresponded to 0.6 – 1.0 mol.%. Hence, the higher alcohols synthesis was optimized using a Cs doping of 1.0 mol.%. Increasing the Cs content on the catalyst shifted the reduction of CuO to Cu to higher temperatures. Not only was the reducibility affected by the Cs content, also the catalyst performance changed significantly as function of the Cs loading. The absence of Cs yielded high amounts of CO₂ and showed high selectivity to methanol. 3.0 mol.% Cs doping decreased the yield of HA, probably due to the blockage of the hydrogenation sites by Cs impregnation. The same tendency was found when ethanol was added to the synthesis gas. As a next step, the amount of ethanol added to the synthesis gas was varied. Ethanol addition improved the

performance of all catalysts regardless of the Cs content. The most favorable $n_{\text{EtOH}} : n_{\text{CO}}$ ratio corresponded to 0.5:1, since it favored the HA production while maintaining the formation of byproducts at acceptable levels. The formation of esters, particularly ethyl acetate, was favored when a $n_{\text{EtOH}} : n_{\text{CO}}$ ratio of 10.0:1 was used. In addition, changes in the preferred reaction path towards higher alcohols were observed when the ethanol to CO ratio was changed. In the absence of ethanol, an aldol-type coupling of methanol derived C_1 intermediates to adsorbed alcohols (or derivatives) was observed, since 2-methyl-1-propanol was identified as a termination product. An excess of ethanol led to higher selectivities towards 1-butanol and 2-butanol suggesting homocoupling of ethanol. At intermediate ratios both reaction paths were followed.

In a next step, CuO/ZnO catalysts were elaborated using different preparation methods and support materials to study their influence on the synthesis of higher alcohols. A CuO/ZnO catalyst was supported on Al_2O_3 by increasing pH precipitation or wet impregnation and compared to a physical mixture. Wet impregnation proved to be the most favorable preparation method since it led to an appropriate interaction between copper and zinc oxide sites required for HA synthesis, which led to higher yields and selectivities to alcohols. The content of CuO/ZnO on the support was optimized to 30 wt.%. The CuO/ZnO catalyst was further supported on activated carbon and SiO_2 by wet impregnation. Al_2O_3 was the most adequate support since it showed the highest selectivity and yield towards HA. The Al_2O_3 supported CuO/ZnO catalyst was additionally prepared by constant pH precipitation and flame spray pyrolysis. The catalysts were then modified with 1.0 mol.% Cs and compared with a Cs-doped commercial catalyst. Similar yields of HA were obtained for both the catalysts obtained via flame spray pyrolysis and wet impregnation, but the alcohol selectivity varied in each case, suggesting the presence of different active sites depending on the preparation method.

For further tests of the catalysts, a continuous downward-flow, high pressure trickle-bed reactor was designed and constructed in-house at the Institute of Catalysis Research and Technology (IKFT). Parameters including the type of flow, temperature profiles, optimal packing of the catalyst bed and mass and heat transfer limitations were considered during the construction of the reactor. The products were analyzed offline, which required good separation of the reaction phases. Methanol synthesis as a well-known target reaction was tested in the first instance with a commercial catalyst to ensure the appropriate functioning of the reactor. The HA synthesis was then optimized by varying the space velocity, reaction temperature and ethanol to CO ratio using a [1.0 mol.% Cs-CuO/ZnO]/ Al_2O_3 catalyst at 8.0 MPa. This catalyst was the best performing during screening studies using a batch reactor. Higher space velocities (19400

L(STP) / kg_{cat} h) limited the formation of byproducts by enhancing the HA yields. Medium temperatures (593 K) ensured a high yield towards HA preventing an undesired sintering of the copper particles, which would lead to deactivation of the catalyst. As for the batch reaction tests, an optimum ethanol to CO ratio was found ($n_{\text{EtOH}} : n_{\text{CO}}$ ratio of 0.3:1). Higher ratios led to an abrupt increase in the formation of byproducts. During the continuous tests also the effect of the ethanol to CO ratio on the preferred reaction path was studied. Probably aldehydes and ketones were reaction intermediates, whereas both HA and esters were final products that were less prone to further C-C coupling reactions. An equilibrium reaction between the aldol and keto form of the product of the coupling of two acetaldehydes, led to either the preferential formation of 1-butanol (higher ratios) or 2-butanol (middle ratios) as the main HA products. Higher ethanol to CO ratios especially favored the formation of ethyl acetate. Apparently, higher amounts of adsorbed ethanol shifted the equilibrium to 3-hydroxy-butanal (aldol), which favored 1-butanol production and additionally favored the coupling of acetaldehyde with ethanol to form ethyl acetate. An internal hydrogen transfer was required to form 1-hydroxy-3-butanone (ketone). Therefore most probably the adsorbed ethanol hindered the hydrogenation function of the copper sites.

In conclusion, the addition of an appropriate amount of ethanol to the synthesis gas feed improved the HA synthesis over Cs modified CuO/ZnO and CuO/ZnO/Al₂O₃ catalysts using both batch and continuous reactors. Important reaction parameters as well as the catalyst materials and preparation methods were modified, but further improvements are still required to scale up the process. Furthermore, *in situ* or *in operando* characterization tests will be helpful to understand the effect of ethanol on the catalyst surface and its influence on the product distribution. An optimization of the quantification of the reaction products in the continuous-flow reactor is recommended to improve the established laboratory plant. An online gas chromatography system is advisable to avoid product losses and to improve the carbon and mass balances.

Kurzfassung

Das derzeitige Interesse an erneuerbaren Energien ist eine Antwort auf die Knappheit und steigende Preise jetziger Energieressourcen sowie einer strengeren Umweltpolitik. In diesem Kontext stellt die Umwandlung von Biomasse ein sehr interessantes Gebiet dar, da sie einen neutralen CO₂-Zyklus sicherstellt. Für den zukünftigen Energiemarkt und die chemische Industrie ist die Umwandlung von Biomasse zu Synthesegas sehr wichtig. Mehrere Kraftstoffe und Chemikalien können durch Reaktionen mit Synthesegas als Edukt an verschiedenen Katalysatoren gewonnen werden. Unter diesen Produkten erscheinen vor allem Alkohole sehr interessant, da sie viele Vorteile zeigen, wenn sie als Kraftstoff oder Kraftstoffzusatz benutzt werden. Zum Beispiel werden bereits heutzutage Fahrzeuge mit Ethanol oder Ethanol/Benzin-Mischungen betrieben. Unabhängig davon zeigen Methanol und Ethanol einige Nachteile im Vergleich zu höheren Alkoholen. Höhere Alkohole weisen eine höhere Toleranz gegenüber Wasser und Feuchtigkeit auf, sind weniger korrosiv und mischen sich besser mit Kraftstoffen. Im Rahmen der Synthese höherer Alkohole wird derzeit an verschiedenen Katalysatorsystemen geforscht, ohne jedoch ausreichende Selektivitäten und Ausbeuten zu erreichen, um ein Scale-up zu ermöglichen. In dieser Arbeit standen modifizierte Methanolsynthese-Katalysatoren im Fokus. Für diese Art von Katalysatoren ist der limitierende Reaktionsschritt das Kettenwachstum von C₁ zu C₂. Aus diesem Grund war das Ziel dieser Arbeit, Ethanol und Synthesegas zu mischen und das Kettenwachstum mit dem Schritt von C₂ zu C₃ zu starten.

Zuerst wurden modifizierte CuO/ZnO-Katalysatoren hergestellt und in der Synthese von höheren Alkoholen in einem Batchreaktor getestet. Dazu wurde ein CuO/ZnO-Katalysator mit Ru oder Cs modifiziert. Cs stellte sich als geeignetere Dotierung heraus, da in Anwesenheit von Ru verstärkt Alkane unter diese Bedingungen produziert wurden. Aus diesem Grund wurde eine Serie von Katalysatoren mit unterschiedlichen Cs-Gehalt (0.3 - 3.0 mol%) hergestellt und in der Synthese von höheren Alkoholen getestet. Eine optimale Cs-Dotierung lag zwischen 0.6 und 1.0 mol%. Deswegen wurde die Synthese höherer Alkohole mit 1.0 mol% Cs optimiert. Eine Erhöhung des Cs-Gehaltes verschob die Reduktion von CuO zu Cu zu höheren Temperaturen. Nicht nur die Reduzierbarkeit des Katalysators wurde durch den Cs-Gehalt beeinflusst, sondern auch die katalytische Aktivität veränderte sich als Funktion des Cs-Gehalts. In Abwesenheit von Cs wurden eine höhere Ausbeute an CO₂ und höhere Selektivitäten zu Methanol beobachtet. Eine Dotierung mit 3.0 mol% Cs hatte schlechtere

Ausbeuten an höheren Alkohole zur Folge, wahrscheinlich aufgrund einer Blockierung der Hydrierungsstellen des Kupfers durch Cs als Folge der Imprägnierung. Dieselbe Tendenz wurde auch beobachtet, wenn Ethanol als Edukt hinzugegeben wurde. Als nächster Schritt wurde die Menge an Ethanol, die zum Synthesegas zugegeben wurde, variiert. Die Zugabe von Ethanol erhöhte in allen Fällen die katalytische Aktivität unabhängig vom Dotierungsgrad. Das beste $n_{\text{EtOH}} : n_{\text{CO}}$ -Verhältnis war 0.5, da es die Ausbeute an höheren Alkoholen steigerte, aber die Nebenprodukte auf einem akzeptablen Niveau beließ. Eine erhöhte Produktion von Estern, hauptsächlich Ethylacetat, wurde bei einem Verhältnis $n_{\text{EtOH}} : n_{\text{CO}}$ von 10.0 gefunden. Zusätzlich, die Änderung des $n_{\text{EtOH}} : n_{\text{CO}}$ -Verhältnisses hatte wichtige Veränderungen des Reaktionsweg zu Höhere Alkohole zur Folge. In Abwesenheit von Ethanol wurde ein Reaktionsweg entsprechend einer Aldolkondensation der von Methanol abstammenden C_1 -Intermediate hin zu adsorbierten Alkoholen beobachtet, da 2-Methyl-1-propanol als Endprodukt gefunden wurde. Ein Überschuss an Ethanol zeigte höhere Selektivitäten zu 1-Butanol und 2-Butanol, die durch eine Homokupplungsreaktion von Ethanol gebildet werden könnten. Mittlere Verhältnisse zeigten beide Reaktionswege.

Im nächsten Schritt wurden CuO/ZnO-Katalysatoren mit verschiedenen Präparationsmethoden auf unterschiedlichen Trägermaterialien hergestellt, um deren Einfluss in der Synthese höherer Alkohole herauszufinden. Ein CuO/ZnO-Katalysator wurde auf einen Al_2O_3 -Träger durch Fällung und Nassimprägnierung aufgebracht und mit einer physikalischen Mischung verglichen. Nassimprägnierung stellte sich als die erfolgreichste Präparationsmethode heraus, da sie einen Katalysator lieferte, der eine gute Wechselwirkung der Aktivkomponenten Cu und ZnO mit dem Träger aufwies, was hohe Ausbeuten und Selektivitäten zu höheren Alkoholen zur Folge hatte. SiO_2 und Aktivkohle wurden als zusätzliche Träger getestet. Al_2O_3 war jedoch der geeignetste Träger, da der Katalysator die höchsten Selektivitäten und Ausbeuten zu höheren Alkoholen zeigte. Auf Al_2O_3 geträgerte Katalysatoren wurden zusätzlich über Fällung bei konstantem pH-Wert und Flammenspraypyrolyse hergestellt. Danach wurden die Katalysatoren mit Cs imprägniert und mit einem Cs-dotierten kommerziellen Katalysator verglichen. Für die mittels Nassimpregnung und Flammenspraypyrolyse hergestellten Katalysatoren wurden ähnliche Ausbeuten gefunden, jedoch wichen die Alkoholselektivitäten voneinander ab. Dies weist auf unterschiedliche aktive Zentren in Abhängigkeit von der Präparationsmethode hin.

Um die Katalysatoren weiter zu testen, wurde ein abwärts durchströmter Strömungsrohrreaktor am Institut für Katalyse Forschung und Technologie geplant und gebaut. Parameter wie

Flusstyp, Temperaturprofile, optimale Katalysatorbettpackung sowie zu Masse- und Wärmeübertragungslimitierungen wurden während der Bauphase betrachtet. Die Reaktionsprodukte wurden offline analysiert, weshalb eine gute Abtrennung der Reaktionsprodukte nötig war. Um die Funktionsweise des Reaktors zu überprüfen, wurde zunächst die Synthese von Methanol als einfache Testreaktion durchgeführt. Die Raumgeschwindigkeit, die Reaktionstemperatur und das EtOH:CO-Verhältnis wurde dann für die Synthese von höheren Alkoholen bei 8.0 MPa über einem [1.0 mol% Cs-CuO/ZnO]/Al₂O₃ Katalysator optimiert. Dieser Katalysator hatte sich in den Screeningreaktionen im satzweisen Betrieb als das vielversprechendste System herausgestellt. Höhere Raumgeschwindigkeiten (19400 L(STP) / kg_{cat} h) erwiesen sich als geeigneter für die Synthese von höheren Alkoholen und schränkten die Bildung von Nebenprodukten ein. Mittlere Temperaturen (593 K) stellten eine höhere Ausbeute sicher ohne zum Sintern des Kupfers beizutragen, was den Katalysator deaktivieren könnte. Wie bei den Batchversuchen wurde ein optimales EtOH:CO-Verhältnis gefunden ($n_{\text{EtOH}} : n_{\text{CO}} = 0.3$). Höhere Verhältnisse zeigten einen plötzlichen Anstieg der Bildung von Nebenprodukten. Auch für die kontinuierlich Tests wurde der Effekt des EtOH:CO-Verhältnis auf den Reaktionsweg analysiert. Wahrscheinlich waren Aldehyde und Ketone Reaktionsintermediate, wohingegen Alkohole und Ester Endprodukte darstellten, welche nicht durch Kupplungsreaktionen weiter umgesetzt wurden. Innerhalb der höheren Alkohole führte eine Gleichgewichtsreaktion zwischen der Aldol- und der Ketoform des Kupplungsprodukts von zwei Acetaldehyd-Molekülen entweder bevorzugt zur Bildung von 1-Butanol (höhere Verhältnisse) oder 2-Butanol (mittlere Verhältnisse). Bei höheren EtOH:CO-Verhältnis wurde die Bildung von Ethylacetat speziell bevorzugt. Offensichtlich verschoben höhere Anteile von adsorbiertem Ethanol das Gleichgewicht zur 3-Hydroxy-butanal (Aldolform), welche die Bildung von 1-Butanol ermöglichte und die Kupplung von Acetaldehyd mit adsorbierten Ethanol zu Ethylacetat vereinfachte. Um die Ketoform zu bilden, wird ein interner Wasserstofftransfer benötigt, den das adsorbierte Ethanol vermutlich durch Blockierung der Hydrierungsfunktionen der Kupferstellen verhinderte.

Zusammenfassend verbesserte die Zugabe einer bestimmten Menge an Ethanol zu Synthesegas die Synthese von höheren Alkoholen an CuO/ZnO und CuO/ZnO/Al₂O₃-Katalysatoren in satzweise und kontinuierlich. Mehrere Reaktionsparameter und der Katalysator selbst wurden modifiziert, jedoch sind für ein Scale-up des Prozesses noch weitere Verbesserungen nötig. Weitere *in situ*- und *in operando*-Characterisierungsstudien wären hilfreich, um den Einfluss von Ethanol auf die Katalysatoroberfläche und die Produktverteilung herauszufinden. Um den

in dieser Arbeit entwickelten kontinuierlichen Reaktor zu verbessern, ist eine Verbesserung der Produktquantifizierung zu empfehlen. Mittels einer Online-GC-Analytik könnten Produktverluste verhindert und die Massen- und Kohlenstoffbilanzen verbessert werden.

Table of contents

ACKNOWLEDGMENTS	I
ABSTRACT	III
KURZFASSUNG	VI
TABLE OF CONTENTS	X
1. INTRODUCTION	1
1.1. GENERAL CONSIDERATIONS.....	1
1.2. SYNTHESIS GAS AS STARTING MATERIAL FOR FUELS AND CHEMICALS	3
1.3. METHANOL SYNTHESIS.....	6
1.3.1. <i>Methanol synthesis catalysts</i>	9
1.3.2. <i>Methanol synthesis mechanism</i>	11
1.4. HIGHER ALCOHOL SYNTHESIS.....	14
1.4.1. <i>Catalysts for higher alcohols synthesis</i>	15
1.4.1.1. Noble metal based catalysts	17
1.4.1.2. Mo based catalysts: sulfides and carbides.....	18
1.4.1.3. Modified Fischer Tropsch catalysts.....	20
1.4.1.4. Modified methanol synthesis catalysts.....	23
1.4.2. <i>Higher alcohol synthesis mechanism over Cu based catalysts</i>	27
1.5. MOTIVATION	29
2. MATERIALS AND METHODS	32
2.1. CATALYST PREPARATION.....	32
2.1.1. <i>Precipitation</i>	32
2.1.2. <i>Wet impregnation</i>	33
2.1.3. <i>Flame spray pyrolysis</i>	34
2.1.4. <i>Catalyst doping</i>	35
2.2. CATALYST CHARACTERIZATION.....	35
2.2.1. <i>Elemental analysis</i>	36
2.2.2. <i>X-Ray Diffraction (XRD)</i>	36
2.2.3. <i>N₂ physisorption</i>	37
2.2.4. <i>Transmission Electron Microscopy (TEM)</i>	37
2.2.5. <i>Temperature Programmed Reduction (H₂-TPR)</i>	38
2.2.6. <i>Thermogravimetric Analysis (TGA)</i>	38
2.2.7. <i>Attenuated Total Reflectance – Infrared Spectroscopy (ATR-IR)</i>	38

2.2.8.	<i>X-Ray Absorption Spectroscopy (XAS)</i>	39
2.3.	CATALYTIC TESTS	41
2.3.1.	<i>Batch reactor</i>	41
2.3.2.	<i>Continuous-flow reactor</i>	43
2.4.	PRODUCT ANALYSIS.....	44
2.4.1.	<i>Gas phase analysis</i>	45
2.4.2.	<i>Liquid phase analysis</i>	45
3.	PREPARED CATALYSTS AND THEIR CHARACTERIZATION	46
3.1.	UNSUPPORTED CATALYSTS.....	46
3.2.	SUPPORTED CATALYSTS.....	53
4.	SYNTHESIS OF HIGHER ALCOHOLS: SCREENING STUDIES IN BATCH REACTORS	63
4.1.	UNSUPPORTED CATALYSTS.....	63
4.1.1.	<i>Influence of metal promoters</i>	65
4.1.1.1.	Effect of Ru doping on the CuO/ZnO catalyst	65
4.1.1.2.	Effect of Cs doping on the CuO/ZnO catalyst.....	66
4.1.2.	<i>Influence of ethanol to carbon monoxide ratio</i>	74
4.1.3.	<i>Influence of reaction temperature</i>	77
4.1.4.	<i>Catalyst characterization after catalytic tests</i>	79
4.1.5.	<i>Conclusions</i>	85
4.2.	SUPPORTED CATALYSTS.....	86
4.2.1.	<i>Effect of preparation method</i>	87
4.2.2.	<i>CuO/ZnO loading on the support</i>	88
4.2.3.	<i>Influence of the support material</i>	89
4.2.4.	<i>Influence of the preparation method of Cs-doped catalysts</i>	90
4.2.5.	<i>Catalysts characterization during and after reaction</i>	93
4.2.6.	<i>Conclusions</i>	95
5.	DESIGN AND CONSTRUCTION OF A HIGH PRESSURE, CONTINUOUS-FLOW REACTOR	97
5.1.	THEORETICAL BACKGROUND	97
5.2.	DESIGN AND CONSTRUCTION CONSIDERATIONS.....	102
5.3.	DETAILS OF THE LABORATORY PLANT.....	106
5.4.	PROOF OF CONCEPT: METHANOL SYNTHESIS REACTION.....	109
5.5.	CONCLUSIONS.....	112
6.	SYNTHESIS OF HIGHER ALCOHOLS: CONTINUOUS-FLOW REACTOR.....	113
6.1.	EFFECT OF SPACE VELOCITY	113
6.2.	INFLUENCE OF THE REACTION TEMPERATURE	116
6.3.	INFLUENCE OF $N_{EtOH} : N_{CO}$ RATIO	119

6.4.	CHARACTERIZATION AFTER REACTION	125
6.5.	CONCLUSIONS.....	127
7.	FINAL REMARKS AND OUTLOOK	129
	REFERENCES.....	133
	SUPPORTING INFORMATION	I
	LIST OF ABBREVIATIONS	XXVII
	LIST OF SYMBOLS.....	XXX
	CURRICULUM VITAE.....	XXXIII
	LIST OF PUBLICATIONS, POSTER/ORAL PRESENTATIONS AND CO-SUPERVISED THESES	XXXV

1. Introduction

1.1. General considerations

In the annual report for 2015 the International Energy Agency (IEA) claim that energy demand has and will continue to increase in all developing countries in the coming years (Figure 1).^{1,2} This rise in demand, despite of efficiency improvements, is linked with the fundamental human need of mobility and economic development.³ Non-renewable sources of energy involve the emission of CO₂, which becomes an additional environmental problem.

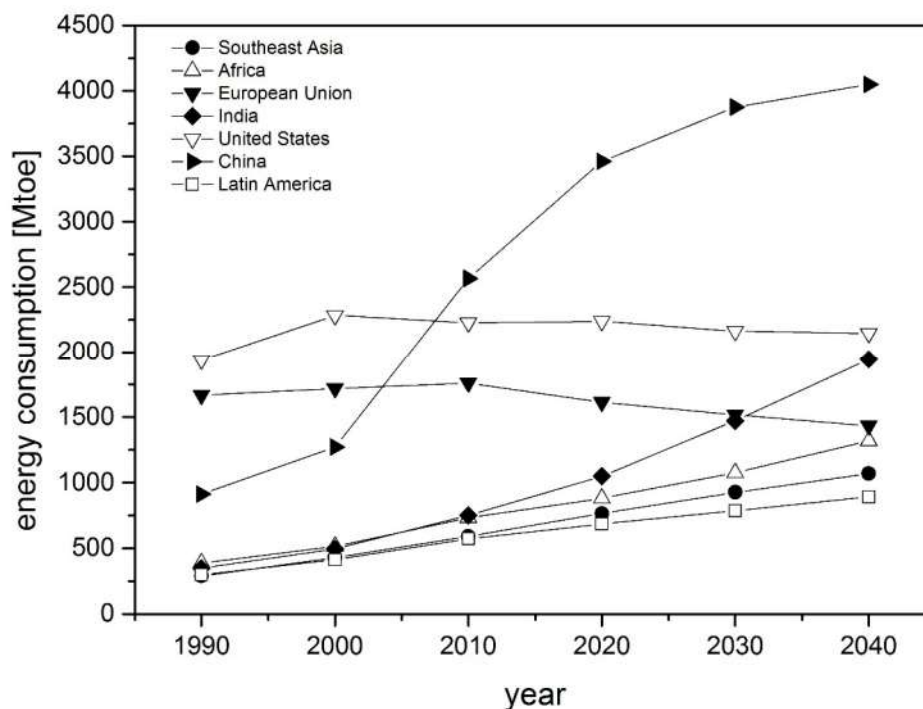


Figure 1: Primary energy demand by selected region in the new policies scenario, 1990-2040. (adapted from ²)

Particularly, oil demand is estimated to increase by 15 % until 2040 in a scenario which considers all publicly announced broad policy commitments and plans,¹ with principal oil consumption predicted for the transport and petrochemical sectors. Therefore finding alternatives for oil derived fuels and chemicals has been a strong focus over the past years. Oil production is predicted to grow until 2040, but at a decreasing rate over the years since it will become more difficult to access. Nevertheless, oil prices could rise again and alternatives to oil derived fuels and chemicals may become economically interesting.¹

In addition to the economic reasons, environmental goals (i.e. new regulations) will determine the use of renewable sources of fuels and chemicals.⁴ Alternatives for transportation systems such as electric cars, fuel cells and biofuels are currently being researched and developed.

Biomass derived products are particularly attractive since they mitigate the release of greenhouse gases (closed CO₂ cycle).^{3, 5, 6} Lignocellulosic feedstocks are appealing since they are inexpensive, abundant, and they do not interfere with food supply.^{7, 8} Different chemical platforms can be obtained from biomass depending on how it is processed.⁸ Four different routes are available: (a) thermochemical, (b) physical (c) chemical and (d) biochemical (fermentation or anaerobic digestion) as presented in Figure 2.^{3, 5-7, 9-14} Particularly, thermochemical processing of biomass will be discussed in more detail in the following paragraphs.

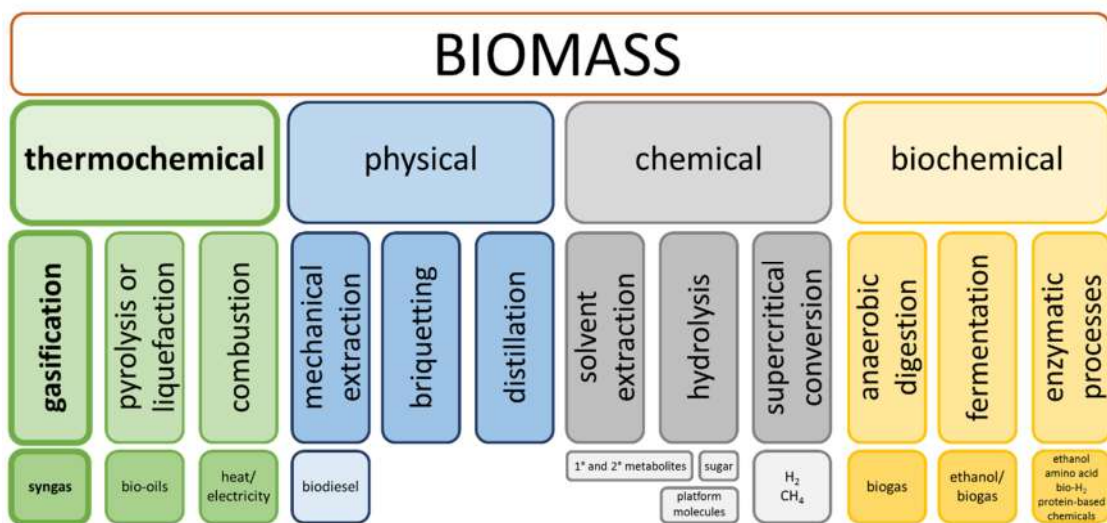


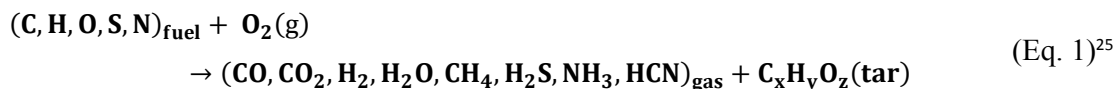
Figure 2: Biomass processing routes and derived products (compiled from ^{5, 7, 9-14}).

All types of biomass processing routes offer different advantages and disadvantages. Any type of biomass is suitable for thermochemical treatment and therefore it offers advantages compared to biochemical processes. Disadvantages include cleaning of the gaseous products and the presence of oxygen containing compounds, alkalis and sulfur in the biomass.⁶ Thermochemical processing leads to bio oils¹⁵ (via pyrolysis or liquefaction), synthesis gas^{6, 16, 17} (via gasification) or heat and electricity¹⁸ (via combustion).^{5, 7, 9-13} The use of bio oils, which after upgrade have similar properties to oil derived fuels, would avoid significant modifications in current transportation infrastructure and the internal combustion engine⁷. The upgrading process involves the elimination of the excess of oxygen contained in the bio oil.^{19, 20} An alternative processing route with several industrial applications is synthesis gas. Synthesis gas

is used as a building block in a variety of catalytic reactions such as Fischer-Tropsch synthesis, methanol synthesis, water gas shift reaction, and higher alcohol synthesis among others.^{3, 11, 21-24} The focus of this thesis is using synthesis gas as starting material. Therefore the production and uses of synthesis gas will be discussed in more details in the next chapter.

1.2. Synthesis gas as starting material for fuels and chemicals

One possibility to obtain synthesis gas corresponds to the direct gasification of biomass (Eq. 1). It is a thermochemical process in which biomass is dried (< 393 K), devolatilized (393 - 623 K) and degasified (623 - 1073 K, preferentially at temperatures higher than 773 K).^{3, 16} The process is performed at temperatures from 873 to 1373 K and pressures between 1 and 3.2 MPa.²⁵ The principal parameters for the design of a gasification process include the type and design of the gasifier, process temperature, flow rates of biomass and oxidizing agents, type and load of catalyst, and type of biomass and its properties.^{6, 11, 16} After the gasification process the produced synthesis gas needs to be cleaned before further use.⁶ An alternative to the direct gasification of biomass involves first the pyrolysis of biomass (to increase its energy density) followed by the gasification of the obtained biofuel.¹⁷



Using synthesis gas as a starting material leads depending on the catalyst and reaction conditions to a variety of products as displayed in Figure 3^{3, 6, 21, 22}, which will be described in more detail in the next paragraphs. Nevertheless, the main goal of this thesis is the synthesis of methanol and higher alcohols.

Several of the products derived from synthesis gas, such as hydrogen, methane, hydrocarbons, methanol and ethanol, are suggested as solutions for long-term storage of excess electrical energy produced from renewable resources. In particular this includes energy produced from sources such as wind, solar or tidal power, where periods of supply do not predictably coincide with periods of electricity demand. The most common way to convert excess electrical energy to chemical compounds corresponds to water electrolysis, which produces hydrogen. An alternative strategy includes the production of CO from the reverse water gas shift reaction (Eq. 13). In general, chemical energy storage is only an appropriate long term storage form since it

offers increased energy density, but suffers from low efficiency in comparison to other energy storage methods such as pumped hydroelectric power and compressed air energy storage.²⁵

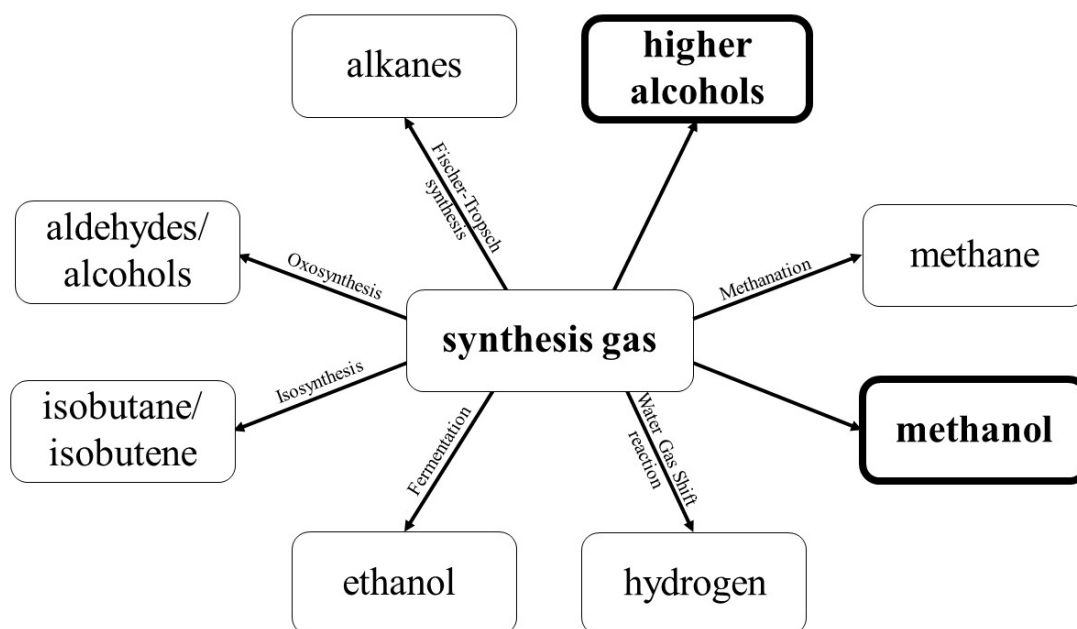


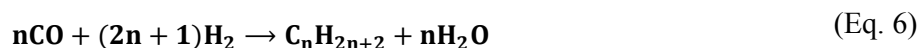
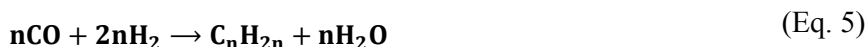
Figure 3: Synthesis gas derived products (adapted from^{11,22}).

The most prominent use of synthesis gas presently is in hydrogen production.^{21,22} H₂ is mainly synthesized via steam methane reforming (Eq. 2 – Eq. 4)²⁴. The production process involves feed pretreatment (desulfurization), steam reforming (Ni catalysts, Ni/Al₂O₃ or Ni/MgAl₂O₄ spinel), water gas shift reaction (Fe or Cu based catalysts) and hydrogen purification.^{4, 22, 24} Typical process conditions are temperatures up to 1273 K and pressures between 2.5 and 3.5 MPa. The formation of carbon depositions on the catalyst and the presence of sulfur in the methane stream are critical for the process. Both lead to deactivation of the catalysts.²⁴

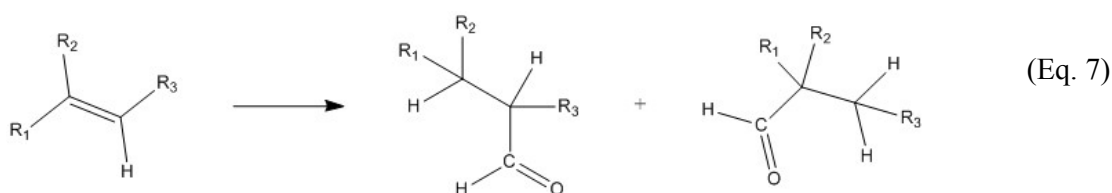


Another application of synthesis gas involves the use of anaerobic bacteria to produce ethanol which is known as synthesis gas fermentation.²² More details regarding the type of microorganisms used for this process can be found in reference ²⁶. The main advantages over other conversion possibilities relies on the selectivity of the biocatalyst, lower energy costs, better resistance to poisoning, and independence of the hydrogen to carbon monoxide ratio.²⁶

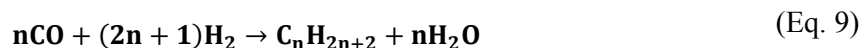
The production of isobutene (Eq. 5) and isobutane (Eq. 6) is known as isosynthesis. This process uses very high temperatures and pressures and is mainly performed over Th or Zr based catalysts.^{22,27,28} Isobutene is used in the synthesis of methyl tert-butyl ether (MTBE) and ethyl tert-butyl ether.²⁷ Currently, synthesis conditions vary from 623 to 723 K and from 0.05 to 10.0 MPa.^{27, 29-31}



Hydroformylation or oxosynthesis is the reaction of synthesis gas with olefinic hydrocarbons over homogeneous Co or Rh complexes to produce a mixture of aldehydes or alcohols (Eq. 7).^{21, 22, 32, 33} Usually, the reaction conditions depend on the activity of the metal, the ligands used and the reactivity of the substrate.³³



Fischer-Tropsch synthesis (Eq. 8 and Eq. 9)²⁴ is traditionally performed over Co or Fe catalysts, but other transition metals have been tested as well (for example Ru or Ni).^{22, 34, 35} Depending on the reaction conditions, the synthesis products include olefins, paraffins and oxygenated compounds in various compositions following the Anderson-Schulz-Flory distribution and, the production of large quantities of heat (exothermic reaction).^{22, 24, 34} The absence of sulfur or aromatics makes Fischer-Tropsch fuels very attractive.²⁴ Typical reaction conditions are pressures between 2.0 and 4.0 MPa and temperatures from 453 to 523 K.⁶ The Fischer-Tropsch reaction is a polymerization reaction, which involves CO adsorption on the surface, dissociation of the adsorbed CO and hydrogenation (chain initiation), insertion of CO molecules followed by hydrogenation (chain growth), chain termination and desorption of the product.^{22, 35} The main catalyst deactivation process corresponds to carbon deposition or coking.²⁴



Methanation (Eq. 10) is principally used for purifying methane or hydrogen streams by removal of CO^{36, 37}, but lately there has been renewed attention to production of synthetic natural gas

(SNG)³⁸. Methane is produced through the Sabatier reaction which is highly exothermic.³⁶⁻³⁸ Supported Ni catalysts are typically used, but also other metals like Ru, Co and Fe are active.³⁶ Usual operation conditions are temperatures between 523 and 973 K.³⁹ The deactivation of the catalyst usually occurs through sulfur poisoning or carbon deposition.³⁸



Alcohol synthesis (methanol and higher alcohols) is an important process for the production of oxygenate fuels, fuel additives and other intermediate feedstocks.⁴⁰⁻⁵⁰ Alcohols have high octane number^{43, 51, 52} and therefore are appropriate additives to fuels. The addition of methanol or ethanol to automotive fuels leads also to some problems due to corrosion of metallic fuel systems and, vapor lock⁵³, for example.⁴³ Additionally, a higher volume based consumption of the fuel is achieved due to the lower energy density of alcohol-containing and alcoholic fuels.²⁵ The use of alcohols as fuels or fuel additives offers the following advantages^{42, 43}:

- Reduction of life-cycle greenhouse gas emissions
- Reduction of toxic exhaust emissions
- Enhancement of the overall energy efficiency
- Reduction of fuel costs

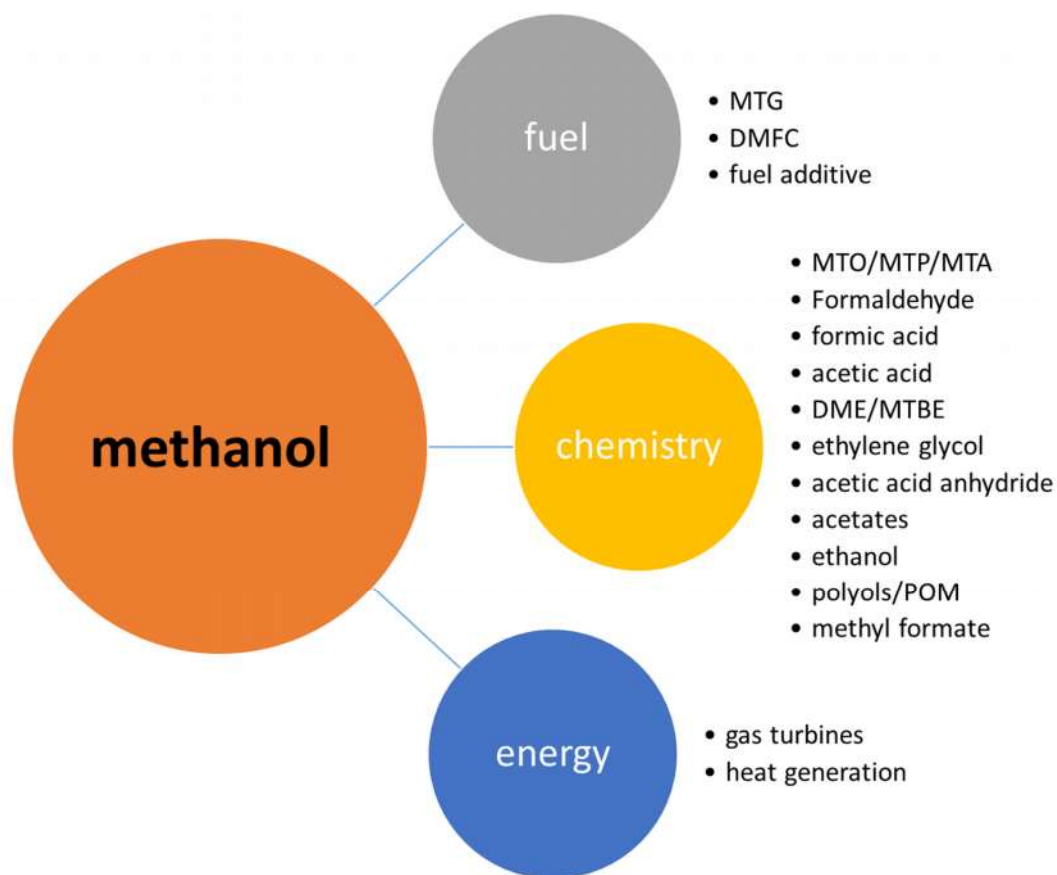
Since the synthesis of methanol and higher alcohols are the main objectives of this thesis, they will be discussed more specifically in the following sections of the introduction.

1.3. Methanol synthesis

Methanol is an important chemical building block which can be used as a source of fuels, energy and a wide range of chemicals as shown in Figure 4. These characteristics make methanol and its derivatives attractive as a replacement for oil based fuels. Several books deal with the topic of the methanol economy^{54, 55} accounting for its feasibility and importance for the future.^{53, 54} The principal methanol consumer is China (43 % of the world consumption). In China, most of the synthesis gas used for methanol synthesis is produced from coal gasification.⁵⁶ 40 % of the global methanol demand are for energy and methanol to olefins (MTO).⁵⁷

The current most important utilization of methanol corresponds to the synthesis of formaldehyde (40-50 %)^{24, 25, 55}, which is used in the wood, pharmaceutical and automotive

industries.⁵⁷ In the energy/fuel sector the current main application is the synthesis of MTBE (20 %), which is used as a gasoline additive and blending component (octane booster).^{25, 55} Pure methanol could also be used as a fuel for internal combustion engines. Despite the fact that its energy content is half that of gasoline, which leads to a higher volume-based consumption, methanol has both a higher octane rating and motor octane number and enables faster and more complete fuel combustion, which makes it a more efficient combustible.^{25, 55} Methanol displays some disadvantages when used as a fuel: some parts of the engine are incompatible (corrosion problems, dilutes ionizable substances and plastic materials) and cold start could be difficult because it lacks of highly volatile compounds (butane, isobutene and propane) which provide ignitable vapors to start the engine.⁵⁵ Alternatively dimethyl ether (DME) can be produced from the dehydration of methanol and used as a replacement for diesel fuels.⁵⁸⁻⁶⁰ The advantages of DME include a high cetane rating and clean burning properties.



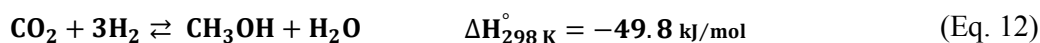
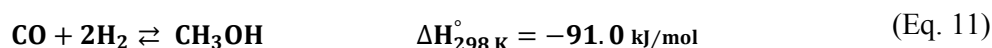
MTG: methanol to gasoline - DMFC: direct methanol fuel cell - MTO: methanol to olefins - MTP: methanol to propylene - MTA: methanol to aromatics - DME: dimethyl ether - MTBE: methyl tert-butyl ether - POM: polyoxymethylene

Figure 4: Chemicals derived from methanol.^{21, 22, 54, 55}

Some important future uses of methanol, considering higher petroleum prices, are in the methanol to olefins (MTO) and methanol to gasoline (MTG) processes. MTO produces ethylene and propylene. It is a two stage process involving firstly DME synthesis, which reacts further to olefins. This process is performed using zeolites (like ZSM-5 or SAPO-34) or a bifunctional catalyst ($\text{WO}_3/\text{Al}_2\text{O}_3$). The MTG is also catalyzed by zeolites (ZSM-5). In the first step also DME is formed, which is dehydrated into light olefins, followed by formation of C_{10} hydrocarbons.⁵⁴

Methanol synthesis has been widely studied in literature and is well developed as an industrial process with efficiencies over 70 %⁵⁵ and selectivities up to 99 %.^{25, 54, 61} Methanol synthesis plants are comprised of a synthesis gas production unit, a methanol synthesis reactor, and a separation and purification section.^{25, 62} The reactor design should consider the fast removal of the heat of reaction, since high temperatures affect the catalyst activity and decrease its lifetime. The synthesis is typically carried out in fixed bed reactors,²⁵ with normal designs including: quench reactors (adiabatic multibed quench systems), adiabatic reactors in series, boiling water reactors and gas-cooled reactors.⁵⁴

Methanol synthesis is an exothermic reaction which formally is written as CO hydrogenation (Eq. 11), but also includes CO_2 hydrogenation and the reverse water gas shift reaction (rWGS) (Eq. 12 and Eq. 13 respectively).^{25, 54, 55} The system is limited by thermodynamic equilibria at the given reaction conditions, because it involves reversible reactions.



This process can be performed at both high and low pressures and temperatures. BASF developed a high temperature and high pressure synthesis (25.0 - 35.0 MPa and 573 - 723 K) over $\text{ZnO}/\text{Cr}_2\text{O}_3$ catalysts.^{24, 25, 54, 55} Currently the synthesis is performed conventionally over copper-zinc oxide-aluminum oxide catalysts (first developed by Imperial Chemical Industries, ICI)⁵⁵ at milder temperatures between 493 and 543 K and pressures between 5.0 and 10.0 MPa.^{24, 25} The Cu/ZnO based catalyst results in high selectivity towards methanol since byproducts are kinetically limited.²⁵ Lower temperatures are chosen to avoid sintering of the copper particles and the formation of byproducts. The required synthesis gas is suggested to be a mixture of H_2 , CO and CO_2 in a ratio of 90:5:5.²⁴ Whereas other authors suggest a ratio S as

the quotient between the difference of the moles of H₂ and CO₂ and the summation of the moles of CO₂ and CO (Eq. 14). For an optimal methanol synthesis this ratio should be equal or close to 2.^{25, 54, 55, 63}

$$S = \frac{(n_{H_2} - n_{CO_2})}{(n_{CO_2} + n_{CO})} \sim 2 \quad (\text{Eq. 14})$$

The synthesis gas required for the methanol production is mostly obtained by steam reforming of natural gas, which requires an addition of CO₂ to achieve the specified S ratio⁵⁵ or coal gasification⁵⁶. Methanol synthesis can be a more environmentally friendly process if biomass gasification is used for the production of the synthesis gas or the synthesis is done directly from CO₂ and a regenerative H₂ source (for example, from water electrolysis).⁶¹ However, in order to use CO₂ as a methanol source, improvements on the catalyst are necessary to achieve better yields.⁶¹

1.3.1. Methanol synthesis catalysts

Industrial methanol synthesis catalysts are typically in the form of cylindrical pellets (diameter and height: 4-6 mm, specific surface area: 60 - 100 m²/g), which typically contain copper oxide (50 - 70 %), zinc oxide (20 - 50 %) and aluminum oxide (5 - 20 %), and do not constitute a supported system.^{25, 61-63} *In situ* reduction with diluted hydrogen at temperatures between 450 and 510 K activates the catalyst by forming dispersed metallic copper particles of typically 5 - 15 nm.^{25, 61, 63} The copper surface area is between 25 and 35 m²/g_{cat}.²⁵ The catalysts are deactivated by a decrease in the amount of active sites.⁶⁴ Typical deactivation of the catalysts occurs by sintering of the copper particles or poisoning by impurities (e.g. sulfur ⁶⁵).^{25, 64, 66, 67} Water presence accelerates the deactivation through sintering, reducing permanently the catalyst activity most probably by affecting the Cu-ZnO synergetic interaction which will be described later in more detail.⁶⁴

Methanol catalysts are known to be structure sensitive. A large copper surface area is one of the most important attributes. ZnO not only acts as a stabilizer and spacer avoiding sintering of the copper particles. It is also believed to exhibit a certain synergy with the copper particles, which give special catalytic attributes to the Cu/ZnO catalyst in comparison to other systems. Additional contributions to the catalyst activity are made by defect structures of the copper nanoparticles. Al₂O₃ is considered as a structural and electronic promoter to increase the catalyst activity and lifetime. Consequently, catalyst preparation plays a decisive role in its

activity. The effect of the preparation steps on the performance of the catalyst is known as chemical memory.^{61, 68-73}

The precise role of ZnO in methanol synthesis is still a disputed topic in the literature. Different hypotheses have been presented so far. It is believed that the high activity of the Cu/ZnO catalyst in comparison to other catalytic systems is most probably due to a synergy between Cu and ZnO. The active site formed as a consequence of this interaction is thought to enable a faster reaction path. One explanation for the observed synergy is the formation of a surface alloy.^{74, 75} Another suggestion is reversible wetting of the copper surface by metallic zinc as a function of the oxidizing potential of the gas, which changes the morphology of the copper particles.⁷⁶

Burch et al.⁷⁷ postulated that ZnO acts as a reservoir for atomic hydrogen and promotes the hydrogen spillover. Evidence of a Cu₃Zn surface alloy has been found by Derrouiche et al.⁷⁵ using X-ray diffraction and UV-vis spectroscopy when the catalyst was reduced at 623 K under hydrogen. This could be avoided when using CO/N₂ as reducing gas. By means of XPS (X-ray Photoelectron Spectroscopy), H₂-TPD (Temperature Programmed Desorption of hydrogen), N₂O-RFC (N₂O Reactive Frontal Chromatography) and H₂-TA (hydrogen Transient Adsorption) Kuld et al.⁷⁴ also suggested the formation of a surface alloy. Additionally, evaluation of the data from XPS and H₂-TPD measurements proved a correlation between the amount of metallic Zn and the decrease in the copper surface area.

Grunwaldt et al.⁷⁸ found additional evidence supporting the wetting/non wetting theory postulated by Clausen et al.⁷⁶. The authors observed a reversible morphology change of the copper particles under more reducing conditions. This change in morphology led to more disk shaped particles and consequently, a higher exposed copper surface area with atoms of lower coordination number. Under these conditions a higher catalytic performance was also observed due to the exposure of the more active Cu (100) and Cu (110) planes.⁷⁸ This phenomenon is only observed when copper particles are supported on ZnO, and was not seen for example on SiO₂.^{76, 78} Changes in the morphology of the copper particles with different pretreatments were also identified by Wilmer and Hinrichsen.⁷⁹ The authors explained these reversible changes through strong metal support interactions (mobile ZnO_x species), which inhibit the further adsorption of hydrogen. In agreement with Grunwaldt et al.⁷⁸, they suggested that more severe reducing conditions could induce to the formation of a surface alloy. Hansen et al.⁸⁰ observed

reversible dynamic changes in the shape of the nanocrystals when they were exposed to different gas environments.

As mentioned in the previous paragraphs, the Cu-ZnO synergetic interaction is of crucial importance for an active catalyst. Therefore special attention to the preparation of the catalyst has to be considered. A recent review regarding the synthesis conditions of methanol catalysts has been published by Behrens and Schlögl.⁶¹ The most common preparation method for this catalyst is by co-precipitation. When performed correctly, this ensures a homogeneous distribution of the copper and zinc oxide particles. The synthesis procedure has been optimized empirically over the years. It involves a constant pH precipitation (6 - 7) of the precursors (usually nitrate salts) with a solution of a basic precipitating agent (i.e. Na₂CO₃) at temperatures between 333 and 343 K.^{61, 68} These titration conditions are chosen to ensure an environment as close as possible to a simultaneous titration of the Cu and Zn cations (the individual cations precipitate at pH 3 and 5, respectively). The direct formation of CuO should be avoided, therefore the solution should not exceed a pH of 9. After the titration, the solution is aged within a period of 30 min to several hours forming hydroxy-carbonate precursors (preferentially zincian malachite and malachite). It has been reported that the formation of the highly substituted zincian malachite (28 % of Zn incorporation) lead to catalysts with the highest activity. This incorporation at an early stage enables the high dispersion of copper particles following precursor decomposition and results in a strong metal support interaction. According to Baltes et al.⁶⁸ the presence of residues of the precursor material after calcination should be beneficial to the catalytic activity.

1.3.2. Methanol synthesis mechanism

The methanol synthesis mechanism has been studied and debated for many years in the scientific community. It was initially assumed that CO was the primary carbon source of methanol, while Cu⁺ cations were considered as the active species. The complete reduction of the copper particles was prevented by CO₂ and H₂O. However, higher concentrations of CO₂ were shown to inhibit the synthesis due to strong adsorption.⁸¹ On the contrary, Chinchén et al.⁸² later proposed CO₂ as the primary carbon source of methanol using isotopic tracers. The authors postulated that CO hydrogenation is only preferred at low concentrations of CO₂ and in the presence of adsorbed oxygen on copper. The same authors could not identify a common intermediate between methanol synthesis and the water gas shift reaction (WGS).

In a more recent publication by Grabow and Mavrikakis⁸³, the authors used a comprehensive mean-field microkinetic model for methanol synthesis and WGS reaction (all input model parameters were calculated by density functional theory on a Cu (111) surface). For the microkinetic model 49 elementary steps were considered. They suggested that 2/3 of the methanol is produced by CO₂ hydrogenation and the rest via CO hydrogenation, discarding the hypothesis of CO acting only as a promoter. The production of methanol via CO₂ involves the following adsorbed intermediates: HCOO* (formate), HCOOH* (formic acid), CH₃O₂* (hydroxymethoxy), CH₂O* (formaldehyde) and CH₃O* (methoxy). The CO hydrogenation considers HCO* (formyl), CH₂O* and CH₃O* as adsorbed intermediates. The potential energy surface (Figure 5) was obtained after fitting the microkinetic model to the experimental data. This diagram suggests that CO hydrogenation is dominant, while adsorbed CO is additionally consumed by a competitive path, the WGS reaction. In Figure 5 also the promoting effect of CO on the CO₂ hydrogenation can be appreciated when comparing the blue path to state 4 with the red path to state 5. According to the authors, the CO promotion could be explained by either the removal of OH* with CO* via the WGS or CO-assisted hydrogenation of HCO*.

Zuo et al.⁸⁴ postulated that methanol is synthesized from CO and CO₂ at different sites using density functional theory. The synthesis from CO occurs at Cu^{δ+} (0 < δ < 1) species.

Kunkes et al.⁸⁵ investigated an industrial methanol catalyst by means of H/D substitution studies. They proposed that (i) the methanol synthesis and the rWGS reaction do not share a common intermediate and (ii) the methanol formation from CO₂ does not occur via a consecutive reverse water gas shift and CO hydrogenation steps. They claimed that formate hydrogenation is the rate determining step for methanol synthesis from CO₂. Both reactions occur in parallel and on different sites.

A kinetic model of the methanol synthesis for a commercial catalyst based on a three-site adsorption model was developed by Park et al.⁸⁶ The model considered Cu, Cu⁺¹ and ZnO as adsorption sites and the simultaneous dosage of CO and CO₂. The maximum methanol concentration and the contribution of both CO and CO₂ hydrogenation were a function of both temperature and CO fraction. The maximum methanol concentration occurred for mixtures containing 90 % of CO. The CO conversion exhibited two opposite behaviors depending on the proximity to the reaction equilibrium. Close to equilibrium, temperature had a negative effect on the CO conversion, because of the exothermicity of the reaction. On the contrary, further from the equilibrium point, temperature had a positive effect since it increased the

reaction rates. Increasing the space velocity decreased the CO conversion due to a reduction of the residence time. Higher pressures increased the concentration of reactants, consequently increasing the CO conversion. The effect of temperature, pressure and space velocity on the CO₂ conversion was minimal due to a compensation by the WGS reaction. These authors claimed that the degree of CO and CO₂ hydrogenation on commercial catalysts is comparable.

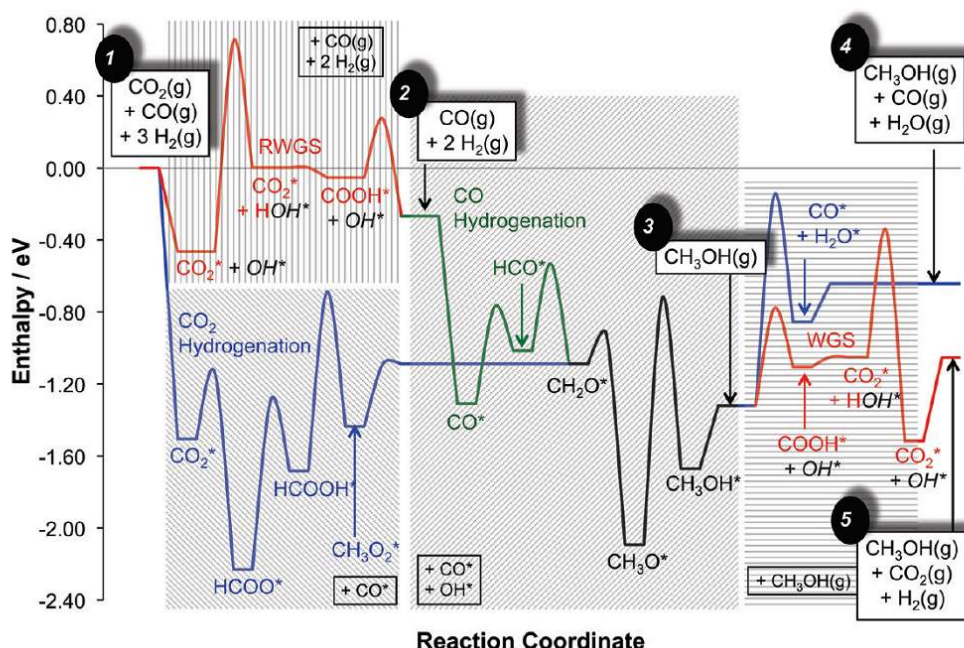


Figure 5: Potential energy surface diagram for methanol synthesis. (reprinted with permission from ⁸³).

In a recent study, Studt et al.⁸⁷ addressed two arguments regarding the methanol synthesis: (1) the preferred carbon source (CO or CO₂) and (2) the Cu-Zn synergy. In a gas switching experiment it was claimed that metallic Cu, in general, allowed the hydrogenation of both CO and CO₂. A ZnO containing Cu catalyst required a mixture of CO/CO₂/H₂ to perform optimally. On the other hand, an MgO supported catalyst exhibited higher activities in a CO/H₂ mixture. Regardless of the support and proven by isotopic-labelled CO₂, the majority of the methanol was produced from CO₂ hydrogenation. On Cu/MgO catalysts CO₂ functioned as a poison (suppressing CO conversion) and a precursor at the same time. The poisoning effect was more marked for more basic supports, like MgO, but the major benefit can be attributed to ZnO. The catalyst was covered by adsorbed formate when exposed to CO₂ containing mixtures. At differential conditions, methanol production increased with CO₂ concentration, but at higher conversions this was not the case because the product was inhibited by water. Therefore the methanol production as a function of CO₂ concentration was shaped as volcano type plot.

Combining density functional theory and microkinetic modeling, it was discovered that in the presence of Zn all intermediates and transition states for the CO₂ hydrogenation are bonded by an oxygen atom. Zn deactivates the surface for CO hydrogenation, whereas it increases the CO₂ hydrogenation. CO promotes the CO₂ hydrogenation because it converts the formed water via the WGS reaction.

1.4. Higher alcohol synthesis

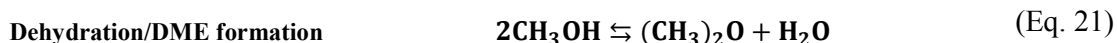
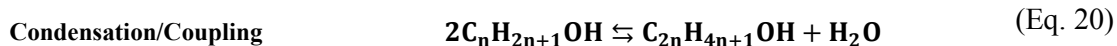
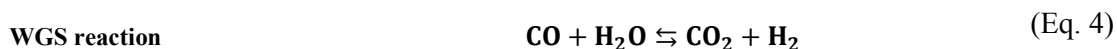
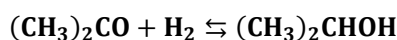
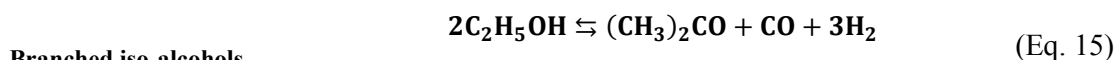
The use of higher alcohols as fuels or fuel additives has several advantages compared to the use of methanol. For instance, methanol is more corrosive and has lower miscibility with gasoline.⁸⁸ Methanol miscibility with water limits the amount of methanol allowed in a blend before phase separation occurs.⁸⁸ Ethanol solubility in diesel is determined by two factors when used in blends: temperature and water content. Separation of the blend has been observed at temperatures below 283 K.⁸⁹ Azeotropic water contained in ethanol is responsible for wet corrosion which damages parts of the engine.⁸⁹ Additionally, higher alcohols (as additives) offer improved lubrication, decrease destruction of engine parts⁴³, and have higher heating values compared to methanol.^{42, 90-92} Higher alcohols are also used as solvents or starting material for other products (Table 1).

Table 1: Products derived from higher alcohols.⁹³

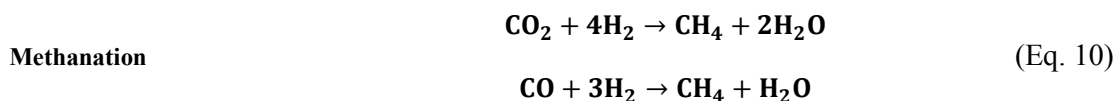
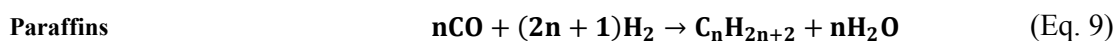
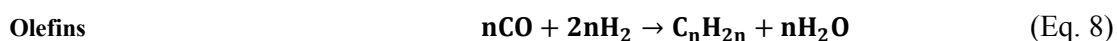
phosphoric acid ester	Solvent, plasticizer, lubricant, flame retardant
citric acid ester	Environmentally friendly plasticizer
aromatic esters	plasticizer
alkanoic acid ester	solvent
fatty acid ester	Lubricant, wax, additive for herbicides
ethoxylate	Surface cleaner, cosmetics
alcohol mixtures	Solvent, floating agent for carbon extraction
nitric acid ester	Additive for raising the cetane number of diesel fuels
sugar ether	Foam concentrate
dialkyl ether	Cosmetics, solvent, latent heat reservoir/storage, printing ink
Guerbet alcohols	Cosmetics, fatty alcohols, tenside

The production of alcohols is a highly exothermic reaction. According to Fang et al.⁴⁰, a successful synthesis of mixed alcohols requires an efficient removal of the reaction heat. Other important factors involve controlling the process temperatures, maximizing yields and minimizing catalyst deactivation by sintering.²² The reactions involved in higher alcohol synthesis are listed below^{11, 22, 49, 50}:

Desired reactions:



Competing reactions:



1.4.1. Catalysts for higher alcohols synthesis

Several catalysts have been studied in the literature for the synthesis of higher alcohols starting from CO/H₂ mixtures. An optimal catalyst for this reaction is a bifunctional catalyst, which combines active sites that favor C-C (chain growth) and C-O (termination step) bond forming reactions and hydrogenation sites.

The synthesis of higher alcohols has been approached with homogeneous and heterogeneous catalysts as displayed in Figure 6. The homogeneous synthesis has focused more on the direct formation of ethanol via homologation.⁹⁴⁻⁹⁶ Chen et al.⁹⁴ performed methanol homologation at 30.0 MPa and 473 K in methanol solutions of amines. The authors tested several catalytic carbonyl complexes containing Fe, Rh, Ru, Mn. They proposed a common pathway for all catalysts. Methylammonium ions were the methyl carriers, the role of nucleophilic methyl acceptors was carried by the transition metal complex anions. Cobalt carbonyls and iodine or cobalt iodide were also used as catalysts for the homologation reaction of methanol to ethanol.⁹⁵ Under the reaction conditions studied (3.0 - 15.0 MPa, 423 - 483 K and H₂ : CO ratios of 0.3:1 - 3:1) the reaction rate was first order with respect to methanol and cobalt concentrations and CO partial pressure. Methanol conversion was 52 % and the selectivity towards ethanol was 74.4 % (13.5 MPa, 468 L, H₂ : CO molar ratio of 2:1). The liquid phase methanol hydrocarbonylation reaction was studied using both heterogeneous Rh and Ru supported on active carbon, and Rh and Ru homogeneous catalysts.⁹⁶ The activity of both homogeneous and heterogeneous catalytic systems were similar. Nevertheless, the authors identified leaching of the active metals from the support during reactions with the heterogeneous catalysts. The leached metals were responsible for the observed activity.

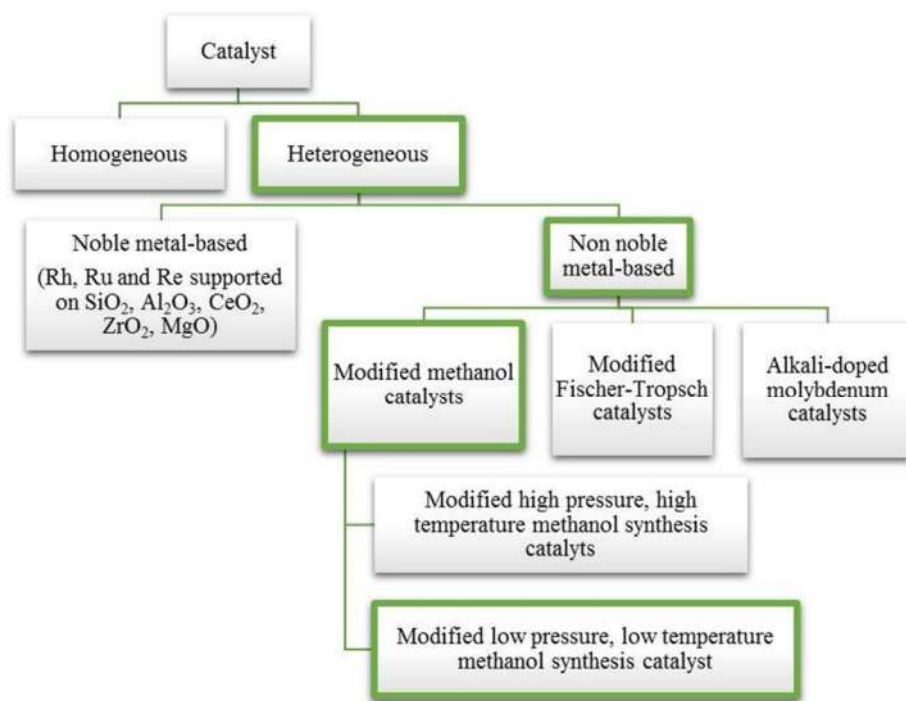


Figure 6: Classification of the catalysts for higher alcohols synthesis.

Even though homogeneous catalysts offer good selectivity for the synthesis of ethanol, disadvantages arise in comparison to heterogeneous catalysts when used on an industrial scale. An industrial scale catalyst should offer easy separation of reaction products from the reactor system (i.e. by filtration). Simple recovery of the catalysts furthermore facilitates catalyst reactivation and reutilization. Heterogeneous catalysts are typically classed as either noble metal or non-noble metal based catalysts. The non-noble metal catalysts are divided into three categories, which present attractive qualities for the synthesis of higher alcohols: (i) modified methanol catalysts, (ii) modified Fischer-Tropsch catalysts and (iii) alkali-doped molybdenum based catalysts. In the following sections, the different categories will be described in more detail, although the main focus of this thesis will be modified methanol synthesis catalysts.

1.4.1.1. Noble metal based catalysts

The synthesis of higher alcohols using noble metal based catalysts has been reported using Re, Rh, and Ru supported on different oxides (SiO_2 , Al_2O_3 , CeO_2 , ZrO_2 , MgO , among others).⁵⁰ Rh supported catalysts are the most widely examined ones, because they have attractive qualities for the synthesis of higher alcohols. Rh has both the ability to bind CO dissociatively and non-dissociatively, thereby enabling the chain growth and consequent alcohol formation via CO insertion.

Rh-based catalysts produce mainly C_{2+} oxygenates, mostly ethanol among the alcohols⁹⁷⁻¹⁰⁰. The product distribution depends on the support and the promoter, as well as the activation process and the reaction conditions used. The support affects the Rh dispersion and consequently the nature of CO adsorption. Several promoters have been tested so far, such as V, La, Ce, Y, Li, Na, K, Mn, Mo, Fe, Sm among others.^{50, 97, 98, 100, 101} The addition of Fe as a promoter to Rh supported catalysts increased the selectivity towards ethanol up to 22%.^{97, 101} Fe favored the adsorption of doubly bonded CO. Also Mn promoters were qualified as very promising.⁵⁰

The effect of pretreatment on the activity of the Rh supported catalyst was studied by Jiang et al.¹⁰² A SiO_2 support was pretreated with C_{1-5} alcohols before preparing a Rh-Mn-Li/ SiO_2 catalyst. An increase of the molecular weight of the alcohol employed in the pretreatment led to higher C_{2+} oxygenates selectivity (77 %) and higher space-time yields (631 $\text{g}/\text{kg}_{\text{cat}} \text{ h}$) until a maximum was reached with the catalysts pretreated with butanol. The authors proposed that the pretreatment enhanced the Rh dispersion and increased the Rh^+/Rh^0 ratio.

Hu et al.¹⁰³ tested the performance of Rh-Mn/SiO₂ under several reaction conditions. Optimal conditions for ethanol synthesis were identified at lower temperatures (< 553 K), higher pressures (5.4 MPa) and H₂ : CO ratio of 2:1. Higher temperatures favored methane synthesis, as shown for several Rh supported catalysts. On the contrary, higher pressures disfavored methane production. Lower H₂ : CO (1:1) ratio increased the selectivity toward CO₂ (WGS reaction) and higher ratios (3:1) increased the methane selectivity. Gogate and Davis¹⁰⁴ compared the hydrogenation of CO, CO₂ and CO/CO₂ mixtures on the Fe promoted Rh/TiO₂ catalysts. The reaction conditions influenced the product distribution significantly. In the case of CO hydrogenation on Rh-Fe/TiO₂ catalysts, the selectivity towards ethanol was appreciable (28 %), but it decreased considerably when CO₂ hydrogenation was performed (6 %). For reactions using mixtures of H₂, CO and CO₂ (H₂ : CO : CO₂ = 10:5:5) a decrease in conversion of about 15 - 20 % was observed in comparison to only CO hydrogenation reactions. The methane selectivity increased from 39 % to 45 % when the gas mixture was used, but the ethanol selectivity remained virtually constant (27 - 29 %).

Recently Surisetty et al.¹⁰⁵ investigated the effect of Rh addition to MWCNT-supported alkali-modified MoS₂ catalysts. The reduction ability and the dispersion of the metal phase increased with rhodium addition due to a strong electronic interaction between Rh and Mo. Similarly to other Rh-containing catalysts, ethanol was the dominant product but higher alcohols were also reported. A selectivity of 16 % towards ethanol and 25 % towards higher alcohols was achieved at 593 K and 8.3 MPa for a 2 wt.% Rh catalysts.

Despite the high selectivity to ethanol achieved with Rh containing catalysts, according to Gupta and Smith⁴¹ they are not so attractive for industrial purposes since the selectivities and yields towards alcohols are not satisfactory enough to overcome the current Rh prices.

1.4.1.2. Mo based catalysts: sulfides and carbides

Mo based catalysts are generally alkali promoted Co, Fe, Ni or Rh supported on MoS₂ or Mo₂C. Typical operation conditions are temperatures between 543 and 603 K, pressures of 7.5 - 28.0 MPa, and H₂ / CO = 1 - 2.^{40, 42} The MoS₂ type catalysts exhibit excellent sulfur tolerance.^{40, 42, 44} The alcohols formed are mainly linear alcohols¹⁰⁶ and follow the Anderson-Schulz Flory distribution.^{42, 44, 49, 107}

The production of alcohols over alkali promoted MoS₂ catalysts in a microreactor between 473 and 673 K was studied by Liu et al.¹⁰⁶ K, Rb and Cs showed similar effects on the synthesis of

higher alcohols. In the case of Rb and K an optimal alkali : Mo ratio was determined as 0.7:1, whereas for Cs it was 0.2:1. Methanol was preferred at lower temperatures, while ethanol exhibited a maximum at intermediate temperatures around 623 K. Propanol and 1-butanol production increased together with the temperature.¹⁰⁶

Moderate basic promotion is desirable. The promotion effect on high surface area MoS₂ catalysts increased in the following order: Li < Na < Cs < Rb < K. On low surface area MoS₂ catalysts, the alcohol space-time yield raised according to K < Rb < Cs.^{44, 49} The promotion with Cs or K of Co-MoS₂/clay catalysts gave higher selectivities towards higher alcohols when K (44.8 %-C) was used as a promoter in comparison to Cs (30.5 %-C) at a GHSV of 2000 h⁻¹ and 563 K.¹⁰⁸ The alcohol productivity raised with increasing reaction temperature, but the selectivity decreased. La and Ni co-modified catalysts were tested in the synthesis of higher alcohols.¹⁰⁹ Ni enhanced the activity (CO conversion raised from 23 to 40 %) and changed the alcohol distribution towards higher alcohols, but simultaneously increased the production of methane. When La was additionally added the hydrocarbon formation decreased. The authors suggested a structure and morphology change of the catalyst due to the La doping, leading to higher Ni dispersion on the surface. Rh modification (0 - 1 wt.%) of a Mo-K/Al₂O₃ catalyst showed an improvement in both catalytic activity (from 19.2 to 56.6 g/l h) and selectivity to alcohols (from 39.4 to 63.7 %-C). The authors attributed these improvements to the simultaneous presence of cationic and metallic Rh species.¹¹⁰ Similar results were also obtained for Pd modified catalysts.¹¹¹ Co addition to a K-Mo/Al₂O₃ catalyst led to an increment in the formation of higher alcohols.¹¹² Co containing catalysts calcined at 773 - 923 K after sulfidation tend to have Co as a sulfide with tetrahedral coordinated structure.

An extensive study on Mo₂C catalysts for the conversion of synthesis gas to higher alcohols was performed by Christensen et al.¹¹³ As for MoS₂ based catalysts K was found to be the most appropriate alkali promoter. Deactivation of the catalyst was observed after 94 h on stream. The authors explained that the deactivation was probably due to the formation of carbonaceous deposits rather than sintering of the metal particles. Additionally, the effect of the addition of Cu as promoter was evaluated. Cu improved higher alcohol productivity by 33 % while maintaining the alcohol distribution at 548 K and 10.0 MPa. Other promoters such as La, Re and Mn did not show positive effects.

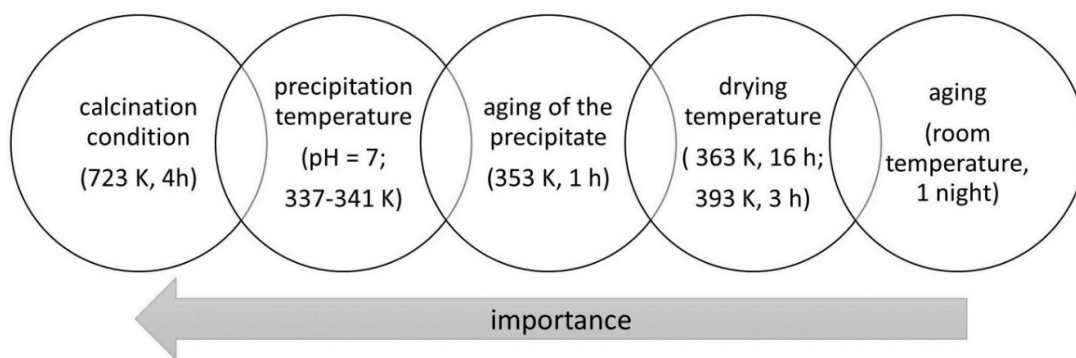
Mo based catalysts appeared to be very promising, particularly because of the sulfur resistance offered by MoS₂ based catalysts. Nevertheless, these catalysts require a continuous feed of H₂S

which provokes contamination by organosulphides.⁴⁴ As an alternative Mo₂C catalysts have recently been investigated. However, high selectivities towards hydrocarbons are still an important issue if not promoted correctly, in addition to water deactivation and the need of an appropriate CO/CO₂/H₂ ratio. Therefore they will not be the focus of this thesis.

1.4.1.3. Modified Fischer Tropsch catalysts

Fischer Tropsch (FT) catalysts based on Co, Ru, Ni and Fe are particularly active for higher alcohols synthesis when modified with promoters, such as transition metals or alkali cations for example.^{43, 49, 50} According to ⁵⁰, products formed over modified-FT catalysts are primarily straight chain alcohols. Typical operating conditions range from 5.0 - 15.0 MPa, 493 - 623 K and 4000 - 8000 h⁻¹ (GHSV). A maximum amount of alkali loading is required in these catalysts to achieve maximum selectivity towards ethanol and higher alcohols. The increase in higher alcohol formation with alkali loading is due to the suppression of hydrocarbon formation. A synergistic interaction between metals that dissociate CO (like Ru and Co) and others that do not dissociate it (like Ir) is necessary. These catalysts are severely affected by the preparation procedure (impregnation sequence, precursors, metal and promoter loading especially).⁴⁹

Mahdavi and Peyrovi¹¹⁴ studied the influence of the preparation procedure on the selectivity and activity in the synthesis of alcohols over Cu/Co₂O₃/ZnO, Al₂O₃ catalysts. The authors ordered the relevant factors that could affect the catalytic performance (Scheme 1). Varying systematically these preparation conditions a conversion of 20 % was achieved with a selectivity towards alcohols of 65 %.



Scheme 1: Importance of the preparation conditions for the synthesis of Cu/Co₂O₃/ZnO, Al₂O₃ catalysts.

In addition, the impregnation sequence of Cu-Co supported on SiO₂ catalysts was analyzed. A strong synergistic effect caused probably by the formation of copper cobalt spinel was observed for co-impregnated catalysts reaching a selectivity of 52 %.¹¹⁵

Several groups of modified Fischer Tropsch catalysts have been studied, for example: (1) FeCuMn, (2) LaCo_xCu_yO_z, and (3) Cu-Co based.

Fe promotion on CuMnZrO₂ and CuMnZnO increased the copper particle dispersion.^{116, 117} For Fe-CuMnZrO₂ catalysts the preparation method directed the selectivity towards branched alcohols when co-precipitation was used and linear ones when wet impregnation was utilized.¹¹⁷ In the case of CuMnZnO catalysts, the increase in catalytic activity was attributed to a synergistic effect between dispersed copper and iron carbides.¹¹⁶ Mn promoted the dispersion of both Cu and Fe species.¹¹⁸ Increasing the Mn concentration for the FeCuMn_{0.5-2.0}ZnO catalyst led to an increase in the CO hydrogenation activity, selectivity to higher alcohols (from a ratio C₂₊-OH / C₁-OH of 1.56 to 1.95) and to hydrocarbons (20 to 29 %). Zn was suggested as an electronic/chemical promoter, with Mn acting as a structural promoter.¹¹⁹

Co and Mo-promoted CuLa₂Zr₂O₇ catalysts were investigated by Chu et al.¹²⁰ Co promotion favored chain growth processes. Mo increased the total conversion by enhancing the hydrogenating properties of the catalyst. The authors suggested the incorporation of C₁-oxygen containing intermediates into alkyl chains as a probable reaction mechanism. Tien-Thao et al.¹²¹ identified an alkali doping between 0.1 and 0.3 wt.% as optimum for nanocrystalline LaCo_{0.7}Cu_{0.3}O₃ perovskites. Li proved to be the most effective dopant. Alkali doping influenced positively the chain growth from both hydrocarbons and alcohols. In general, the alcohol selectivity was between 26 - 49 %

Cao et al.¹²² compared Cu/ZnO, Cu/Co/ZnO and Cu/Co/ZnO/Al₂O₃ catalysts for the synthesis of higher alcohols. Cu sites were blocked by Co reducing methanol synthesis rates, nevertheless this did not affect methane and ethanol production. A Cu-Co alloy formation was suggested implying a dual site mechanism.¹²³ The formation of alcohols most probably occurred through the reaction of hydrocarbonated species with a C₁ oxygenate.¹²⁴ Strong Cu-Co interaction was also identified using temperature programmed reduction and X-ray photoelectron spectroscopy.¹²⁵ Volkova et al.¹²⁶ attributed to the CuCo alloy the formation of cobalt carbides (Co₂C), which were responsible for the activation of CO non-dissociatively, therefore enabling synthesis of oxygenates. Similar studies revealed that CO is coordinated to sites where Cu and Co atoms interact.¹²⁷ More recently, a strong interaction between Cu and Co particles was

identified by X-ray absorption spectroscopy confirming the presence of a mixed spinel phase (CuCo_2O_4).¹²⁸ In the reduced catalysts evidence of bimetallic Cu and Co was observed. The addition of Cu to the Co catalyst led to an increase in higher alcohol selectivity from 2 % to 23 %, but a decrease in the CO conversion. The authors suggested that bimetallic particles are responsible for the synthesis of higher alcohols. Density functional theory coupled to a microkinetic model were used to identify the preferred active site and the optimum composition to synthesize higher alcohols over CuCo supported catalysts.¹²⁹ According to the simulation, Co rich CuCo sites (alloy) were the most active towards higher alcohol synthesis. When alkalinized or basic oxide-supports were used carbonyl ions ($\text{Co}(\text{CO})_4^-$) were identified by infrared spectroscopy of CO adsorption. No CuCo alloy was formed in this case.¹³⁰ The carbonyl ions were suggested as an intermediate in the CO insertion step for the oxygenate formation.

Promotion with K on $\text{Co}_2\text{O}_3/\text{CuO}/\text{ZnO}/\text{Al}_2\text{O}_3$ catalysts showed a moderate selectivity towards higher alcohols.¹³¹ The selectivity increased from 1.1 % to values between 3.8 and 5.0 % depending on the K loading. The effect of alkali doping (Li, Na, K, Rb, Cs) was also studied on Zn promoted CuCoCr catalysts.¹³² The influence of different alkali metals depended on both temperature and catalyst composition. In the absence of Zn the highest selectivity towards higher alcohols was found for Na (34 %) doped catalysts at 573 K, whereas at 623 K potassium proved to be more effective. In the presence of Zn at 623 K Li and Cs showed higher selectivities. Doping of Co catalysts with Na allowed a shift in the selectivity from hydrocarbons towards alcohols reaching values up to 28 %, with 77 % of the total alcohols having more than 5 C atoms. The presence of alkali metal resulted in a decrease of the Co particle size, its reducibility and an increase in the surface basicity.¹³³ Simulation results were also tested experimentally on K doped CuCoMo catalysts.¹²⁹ The results showed that the yield of higher alcohols increased two orders of magnitude in comparison to a benchmark catalyst (K-CuCoCr).

Different supports were tested for the CuCo catalysts (Al_2O_3 , SiO_2 and carbon nanotubes) by Wang et al.¹³⁴ Al_2O_3 proved to be the most effective support allowing an increase in the metal dispersion and formation of the active Cu-Co bimetallic species.

Modified Fisher-Tropsch catalysts promoted solely with Fischer Tropsch elements exhibit also high selectivities towards hydrocarbons, therefore promoters are required for their application. To optimize the catalyst performance, theoretical calculations are a useful tool.¹³⁵⁻¹³⁸ An

interesting combination is achieved when CuCo catalysts are used since they offer a combination between two of the required characteristics for a successful higher alcohol synthesis as suggested from calculations by Medford et al.⁴⁸ Even though these catalysts will not be the central topic of this thesis, promotion with Ru (well-known Fischer-Tropsch element) will be addressed.

1.4.1.4. Modified methanol synthesis catalysts

Modified methanol synthesis catalyst are classified into two categories depending on the optimal operation conditions of the catalyst:

- High pressure, high temperature methanol synthesis catalysts
- Low pressure, low temperature methanol synthesis catalysts

High pressure, high temperature methanol synthesis catalysts

It is well known that ZnO/Cr₂O₃ catalysts are active for methanol synthesis. Alkali-doped ZnO/Cr₂O₃ have been tested for the production of higher alcohols.¹³⁹⁻¹⁴⁵ These catalysts were originally non-selective and produced high quantities of hydrocarbons, however improved alcohol productivity and selectivity have been obtained using heavy alkali dopants. The process conditions include temperatures between 673 and 723 K and pressures between 6.9 and 25.5 MPa. The main alcohol products consist of methanol and isobutyl alcohols.^{141, 145}

Tronconi et al.¹⁴⁵ studied the synthesis of higher alcohols over potassium-promoted ZnO/Cr₂O₃ catalysts, concluding that methanol formation occurred quickly in comparison to higher alcohols. Addition of CO₂ inhibited the production of higher alcohols, affecting branched alcohols to a higher extent than linear ones.

These type of catalysts were studied to obtain an appropriate mixture of methanol/isobutanol (ratio of 1:1), which is considered ideal for MTBE synthesis.^{140-144, 146-149} Firstly, K or Cs promoted commercial Zn/Cr spinel catalysts were tested. Catalysts doped with 1 wt.% K showed the highest isobutanol production (38 g/kg h), but also the highest hydrocarbon production (23 g/kg h).¹⁴¹ On the other hand, the 3 wt.% Cs doped catalyst showed the highest total alcohol production (214 g/kg h), alcohol selectivity (81 %) and isobutanol production rate (116 g/kg h) with a low hydrocarbon production rate (11 g/kg h).¹⁴² Surface characterization results demonstrated that alkali promoters were bonded to the Cr as chromate or dichromate species. The Zn/Cr spinel structure acted only as a high surface-area support.

Excess ZnO improved the catalysts performance, enhancing the isobutanol yield and the total alcohol selectivity for Cs or K doped catalysts.¹⁴⁷ Addition of Pd as a second promoter to the catalysts lead to enhanced productivities of total alcohols and isobutanol, since it decreased the production of hydrocarbons.^{140, 143} The highest isobutanol production rate (154 g/kg h) and lowest methanol to isobutanol ratio (0.35:1 mole ratio) were found for 5 wt.% Cs- promoted Pd/Zn/Cr catalysts with an excess of ZnO.^{144, 149} An adequate catalyst stability was observed, no change in the product stream composition occurred during the 5-day tests.

The presence of Cr was not fundamental in the performance of the catalysts, therefore it was partially replaced with Mn.¹⁴⁰ The addition of Mn to catalysts solely promoted with Cs was beneficial, but for catalysts promoted with both Cs and Pd was worse for the catalytic performance. Contrary to the findings of this study, catalysts promoted with K and Pd exhibited an increase in their catalytic properties.

Verkerk et al.¹⁵⁰ summarized aspects from the molecular kinetics and the reaction mechanism for isobutanol synthesis from synthesis gas. Methanol formation and water gas shift reaction were in equilibrium under typical reaction conditions. The expected ketone and aldehyde products coexisted with their corresponding alcohols, but their amount was limited due to the high partial pressure of hydrogen. The chain growth mechanism was kinetically controlled and consisted of C₁-addition and aldol-type condensation steps. Isobutanol (preferred end product) and other β-branched oxygenates were the final products due to steric hindrance and the lack of two α-hydrogens needed for aldol-condensation reactions. Commonly, the reaction of two C₁-intermediates to a C₂-intermediate is viewed as the limiting step in the overall chain growth mechanism.

Although high temperature, high pressure modified methanol synthesis catalysts are particularly stable, optimal operation conditions would involve elevated operation costs and extensive security considerations if applied at an industrial level.

Low pressure, low temperature methanol synthesis catalysts

According to several authors^{41-43, 151}, the following are the most important characteristics of the low pressure, low temperature methanol synthesis catalysts, including Cu/ZnO/Cr₂O₃, Cu/ZnO/Al₂O₃. These operate in a temperature and pressure range between 523 and 573 K and from 2.0 to 10.0 MPa, respectively^{41, 43} and H₂/CO ratio of 0.45:1 - 2.33:1⁴¹, preferably around 1:1⁴². Higher contact time also favors higher alcohols synthesis.⁴¹ Higher pressures are favorable to reduce the hydrocarbon selectivity.⁴³ The main products are methanol and

isobutanol.^{41-43, 151} CO₂ contained in the feed stream inhibits the synthesis of higher alcohols.^{41, 42, 151} These catalysts achieve a high CO conversion, but with poor selectivities and yields towards alcohols.^{41, 43} Temperatures above 573 K are not recommended due to sintering of copper.^{41, 43} Ethanol could be produced via CO hydrogenation or methanol homologation (predominant mechanism¹⁵¹), but both reactions are linked to side reactions (methanation and water-gas shift reaction).⁴¹ An optimum amount of alkali promoter is used to enhance ethanol and higher alcohol selectivity.^{41, 151} The promotion effect of alkali metals is considered to neutralize the acidity of the catalysts and suppress undesired side-reactions. The effect promotion of the alkali on the catalyst followed the sequence Cs > Rb > K > Na > Li.^{42, 151} Control of the metal particle size and shape is desirable, because the ability of the promoter to alter the catalyst depends on the synthesis method and subsequent conditioning.

Doping Cu/ZnO catalysts with Cs increased the methanol yield as a function of the Cs nominal concentration until 1 mol.% Cs, higher concentrations resulted in higher oxygenate selectivity.¹⁵² Cs doping increased the concentration and reactivity of surface hydroxyl groups, promoting the formation of intermediates to the synthesis of methanol and ethanol. An excess of Cs could poison the hydrogenation activity of the catalyst, thereby altering the methanol synthesis ability to a greater extent than the higher oxygenate formation. Nunan et al.¹⁵³ described the mechanism of higher alcohol synthesis over Cs-doped Cu/ZnO catalysts from synthesis gas. Details will be discussed in the following section. Nunan et al.¹⁵⁴ showed successful utilization of Al₂O₃ and Cr₂O₃ as supports for the Cs-doped Cu/ZnO catalysts. The addition of Cr₂O₃ enhanced the alcohol synthesis rate under higher alcohols synthesis conditions while maintaining the selectivity of Cs-Cu/ZnO catalysts. But higher Cs loadings were necessary to balance the acidity of Cr₂O₃.

In early studies on Cu-based catalysts for the synthesis of higher alcohols, Berndt et al.¹⁵⁵ proposed that higher alcohols synthesis was very sensitive to the pore structure of the CuO/ZnO/MeO_x catalysts (Me: Mn or Al). The smaller the pores, the higher the activity towards higher alcohol synthesis. This was attributed to a high coverage of the surface with C₁-intermediates, which facilitated the slow C₁ to C₂ chain growth step. The produced methanol cannot evacuate the pores so easily, allowing the synthesis of higher alcohols. The authors also proposed that the formation of higher alcohols occurred at Cu-sites or at the interface to zinc oxide.

Further investigations on K-doped CuO/ZnO/Al₂O₃ were performed by Boz et al.¹⁵⁶ The authors claimed that lower alkali loading (0.5 wt.%) favored higher alcohol yield, especially isobutanol (> 1.6 %). The addition of an optimum amount of K balanced the amount of Cu⁰ / Cu⁺¹ sites necessary for higher alcohol synthesis. On these catalysts, the methanol reaction was faster than higher alcohol and methane synthesis, but the latter had favorable thermodynamics compared to methanol (favored by higher temperatures). A peak in the aldehyde selectivity with increasing contact time, suggested that aldehydes are intermediates to secondary products, probably by the aldol condensation mechanism. At the beginning of the reaction a significant deactivation of the catalyst took place, reaching stabilization after a period of 10 hours on stream.

Klier et al.¹⁵⁷ proposed that the C₁ intermediate had to be converted to a C₂ oxygenate before the aldol C-C bond formation step to form higher alcohols from lower alcohols could occur. For alkali-promoted copper-based catalysts the path that couples two methanol molecules was preferred over the methanol-CO reaction. This was presented as the limiting reaction step. Alkali-promotion lowers the activation energy of the cis-trans isomerization over larger cations (Cs > Rb > K > Na) favoring the aldol coupling. The authors also confirmed that aldol synthesis does not occur in β-branched aldehydes; consequently isobutanol is a major terminal product.

Hilmen et al.¹⁵⁸ studied the synthesis of higher alcohols on copper catalysts supported on alkali-promoted basic oxides (K-Cu_yMg₅CeO_x and Cs-Cu/ZnO/Al₂O₃). The formation of higher alcohols was favored with higher temperatures and low space velocities. The increase of oxygen coverage of the basic sites on the surface of the catalysts due to the presence of an oxidant (CO₂ or water) inhibited the formation of methanol and higher alcohols. This effect was more pronounced in catalysts with lower Cu content. The more basic sites of Mg₅CeO_x were more efficiently covered by CO₂. This effect could be weakened by the addition of Pd to the catalyst. Even though higher Cu-contents in the catalysts favored the synthesis of isobutanol, they had lower isobutanol selectivity (increase in methyl acetate and hydrocarbon selectivity). The alkali-promoters blocked the acid sites, preventing the synthesis of dimethyl ether and hydrocarbons. Lower alcohols played a role as chain initiators during the higher alcohol synthesis. According to the calculations for the chain growth probabilities, the step from C₁ to ethanol and from iso-C₄ chains to higher alcohols were lower than other steps.

An interesting approach to the present study is the utilization of double bed reactors for the synthesis of higher alcohols. In the first bed short-chain alcohols were produced which, in the

subsequent bed, grew further to branched alcohols. This proved the feasibility to produce higher alcohols from synthesis gas and ethanol (or other polyols) using alkali modified-high temperature methanol catalysts.^{139, 159, 160}

The addition of short-chain alcohols or intermediates to the synthesis gas has been used to analyze the reaction path and mechanism to form higher alcohols.^{153, 157, 161-165} Campos-Martín et al.¹⁶¹ incorporated different alcohols (methanol, ethanol or 1-propanol) in the synthesis gas feed stream to the high pressure hydrogenation of CO to produce higher alcohols over Cu-Zn-Cr oxide catalysts. The feeding of C_nOH , enhanced the $C_{n+1}OH$ yield. The most difficult step being the chain growth from methanol to ethanol. Beretta et al.¹⁶⁴ incorporated selected reaction intermediates over Cs-doped Zn-Cr-oxide catalysts which confirmed a kinetic model assuming aldehydes and ketones as reactive species.¹⁶⁶ Ethanol addition to the synthesis gas strongly promoted the formation of C_{3-5} linear alcohols, 2-methyl alcohols (moderate in the case of isobutanol), 2-butanone, 3-pentanone and 2-methyl-3-pentanone.

Cu based catalysts are attractive for further applications, since they are produced in a similar way to the well-known methanol synthesis catalyst. Particularly, alkali doping seemed to increase the higher alcohols synthesis rates. Nevertheless improvements are still required. Therefore this type of catalysts was chosen for this thesis since they seemed to be attractive for further industrial applications.

1.4.2. Higher alcohol synthesis mechanism over Cu based catalysts

A summary of the several reaction mechanisms for modified methanol synthesis catalysts proposed in the literature has been recently reviewed by Gupta et al.⁴¹ One of the most relevant mechanisms for undoped and Cs-doped CuO/ZnO catalysts which is interesting for our study has been proposed by Nunan et al.^{153, 163} and was later on complemented by other authors¹⁶⁷⁻¹⁷⁰. The carbon chain growth occurred in a stepwise manner. The preferred carbon chain growth path depended on the reaction step taking place. Methanol was produced directly from CO/H₂ similarly to a traditional methanol synthesis. The C₁ to C₂ chain growth was suggested to occur by the coupling of two methanol derivatives (e.g. nucleophilic attack of formyl/formate on formaldehyde) rather than CO insertion. The mechanistic differences between Cs doped and undoped catalysts were more evident for the C₂ to C₃ step, but the synthesis rate in all steps was promoted by Cs. The preferred path in the presence of Cs was described as an aldol-reaction based β -carbon additions of oxygen-containing C₁ intermediates derived from

methanol. For undoped catalysts, the C_2 to C_3 step occurred by linear chain growth and/or aldol-reaction based β -carbon additions. Two different β -additions were identified; aldol coupling with oxygen retention reversal $\beta(R)$ (retention of the alcoxide oxygen), and normal aldol coupling $\beta(N)$ (retention of the keto oxygen), the first one favored for C_2 to C_3 step in the case of Cs doping. The coupling of a C_1 and C_2 intermediate via aldol-like reaction patterns was often faster than the coupling of two C_1 intermediates. The role of Cs was to stabilize the required formyl species by activating the C-H bonds in formaldehyde. Aldehydes, ketones and methyl esters present in the mixture were in equilibrium with their corresponding alcohols.

Smith et al.¹⁶⁹ developed a kinetic model for alcohol synthesis over a Cs-promoted Cu/ZnO catalyst based on Nunan et al. description of the reaction mechanism¹⁵³. An agreement between the calculated and experimental product distribution was observed for several experimental conditions. The most important C-C bond forming reactions of the model were linear growth by addition of an oxygenated C_1 intermediate to an alcohol chain (linear alcohols) and β -addition aldol condensation type mechanism between an oxygenated C_1 intermediate and an aldehydic C_n intermediate (2-methyl-branched primary alcohols). It was predicted that β -addition dominated over linear growth. β -addition was more effective at C_2 than at C_n ($n \geq 3$). At temperatures higher than 573 K linear growth alcohol-forming reactions have higher rates than ester-forming reactions. Nevertheless, the model was still based on assumptions and simplifications, the most important being: (i) differential reactor regime and (ii) irreversibility of the growth and termination steps.

Xu and Iglesia¹⁷⁰ studied the carbon-carbon bond formation pathways for two different types of catalysts, K-Cu_{0.5}Mg₅CeO_x and Cs-Cu/ZnO/Al₂O₃. For each catalyst a different reaction pathway was identified. In the case of K-Cu_{0.5}Mg₅CeO_x ethanol was formed predominantly from CO. In the case of Cs-Cu/ZnO/Al₂O₃, ethanol was produced via a coupling reaction of two methanol molecules, resembling the reaction pathway of Cs-promoted/Cu/ZnO catalysts. The occurrence of another reaction pathway was attributed to the effect of Cs-promotion. Two possibilities were discussed, either it could be the different effect on the acidity of the catalyst (K and Cs) or the higher density of Cu sites on the Cs-promoted catalyst, which led to a higher local concentration of formaldehyde (required for the ethanol synthesis). The coupling pathway exhibited a higher overall synthesis rate of ethanol. On both catalysts, the formation of 1-propanol and isobutanol proceeded via a sequential C_1 -addition (resembling an aldol condensation reaction).

Considering all aspects mentioned during the introductory section, during the course of this thesis the synthesis of higher alcohols over unsupported and supported modified CuO/ZnO is described. Different parameters were first screened using batch reactors. In parallel, a continuous setup was built to test selected catalysts and screen reaction parameters which would favor the synthesis of higher alcohols.

1.5. Motivation

Worldwide interest in decreasing consumption and dependency on fossil fuels is important for a variety of environmental and economic reasons. Renewable sources such as biomass are an important source of fuels and chemicals since they ensure a CO₂ neutral cycle. As mentioned above, several biomass processing routes have been developed over past years. Thermochemical processing of biomass, specifically gasification, leads to synthesis gas. Synthesis gas serves as a starting material for several products, including methanol or higher alcohols.

Alcohols from renewable sources are expected to contribute towards reducing energy dependency on fossil fuels in the near future and to be used as chemical storage for excess electrical energy generated from solar and wind. Even though all questions regarding methanol synthesis have not yet been solved, it is a developed process at laboratory and industrial scale. On the other hand, higher alcohols synthesis is a topic still under development. Several homogeneous and heterogeneous catalytic systems have been studied over the years. Among the heterogeneous catalysts, significant attention has been paid to modified Fischer-Tropsch catalysts, Mo based catalysts and modified methanol synthesis catalysts. Unfortunately, so far the yields and selectivities towards higher alcohols using synthesis gas as a reactant have not been promising enough to develop an industrialized process. Further improvements are therefore required. As shown by Medford et al.⁴⁸ by theoretical calculations, only a small region on the selectivity map exists where methane formation is not the dominant reaction and C-O bond cleavage occurs selectively enough to enable the formation of surface species which lead to higher alcohols. As derived from this modelling approach no pure metal lies in this region, therefore either alloyed particles or dopants are required. Even though several authors mentioned previously approach the higher alcohols synthesis by alloying different transition metals or adding dopants, for the purpose of this thesis attention is focused on modified methanol synthesis catalysts. For this type of catalysts, the slowest reaction step is known to

be the C₁ to C₂ chain growth.^{155, 157} Moreover, it is well known that the preparation method of the catalysts has a major influence on their catalytic performance, therefore it is of critical importance for the process.

The main goals of this thesis are overcoming the slowest reaction step by adding the C₂ alcohol ethanol as a reactant, developing an apparatus and methodology to test catalysts in the higher alcohols synthesis from synthesis gas and ethanol using a continuous reactor and, identifying active and selective catalysts for this reaction and suitable process conditions which would enable application at a larger scale. In order to achieve these goals, the following topics are addressed in this thesis:

CuO/ZnO	preparation of traditional methanol synthesis catalyst
	<ul style="list-style-type: none">• Cs or Ru doping to tune higher alcohol synthesis
Batch reactions	unsupported catalysts
	<ul style="list-style-type: none">• dopant• dopant concentration• ethanol to CO ratio
Batch reactions	supported catalysts
	<ul style="list-style-type: none">• support• CuO/ZnO loading on support• preparation method• reaction parameters
Continuous reaction	supported catalysts
	<ul style="list-style-type: none">• design and construction of continuous-flow reactor• test continuous-flow reactor with well known reaction. Case study: methanol synthesis• higher alcohol synthesis in continuous-flow reactor. Identification of reaction parameters

Herein, the synthesis of traditional methanol synthesis catalysts (CuO/ZnO) promoted with Ru or Cs has been investigated. After modification the catalysts are screened for the ability to tune the methanol synthesis towards higher alcohol synthesis using a batch reactor. Different preparation methods (precipitation, wet impregnation and flame spray pyrolysis) and supports (Al₂O₃, SiO₂ and active carbon) are compared to find the most suitable catalyst to be further tested in a continuous reactor. Cs is selected as it is the most effective alkali promoter for the higher alcohol synthesis^{157, 171} and Ru is chosen as it is a well-known element for Fischer-Tropsch synthesis³⁴.

Depending on the doping of the catalyst different reactions mechanisms occur on the surface, therefore the product distribution changes as a function of the dopant. In the corresponding sections the specific reaction mechanism are described in detail. Additionally, the effect of ethanol in the homologation reaction and also the potential redirection towards ethanol coupling are investigated by changing the ethanol to synthesis gas ratio. Potential changes in the reaction mechanism as a consequence of the presence of ethanol are evaluated, which could also be interesting for the synthesis of higher alcohols starting from synthesis gas. The design and construction steps of a continuous-flow reactor are presented. Optimization of the reactor packing and the catalyst particle size is performed to avoid heat and mass transfer limitations. The well-known synthesis of methanol from a CO/H₂/CO₂ mixture is in this case used as a proof of concept of the reactor and as an example study allowing also the evaluation of the reactor performance. Finally, in order to elucidate structure-activity relationships and to understand the stability of the catalysts, they are characterized with both *ex situ* and *in situ* techniques.

In summary, this work is concerned with the development of apparatus and methodology for higher alcohol synthesis under batch and continuous flow conditions. Several parameters are screened with the aim of moving towards an industrially relevant and renewable process in future.

2. Materials and methods

2.1. Catalyst preparation

For this study, Cu based catalysts were prepared by both increasing and constant pH precipitation, wet impregnation and flame spray pyrolysis (inc_pH, const_pH, wi and fsp in the following). First, a standard CuO/ZnO catalyst was prepared by increasing pH precipitation (inc_pH) and doped with different promoters to study their influence on the selectivity and yield towards higher alcohols in a batch reactor. Since Cs turned out to be the most effective promoter in agreement to literature presented in the introduction (section 1.4.1.3), it was chosen to perform all further tests. Al₂O₃, SiO₂ and activated carbon were tested as supports for the Cs doped CuO/ZnO catalyst also in a batch reactor. Additionally, the CuO/ZnO loading on the support and the preparation method were varied. 10, 20 and 30 wt.% CuO/ZnO contents were compared.

A summary of the weighted amounts of precursors and supports is shown in Table 2.

Table 2: Calculated precursor mass for catalysts synthesis.

Catalyst	Calculated mass of precursor [g]		
	[Cu(NO ₃) ₂]·3H ₂ O	[Zn(NO ₃) ₂]·6H ₂ O	Al ₂ O ₃ / SiO ₂ / AC
CuO/ZnO [inc_pH]	28.6	82.2	-
CuO/ZnO/Al ₂ O ₃ [10 wt.%; wi]	0.7	2.1	6.8
CuO/ZnO/Al ₂ O ₃ [20 wt.%; wi]	1.4	4.1	6.0
CuO/ZnO/support [30 wt.%; wi]	4.3	12.3	10.5
CuO/ZnO/support [30 wt.%; inc_pH]	2.2	6.2	5.3
CuO/ZnO/support [30 wt.%; const_pH]	1.4	4.1	3.5

inc_pH: increasing pH precipitation; wi: wet impregnation; const_pH: constant pH precipitation.

2.1.1. Precipitation

Standard unsupported CuO/ZnO catalysts (30:70 mol.% Cu : ZnO) were prepared by increasing pH precipitation (inc_pH). The precipitation was performed at 343 K and an ageing period of

1 h in the mother solution without controlling the pH in a similar way as presented by Nunan et al.¹⁵³ and Herman et al.¹⁷² A 1 M solution was prepared using 28.6 g of $[\text{Cu}(\text{NO}_3)_2] \cdot 3\text{H}_2\text{O}$ (Honeywell, purum p.a., 98 - 103 % (RT)) and 82.6 g of $[\text{Zn}(\text{NO}_3)_2] \cdot 6\text{H}_2\text{O}$ (Honeywell, purum p.a., crystallized, ≥ 99 %, (KT)) as precursor and 380 ml distilled water. The solution was agitated for 1 h before titration to ensure sufficient mixing and dilution of the salts. A 1 M aqueous solution of 106 g of Na_2CO_3 (Roth, ≥ 99.5 % p.a. ACS, water free) and 1000 ml of distilled water was used to titrate the precursor solution up to a pH value of 7.5. The Na_2CO_3 solution was added dropwise. The precipitate was filtrated right after the ageing period, washed with 1500 ml distilled water and dried over night at 353 K. The precursor was calcined at 623 K for 5 h to form the standard CuO/ZnO catalyst.

Before the catalysts were supported on Al_2O_3 (Alfa Aesar, catalysts support - high surface area, 1/8" pellets), SiO_2 (Alfa Aesar, catalysts support - high surface area, 1/8" pellets) or activated carbon (Fluka Analytical, activated charcoal Norit ROX 0.8, rods 0.8 mm diameter), the support pellets were crushed and sieved between 250 μm and 500 μm . The titration followed in an analogous way as for the standard catalyst with the distinction that the different supports were additionally placed in the solution of precursors and the titration was ended when the solution reached a pH of 7. The amount of Cu and Zn precursors in the solution was varied to achieve a final content of 10, 20 and 30 wt.% of CuO/ZnO on the support. The supported catalysts were calcined in the same way as the unsupported ones. The activated carbon catalysts were calcined under a N_2 atmosphere using analogous conditions as for the other catalysts.

Al_2O_3 supported catalysts (30 wt.% of CuO/ZnO) were additionally synthesized by constant pH precipitation (const_pH) at 338 K. The metal precursor solution was prepared in the same way as for the supported catalysts. A 1 M solution of Na_2CO_3 was also used for titrating the solution. The pH was kept in a range between 6.0 and 6.5 during the complete titration. The metal precursors and the Na_2CO_3 solutions were dosed simultaneously in a flask which contained 400 ml distilled water and 3.5 g of Al_2O_3 . After the titration, the ageing, washing, drying and calcination of the catalysts followed as described previously.

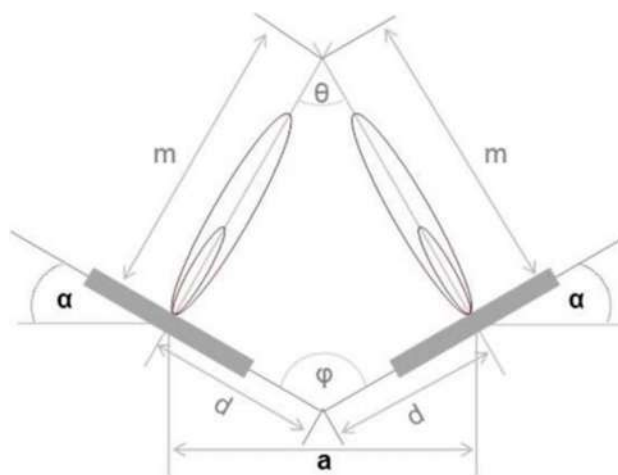
2.1.2. Wet impregnation

Al_2O_3 , SiO_2 or activated carbon supported CuO/ZnO catalysts were also prepared by wet impregnation (wi). A solution of 4.3 g $[\text{Cu}(\text{NO}_3)_2] \cdot 3\text{H}_2\text{O}$ and 12.3 g $[\text{Zn}(\text{NO}_3)_2] \cdot 6\text{H}_2\text{O}$ in 60 ml distilled water was prepared. The desired amount of support was added. For the 30 wt.%

CuO/ZnO, catalyst 10.5 g were required. The solution was heated to 313 K and stirred at 150 rpm for 1 h. The water was evacuated under low vacuum at these conditions. As for the precipitated ones, the catalysts were dried over night at 353 K and then calcined at 623 K for 5 h.

2.1.3. Flame spray pyrolysis

As an alternative preparation method flame spray pyrolysis (fsp) was used.¹⁷³ The flame spray pyrolysis was performed using a two nozzle set up^{174, 175} a recent extension of the one nozzle set up previously used at ITCP^{176, 177}. Two precursor solutions were prepared. The first solution contained 0.774 g copper (II)-acetylacetonate (Fluka Chemika, > 97 %) and 1.515 g zinc acetate dehydrate (Fluka Chemika, > 99.0 %) dissolved in a mixture of 100 ml methanol (VWR Chemicals, HiPerSolv CHROMANORM, for HPLC - Gradient grade) and acetic acid (Merck, for synthesis, 99 -100 %) (70/30; v/v) giving a total metal concentration of 0.09 M. For the second solution, 12.877 g of aluminium nitrate nonahydrate (Merck, EMSURE for analysis) were dissolved in 100 ml methanol and acetic acid (50/50; v/v) giving a concentration of 0.34 M. Each precursor solution was filled in 50 ml syringes and placed in a syringe pump (World Precision Instruments). The two solutions were simultaneously fed to the two FSP nozzles at 5 ml/min, consequently they were released through a steel capillary of 0.413 mm diameter (Hamilton syringes, KF6, gauge 22) and dispersed with 5 NI/min oxygen gas flow at 0.3 MPa back pressure. The dispersed solutions were ignited by a supporting flame of 0.75 NI/min methane gas and 1.6 NI/min oxygen gas flow. The nozzle distance d in Scheme 2 was adjusted to 7 cm and the angle θ was set to 120°.



Scheme 2: Two nozzle flame spray pyrolysis set up.

The product particles were collected on a glass fiber filter (Whatman GF6, GE) in a cylindrical filter holder 80 cm over the flame connected with a vacuum pump (R5, Busch). Finally, the solid powder was collected by scratching it off the filter with a spatula and sieving it with a particle sieve with a mesh size of 600 μm .

2.1.4. Catalyst doping

After the preparation of the undoped catalysts, they were doped with either Cs (0.3 - 3.0 mol.%) or Ru (0.5 and 1.0 mol.%) by a subsequent wet impregnation. The standard CuO/ZnO catalyst (7 g) together with the corresponding Cs (0.0469 - 0.4764 g HCOOCs (Sigma Aldrich, 98%)) or Ru (0.1149 and 0.2354 g $\text{RuCl}_3 \cdot x\text{H}_2\text{O}$ (Alfa Aesar, 99.9 % (PGM basis), Ru 38 % min)) precursor were diluted in 100 ml of ethanol or 140 ml of water, respectively. The doped catalysts were dried and calcined for a second time at the same conditions as previously.

The doping with Cs of the supported catalysts was performed in the same way as for the undoped catalysts. The amount of Cs precursor was adapted to result in a 1 mol.% Cs doping relative to the content of CuO/ZnO on the catalyst support.

2.2. Catalyst characterization

Characterization of catalysts before, during and after reaction is an important field in catalysis since it allows understanding and correlating the changes in the catalyst system due to exposure to the reaction environment and investigating the nature of an active catalyst.

The analytical methods used herein to characterize catalysts both *in situ* and *ex situ* are presented below. *Ex situ* characterization involves measuring the state of the catalyst before and after the reaction, whereas *in situ* characterization measures either the catalyst during its transformation in a special chemical environment (e.g. during temperature programmed reduction, TPR) or the catalytic activity and catalyst itself during the reaction (*in operando*, not the focus in this work).

First the method is described briefly and afterwards a detailed explanation on how each method was applied to the specific system is given.

2.2.1. Elemental analysis

Elemental analysis is a tool that enables either qualitative or quantitative determination of the elemental or isotopic composition of a particular material. In this case it allows verification of the catalyst composition and evaluation of the effectiveness of the preparation method.

For elemental analysis the catalysts were dissolved in 5 ml of concentrated HNO₃, 1 ml of concentrated HCl and 0.5 ml of H₂O₂ using a microwave reactor (Anton Paar, 600 W, 45 min) at a maximum temperature of 513 K and a maximum pressure of 6.0 MPa. The composition of the catalysts in the as-prepared state and after reaction was probed by Inductively Coupled Plasma - Optical Emission Spectroscopy (ICP-OES) with an Agilent 725-ES instrument. Argon was used as carrier and plasma gas. The plasma was created by a 40 MHz high-frequency generator. The Cs and Ru content in the catalysts were determined by Atomic Absorption Spectroscopy (AAS) using a VARIAN Zeeman SpectrAA 800.

2.2.2. X-Ray Diffraction (XRD)

XRD is commonly used in catalysis to identify crystalline phases within a solid material and to give an estimation of the crystallite size. The sample is irradiated with X-rays, resulting in elastic scattering of the incoming X-ray photons by periodically spaced lattices of atoms. The scattered X-rays are detected in order to construct X-ray patterns of a particular sample. Using the Bragg equation, X-rays diffracted constructively by crystal planes allow the calculation of lattice spacings which are characteristic of specific crystal structures or phases. One of the limitations of XRD is the incapability of detecting either amorphous or too small particles which are common in catalytic systems.

The calcined, reduced and used catalysts were analyzed by powder XRD on rotating sample holders with a PANalytical X'pert PRO Diffractometer with Cu K_α radiation (Ni filter, 40 mA, 45 kV). The XRDs were recorded from 20 to 80° for 30 min (step size: 0.0170°, scan step time: 0.51s). The Scherrer equation¹⁷⁸ (Eq. 22) was used to estimate the crystallite size of Cu, CuO and ZnO from selected XRD reflections. LaB₆ was used as standard to correct the instrumental line broadening. The Cambridge Structural Database (CSD) from the Cambridge Crystallographic Data Centre was used for analysis and reflection fitting of the diffractograms.¹⁷⁹

$$d = \frac{K \cdot \lambda}{\beta \cdot \cos \theta} \quad (\text{Eq. 22})$$

K: crystallite shape factor ($K = 0.9$), λ : wavelength of the X-rays ($\lambda = 1.540598 \text{ \AA}$), β : full width at half maximum of the X-ray reflection in radians and θ : Bragg angle.

2.2.3. N_2 physisorption

N_2 physisorption experiments allow the determination of the specific surface area and pore volume of a catalyst by evaluating the adsorption isotherms with, for example, the Brunauer-Emmet-Teller model (BET). The surface area determined by the BET model includes external and accessible internal pore surface. For this thesis it was used to identify structural changes in the catalysts before and after treatment. It also enabled the determination of the porosity of the sample according to the shape of the adsorption isotherm.

The specific surface area of the calcined and used catalysts was obtained by N_2 physisorption at 77 K (Belsorp mini II, Bell, Japan. Inc.). The catalysts were evacuated at 573 K under vacuum for 2 h. The specific surface area was determined using the multipoint BET theory in the $p/p_0 = 0.05$ - 0.3 range. The shape of the adsorption-desorption curve indicated a Type-II isotherm.

2.2.4. Transmission Electron Microscopy (TEM)

TEM is an imaging technique which enables the determination of size and shape of a material. The material is irradiated with a high energy and high intensity electron beam which passes through several lenses to be focused. A two-dimensional projection of the sample is obtained from the transmitted electrons, which contrast is dependent of the density and thickness of the sample. In consequence, information regarding the morphology, crystallography and chemical composition of a material is obtained. Particularly in catalysis, TEM is used for obtaining particle size distribution. TEM can be also coupled with energy dispersive X-ray spectroscopy (EDX) to determine elemental composition of a sample. One disadvantage of TEM is that it can only measure relatively thin or less dense samples due to high attenuation of electrons during transmission.

TEM images were measured in an FEI Titan 80 - 300, 300kV. An Au grid with a carbon film was used to mount the samples. Elemental distribution was indicated by EDX. The particle size

distribution was acquired from the STEM images and the lattices spacing were obtained from HRTEM images.

2.2.5. Temperature Programmed Reduction (H₂-TPR)

H₂-TPR gives information on the reduction behavior of a sample. For catalysis this technique allows the identification of the temperature necessary to achieve the complete reduction of the catalyst.

To select an appropriate reduction temperature and to study the reduction behavior, temperature programmed reduction in hydrogen (H₂-TPR) experiments were performed in a Micromeritics AutoChem HP 2950. The catalysts (~100 mg) were reduced in a 10 % H₂/Ar stream (~30 ml/min, standard temperature and pressure, STP) with a heating rate of 5 K/min from room temperature until 873 K. A pretreatment was performed to eliminate adsorbed water by heating up until 423 K at 5 K/min under inert atmosphere. To determine the reduced amount of the metals on the catalysts, it was assumed that only CuO and RuO₂ can be reduced. The effect of a second calcination on the reduction behavior was independently studied for the standard CuO/ZnO catalyst.

2.2.6. Thermogravimetric Analysis (TGA)

TGA gives information on changes in the physical or chemical properties of materials as a function of increasing temperature or as a function of time. It is normally used to determine characteristics of materials which involve mass losses or gains, such as decomposition, oxidation or loss of volatiles.

The analysis was performed using a Mettler Toledo TGA/STDA 851 to study the potential carbon depositions on the catalysts surface. It was conducted at a heating rate of 10 K/min from room temperature to 1173 K under pure O₂ (60 ml/min, STP).

2.2.7. Attenuated Total Reflectance – Infrared Spectroscopy (ATR-IR)

The ATR-IR technique allows solids or liquids to be examined directly by infrared spectroscopy without further preparation. With this method it is possible to identify species adsorbed on the catalyst surface and the structure of the surface. This method is particularly interesting in catalysis since it allows the *in situ* analysis of samples.

The FT-IR spectra were obtained using a Varian 660-IR FT-IR spectrometer equipped with an Attenuated Total Reflection (ATR)-IR element (diamond) operating with a resolution of 2 cm^{-1} and 8 scans ($230 - 4000\text{ cm}^{-1}$). This technique was also used to identify potential carbon depositions on the catalyst surface.

2.2.8. X-Ray Absorption Spectroscopy (XAS)

XAS involves the absorption of X-rays by a sample and the excitation/ejection of a core electron which is then backscattered by the neighboring atoms. XAS is typically divided between X-ray Absorption Near Edge Spectroscopy (XANES) and Extended X-ray Absorption Fine Structure (EXAFS). XANES involves the interaction of an ejected electron with low kinetic energy and valence electrons. EXAFS reflects the backscattering of neighboring atoms and the interference with the outgoing electron. Both parts of the spectrum give different information about the absorbing atom and its surroundings that is very interesting in catalysis, such as the structure of active phases, lattice distances, coordination number and oxidation state of the catalyst. As the electronic structure of each element is unique, XAS is an elementally specific technique. Due to the high penetration of X-rays through matter, a wide range of sample types can be studied, including solids, liquids and gases. This makes XAS a powerful and versatile technique in catalysis.

Two different experiments using XAS were performed to identify (i) the effect of Cs doping on the reduction of the Cu/ZnO and CuO/ZnO/Al₂O₃ catalysts and (ii) the influence of different gas atmospheres in the oxidation state of a 1 mol.% Cs-CuO/ZnO/Al₂O₃.

The calcined catalysts were tested in a 1.0 mm quartz capillary at 0.1 MPa (wall thickness = 0.02 mm). The catalysts were diluted in Al₂O₃ and sieved between 100 and 200 μm . The catalyst bed was fixed in the capillary with quartz wool. The gas dosing system allowed mixing of different gases; typically a flow of 50 ml/min was used. Water and ethanol were delivered with the whole gas mixture flow through a saturator at ambient temperature. The product stream was connected to a mass spectrometer for analysis (Pfeiffer Vacuum – ThermoStar GSD 320 T1 with yttrium iridium filament, 2-m capillary). The XAS data were obtained in transmission mode for the Cu-K (8.9879 keV) edge.

The influence of Cs doping on the unsupported catalysts (diluted in Al₂O₃ in a ratio of 1:3) was determined by temperature programmed reduction (TPR). The catalysts were reduced at 5 K/min from room temperature to 673 K under 5 % H₂/He. EXAFS was measured at the initial

state (room temperature, calcined catalyst), at the end of the TPR (673 K, reduced catalyst) and final state (room temperature, reduced catalyst). During the TPR XANES spectra were recorded. The measurements were done at ANKA synchrotron facility.

For the second type of experiments a calcined 1 mol.% Cs-CuO/ZnO/Al₂O₃ catalyst (diluted in Al₂O₃ in a ratio of 1:2) was tested as shown in Figure 7 at ANKA. First a TPR was performed at the same conditions as presented before. The set up was heated again to 593 K (same temperature as in the batch reactor tests) and the surrounding gas atmosphere was change to the following conditions:

- CO/H₂: synthesis gas in a ratio 2 % CO and 2 % H₂ in He
- CO/H₂/EtOH: synthesis gas with ethanol
- CO/H₂/CO₂: synthesis gas with 0.5 % CO₂ (pure CO₂)
- CO/H₂/CO₂/H₂O: synthesis gas, CO₂ and water.

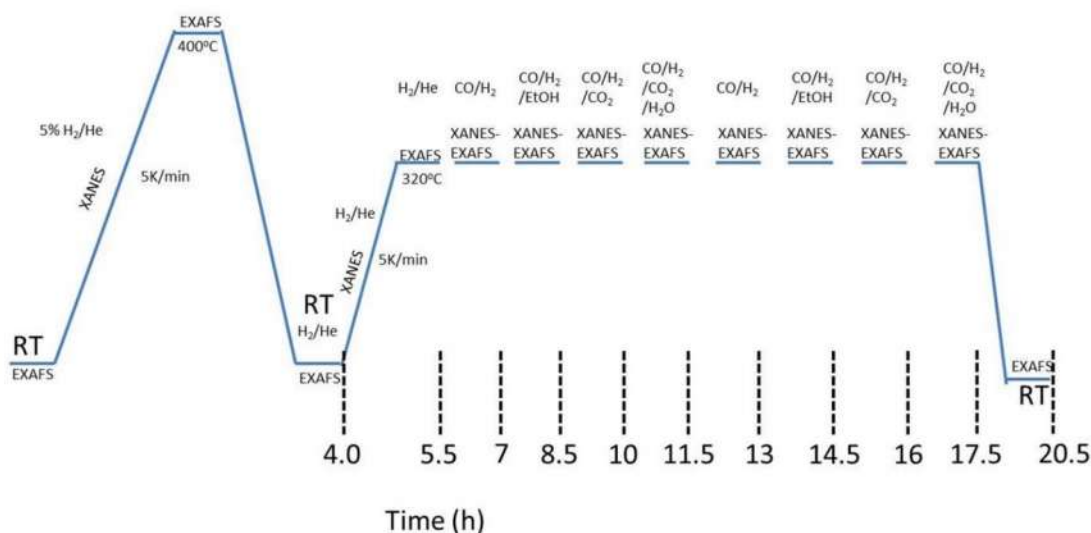


Figure 7: XAS experimental procedure for the 1 mol.% Cs- CuO/ZnO/Al₂O₃ catalyst.

The gases fed to the reactor to achieve the previous conditions corresponded to 5 % H₂/He, 4.5 % CO/He and pure He. After the first cycle, the catalyst was regenerated in synthesis gas and a second cycle following the same combinations was performed. Finally, the capillary was cooled to room temperature. XANES and EXAFS were recorded as shown in Figure 7. Cu, CuO, Cu₂O, CuCO₃·Cu(OH)₂, Cu(OH)₂, C₄H₆CuO₄ and a precursor pellet were measured as references for the linear combination analysis.

2.3. Catalytic tests

The prepared catalysts were tested in both batch and continuous-flow reactors in the synthesis of methanol and higher alcohols. In the following sections the experimental procedure followed during the tests is described in detail. In general, batch reactions were performed to screen the catalysts and to choose the most adequate catalyst to be further tested in the continuous-flow reactor which was built up new within this thesis. Continuous-flow experiments were performed to screen and optimize reaction parameters on selected catalysts.

2.3.1. Batch reactor

Higher alcohol synthesis was performed in a 100 ml batch reactor (Parr Instruments Co.) for the unsupported catalysts and in a 200 ml batch reactor (newly constructed in this thesis) for the supported ones.

The 100 ml reactor was heated with an oven and cooled down with an ice/water bath. The agitation of the reaction medium was performed with a traditional impeller at 1700 rpm. The 200 ml batch reactor was heated with a sand bath and cooled also with an ice/water bath. To ensure better mass transfer between the liquid and gas phases, the autoclave was equipped with a gas entrainment impeller, which allowed better mixing of the phases. The reactor material was Inconel. The pressure and temperature data was monitored and stored online (data acquisition: Agilent 34972A LXI Data Acquisition/Switch Unit and data processing: Agilent Benchlink Data Logger 3) during the complete reaction. In both reactors a thermocouple inside the reactor was used to control the temperature. In the case of the 100 ml reactor the temperature was controlled with a Parr 4848 reactor controller, whereas for the 200 ml reactor the temperature was controlled by regulating the sand bath temperature with a ECO24 (PMA) controller. A pressure sensor was used to monitor the pressure as the reaction proceeded. Both reactors allowed a maximum temperature and pressure of 773 K and 35.0 MPa, respectively.

Standard reaction conditions included a reaction time of 3 h, a temperature of 593 K, CO to H₂ ratio of 1:1, an initial synthesis gas pressure of 5.0 MPa, 1 g of catalyst and 30 g of liquid phase (cyclohexane, ethanol or mixtures of both). The liquid phase was cyclohexane (ethanol free reaction mixture), ethanol ($n_{\text{EtOH}} : n_{\text{CO}} = 10.0:1$) or a cyclohexane/ethanol mixture ($n_{\text{EtOH}} : n_{\text{CO}} = 0.5:1$ and $0.9:1$). Cyclohexane was used as a solvent to allow the study of the influence of ethanol in the higher alcohol synthesis. The amount of ethanol in liquid phase was selected in

order to vary the ethanol to CO ratio between $0.5:1 \pm 0.05$ and $0.9:1 \pm 0.05$. Note that experiments were conducted with both pre-reduced and calcined catalysts. To ensure the reproducibility of the experiments, the catalysts were used in an oxidized state due to the instability of the reduced catalyst on exposure to air. In the supporting information more details regarding the carbon balance, CO and ethanol conversions, product selectivities and yields for the reproducibility tests are found (Table S 18, Table S 19 and Figure S 2). The catalysts were reduced during the reaction. Additionally the standard catalyst was tested under inert atmosphere (Ar) using only ethanol as a reaction medium. For comparison, a commercial catalyst doped by wet impregnation with 1.0 mol.% Cs was additionally tested.

To circumvent potential internal and external mass transfer limitations a fine catalyst powder was used (sieve fraction $< 250 \mu\text{m}$) and the agitation speed was set at the maximum possible.¹⁸⁰

The residual activity of the 100 ml reactor was evaluated for the $n_{\text{EtOH}} : n_{\text{CO}} = 10.0$ conditions which was rather low (Table S 17).

Total conversion (X), CO conversion (X_{CO}), ethanol conversion (X_{EtOH}), selectivities (S_i) and the yields (Y_i) were calculated according to the equations Eq. 23 to Eq. 27 using data obtained from gas chromatography analysis as described in section 2.4. The values are expressed in terms of the number of carbons of each calibrated component ($v_{C,i}$) and are noted as %-C. n_i is assigned to the number of moles of each component. No distinction was made between the ethanol and CO produced during the reaction, and that which was initially fed to the reactor. The yields and selectivities for the batch reactor experiments were calculated from the gas chromatography with flame ionization detector (GC-FID) analysis for the calibrated products, excluding the products only identified by gas chromatography coupled to a mass spectrometer (GC-MS). The total mass balance (Eq. 28) was determined in terms of the mass of liquid (m_{liquid}), gas (m_{gas}) and catalyst (m_{cat}) before and after the reaction at room temperature. The catalyst mass was included to avoid the mass losses related to a separation step between the liquid and the catalyst after the reaction. The gas mass was calculated considering the gas composition, the pressure inside the reactor and assuming that the volume of gas phase was the same before and after the experiment. For the calculations an ideal gas was considered. The C-balances (Eq. 29) were calculated based on the ratio between the initial C-moles from ethanol and CO and the calibrated products after the reaction.

$$X = \frac{(\mathbf{v}_{C,EtOH} \cdot \mathbf{n}_{EtOH} + \mathbf{n}_{CO})_{initial} - (\mathbf{v}_{C,EtOH} \cdot \mathbf{n}_{EtOH} + \mathbf{n}_{CO})_{final}}{(\mathbf{v}_{C,EtOH} \cdot \mathbf{n}_{EtOH} + \mathbf{n}_{CO})_{initial}} \cdot 100 \quad (\text{Eq. 23})$$

$$X_{CO} = \left(1 - \frac{\mathbf{n}_{CO_{final}}}{\mathbf{n}_{CO_{initial}}}\right) \cdot 100 \quad (\text{Eq. 24})$$

$$X_{EtOH} = \left(1 - \frac{(\mathbf{v}_{C,EtOH} \cdot \mathbf{n}_{EtOH})_{final}}{(\mathbf{v}_{C,EtOH} \cdot \mathbf{n}_{EtOH})_{initial}}\right) \cdot 100 \quad (\text{Eq. 25})$$

$$Y_i = \left(\frac{\mathbf{v}_{C,i} \cdot \mathbf{n}_i}{(\mathbf{v}_{C,EtOH} \cdot \mathbf{n}_{EtOH} + \mathbf{n}_{CO})_{initial}}\right) \cdot 100 \quad (\text{Eq. 26})$$

$$S_i = \left(\frac{\mathbf{v}_{C,i} \cdot \mathbf{n}_i}{(\mathbf{v}_{C,EtOH} \cdot \mathbf{n}_{EtOH} + \mathbf{n}_{CO})_{initial} - (\mathbf{v}_{C,EtOH} \cdot \mathbf{n}_{EtOH} + \mathbf{n}_{CO})_{final}}\right) \cdot 100 \quad (\text{Eq. 27})$$

$$\text{total mass balance} = \left(\frac{(\mathbf{m}_{liquid} + \mathbf{m}_{gas} + \mathbf{m}_{cat})_{final}}{(\mathbf{m}_{liquid} + \mathbf{m}_{gas} + \mathbf{m}_{cat})_{initial}}\right) \cdot 100 \quad (\text{Eq. 28})$$

$$C - \text{balance} = \left(\frac{\mathbf{v}_{C,i} \cdot \mathbf{n}_i + (\mathbf{v}_{C,EtOH} \cdot \mathbf{n}_{EtOH} + \mathbf{n}_{CO})_{final}}{(\mathbf{v}_{C,EtOH} \cdot \mathbf{n}_{EtOH} + \mathbf{n}_{CO})_{initial}}\right) \cdot 100 \quad (\text{Eq. 29})$$

2.3.2. Continuous-flow reactor

For further testing of the catalysts and reaction parameters the most active catalyst was selected and was tested in a continuous-flow reactor with downward flow. A trickle-bed reactor was chosen to test the catalyst. This section presents a typical reaction procedure. Basic considerations during the design of a trickle-bed reactor in general and the design and construction details of the reactor used during this thesis are presented in chapter 5.

In a typical reaction, the catalyst was packed as described in chapter 5, sections 5.2 and 5.3. The cooling system was set at 258 K. Firstly the reactor was flushed with pure N₂. The catalyst was then reduced with a 10 % H₂/N₂ stream (500 ml/min) at atmospheric pressure while heating to 673 K at 10 K/min. The temperature was maintained at 673 K for 1 h. After reduction, the catalyst was cooled back to 473 K with the same reductant gas. The gas was switched to bypass and the synthesis gas mixture was adjusted to the desired values. The volumetric flows were

verified using a Drycal. The composition of the gas was measured also flowing through bypass with the micro GC. The flow was redirected to the reactor and the pressure was slowly increased to reaction pressure (usually 8.0 MPa). After the pressure was reached, the temperature was set to the desired value also heating at a rate of 10 K/min. Once the temperature was stable, the dosage of ethanol was started. The gas phase was measured online, whereas the liquid products were collected for 60 min before completely emptying the phase separator. The collected liquid was weighted and its volume was determined for quantification of this phase. An average of the gas phase composition during the time in which the liquid was collected was used for calculation of the carbon balance and conversion.

The CO and ethanol conversion, yields, selectivities and carbon balance were calculated in a similar way as for the batch reactor tests Eq. 24 - Eq. 27 and Eq. 29 with the difference that an average of all sampling points was taken and instead of the molar quantities the molar flows were considered. In the case of the mass balance (Eq. 28), only the mass flow of the liquid and gas were considered for the calculation.

2.4. Product analysis

Products from both batch and continuous-flow reactor setups were analyzed by gas chromatography (GC). In general, GC is used for quantifying the composition of mixtures of gases or liquids. Liquid samples need to be vaporized before analysis. Regardless if a liquid or a gaseous sample is handled, the sample is carried with an inert gas (mobile phase) through a heated column (stationary phase) which selectively separates the components according to particular chemical properties (polarity, chirality, volatility among others). The column is selected and tailored to the specific application. Several types of detectors may be located after the column to identify the different constituents of the sample. For this thesis the analysis was performed with a Flame Ionization Detector (FID), Mass Spectrometer (MS) and Thermal Conductivity Detector (TCD). In an FID the analytes are introduced to a high temperature hydrogen/air flame which decomposes the sample releasing ions and electrons which generate a current monitored by the detector. A MS ionizes and fragments the sample according to their mass to charge ratio. The detector registers the charge induced by the ions. A TCD compares thermal conductivity of the product stream with that of an inert reference gas. The detector consists of two conducting filaments.

2.4.1. Gas phase analysis

The gas phase was analyzed with a Thermo Scientific C2V-200 2-channel micro gas chromatograph (μ -GC) equipped with a thermal conductivity detector. The first channel corresponded to a Divinylbenzene type QS column (QS-BND) at 353 K. It was used to separate CO₂ and C₂₋₄ hydrocarbons. The second channel was a Molecular sieve column (MS5A) at 373 K for the batch reactions and 353 K for the continuous reactor, which allowed analyzing H₂, CO, N₂ and CH₄. The carrier gas was Helium. The micro GC was calibrated using 9 different gas standards.

2.4.2. Liquid phase analysis

The liquid phase was analyzed with a gas chromatograph (GC-2010 Plus) equipped with a flame ionization detector (FID-GC, Shimadzu). The gas chromatograph was equipped with a polar Restek column (Rxi®-624Sil MS). Additionally, the liquid phase was analyzed with a gas chromatograph coupled with a mass spectrometer (GC-MS, QP2010, Shimadzu) equipped with a Restek column (Rxi®-5Sil MS for experiments in the batch reactor and Rxi®-624Sil MS for experiments in the continuous-flow reactor). The following compounds were calibrated for quantification: methanol, ethanol, diethyl ether, 2-propanol, 1-propanol, butanal, ethyl acetate, 2-butanone, 2-butanol, 2-methyl-1-propanol, butanol, 1,1-diethoxy ethane, 1-pentanol, ethyl butyrate, butyl acetate and 1-hexanol. For the experiments in the continuous reactor the rest of the compounds were identified by GC-MS. Since both GCs had the same type of column it was possible to assign the uncalibrated compounds of the GC-FID. Using the effective carbon number method the concentration of the uncalibrated compounds was determined using 2-butanol as standard (Eq. 30). The effective carbon number values were obtained from Scanlon and Willis¹⁸¹.

$$\text{conc}_{i,\text{uncalibrated}} = \left(\frac{\text{Area}_i \cdot \text{MW}_i}{\text{ECN}_i} \right)_{\text{uncalibrated}} \cdot \left(\frac{\text{conc}_{2\text{-butanol}} \cdot \text{ECN}_{2\text{-butanol}}}{\text{Area}_{2\text{-butanol}} \cdot \text{MW}_{2\text{-butanol}}} \right) \quad (\text{Eq. 30})$$

3. Prepared catalysts and their characterization

In the following chapter, characterization of both unsupported (section 3.1) and supported catalysts (section 3.2) in their as prepared form is presented. The catalysts were characterized by *in situ* and *ex situ* methods. The characterization methods are described in section 2.2 of the experimental.

3.1. Unsupported catalysts

The unsupported catalysts were characterized in their as prepared form to identify the effect of doping the catalysts with promoters, and to compare them after exposure to the reaction environment. CuO/ZnO catalysts were prepared by increasing pH precipitation (inc_pH) as described in section 2.1.1 followed by wet impregnation of the promoters. Elemental analysis and specific surface area of the as prepared catalysts are presented in Table 3 and Table 4.

As shown in Table 3, results obtained from the elemental analysis generally differed from the calculated values. The values displayed in Table 3 correspond to an average of two measurements. The Cu and Zn contents determined by ICP-OES were higher than expected in all catalysts, whereas the Cs and Ru contents were lower. Nevertheless, a quite good agreement was obtained.

Table 3: Elemental composition of the as prepared unsupported catalysts.

Catalyst	Measured [wt.%]			Calculated [wt.%]		
	Cs/Ru*	Cu	Zn	Cs/Ru	Cu	Zn
CuO/ZnO	-	24.4	60.7	-	23.5	56.7
0.3 mol.% Cs-CuO/ZnO	0.3	25.1	61.7	0.5	23.4	56.4
0.6 mol.% Cs-CuO/ZnO	0.9	25.2	61.6	1.0	23.2	56.1
1.0 mol.% Cs-CuO/ZnO	1.4	25.0	58.2	1.7	23.1	55.7
3.0 mol.% Cs-CuO/ZnO	4.4	23.7	58.1	4.8	22.3	53.8
0.5 mol.% Ru-CuO/ZnO	0.3	25.7	61.5	0.6	23.3	56.2
1.0 mol.% Ru-CuO/ZnO	1.4	24.0	57.0	1.3	23.1	55.7

*Cs and Ru content measured by AAS.

The specific surface area changed slightly by doping the catalysts with promoters as it can be seen in Table 4. Doping with 0.3 - 1.0 mol.% Cs caused a slight decrease in the total surface area. For the 3.0 mol.% Cs doping a decrease of 15 m²/g in the surface area was observed. Ru doping influenced the specific surface area in a similar way. Even though the decrease in the specific surface area was more pronounced as the doping increased, for all catalysts the decrease can be explained by the subsequent addition of Cs/Ru by a second wet impregnation. This may have led to a restructuring of the surface of the material due to the basicity of the impregnating solution¹⁶⁸ or because of the second calcination after doping the catalysts. To test the effect of a second calcination on the surface area the standard catalyst (45 m²/g) was calcined a second time at 623 K and a decrease of the surface area to 35 m²/g was observed.

Table 4: Specific surface area of as prepared unsupported catalysts.

Catalyst	Specific surface area
	[m ² /g]
CuO/ZnO	45/35*
0.3 mol.% Cs-CuO/ZnO	40*
0.6 mol.% Cs-CuO/ZnO	40*
1.0 mol.% Cs-CuO/ZnO	40*
3.0 mol.% Cs-CuO/ZnO	30*
0.5 mol.% Ru-CuO/ZnO	40*
1.0 mol.% Ru-CuO/ZnO	30*

*Catalyst calcined two times.

The promotion of CuO/ZnO catalysts with Cs or Ru affected also the reduction process of the catalysts. Therefore H₂-TPR experiments were performed and their results are summarized in Table 5. The theoretical reduction volume represents the ratio between the stoichiometric volume of hydrogen consumed for a full reduction of the catalyst and the weighted mass of catalyst for the H₂-TPR experiment. Full reduction profiles are presented in Figure 8 and Figure 9. The hydrogen consumption was determined by calculating the area under the TPR profile and comparing it to the theoretical reduction volume. The instrument was calibrated to correlate the hydrogen consumption and the TCD signal.

For the standard catalyst (CuO/ZnO), the main reduction peak was found at 439 K. It showed two shoulders, one each at lower and higher temperatures from the main reduction peak. In comparison to pure CuO reduction, the shape of the reduction peak changed when ZnO was

present. Pure CuO exhibited a single reduction peak, whereas for the CuO/ZnO catalyst a shoulder in the lower temperature region was observed (Figure 9).

Additionally, ZnO enhanced the reducibility of the catalyst by lowering the reduction temperature in comparison to pure CuO.¹⁸³ The main reduction peak shifted from 510 K to 439 K, but the start of the reduction was at the same temperature. The shape of the reduction peak of the standard catalyst agreed with the ones presented by Fierro et al.¹⁸³ and Kniep et al.⁷¹ Nevertheless, the maximum of the reduction peak was located 15 - 30 K lower than the temperatures reported by the previous authors. This could be a consequence of the different conditions used for the TPR or due to a different catalyst synthesis method^{71, 183-185}. The two shoulders next to the main reduction peak could be attributed either to a stepwise reduction of copper^{71, 186, 187} or to an inhomogeneous size distribution of the copper particles.

Fierro et al.¹⁸³ interpreted the observed shoulder by considering the presence of two different reducible copper species. Highly dispersed and intimately contacted copper particles on ZnO would enable an easy reduction of the copper species (cf. XRD and TEM results). A stepwise reduction from CuO to Cu₂O and then to Cu was identified using CO as probe molecule instead of H₂ by Pike et al.¹⁸⁷ The authors studied the reduction of CuO nanoparticles by means of *in situ* Time-Resolved X-ray Diffraction (TR-XRD).

Table 5. Temperature programmed reduction with hydrogen (H₂-TPR) of the unsupported catalysts.

Catalyst	Maximum reduction peak	Theoretical reduction volume	H ₂ consumption *
	[K]	[cm ³ /g]	[%]
pure CuO	510	281	100
CuO/ZnO	439	83	94
0.3 mol.% Cs-CuO/ZnO	468	83	98
0.6 mol.% Cs-CuO/ZnO	459	82	95
1.0 mol.% Cs-CuO/ZnO	492	81	99
3.0 mol.% Cs-CuO/ZnO	551	78	99
0.5 mol.% Ru-CuO/ZnO	460	87	99
1.0 mol.% Ru-CuO/ZnO	470	91	92

*From possible theoretical value.

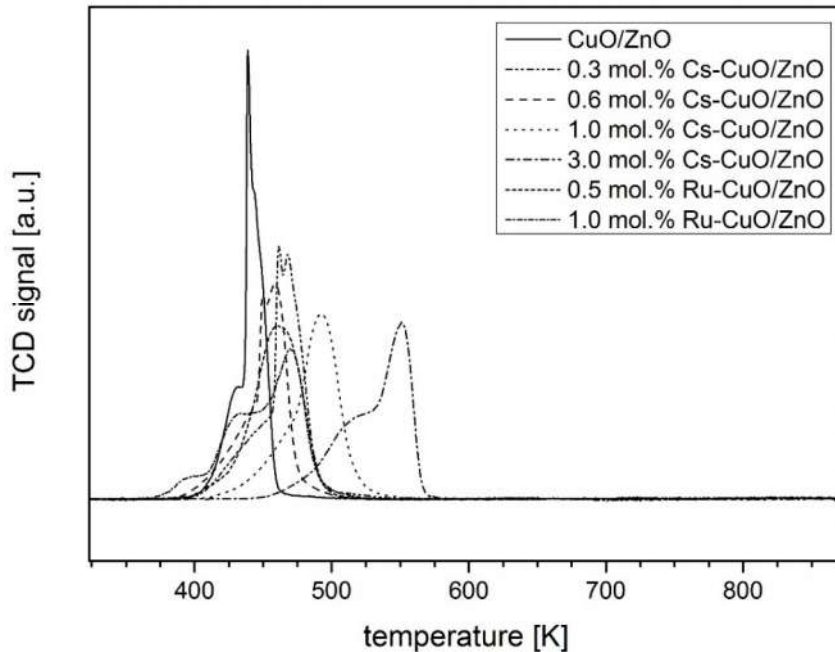


Figure 8: H₂-TPR profiles of different Cs/Ru-doped catalysts (pretreatment: heated to 423 K with 5 K/min under Ar. TPR experiment: heated from 273 K to 873 K with 5 K/min under 10 % H₂/Ar, 30 ml/min, STP, ~100 mg).¹⁸²

The presence of Cs or Ru delayed the main reduction peak from 439 K (standard catalyst) to a value between 460 K and 551 K (depending on the doping) and modified the profile shape in accordance with literature reports.^{161, 186} Nevertheless, the reduction still occurred at lower temperatures than for pure CuO, except for the 3 mol.% Cs-CuO/ZnO catalyst. The reduction peak changed from a sharp peak to a broader one of lower intensity. However, the hydrogen consumption was similar and close to the possible theoretical value for all experiments, as shown in Table 5. Hence, all catalysts were completely reduced after the TPR experiment. The left shoulder (lower temperature) was maintained despite the Cs or Ru doping. The two reduction peaks overlapped at Cs loadings larger than 1 mol.%, which was also the case for the Ru-doped catalysts. With higher Cs content on the catalyst the reduction temperature was larger, except for Cs doping between 0.3 and 0.6 mol.%.

For low Cs doping a difference with the standard catalyst was not observed at the start of the reduction profile, since both reduction processes started at the same temperature. The difference was observed at the end of the reduction process, since for lower doping it ended at 533 K (approximately 60 K higher than for the standard catalyst). At higher Cs loadings the reduction even started at higher temperatures. The subsequent impregnation with Cs might

have led to a blockage of the small copper particles, thereby causing a shift in the reduction temperature induced by Cs doping. Similar observations were presented by Campos-Martín et al.¹⁶¹ The authors suggested that a close interaction of copper and cesium hampered the hydrogen dissociation, which retarded the reduction. The 1.0 mol.% Ru catalyst showed a stepwise reduction divided into three steps. The reduction step at lower temperatures was assigned to the reduction of RuO₂ to Ru. Ru doping did not shift the reduction of copper oxide to lower temperatures.

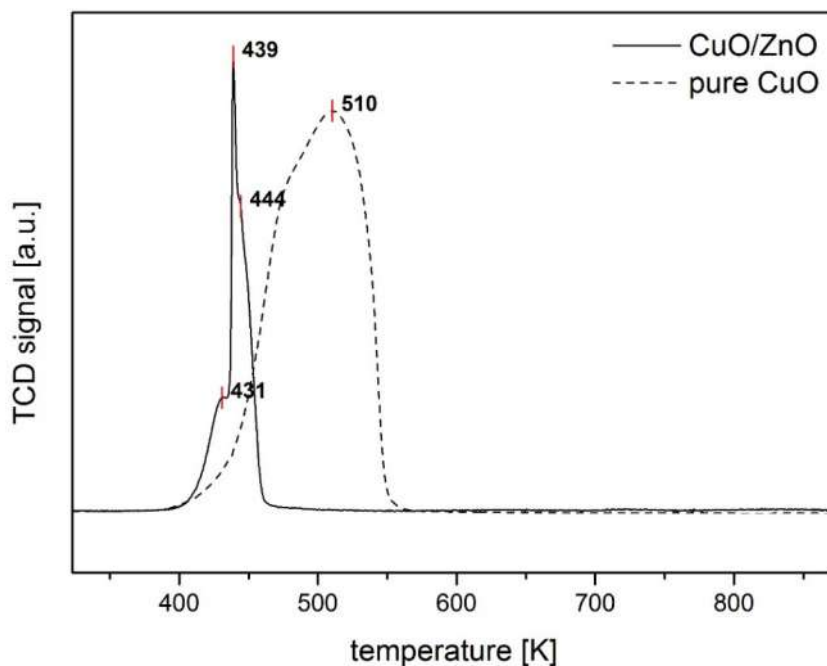


Figure 9: H₂-TPR profiles of CuO/ZnO and pure CuO (pretreatment: heated to 423 K with 5 K/min under Ar. TPR experiment: heated from 273 K to 873 K with 5 K/min under 10 % H₂/Ar, 30 ml/min, STP, ~100 mg).

Powder X-ray diffraction patterns of the fresh calcined catalysts were measured and are displayed in Figure 10. After calcination of the precursors, CuO and ZnO phases were formed regardless of the amount of Cs doping. A slight discrepancy in the XRD patterns for the different levels of Cs doping was observed in the 2θ range from 27° to 29°. This reflections could not be assigned to any measured pattern. Presumably, they are related to the Cs content in the catalyst since a difference in their height is accounted. As the Cs doping was increased, the reflection between 28 and 28.5° became more intense, except for the 4.0 mol.% Cs doping. Another reflection at approximately 27.5° also appeared with increasing the Cs content in the

catalyst. For the 4.0 mol.% Cs catalyst this reflection was broader in comparison to the other Cs concentrations.

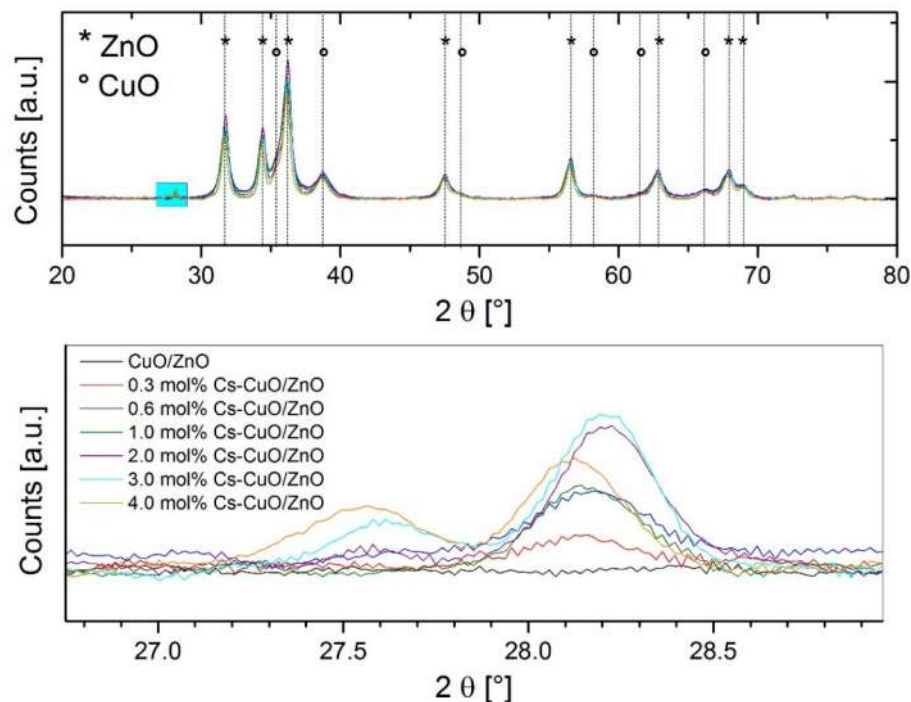


Figure 10: X-ray diffraction patterns in the 2θ range from 20° to 80° for doped and undoped CuO/ZnO fresh calcined catalysts (top). Zoom in the 2θ range from 27° to 29° for doped and undoped CuO/ZnO fresh calcined catalysts (bottom). *: ZnO and $^\circ$: CuO.

Independent of the Cs content, all catalysts showed reflections of similar intensities and width, therefore a similar particle size could be expected according to the Scherrer equation. Since a similar particle sizes were expected from the XRD, the particle size distribution was determined only for one catalyst by HRTEM. As an example, an HRTEM image of the 0.6 mol.% Cs-CuO/ZnO fresh calcined catalyst is shown in Figure 11. A broad copper particle size distribution between 1 and 24 nm was observed (average of 8 nm). This could explain the observed shape in the reduction profile during the TPR experiments. As in the XRD patterns, both CuO and ZnO phases were identified.

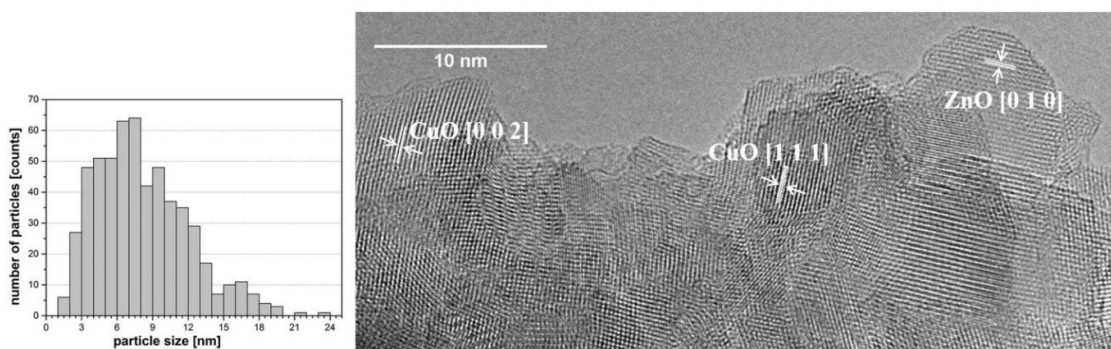


Figure 11: Particle size distribution and selected HRTEM image of the 0.6 mol.% Cs-CuO/ZnO after calcination.

To understand the effect of Cs doping in the reduction of the CuO/ZnO catalyst, *in situ* TPR using X-ray absorption near edge structure (XANES) spectroscopy in 5 % H₂/He atmosphere was performed. As in the case for the laboratory experiments, the reduction of the catalysts was a function of the Cs content. As an example, a comparison between a 3 mol.% Cs and a 4 mol.% Cs doped catalysts was performed as presented in Figure 12. Higher Cs contents in the catalysts led to a shift in the start of the reduction. Nevertheless both catalysts reached a 100 % reduction at the same temperature.

Note that the temperature reported in Figure 12 does not necessarily correspond to the one reported for the H₂-TPR since for the XAS experiments only the temperature of the gas blower was recorded. The real temperature of the capillary is dependent on the position of the capillary relative to the gas blower. For the linear combination analysis the first and last spectra recorded at room temperature were used. From the linear combination analysis, identification of the metallic copper fraction at a certain temperature is possible. For example, at 450 K the metallic copper fraction for the 3.0 mol.% Cs doped catalyst corresponded to approximately 80%, whereas for the 4.0 mol.% doped catalyst nearly all of the copper species were still oxidized at this temperature. When 500 K were reached, both of the catalyst were almost completely in a reduced state.

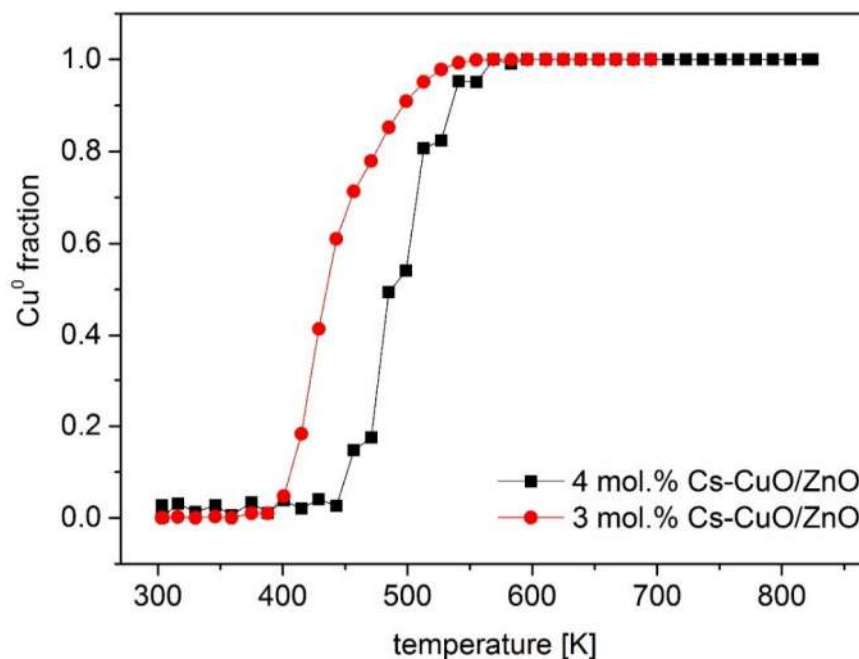


Figure 12: Fraction of metallic Cu obtained using linear combination analysis of XANES spectra (reference XAS-spectrum: first and last spectra at room temperature) during reduction in 5 % H₂/He reaction atmosphere for differently Cs-doped CuO/ZnO catalysts.

3.2. Supported catalysts

Before testing the synthesis of higher alcohols in a continuous-flow reactor, catalysts supported on Al₂O₃, SiO₂ and activated carbon were prepared to study the effect of different supports on the product distribution and activity. A commercial catalyst is also shown for comparison purposes. As for the unsupported catalysts, the supported catalysts were characterized using the same experimental techniques. Some of the data presented in this section were obtained during a joint research project with Marc-André Serrer within the frame of his bachelor thesis.¹⁸⁸

The elemental composition of the supported catalysts as prepared is presented in Table 6. In general a good agreement between calculated and measured values was obtained. In the case of the catalysts prepared in the laboratory, they were supported catalysts whereas the commercial one Al₂O₃ is just an additional promoter. The specific surface area of the support materials are presented in Table 7. In Table 8 and Table 9 the specific surface area of each catalyst is displayed.

In general, after preparation of the catalysts some of the specific surface area of the support was lost probably due to blockage of the pores by CuO/ZnO addition. Variation of the preparation method affected the specific surface area of the resulting catalysts to a different extent. Regardless of the support, wet impregnation seemed to decrease the surface area to a higher extent in comparison to the other preparation methods.

Table 6: Elemental composition of the as prepared supported catalysts.

Catalyst	Measured [wt.%]			Calculated [wt.%]		
	Al/Si	Cu	Zn	Al/Si	Cu	Zn
CuO/ZnO/Al ₂ O ₃ _wi	31.0	7.2	16.2	36.4	7.3	17.7
CuO/ZnO/Al ₂ O ₃ _inc_pH	35.3	7.8	18.5	36.4	7.3	17.8
CuO/ZnO/Al ₂ O ₃ _const_pH	34.6	7.8	17.6	36.4	7.4	17.7
CuO/ZnO/Al ₂ O ₃ _fsp	28.0	6.0	14.9	36.4	7.4	17.7
CuO/ZnO/SiO ₂ _wi	38.4	6.3	16.7	32.2	7.4	17.6
CuO/ZnO/SiO ₂ _inc_pH	28.6	8.3	20.0	32.2	7.3	17.6
CuO/ZnO/AC_wi	-	9.0	23.0	-	7.4	17.7
CuO/ZnO/AC_inc_pH	-	6.8	16.5	-	7.4	17.7
Cu/ZnO/Al ₂ O ₃ _com	4.5	50.5	21.2	-	-	-

wi: wet impregnation. inc_pH: increasing pH precipitation. const_pH: constant pH precipitation. fsp: flame spray pyrolysis. com: commercial methanol catalyst. AC: activated carbon.

Table 7: Specific surface areas of support materials.

Catalyst	Al ₂ O ₃	SiO ₂	AC*
Specific surface area [m ² /g]	220	135	1820

*AC: activated carbon.

As observed in Table 8, different CuO/ZnO loadings (30, 20 and 10 wt.%) on the support decreased the specific surface area almost proportionally to the amount of CuO/ZnO for catalysts prepared via wet impregnation. This also evidenced the blocking of the support pores by the CuO/ZnO. Additional preparation methods were tested for Al₂O₃ support. The influence of each preparation method on the specific surface area of the catalysts is also displayed in Table 8. Additionally, a commercial catalyst is shown for comparison.

The lowest specific surface area was obtained for the commercial catalyst (90 m²/g). This is expected since most of the specific surface area in catalysts is generally given by the support. The two types of precipitations gave similar specific surface areas with differences within the

limits of accuracy of the method. In contrast to the other preparation methods, for the catalyst prepared by flame spray pyrolysis the support material and the active components were synthesized at the same time. The specific surface area for this catalyst corresponded to 100 m²/g.

Table 8: Specific surface areas of as prepared CuO/ZnO/Al₂O₃ supported catalysts.

Preparation method	inc_pH	const_pH	fsp	com	wi [30 wt.%]	wi [20 wt.%]	wi [10 wt.%]
Specific surface area [m ² /g]	180	170	100	90	160	170	200

inc_pH: increasing pH precipitation. const_pH: constant pH precipitation. fsp: flame spray pyrolysis. com: commercial methanol catalyst. wi: wet impregnation.

The catalysts supported on activated carbon resulted in the highest decrease in the specific surface area respect to the support area (990 and 630 m²/g lower with respect to the surface area of the support material for wet impregnation and precipitation, respectively). The precipitated SiO₂ supported catalysts did not show any changes in the specific surface area.

Table 9: Specific surface areas of as prepared SiO₂ and activated carbon supported catalysts by wet impregnation and increasing pH precipitation.

Catalyst	CuO/ZnO/SiO ₂ wi	CuO/ZnO/SiO ₂ inc pH	CuO/ZnO/AC wi	CuO/ZnO/AC inc pH
Specific surface area [m ² /g]	70	130	830	1190

wi: wet impregnation. inc_pH: increasing pH precipitation. AC: activated carbon.

Like for the unsupported catalysts, H₂-TPR profiles were measured to determine the effect of the preparation method as well as Cs impregnation on the supported catalysts. Figure 13 (a) presents a comparison between CuO/ZnO catalysts supported on Al₂O₃, SiO₂ and AC prepared by wet impregnation and a CuO/ZnO/Al₂O₃ prepared by increasing pH precipitation. Figure 13 (b) shows a comparison between several Cs-doped catalysts prepared by different methods and an undoped catalyst.

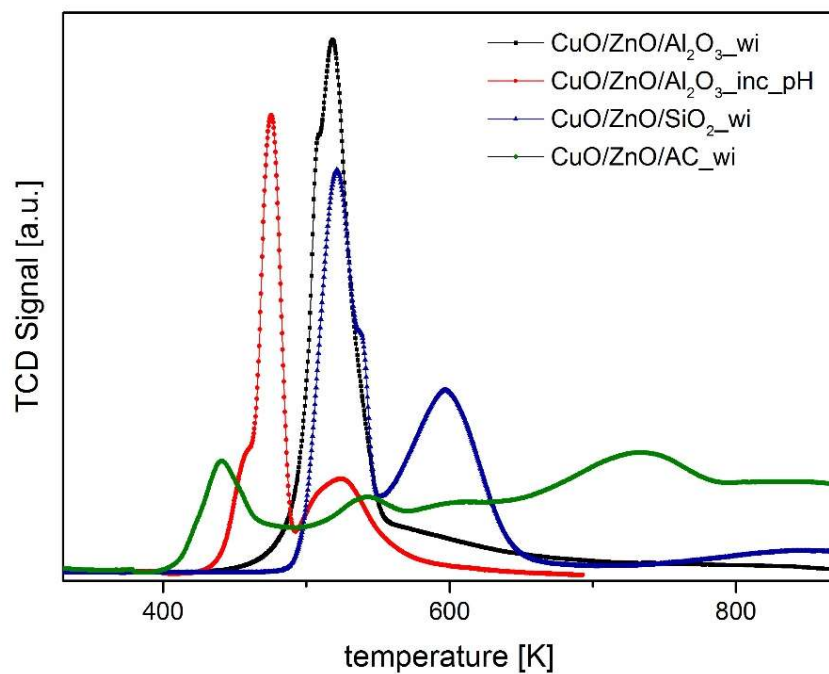
A CuO/ZnO/Al₂O₃ catalyst prepared by wet impregnation gave a different H₂-TPR profile in comparison to a CuO/ZnO/Al₂O₃ catalyst prepared by increasing pH precipitation (Figure 13 (a)). For the catalyst prepared by increasing pH precipitation (red curve), the reduction started at a temperature 20 K lower than for the catalyst prepared by wet impregnation (black curve). Regardless of the preparation method the reduction process of both catalysts ended at similar temperatures, approximately at 600 K. The CuO/ZnO/Al₂O₃_inc_pH catalyst exhibited two main reduction peaks at 475 and 524 K (Figure 13 and Table 10). The first reduction peak showed a shoulder in the lower temperature region. In the case of CuO/ZnO/Al₂O₃_wi only

one main reduction peak also with a shoulder in the lower temperature region was observed. The different characteristics of both reduction profiles could be a consequence of either different particle sizes or a sequential reduction $\text{Cu}^{2+} \rightarrow \text{Cu}^{1+} \rightarrow \text{Cu}^0$ as mentioned in section 3.1 for unsupported catalysts.

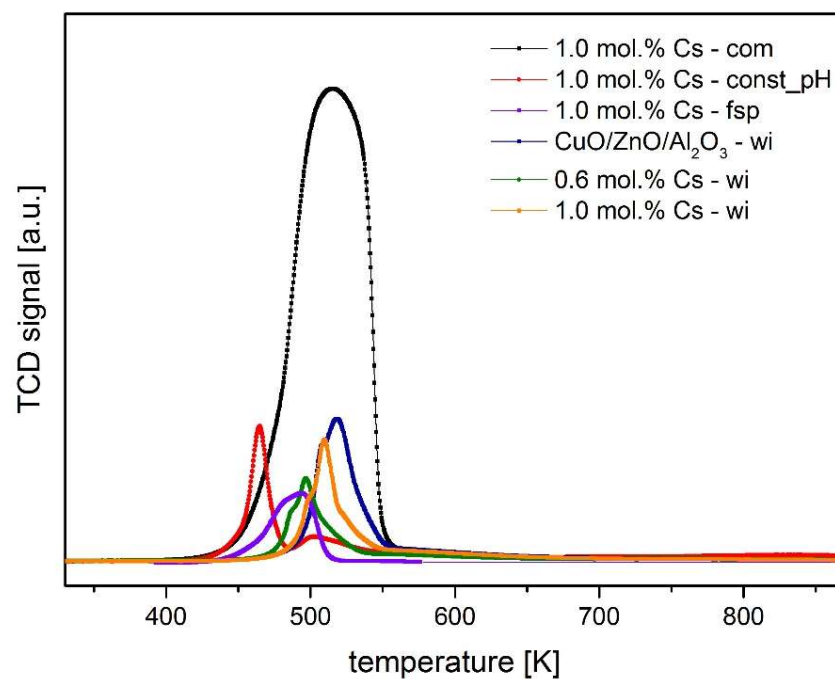
The wet impregnation method was also used to prepare catalysts supported on AC (green curve) and SiO_2 (blue curve). Their H_2 -TPR profiles are also presented in Figure 13 (a). The activated carbon support most probably featured functional groups that also interacted with H_2 or reduced leading to an unstable baseline during the experiment. It was not possible to identify precisely a CuO reduction peak, which was located between 400 and 600 K for the other catalysts. In the case of the catalyst supported on SiO_2 , two main reduction peaks were observed (521 and 597 K, Figure 13 (a) and Table 10). The peak at 521 K showed a shoulder at higher temperatures than the maximum. The reduction peak at 521 K was located in the same temperature region as the one for the $\text{CuO}/\text{ZnO}/\text{Al}_2\text{O}_3_{\text{wi}}$ and as the second peak for the $\text{CuO}/\text{ZnO}/\text{Al}_2\text{O}_3_{\text{inc_pH}}$, this could indicate that the copper particles that are reduced in this region have similar characteristics. The peak located at 597 K could be due to copper particles which are more difficult to reduce provoked probably by interactions with the support.

Different catalysts with an analogous composition are shown in Figure 13 (b) and compared with a Cs modified commercial catalyst (black curve). All catalysts feature the same CuO, ZnO and Al_2O_3 molar composition, but were synthesized using the different preparation methods described in section 2.1. The catalysts were afterwards impregnated with Cs always maintaining a 1 mol.% Cs in relation to the moles of CuO and ZnO present in the catalyst. Note that the same amount of catalyst was used for the TPR experiments, but the copper content in the commercial catalyst exceeded the one of the prepared catalysts. For the catalyst prepared by constant pH precipitation (red curve), copper particles that reduced at lower temperatures in comparison to the catalyst prepared by wet impregnation or flame spray pyrolysis were present, which indicated small particles.

The Cs modified commercial catalyst exhibited a single peak with a maximum at 517 K, which was located in the same temperature region than the catalysts prepared by wet impregnation and the second peak of the catalysts prepared by constant pH precipitation. The catalysts prepared by flame spray pyrolysis showed a single reduction peak at 493 K. For this catalyst the reduction ended at lower temperatures in comparison to the other catalysts presented in Figure 13 (b).



(a)



(b)

Figure 13: H₂-TPR profiles of: (a) CuO/ZnO/support and (b) Cs-doped CuO/ZnO/Al₂O₃ catalysts (pretreatment: heated to 423 K with 5 K/min under Ar. TPR experiment: heated from 273 K to 873 K with 5 K/min under 10 % H₂/Ar, 30 ml/min, STP, ~100 mg). wi: wet impregnation. inc_pH: increasing pH precipitation. const_pH: constant pH precipitation. fsp: flame spray pyrolysis. com: commercial methanol catalyst. AC: activated carbon.

In the same Figure, CuO/ZnO/Al₂O₃_wi catalysts with varying Cs loadings are shown. Regardless of the Cs doping a single reduction peak was still present. Cs presence shifted the reduction peak to lower temperatures unlike for the unsupported catalysts (Figure 8). Lower Cs content (0.6 mol.%) shifted the reduction temperature to lower temperatures in comparison to 1.0 mol.%. In general supported catalysts reduced at higher temperatures than unsupported ones.

As for the unsupported catalysts, *in situ* H₂-TPR XAS experiments were performed for supported catalysts (Figure 14). In this case no effect of Cs doping on the catalyst was observed. The reduction finished at temperatures between 550 and 600 K, similarly to the conventional TPR experiments.

Table 10: TPR results of the supported catalysts.

Catalyst	Reduction peaks
	[K]
CuO/ZnO/Al ₂ O ₃ _wi	518
CuO/ZnO/Al ₂ O ₃ _inc_pH	475 / 524
CuO/ZnO/Al ₂ O ₃ _const_pH*	461 / 498
CuO/ZnO/Al ₂ O ₃ _fsp*	493
CuO/ZnO/SiO ₂ _wi	521 / 597
CuO/ZnO/SiO ₂ _p*	455 / 526
CuO/ZnO/AC_wi	-
CuO/ZnO/Al ₂ O ₃ _com*	517

*: not shown in Figure 13. wi: wet impregnation. inc_pH: increasing pH precipitation. const_pH: constant pH precipitation. fsp: flame spray pyrolysis. com: commercial methanol catalyst. AC: activated carbon.

XRD patterns for the supported catalysts are presented in Figure 15 (a, b and c). Figure 15 (a) shows a comparison between the support materials and the catalysts obtained via wet impregnation. In all cases the support is clearly identified in the catalyst diffraction pattern. For all catalysts reflections of ZnO and CuO were identified. In the case of the AC supported catalyst also Cu₂O was detected.

The influence of the CuO/ZnO loading on Al₂O₃ is presented in Figure 15 (b). With increasing amount of CuO/ZnO the reflections of both ZnO and CuO became more intense. This reflected an increase in their particle size. Probably a higher availability of CuO/ZnO contributed to the agglomeration during the impregnation.

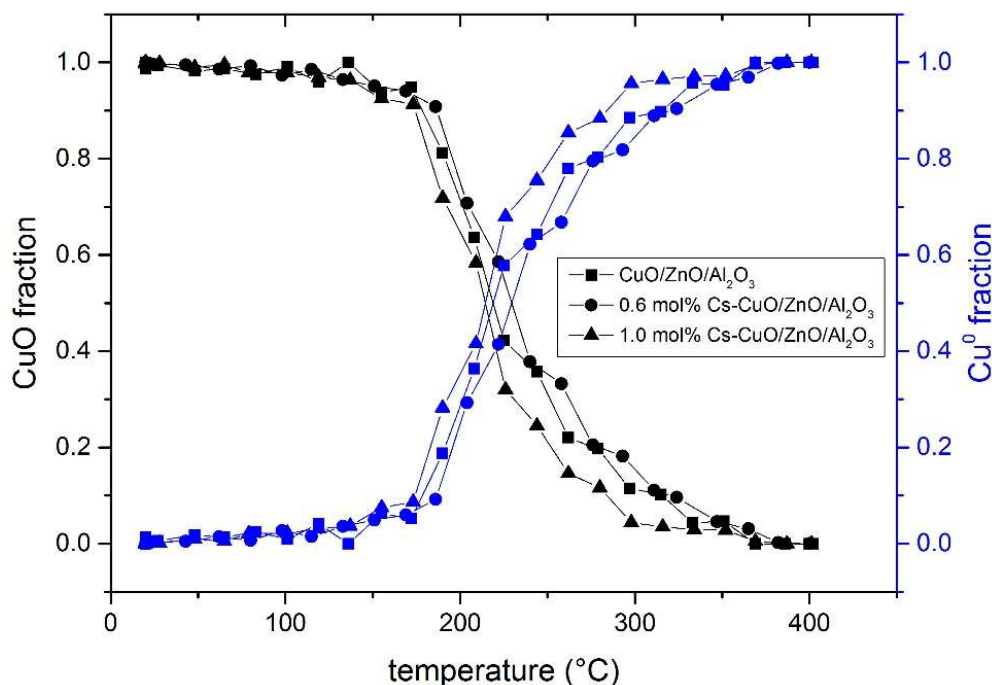
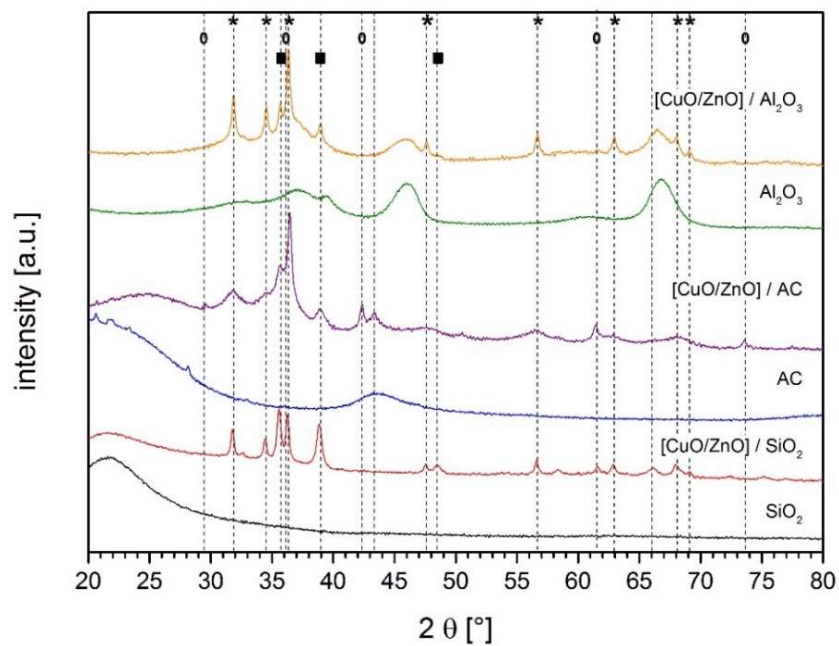


Figure 14: Fraction of metallic Cu and CuO obtained using linear combination analysis of XANES spectra (reference XAS-spectrum: first and last spectra at room temperature) during reduction in 5 % H₂/He reaction atmosphere for Cs-doped and undoped CuO/ZnO/Al₂O₃ catalysts.

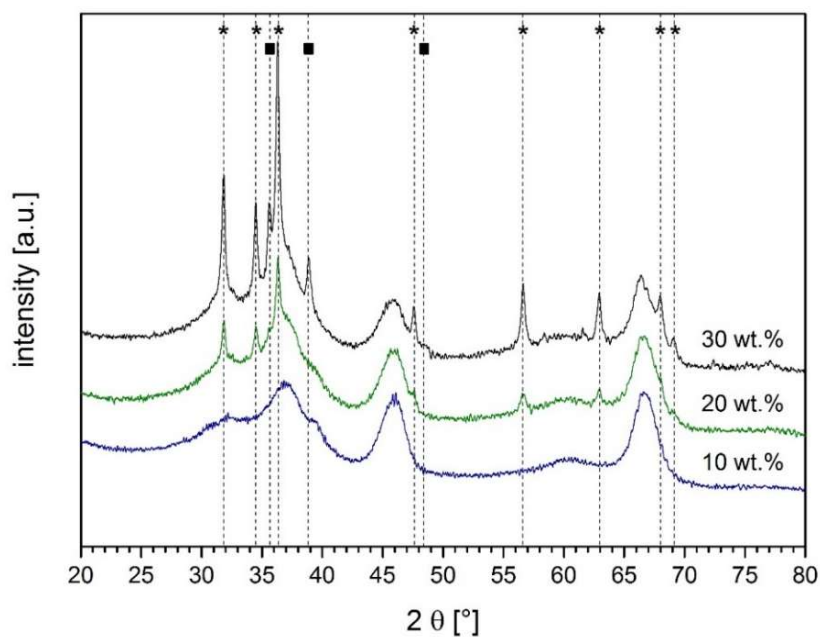
Figure 15 (c) presents XRD patterns for catalysts supported on Al₂O₃ prepared by different methods compared to a commercial methanol synthesis catalyst. In all cases reflections of both CuO and ZnO could be identified. Al₂O₃ reflections were identified regardless of the preparation method. The commercial catalysts showed additional reflections at 2θ values lower than 30°. Probably these reflections were caused by residues from the precursors. In addition, the reference catalyst did not show reflections from Al₂O₃ due to its very low concentration as expected for a typical methanol synthesis catalyst (see further in section 1.3.1). Constant pH precipitation compared to increasing pH precipitation showed higher intensities for ZnO reflections whereas CuO reflections appeared to have the same intensity. The catalysts prepared by wet impregnation showed narrower and more intense reflections both for CuO and ZnO. This indicated that this preparation method led to bigger particles. The catalyst prepared by flame spray pyrolysis showed less intense reflections. The Al₂O₃ reflections were narrower for this catalyst, which indicated a more crystalline material. The CuO reflections overlapped with the Al₂O₃ and ZnO reflections. Their low intensity implied small crystallite sizes.

The catalysts were reduced and characterized by HRTEM. Attention was paid to avoid exposition of the catalysts to air to keep them in a reduced state. [1 mol.% Cs-Cu/ZnO] / Al₂O₃

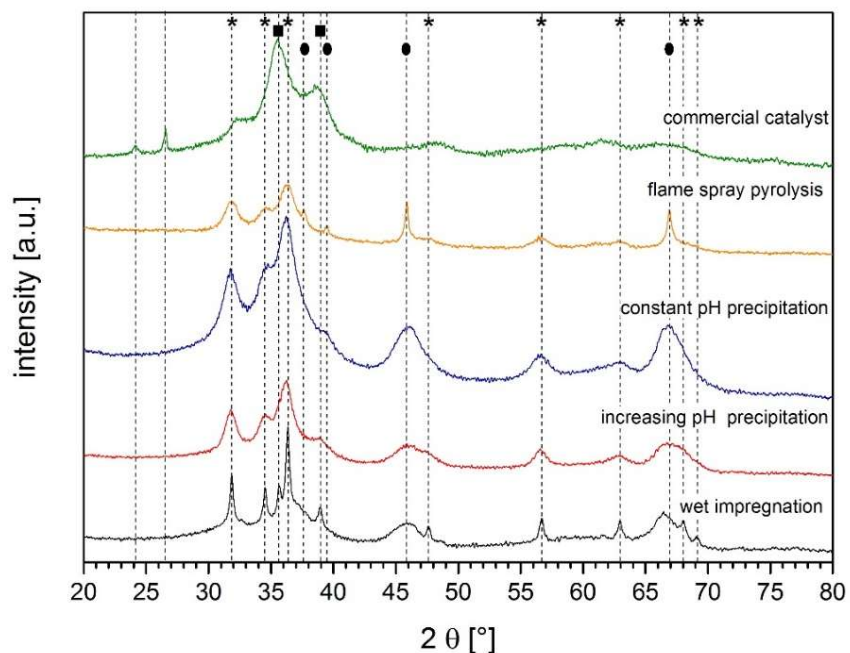
prepared by wet impregnation and constant pH precipitation were selected and their characterization results are compared in Figure 16. For the supported catalysts the particle size distribution was narrower in comparison to the unsupported ones (Figure 11). For both catalysts an average particle size between 3 and 5 nm was found. A broader particle size distribution was found for the catalyst prepared by constant pH precipitation.



(a)

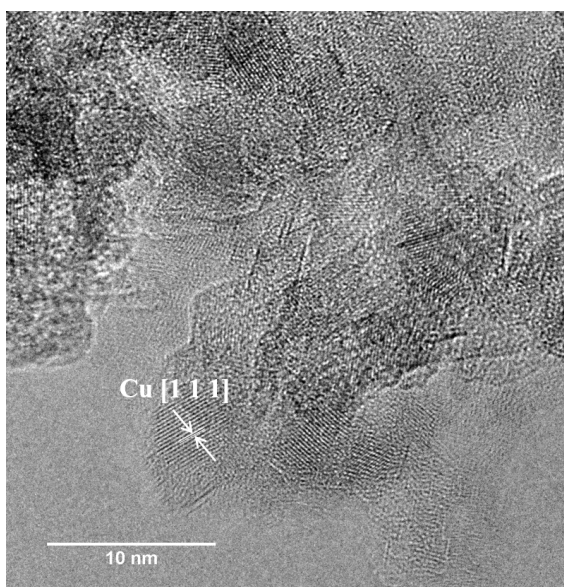
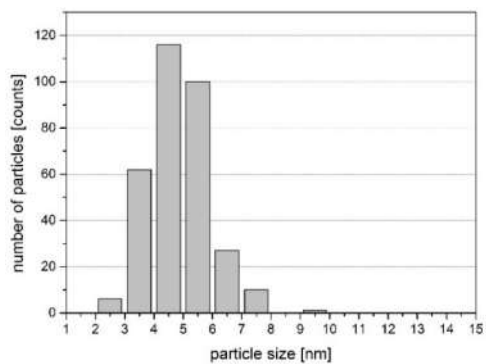


(b)

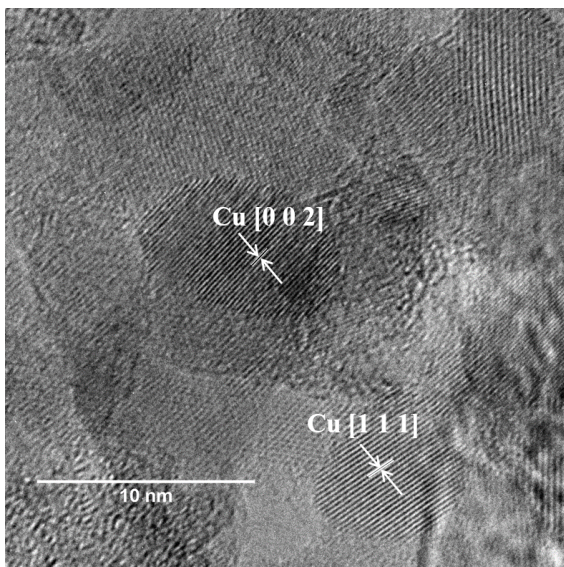
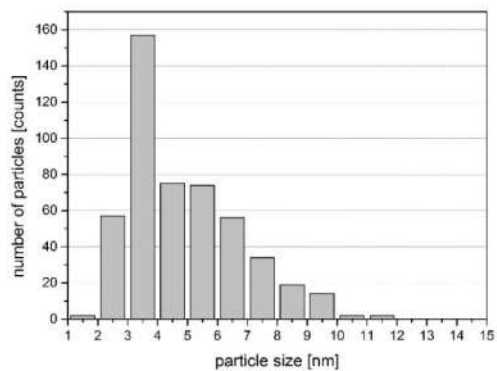


(c)

Figure 15: X-ray diffraction patterns for supported CuO/ZnO fresh calcined catalysts: (a) on different supports; (b) with different amounts of CuO/ZnO on Al₂O₃ and (c) Al₂O₃ supported catalysts from different preparation methods. *: ZnO, ▪: CuO and ◦: Cu₂O, •: Al₂O₃. AC: activated carbon



(a)



(b)

Figure 16: Particle size distribution and selected HRTEM images of the [1 mol.% Cs-Cu/ZnO] / Al₂O₃ prepared by: (a) wet impregnation and (b) constant pH precipitation.

4. Synthesis of higher alcohols: screening studies in batch reactors

The following chapter summarizes the results of catalytic studies on the synthesis of higher alcohols under batch operation conditions.

The first section (4.1) shows the effect of doping (either with Cs or Ru), ethanol to CO ratio and reaction temperature on the higher alcohol synthesis. For this part of the screening unsupported catalysts were used.

The second section (4.2) presents results from parameter screening tests on supported catalysts. The influence of the preparation method of the CuO/ZnO/Al₂O₃ catalyst, the CuO/ZnO loading on the support, and the type of support were analyzed. Both unsupported and supported catalysts were characterized after reaction.

4.1. Unsupported catalysts

The unsupported catalysts were tested in a batch reactor at 593 K for the synthesis of higher alcohols using a CO to H₂ ratio of 1:1. The ethanol to CO ratio was adjusted by varying the amount of ethanol and cyclohexane (initial synthesis gas pressure of 5.0 MPa, either in pure cyclohexane, $n_{\text{EtOH}} : n_{\text{CO}} = 0.5:1, 0.9:1, 10.0:1$ or only ethanol in Ar, cf. chapter 2, section 2.3.1). The reaction time was fixed at 3 hours to ensure a representative interval in comparison to the heating and cooling processes. The overall mass balance was around 95 % (complete reaction data are found in Table S 1 to Table S 5 in the supporting information). The results presented in this section resulted in a publication in a peer-reviewed journal.¹⁸²

Different parameters regarding the higher alcohol synthesis were studied during the catalysts screening in batch reactors as mentioned in the experimental part. To facilitate the presentation of the data, they will be displayed separately during this section. The presented Figures (Figure 18 to Figure 24 and Figure 27) group the reaction products in categories for easier analysis. Further details can be found in the supporting information (Table S 1 to Table S 16). First, the effect of two different promoters (Ru and Cs) on the unsupported CuO/ZnO catalyst will be shown. Next, the influence of different ethanol to CO ratios in the higher alcohol synthesis will be presented. In addition to the catalytic activity results, characterization of selected catalysts

after reaction will be shown to correlate them with the catalytic test results. Data regarding calibrated products will be analyzed.

In general, different temperature profiles (area marked by the dotted lines in Figure 17) were noticed depending on the reaction medium present (cyclohexane, ethanol or mixtures). It is presumed that a phase change dependent on the ethanol content in the mixture took place. In the ethanol free and $n_{\text{EtOH}} : n_{\text{CO}} = 0.5:1$ experiments this probably occurred at 563 K and 8.9 MPa. In the tests with $n_{\text{EtOH}} : n_{\text{CO}} = 10.0:1$ it occurred at 513 K and 9.4 MPa. Prior to the first dotted line all heating profiles showed similar behavior. For the $n_{\text{EtOH}} : n_{\text{CO}} = 10.0:1$ ratio reaction, the pressure increased abruptly and it continued increasing until the end of the reaction time, even though the temperature stabilized. This could indicate the formation of more volatile or gaseous products. This was not the case for the other reaction conditions where the pressure in the reactor slightly decreased. Note that the reaction occurred above the critical temperature/pressure for the pure solvents ethanol and cyclohexane, which are 514 K and 6.3 MPa and 554 K and 4.1 MPa, respectively (c.f. NIST Chemistry Webbook.¹⁸⁹).

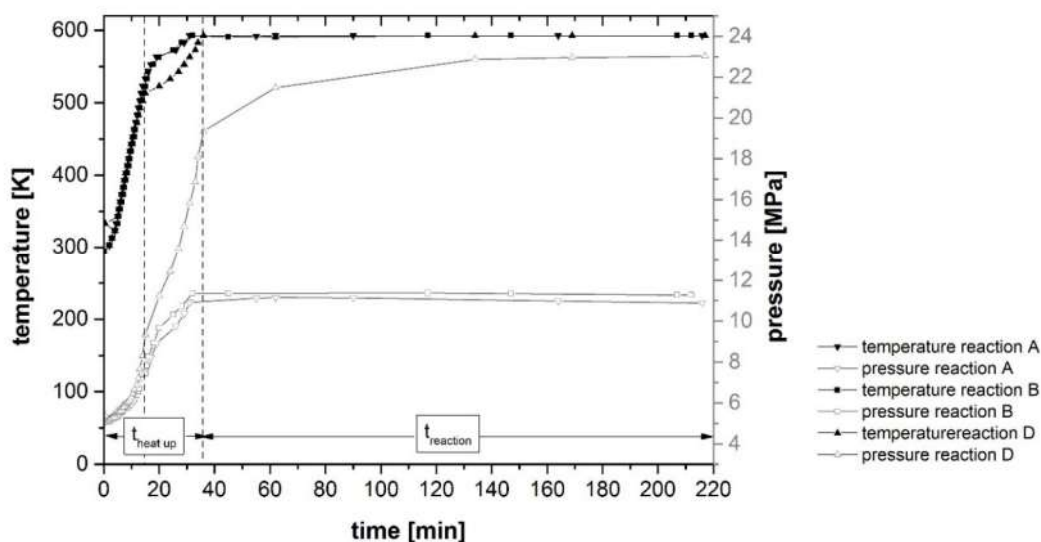


Figure 17: Batch reactor heating profiles for the experiments with CuO/ZnO catalysts in the reactions: A: ethanol free, B: $n_{\text{EtOH}} : n_{\text{CO}} \sim 0.5:1$, and D: $n_{\text{EtOH}} : n_{\text{CO}} \sim 10.0:1$; conditions: $T=593$ K, $p_{\text{start}}= 5.0$ MPa, 1 g catalyst, $\text{H}_2:\text{CO}=1:1$, reaction time = 3 h, liquid phase: A= 30 g cyclohexane, B: ~ 28.6 g cyclohexane and ~ 1.4 g ethanol, D: 30 g ethanol.

4.1.1. Influence of metal promoters

4.1.1.1. Effect of Ru doping on the CuO/ZnO catalyst

The effect of Ru promotion of CuO/ZnO catalysts on the yield towards higher alcohols in comparison to the standard CuO/ZnO catalyst are presented in Figure 18 and Figure 19. Both in the absence (Figure 18) and in the presence of ethanol ($n_{\text{EtOH}} : n_{\text{CO}} = 0.5:1$, Figure 19) the doping with Ru favored the production of alkane and alkene products and did not promote the synthesis of higher alcohols. The formation of C_{2-3} alkanes was induced by the addition of ethanol in a ratio of $n_{\text{EtOH}} : n_{\text{CO}} \sim 0.5:1$ (Figure 19) for all catalysts. The yield increased from 0.1 to 2.0 %-C and 0.2 to 3.3 %-C for the 0.5 mol.% and 1.0 mol.% Ru doped catalysts respectively. For the standard catalyst, the yield increased from 0.6 %-C to 1.6 %-C. Ethanol was dehydrated to ethylene and then hydrogenated to form ethane. Especially for the standard CuO/ZnO catalyst the production of other oxygenates was enhanced (0.1 %-C to 3.0 %-C). This implies that side reactions, such as Fischer-Tropsch synthesis or ester formation, were favored instead of higher alcohol synthesis.

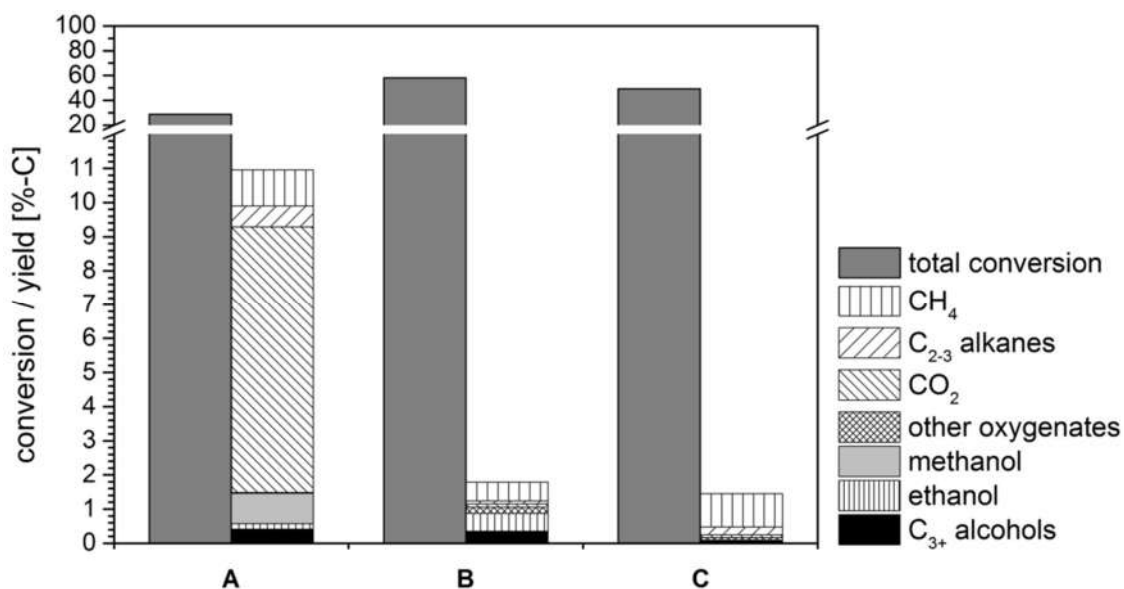


Figure 18: Product yield in the higher alcohols synthesis with $\text{H}_2 : \text{CO}=1:1$ at 593 K, 5.0 MPa in the absence of ethanol over 1 g of the following catalysts: A: CuO/ZnO, B: 0.5 mol.% Ru-CuO/ZnO and C: 1.0 mol.% Ru-CuO/ZnO. (reaction time = 3 h, liquid phase= 30 g cyclohexane).¹⁸²

As expected for Fischer-Tropsch elements as dopants, the reaction mechanism was changed in comparison to Cs-doped catalysts. For Ru-doped catalysts even though the formation of higher alcohols was limited, linear alcohols were preferred instead of branched ones.⁵⁰ As an example, among the calibrated products 1-propanol and 1-butanol were produced for the ethanol free

reaction using a 0.5 mol.% Ru containing catalyst. For the same reaction methanol and 2-methyl-1-propanol were the preferred alcohol products using a CuO/ZnO catalyst.

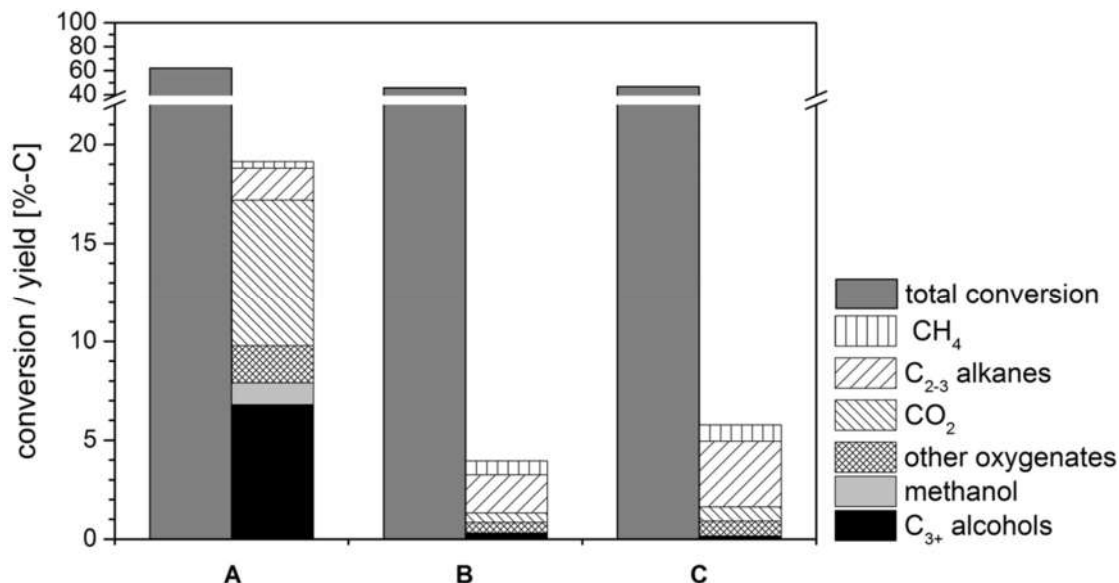


Figure 19: Product yield in the higher alcohols synthesis with $H_2 : CO=1:1$ and $n_{EtOH} : n_{CO} \sim 0.5:1$ at 593 K, 5.0 MPa over 1 g of the following catalysts: A: CuO/ZnO, B: 0.5 mol.% Ru-CuO/ZnO and C: 1.0 mol.% Ru-CuO/ZnO. (reaction time = 3 h, liquid phase= ~ 28.6 g cyclohexane and ~ 1.4 g ethanol).¹⁸²

4.1.1.2. Effect of Cs doping on the CuO/ZnO catalyst

As an alternative to Ru doping, Cs was investigated as a promoter. In comparison to Ru, Cs proved to be more effective. Cs-containing catalysts increased the yield of higher alcohols compared to the standard catalyst, regardless of the reaction conditions used. The effect of Cs was particularly more pronounced for the ethanol free reaction and the reaction with $n_{EtOH} : n_{CO} = 0.5:1$ compared to the ratio of $n_{EtOH} : n_{CO} = 10.0:1$. To simplify the understanding of the data, the effect of Cs will be presented separately for the different reaction conditions.

Ethanol free conditions: To compare the effect of Cs doping with literature data presented in the introduction section, catalytic tests in the absence of ethanol were performed. Figure 20 presents the effect of different levels of Cs doping on the product yield in the synthesis of higher alcohols for these conditions. The influence of Cs promotion on the alcohol selectivity is displayed in Figure 21. In agreement with literature^{153, 163, 167, 170, 190}, Cs doping favored the production of higher alcohols in comparison to the standard catalyst. The presence of Cs induced a change in the reaction mechanism towards a chain growth process. Cs loadings between 0.3 and 1.0 mol.% resulted in the most favorable doping. The higher alcohols yield

for these catalysts increased to values between 2.2 and 2.5 %-C. As the Cs content on the catalyst was further increased to 3.0 mol.% Cs, the CO conversion decreased again to a value similar as for the standard catalyst. H₂-TPR presented in section 3.1 (Figure 8) back up these results since copper is significantly more difficult to reduce and probably Cs blocked the copper sites in this catalyst. In terms of conversion and selectivity towards higher alcohols a Cs loading of 0.3 - 1.0 mol.% was also ideal (Figure 21). The conversion increased up to 59 % (0.6 mol.% Cs doping) and the selectivity up to 4.6 %-C (1 mol.% Cs loading) in comparison to 29 % and 1.4 %-C for the undoped catalyst, respectively. In agreement with the reaction mechanism proposed in literature^{161, 162}, Cs doping enhanced the 1-propanol and 2-methyl-1-propanol yields.

Even for the standard catalyst a rather low methanol selectivity was observed most probably explained by the higher reaction temperature (593 K vs. typically 493 - 523 K in methanol synthesis)²⁴, the lower H₂ : CO ratio of 1:1^{41, 156} and the long residence times in the batch reactor.^{156, 191} Nevertheless, in comparison to the selectivity towards higher alcohols, as observed in Figure 21, methanol was favored by the standard catalyst reaching a selectivity of 3.1 %-C. The reaction conditions played an important role in directing the product distribution. Lower temperatures favored methanol synthesis whereas higher temperatures shifted the selectivity towards higher alcohols (and CO₂).^{156, 161, 191} In comparison to continuous processes, reactions in batch reactors are performed using higher residence time, which may enhance further reactions, i.e. chain growth (higher alcohols), side reactions to methane or other hydrocarbons and oxygenates. The methanol synthesis rate does not only depend on the temperature and residence time; the water amount in the reaction mixture and the Cs content on the catalyst are also important factors.¹⁹² Higher water contents could lower the yields of methanol. The methanol yield remained unchanged for a Cs doping of 0.3 - 0.6 mol.% (1.1 and 0.9 %-C, respectively) and the standard catalyst (0.9 %-C), but it decreased for higher Cs loadings. In general, higher Cs loadings resulted in a decrease of the overall yield of the desired products from 2.5 %-C (0.6 mol.% Cs) to 0.2 %-C (3.0 mol.% Cs). As derived from the H₂-TPR results, the hydrogenation ability at the Cu/ZnO was hindered by Cs impregnation. This inhibited the bifunctionality required for an active catalyst. In addition, the conversion to calibrated products decayed (Table S 6 and Table S 7). A maximum yield of higher alcohols for Cs doping between 0.3 - 0.5 mol.% Cs for Cu/ZnO based catalysts in a fixed-bed continuous-flow reactor was also reported by Nunan et al.¹⁵³.

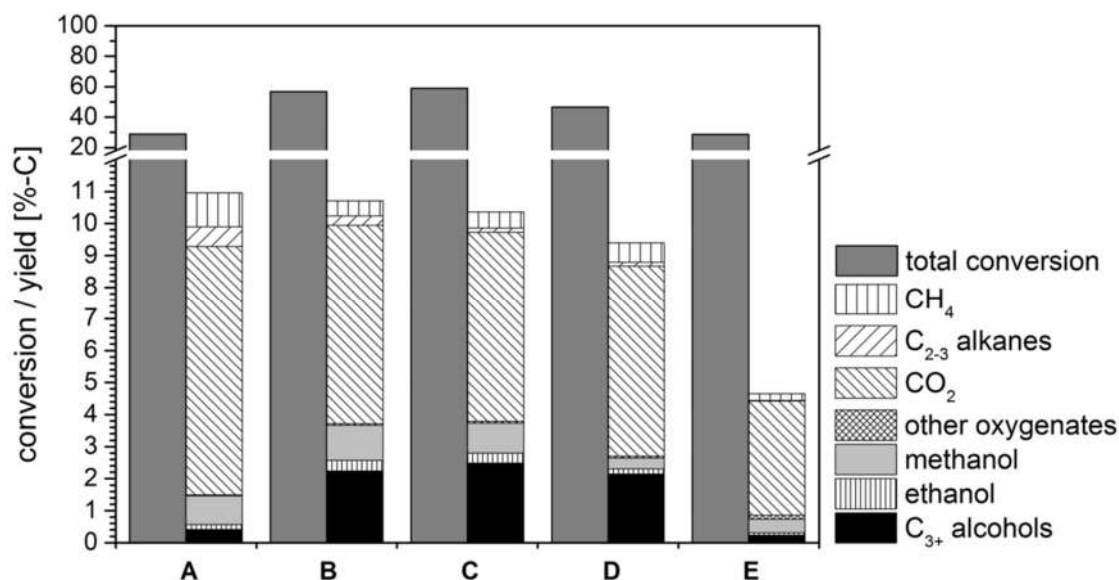


Figure 20: Product yield in the higher alcohols synthesis with $H_2:CO=1:1$ at 593 K, 5.0 MPa in the absence of ethanol over 1 g of the following catalysts: A: CuO/ZnO, B: 0.3 mol.% Cs-CuO/ZnO, C: 0.6 mol.% Cs-CuO/ZnO, D: 1.0 mol.% Cs-CuO/ZnO and E: 3.0 mol %Cs-CuO/ZnO (reaction time = 3 h, liquid phase= 30 g cyclohexane).¹⁸²

As outlined in the introduction (section 1.4.2), Cs-doped CuO/ZnO catalysts follow a different mechanism in comparison to non-promoted catalysts in the higher alcohol synthesis. Cs presence favors an aldol-type condensation, which facilitates the formation of branched alcohols as termination products. On Cs-modified catalysts, the preferred path for ethanol formation is proposed as the reaction of two methanol-derived species.^{41, 153, 163, 167, 170} Subsequent C-C bond formation reactions between C_{2+} intermediates (derived from ethanol or higher alcohols) and oxygen-containing C_1 -species can occur via aldol-like reactions.^{153, 167, 170}

In accordance with the proposed mechanism, the main higher alcohol product in terms of yield and selectivity was 2-methyl-1-propanol (Figure 21, Table S 6 and Table S 7 in the supporting information). It is formed by an aldol-type reaction via insertion of formyl or formate intermediates (originated from methanol) to the β -carbon atom of an adsorbed alcohol (originated from 1-propanol). This alcohol is the preferred termination product due to steric and electronic effects.¹⁵³ 1-propanol could be either formed by linear insertion of a C_1 intermediate to an ethanol derivate or by an aldol-type condensation of an oxygen containing C_1 -species to an adsorbed ethanol derivate. Two types of aldol-type condensations have been proposed by Nunan et al.¹⁵³ depending from which species the oxygen during the aldol condensation was retained. If the oxygen of the adsorbed alcohol was retained it was termed a normal aldol coupling, whereas it was named aldol coupling with oxygen retention reversal if the oxygen of the C_1 intermediate was retained. The retention of the oxygen containing C_1

intermediate is particularly favored during the chain growth step from ethanol to 1-propanol when Cs is present in the catalyst.¹⁶² This type of aldol-type condensation is faster than the linear chain growth and therefore would enhance the production of higher alcohols. Cs cations enabled the bonding of the β -ketoalkoxide intermediate via its anionic oxygen allowing the full hydrogenation of the keto group.^{153, 157, 162}

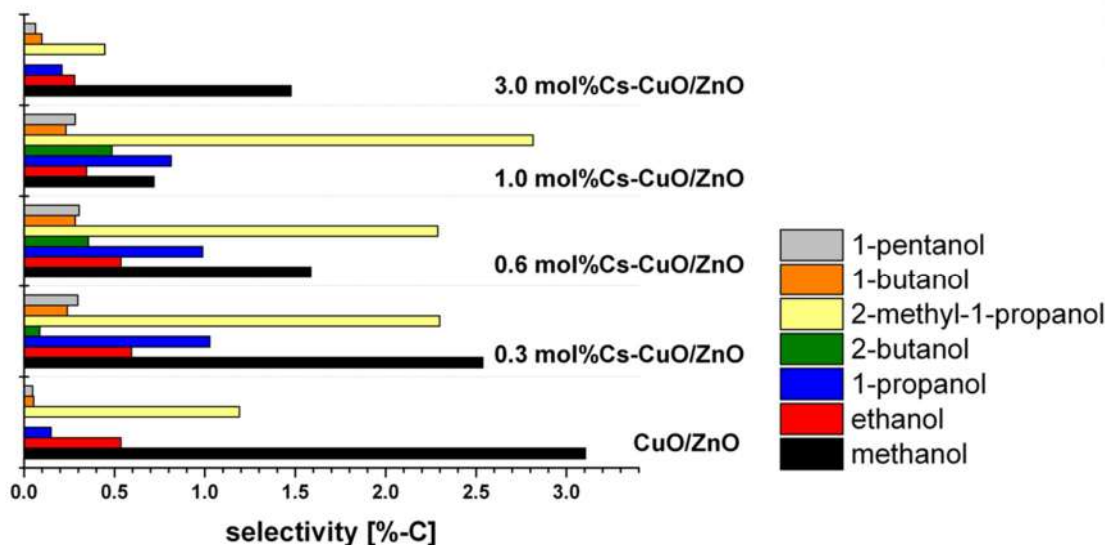


Figure 21: Alcohol selectivity in the higher alcohols synthesis with $H_2:CO=1:1$ at 593 K, 5.0 MPa in the absence of ethanol over 1 g of the following catalysts: A: CuO/ZnO, B: 0.3 mol.% Cs-CuO/ZnO, C: 0.6 mol.% Cs-CuO/ZnO, D: 1.0 mol.% Cs-CuO/ZnO and E: 3.0 mol.% Cs-CuO/ZnO (reaction time = 3 h, liquid phase= 30 g cyclohexane).

For the chain growth from 1-propanol to 2-methyl-1-propanol both types of aldol-type condensation occurred almost in an equal way.¹⁵³ Other quantified higher alcohols were 2-butanol, 1-butanol, 1-pentanol and 1-hexanol (traces). Their yields and selectivities were also maximized at a Cs-dopings between 0.3 and 1.0 mol.% (Table S 6 and Table S 7 in the supporting information). For a doping of 3 mol.% Cs the yield of 2-butanone increased from 0.03 - 0.06 %-C (standard catalyst and Cs doping below 1.0 mol.%) to 0.12 %-C. The homocoupling of ethanol leads to formation of 2-butanone or after subsequent hydrogenation 2-butanol.¹⁹³ Even though the 3.0 mol.% Cs-CuO/ZnO catalyst produced 2-butanone, it was not further hydrogenated extensively to 2-butanol, probably as a consequence of the blocking of the hydrogenation sites by Cs. Regarding the gaseous products, Cs doping lowered the yields and selectivities towards carbon dioxide, methane, ethane and propane (Table S 6 and Table S 7 in the supporting information).

The gas phase composition did not change as significantly as the liquid products as a function of Cs content on the catalyst. Nevertheless, among the calibrated reaction products, the yield

of gaseous products was larger than that of the liquid phase products. The gaseous side product with the most significant yield was CO₂, which was probably formed via the water gas shift reaction (Eq. 4) or the reduction of the catalyst with CO. Klier et al.¹⁹² showed that Cs doping on Cu/ZnO promotes the water gas shift reaction. The necessary water for the shift reaction was produced either during the reduction of the catalysts with hydrogen or via the alcohol synthesis reactions (Eq. 17, Eq. 18 and Eq. 20). The water gas shift reaction might be to a certain extent favorable because it removes water from the surface of the catalyst. The water formed during the reaction could potentially contribute to the thermal sintering of the catalyst. Methane yield decreased with Cs content in the catalyst from 1.1 to 0.2 %-C for CuO/ZnO and 3 mol.% Cs-CuO/ZnO, respectively. The decrease was not linear, e.g. it remained at 0.5 - 0.6 %-C from 0.3 to 1.0 mol.% Cs-CuO/ZnO.

n_{EtOH} : n_{CO} = 0.5:1 conditions: Figure 22 presents the effect of ethanol in a ratio of $n_{EtOH} : n_{CO} \sim 0.5:1$ on the product yields during the higher alcohols synthesis for Cs promoted CuO/ZnO catalysts. In general, the selectivity and yield towards higher alcohols was favored when ethanol was present indicating that ethanol or ethanol derivatives ameliorate the chain growth to higher alcohols as also reported by Nunan et al.¹⁶²

In comparison to the reactions in the absence of ethanol, the yield towards higher alcohols increased up to 12.8 %-C (0.6 mol.% Cs-CuO/ZnO). However, side reactions were also enhanced to result in mainly oxygenated products, especially esters like ethyl acetate and butyl acetate and ketones like 2-butanone. For example, the yield towards higher oxygenates increased from 0.1 %-C to 2.3 %-C for the 1 mol.% Cs-doped catalyst when ethanol was added in a ratio $n_{EtOH} : n_{CO} \sim 0.5:1$. The alcohol distribution also changed, and 2-methyl-1-propanol was not the main higher alcohol product. Instead the selectivity was shifted to 1-propanol, 2-butanol and 1-butanol, which underline the fast C-C-formation reaction with ethanol. Additionally, similar products as reported by Beretta et al.¹⁶⁴ over Cs-promoted Zn-Cr-oxide based catalysts were detected, e.g., 2-methyl alcohols and ketones (3-pentanone). This supports the occurrence of aldol-type condensation reactions. Hence, 1-propanol was the most favored product for Cs doping between 0.6 - 3.0 mol.% (yields between 4.9 - 6.9 %-C). For the 0.3 mol.% Cs catalyst, 1-propanol (3.9 %-C) and 2-butanol (4.4 %-C) were produced to a similar extent. The undoped catalyst preferred the production of 2-butanol (3.5 %-C) instead of 1-propanol (1.4 %-C). Interestingly, also the 3.0 mol.% Cs catalyst, which was not particularly active in the production of higher alcohols during the ethanol free reaction, showed a similar yield of 1-propanol (4.9 %-C) and produced 1-butanol (2.1 %-C) as the second preferred higher

alcohol product. From the marked increase of 1-propanol after adding ethanol to the reaction, we can conclude that ethanol rapidly reacted with the C₁ products. Mechanisms based on aldol-type reactions with C-C bond formation via β-carbon addition of C₁ intermediates^{153, 170} would result in the synthesis of mainly 2-methyl-1-propanol as a termination product. The presence of ethanol, however, seemed to deteriorate this route. Probably aldol-type reactions continued to be favored, but instead of the addition of an oxygen containing C₁ intermediate, oxygen containing C₂ intermediates could also be added leading to 1-butanol and 2-butanol directly.

As for the ethanol free reactions, during the aldol-type coupling, the oxygen could be retained either from the adsorbed alcohol or the oxygen containing intermediate. If the oxygen from the C₂ intermediate was retained, 2-butanol was formed as a product. If the oxygen from the adsorbed alcohol was retained, 1-butanol was formed. Another product that was not formed during the ethanol free reactions is 2-propanol, which might have been formed by the hydrogenation of acetone. Acetone could be produced directly from ethanol as suggested by Gines and Iglesia.¹⁹³ In comparison to the ethanol free reaction, the yield of 2-methyl-1-propanol decreased for the catalysts with Cs doping between 0.3 - 1.0 mol.% (for example, for the 0.6 mol.% Cs-doped catalyst it decreased from 1.3 %-C to 0.8 %-C), but was maintained for the standard catalyst (0.3 to 0.4 %-C). Methyl propionate was identified for the 3.0 mol.% Cs-doping (by GC-MS) instead of 2-methyl-1-propanol. Finally, also the methanol yield and selectivity were different from the tendency observed for the ethanol free reaction (Figure 20 and Figure 21). Increasing Cs doping enhanced the selectivity towards methanol except for 0.3 mol.% Cs doping. The selectivity and yield towards 2-butanol was also enhanced under the reaction conditions employed (Table S 8 and Table S 9 in the supporting information) supporting the reaction pathway proposed by Gines and Iglesia.¹⁹³

As a consequence of ethanol addition, side products were enhanced as mentioned in the previous paragraphs, but particularly ketones and esters. Elliot and Penella¹⁹⁴ investigated CuO/ZnO/Al₂O₃ catalysts in the reaction of linear primary alcohols under different gas atmospheres (N₂ or CO) and studied the influence of the conditions on the selectivity of oxygenates. The experiments were conducted at a temperature of 558 K and pressures of 0.1 or 6.5 MPa using a fixed bed reactor. According to the authors, the main condensation products of the reaction of a C_nH_{2n-1}OH alcohol (n: 2 - 4) were the corresponding aldehydes, esters with 2n carbon atoms and ketones with 2n or 2n-1 carbon atoms. For reactions at 6.5 MPa using N₂ atmosphere the preferred products were the esters, whereas under the same conditions but using CO the ketones with 2n carbon atoms predominated.

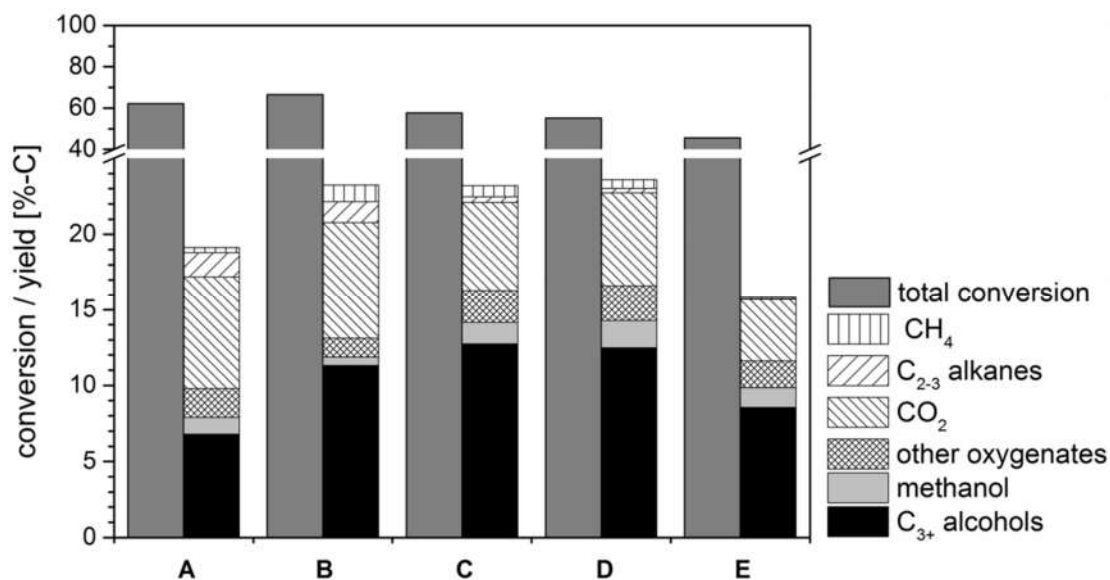


Figure 22: Product yield in the higher alcohols synthesis with $\text{H}_2 : \text{CO} = 1:1$ and $n_{\text{EtOH}} : n_{\text{CO}} \sim 0.5:1$ at 593 K, 5.0 MPa over 1 g of the following catalysts: A: CuO/ZnO, B: 0.3 mol.% Cs-CuO/ZnO, C: 0.6 mol.% Cs-CuO/ZnO, D: 1.0 mol.% Cs-CuO/ZnO and E: 3.0 mol.% Cs-CuO/ZnO. (reaction time = 3 h, liquid phase = ~28.6 g cyclohexane and ~1.4 g ethanol).¹⁸²

The results presented by Elliot and Penella¹⁹⁴ agreed well with the products formed during the reactions with a $n_{\text{EtOH}} : n_{\text{CO}}$ ratio of 0.5:1. Ethyl acetate and 2-butanone were detected as the main oxygenate products, while acetaldehyde and acetone could not be found. Acetaldehyde was formed from the dehydrogenation of ethanol. It is expected to react rapidly by acting as an intermediate. Ethyl acetate can form via acetaldehyde reactions with ethanol¹⁹³ and it was not a significant product for the ethanol free reaction. The production of acetaldehyde¹⁹⁵ and ethyl acetate was also detected during the ethanol steam reforming on Cu/ZnO/Al₂O₃ catalysts for temperatures under 600 K.¹⁹⁶ Oxygenates were particularly favored for catalysts containing 30 wt.% copper. The authors suggested that acetaldehyde formation is favored by longer contact times and it was considered as the first step of a two-step reaction. The second step, depending on the content of water in the reacting mixture, could be shifted towards ethyl acetate (low content) or acetic acid (high content). The formation of ethyl acetate was more related to the temperature and conversion, whereas acetic acid formation depended mostly on the water content. Since CO was present in the reaction mixture a low content of water was expected as a consequence of the water gas shift reaction, accordingly ethyl acetate was favored as a product instead of acetic acid under the reaction conditions used during this study. 2-Butanone was formed by the self-condensation of acetaldehyde followed by the dehydration/hydrogenation of the keto form.¹⁹³

The yield of gaseous products was similar to that observed under the ethanol free conditions (Table S 7 and Table S 9 in the supporting information), but the ethane yield and selectivity were increased for all the catalysts due to dehydration/hydrogenation reactions.

$n_{EtOH} : n_{CO} = 10.0:1$ conditions: Further increase of the $n_{EtOH} : n_{CO}$ ratio to 10.0:1 led to a pressure after heating up to 593 K which was 10 MPa higher (Figure 17) compared to the pressure when cyclohexane was used as reaction medium (ethanol free and $n_{EtOH} : n_{CO} \sim 0.5:1$ reaction conditions). As depicted in Figure 23, the yield of higher alcohols decreased to 3 - 5 %-C and the production of ethyl acetate increased abruptly to 13 - 17 %-C. The raise in the selectivity towards ethyl acetate could occur as a consequence of the pressure increase.¹⁹⁷ Under these conditions, homocoupling of ethanol or its derivatives as well as redox-reactions resulted in ethyl acetate, 1-butanol, 2-butanol, 2-butanone and ethane. Hardly any production of higher alcohols via homologation, e.g. to 1-propanol, was found (Table S 11 and Table S 12).

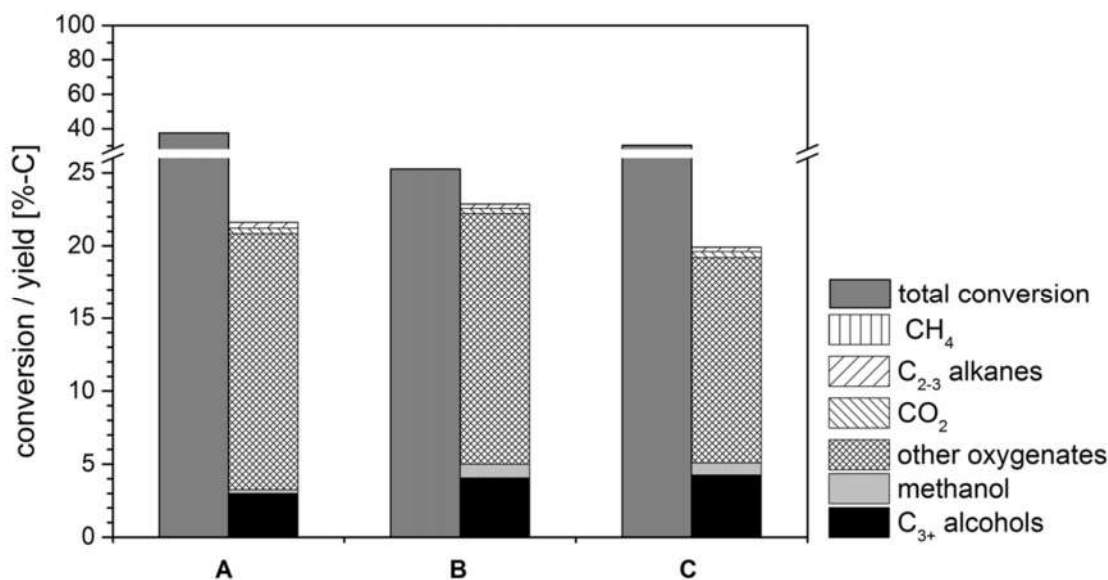


Figure 23: Product yield in the higher alcohols synthesis with $H_2 : CO=1:1$ and $n_{EtOH} : n_{CO} \sim 10.0:1$ at 593 K, 5.0 MPa over 1 g of the following catalysts: A: CuO/ZnO, B: 0.3 mol.% Cs-CuO/ZnO, C: 0.6 mol.% Cs-CuO/ZnO. (reaction time = 3 h, liquid phase= 30 g ethanol).¹⁸²

As for the other reaction conditions, Cs enhanced the yield of higher alcohols but increased the formation of side products at the same time. The yields towards the principal higher alcohol products were 2-butanol (1.7 - 2.2 %-C) and 1-butanol (0.6 - 1.9 %-C), but also the yields were lower than for the $n_{EtOH} : n_{CO} \sim 0.5$ reaction conditions. Probably, 2-butanol and 1-butanol were formed from ethanol through coupling reactions, which also explained its presence at $n_{EtOH} : n_{CO} = 0.5:1$ conditions.^{193, 198, 199} Hydrogen was the main constituent of the gaseous phase (\sim

80 mol.%). It was most probably produced during the ethyl acetate formation. The main carbon containing gaseous phase products were CO₂ and ethane, but their yields decreased considerably. The preference to form ethyl acetate instead of 2-butanone as a side product under these reactions conditions could be merely an effect of the pressure increase or a consequence of the solvent used for each reaction. Ethanol is a polar protic solvent in comparison to cyclohexane which is an apolar solvent. This change in polarity could lead to other intermediates favoring the ester formation.

In summary, compared to the experimental data on Ru presented in section 4.1.1.1, Cs was proven to be a more appropriate dopant in the syntheses of higher alcohols with CuO/ZnO catalysts regardless of the $n_{\text{EtOH}} : n_{\text{CO}}$ ratio used. Cs as dopant enhanced the synthesis of higher alcohols by shifting the reaction mechanism to an aldol-type coupling of oxygen containing C₁ intermediates with adsorbed alcohols. An optimum level of Cs on the catalyst was found to be between 0.3 and 1.0 mol.% for all tested reaction conditions. The shift in the reaction mechanism led to the formation of 2-methyl-1-propanol as the final step in the ethanol free reaction. As ethanol was added to the reaction medium, the product distribution shifted and 1-propanol, 2-butanol and 1-butanol were the preferred products. As a consequence of ethanol addition also side products were enhanced, particularly ketones and esters.

4.1.2. Influence of ethanol to carbon monoxide ratio

Figure 24 compares the CuO/ZnO and 0.3 mol.% Cs-CuO/ZnO catalysts, respectively, under all reaction conditions used. Additionally, a $n_{\text{EtOH}} : n_{\text{CO}}$ ratio of $\sim 0.9:1$ experiment was performed to analyze the effect of the $n_{\text{EtOH}} : n_{\text{CO}}$ ratio in the product distribution while a synthesis gas-free experiment was used to elucidate the participation of CO in the reaction path. Figure 25 presents the alcohol selectivity for the different reaction conditions. More details on the product yield and selectivities for the different reaction conditions can be found in the supporting information (Table S 6 to Table S 12).

The optimal $n_{\text{EtOH}} : n_{\text{CO}}$ ratio for maximizing the yield of higher alcohol was found to be $\sim 0.9:1$ (reaction C in Figure 24) resulting in a yield of 10 %-C and 16 %-C selectivity for the CuO/ZnO catalyst and a yield of 12 %-C and 21 %-C selectivity for the 0.3 mol.% Cs-CuO/ZnO catalyst. Nevertheless, these reaction conditions also favored the synthesis of higher oxygenates (yield: 2.9 %-C and 8.1 %-C, respectively), but to a lesser extent than that of higher alcohols. This result suggests that an optimal $n_{\text{EtOH}} : n_{\text{CO}}$ ratio is achievable where the yield of higher alcohols

is maximized and other side products are still in an acceptable range. The methanol yield appeared to be independent of the reaction conditions A-C. A high $n_{\text{EtOH}} : n_{\text{CO}}$ ratio inhibited the production of methanol in comparison to the other reaction conditions for the standard catalyst. In the absence of synthesis gas, no methanol was detected. Hence, methanol was probably solely produced from synthesis gas. Interestingly, the higher alcohol yield was higher in the absence of synthesis gas (Reaction E in Figure 24 (a) compared to reaction D with a ratio of $n_{\text{EtOH}} : n_{\text{CO}} = 10.0:1$).

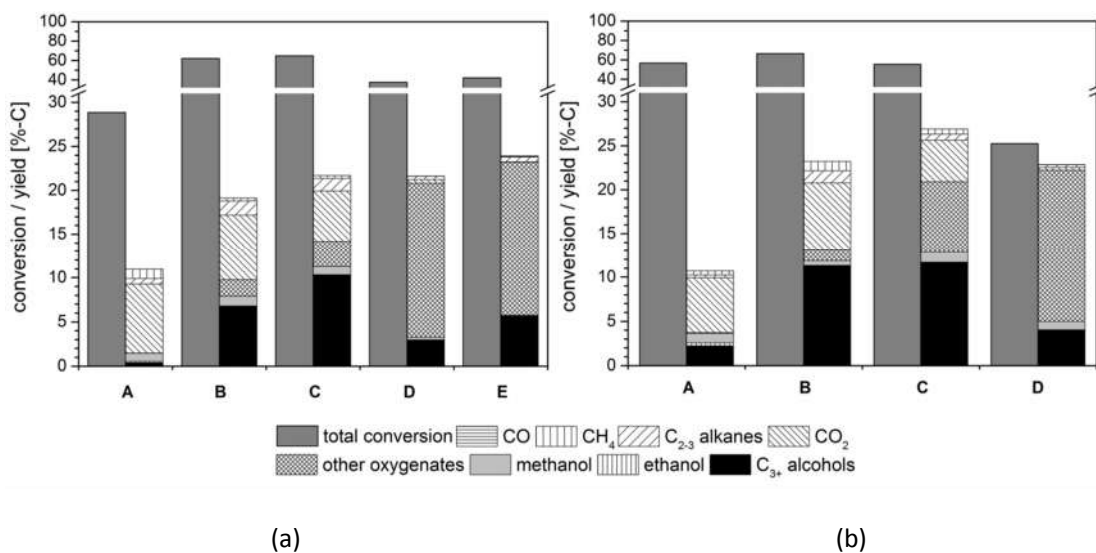


Figure 24: Product yield in the higher alcohols synthesis with $\text{H}_2 : \text{CO}=1:1$ (except: E (Ar) at 593 K, 5.0 MPa over 1 g of the following catalysts (a) CuO/ZnO and (b) 0.3 mol.% Cs-CuO/ZnO catalysts in the reactions: A: ethanol free, B: $n_{\text{EtOH}} : n_{\text{CO}} \sim 0.5:1$, C: $n_{\text{EtOH}} : n_{\text{CO}} \sim 0.9:1$, D: $n_{\text{EtOH}} : n_{\text{CO}} \sim 10.0:1$ and E: ethanol (in Ar, CO and H_2 - free); conditions: reaction time = 3 h, liquid phase: A= 30 g cyclohexane, B: ~28.6 g cyclohexane and ~1.4 g ethanol, C: ~27.5 g cyclohexane and ~2.5 g ethanol, D,E: 30 g ethanol.¹⁸²

The productivity increased with ethanol addition up to an $n_{\text{EtOH}} : n_{\text{CO}} = 0.9:1$. The alcohol selectivity changed as the amount of ethanol in the reaction medium was increased. Ethanol free reactions favored products derived from aldol-type coupling of C_1 intermediates. When an excess of ethanol was present, products derived from aldol-type coupling of C_2 intermediates were preferred. For intermediate ratios alcohols derived from both reaction paths were detected. In line with the observations in the previous sections, both Cs and ethanol addition had a beneficial effect on the synthesis of higher alcohols.

In general, the formation of all products derived from CO like CO_2 (from the water gas shift reaction) and methanol were reduced or completely inhibited for reactions with an excess of ethanol. Most probably the catalyst surface was covered completely by ethanol, hindering CO and H_2 adsorption on the active sites. This is also verified in Figure 26, since the reaction was

selective to ethanol derived products in a similar way, regardless of the presence of CO. The preference of ethyl acetate instead of 2-butanone as byproduct could also be related to the reduced hydrogenation ability of the catalyst surface. Adsorbed hydrogen is required for several steps in the formation of 2-butanone (acetaldehyde formation and alkene hydrogenation). The high selectivity towards 2-methyl-1-propanol for the reaction in Ar did not agree with the observed reaction path for the conditions used in Figure 26, since this alcohol is produced from an aldol type coupling of an oxygen-containing C₁ intermediate with an adsorbed 1-propanol derivate (both alcohols were not identified).

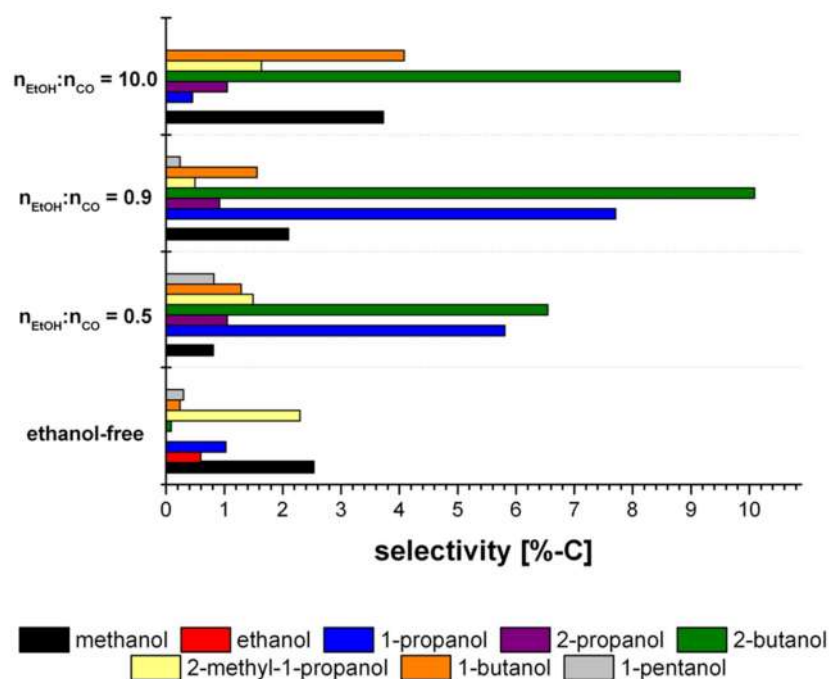


Figure 25: Alcohol selectivity in the higher alcohols synthesis with H₂ : CO=1:1 at 593 K, 5.0 MPa over 1 g of 0.3 mol.% Cs-CuO/ZnO catalyst in the reactions: ethanol free (30 g cyclohexane), n_{EtOH} : n_{CO} ~ 0.5:1 (~28.6 g cyclohexane and ~1.4 g ethanol), n_{EtOH} : n_{CO} ~ 0.9:1 (~27.5 g cyclohexane and ~2.5 g ethanol) and n_{EtOH} : n_{CO} ~ 10.0:1 (30 g ethanol); conditions: reaction time = 3 h.

In section 4.1.1.2., the changes in the product distribution towards 1-propanol, 2-butanol and 1-butanol were explained through a shift from an aldol-type coupling of oxygen containing C₁ intermediates, to an aldol-type coupling of oxygen containing C₂ intermediates with adsorbed alcohols. The optimal n_{EtOH} : n_{CO} ratio was found to be 0.5:1, which increased the higher alcohols production, but still did not significantly enhance the synthesis of side products.

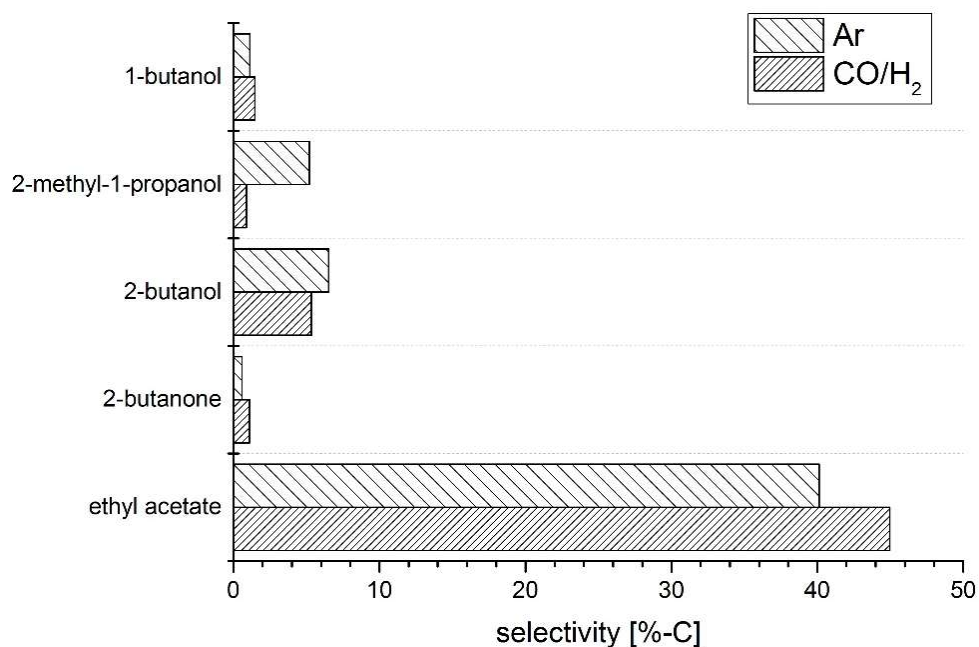


Figure 26: Selectivity in the higher alcohols synthesis at 593 K, 5.0 MPa over 1 g of CuO/ZnO catalyst for the reaction with $n_{\text{EtOH}} : n_{\text{CO}} \sim 10.0:1$ in $\text{H}_2 : \text{CO}=1:1$ or Ar; conditions: reaction time = 3 h, liquid phase: 30 g ethanol.

4.1.3. Influence of reaction temperature

After identifying the most suitable catalyst and $n_{\text{EtOH}} : n_{\text{CO}}$ ratio, the influence of the reaction temperature (533, 563 and 593 K) was tested using a 1 mol.% Cs-CuO/ZnO catalyst and the 200 ml batch reactor. Yields and conversions of CO and ethanol, respectively, are presented in Figure 27 and Table 11, respectively. In Figure 28, the alcohol selectivity as a function of temperature is displayed. More details regarding the yields and selectivities are presented in the supporting information (Table S 13).

In general, both the CO and ethanol conversion increased with temperature (Table 11). Ethanol conversion was dominant in comparison to CO conversion. At 593 K, ethanol conversion reached 65 %, whereas CO conversion was 30 % and therefore more products involving reactions of ethanol or its derivatives were expected. The yield towards higher alcohols also increased with temperature, in addition to an increase in the side products (mostly CO₂ and other oxygenates). The methanol yield did not follow the expected trend for a methanol synthesis catalyst, since the yield at 533 K was lower than at higher temperatures. Nevertheless, the methanol selectivity did follow the expected tendency as presented in Figure 28. Lower temperatures favored methanol instead of longer-chain alcohols. At 533 K, only products obtained by aldol-type coupling of oxygen containing C₁ intermediates to alcohols derivatives

were observed, such as 1-propanol and 2-methyl-1-propanol. As the temperature was increased, also 1-butanol and 2-butanol were present among the formed products, most probably by an aldol-type coupling of oxygen containing C₂ intermediates with ethanol derivatives.

Table 11: Effect of temperature on the carbon balance, CO-conversion and ethanol conversion in the higher alcohols synthesis ($n_{\text{EtOH}} : n_{\text{CO}}=0.5:1$) using a 1 mol.% CuO/ZnO catalyst in a 200 ml batch reactor.

Temperature [K]	Units	533	563	593
C-balance	%	88.4	74.1	70.7
CO conversion	%-C	1.8	15.9	30.4
Ethanol conversion	%-C	29.0	48.8	63.7

The selectivities obtained using the 200 ml autoclave did not correspond exactly with the results obtained for the 100 ml batch reactor (Figure 28, Table S 13 and Table S 8). In general, the same type of products were formed, but the yields and selectivities differed from each other. For example, for the 200 ml reactor the selectivities for methanol, 1-propanol and 2-butanol were 7.5, 8.7 and 1.6 %-C, respectively. In contrast, for the 100 ml autoclave they resulted in 3.3, 11.4 and 5.9 %-C for the same products. Note that the amount of catalyst contained in the reactor was different for each reaction.

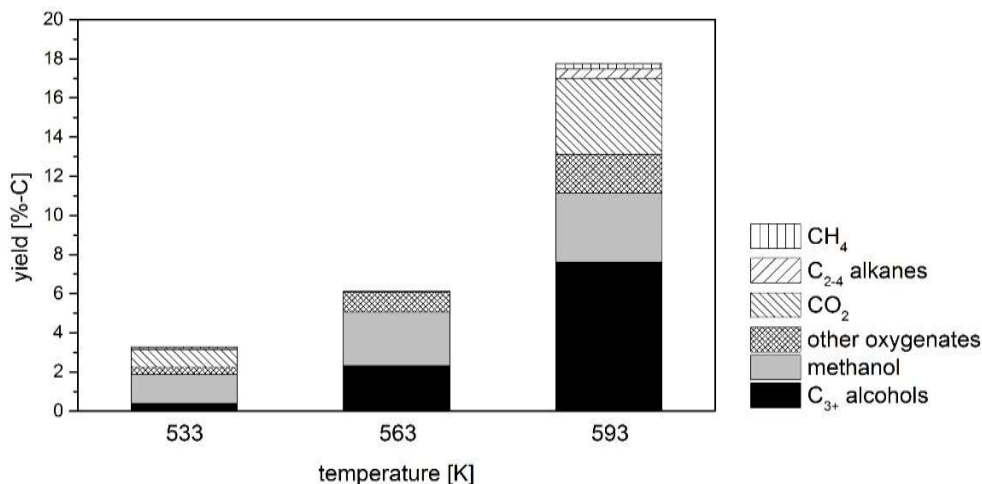


Figure 27: Influence of temperature on the product yields in the higher alcohol synthesis with H₂ : CO=1:1, 5.0 MPa over 0.5 g of 1.0 mol.% Cs-CuO/ZnO catalyst in the reaction $n_{\text{EtOH}} : n_{\text{CO}} \sim 0.5:1$ (~47.4 g cyclohexane and ~2.6 g ethanol); conditions: reaction time = 3 h.

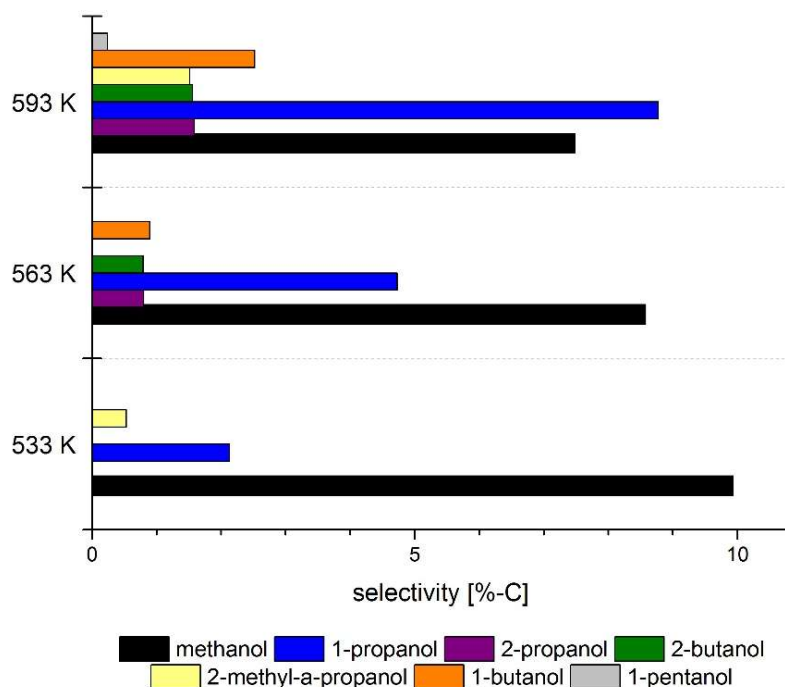


Figure 28: Influence of temperature on the alcohol selectivity in the higher alcohol synthesis with H_2 : $CO=1:1$, 5.0 MPa over 0.5 g of 1.0 mol.% Cs-CuO/ZnO catalyst in the reaction $n_{EtOH} : n_{CO} \sim 0.5:1$ (~47.4 g cyclohexane and ~2.6 g ethanol); conditions: reaction time = 3 h.

4.1.4. Catalyst characterization after catalytic tests

The catalysts were characterized after the different reactions to elucidate the relationship between the catalytic activity and selectivity and the properties of each catalyst. The total surface area of selected catalysts after the different reactions is presented in Table 12. The variation of the reaction medium altered to a different extent the total surface area.

Table 12: Specific surface areas of selected catalysts after reaction.

Catalyst	After reaction			
	Ethanol free	$n_{EtOH} : n_{CO} \sim 0.5$	$n_{EtOH} : n_{CO} \sim 10.0$	Ethanol in Ar (CO and H ₂ -free)
	[m ² /g]	[m ² /g]	[m ² /g]	[m ² /g]
CuO/ZnO	34	40	6	11
0.6 mol.% Cs-CuO/ZnO	32	23	14	n.d.
3.0 mol.% Cs-CuO/ZnO	11	14	n.d.	n.d.
0.5 mol.% Ru-CuO/ZnO	45	21	n.d.	n.d.

n.d.: not determined.

In general, the surface area was lower after the reaction in comparison to the data presented in section 3.1, Table 4. A high amount of ethanol had the largest effect on the surface area for both the undoped catalyst and the catalyst doped with 0.6 mol.% Cs. Note that upon shifting the reaction conditions to an excess of ethanol, the catalysts showed strong leaching (Table 13). The reduction in the specific surface area of the catalysts under these conditions might not only be due to a higher solvation of the leached ions but also by the intermediates involved in the ethyl acetate production, presumably also the formation of acetic acid.

Table 13: Elemental composition of selected catalysts after reaction determined by ICP-OES.

Catalyst	Ethanol free			$n_{\text{EtOH}} : n_{\text{CO}} \sim 0.5$			$n_{\text{EtOH}} : n_{\text{CO}} \sim 10.0$			Ethanol in Ar (CO and H ₂ -free)		
	[wt.%]			[wt.%]			[wt.%]			[wt.%]		
	Cs/Ru*	Cu	Zn	Cs/Ru*	Cu	Zn	Cs/Ru*	Cu	Zn	Cs/Ru*	Cu	Zn
CuO/ZnO	-	25.1	57.1	-	24.5	58.3	-	24.5	62.4	-	25.1	62.2
0.6 mol.% Cs- CuO/ZnO	1.0	25.0	59.7	0.9	28.0	62.5	0.1	25.8	62.0	n.d.	n.d.	n.d.

*Cs and Ru content measured by AAS. n.d.: not determined.

As presented in Table 13 and Table 14, the elemental composition of copper and zinc was not altered after the reactions in comparison to the data presented in Table 3, but the Cs in the catalysts leached for the $n_{\text{EtOH}} : n_{\text{CO}} \sim 10.0:1$ reactions. Even though it is not supported by the elemental analysis of the catalysts, the colorless solution turned turquoise evidencing contributions of leached Cu provoked by the ethanol or acids formed during the reaction. This was further verified by analyzing the liquid product using the standard catalyst. Copper and zinc were identified in the solution in a concentration of 330 $\mu\text{g/ml}$ and 120 $\mu\text{g/ml}$ ($n_{\text{EtOH}} : n_{\text{CO}} \sim 10.0:1$ reaction) and 60 $\mu\text{g/ml}$ and 610 $\mu\text{g/ml}$ (CO and H₂-free reaction) respectively. The leaching could be favored in the presence of liquid products after the cooling down of the reactor.

In Figure 29, the X-ray diffraction patterns for two selected catalysts are shown for the calcined form and after the different reactions. For the calcined samples, reflections attributable to CuO and ZnO were identified, whereas for the catalysts after the different reaction typical patterns for Cu and ZnO were found. The reflections for ZnO of the calcined samples were broader and less intense compared to those after reaction, which implies a growth of the particles during the reduction. Even though the catalyst was in oxidized form at the beginning of the reaction,

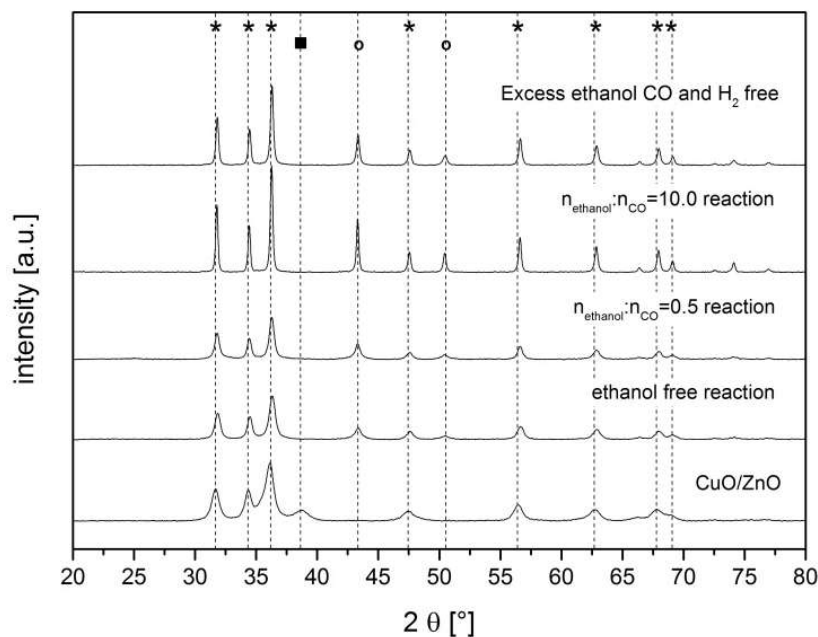
the reducing environment of the gas phase at 593 K successfully reduced the catalyst as it can be derived from Figure 29.

Table 14: Elemental composition of selected catalysts after reaction determined by ICP-OES.

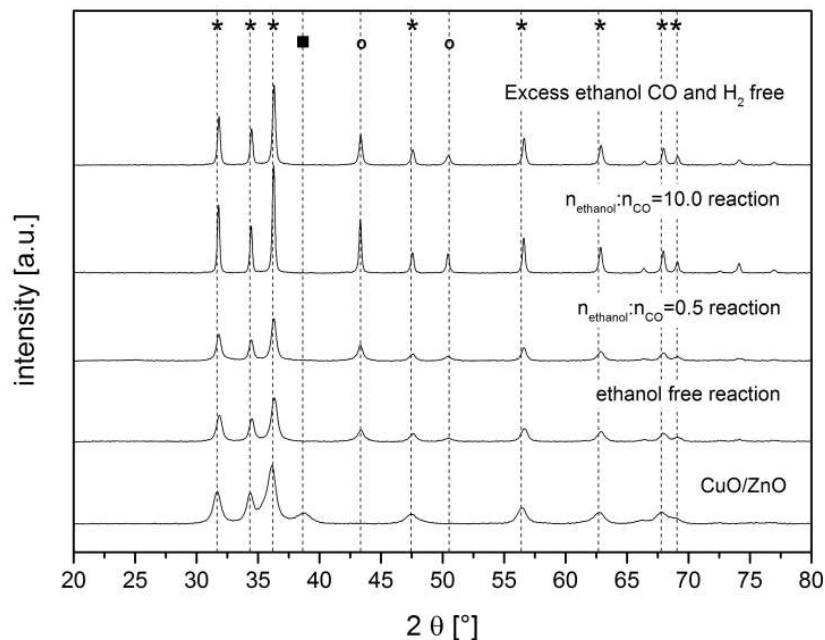
Catalyst	Ethanol free [wt.%]			$n_{\text{EtOH}}: n_{\text{CO}} \sim 0.5$ [wt.%]		
	Cs/Ru*	Cu	Zn	Cs/Ru*	Cu	Zn
3.0 mol.% Cs-CuO/ZnO	4.2	24.2	57.1	4.8	25.6	57.7
0.5 mol.% Ru-CuO/ZnO	0.5	26.2	60.8	0.5	27.1	58.2

*Cs and Ru content measured by AAS.

For the same catalyst, utilizing a high amount of ethanol as reaction medium increased the intensity of the reflections (Figure 29), which implies a growth in the copper particle size that was also verified by the calculation with the Scherrer equation presented in Table 15. These results are in agreement with the ones presented previously for the total surface area, which imply that the highly reactive ethanol medium did not only provoke leaching of the metals but also the sintering of the copper metal particles on the altered support. The sintering of the particles was less pronounced for the ethanol free reaction and conditions with $n_{\text{EtOH}}: n_{\text{CO}} = 0.5:1$. The sintering of the copper particles could be probably one of the main reasons for deactivation.²⁰⁰



(a)



(b)

Figure 29: X-ray diffraction patterns for (a) CuO/ZnO, (b) 0.6 mol.%Cs-CuO/ZnO fresh calcined and after the different reaction conditions. *: ZnO, ■: CuO and °: Cu.

The Cu and ZnO crystallite sizes for the used catalysts were estimated using the Scherrer equation (Table 15). As expected from the results of the specific surface area measurements, the ZnO crystallite size increased after the reaction; the same was found for copper due to the reduction of the catalyst. The most pronounced growth was observed for the the $n_{\text{EtOH}} : n_{\text{CO}} \sim 10.0:1$ reaction. The sintering was furthermore related to the Cs content in the catalysts. It was more pronounced for higher Cs doping for all reaction conditions, except for the reaction with $n_{\text{EtOH}} : n_{\text{CO}} \sim 10.0:1$.

Table 15: Crystallite size determined by the Scherrer equation of selected catalysts.

Catalyst	After ethanol free reaction		After $n_{\text{EtOH}}:n_{\text{CO}} = 0.5$ reaction		After $n_{\text{EtOH}}:n_{\text{CO}} = 10.0$ reaction	
	Cu	ZnO	Cu	ZnO	Cu	ZnO
	[nm]	[nm]	[nm]	[nm]	[nm]	[nm]
CuO/ZnO	11	14	15	22	54	48
0.6 mol.% Cs-CuO/ZnO	15	19	25	32	35	39
3.0 mol.% Cs-CuO/ZnO	29	27	50	36	n.d.	n.d.

n.d.: not determined. Particle size determined from reflections at $2\theta = 43^\circ$ for Cu and at $2\theta = 56^\circ$ for ZnO.

After the reaction with $n_{\text{EtOH}} : n_{\text{CO}} = 0.5:1$, the 0.6 mol.% Cs-CuO/ZnO was analyzed by means of TEM (Figure 30). A broad particle size distribution was obtained, with the majority of the

particles between 3 and 12 nm (average 10 nm). In the HRTEM images Cu was identified in [1 1 1] and [0 0 2] orientations. ZnO was found mainly in the [0 1 1] and [0 1 0] orientations, but also as presented in Figure 30 the [0 0 2] was observed. In agreement with the particle size determined by XRD, the average copper particle size increased after reaction in comparison to the copper oxide size obtained from HRTEM data before reaction.

Potential deactivation of the catalysts via carbonaceous deposits was discarded since TGA and ATR-IR analyses did not show any signs of coke formation (Figure 31 and Figure 32). Most probably they were removed through the reaction with CO, H₂, H₂O and CO₂.²⁰¹ The deactivation most likely occurred during the reaction due to thermal sintering of the copper species.

Thermogravimetric analysis was used to study the potential carbon deposition on the 0.6 mol.% Cs-CuO/ZnO catalysts after the reactions (ethanol free, $n_{\text{EtOH}} : n_{\text{CO}} = 0.5:1$ and $n_{\text{EtOH}} : n_{\text{CO}} = 10.0:1$). As a reference, the 0.6 mol.% Cs-CuO/ZnO catalyst was also analyzed to compare the results.

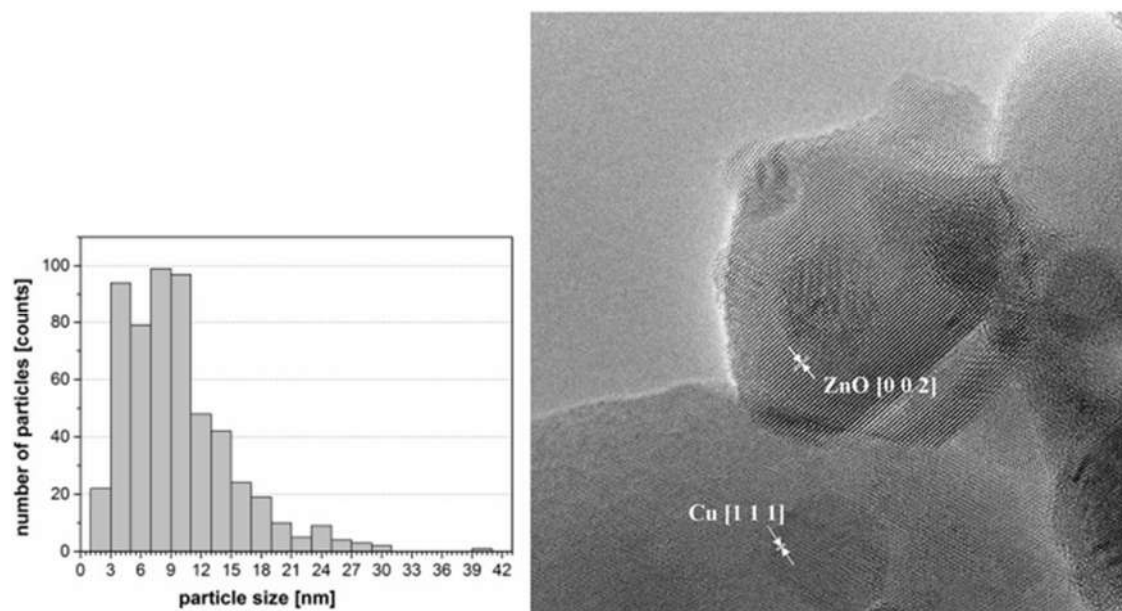


Figure 30: Particle size distribution and a selected HRTEM image of the 0.6 mol.% Cs-CuO/ZnO after the reaction with $n_{\text{EtOH}} : n_{\text{CO}} = 0.5:1$.

Below 423 K the mass losses could be attributed to water adsorbed on the surface of the catalysts (Figure 31). The reference catalyst showed a slight decrease of its mass (2%) until 873 K, afterwards a mass increase was observed. The catalyst after used in the ethanol free reaction featured the largest decrease in its mass in comparison to the reference catalyst, which

could indicate the presence of carbonaceous deposits on the surface of the catalyst. For the reaction conditions with ethanol present in the reaction medium, the catalyst initially gained weight which indicated its reoxidation. At temperatures higher than 573 K, for the catalyst after the $n_{\text{EtOH}} : n_{\text{CO}} = 0.5:1$ reaction a weight loss of approximately 2.5 % was observed. In the case of the catalyst after the $n_{\text{EtOH}} : n_{\text{CO}} = 10.0:1$ reaction, no further weight losses were identified after reoxidation. No strong evidence of carbonaceous deposits was found.

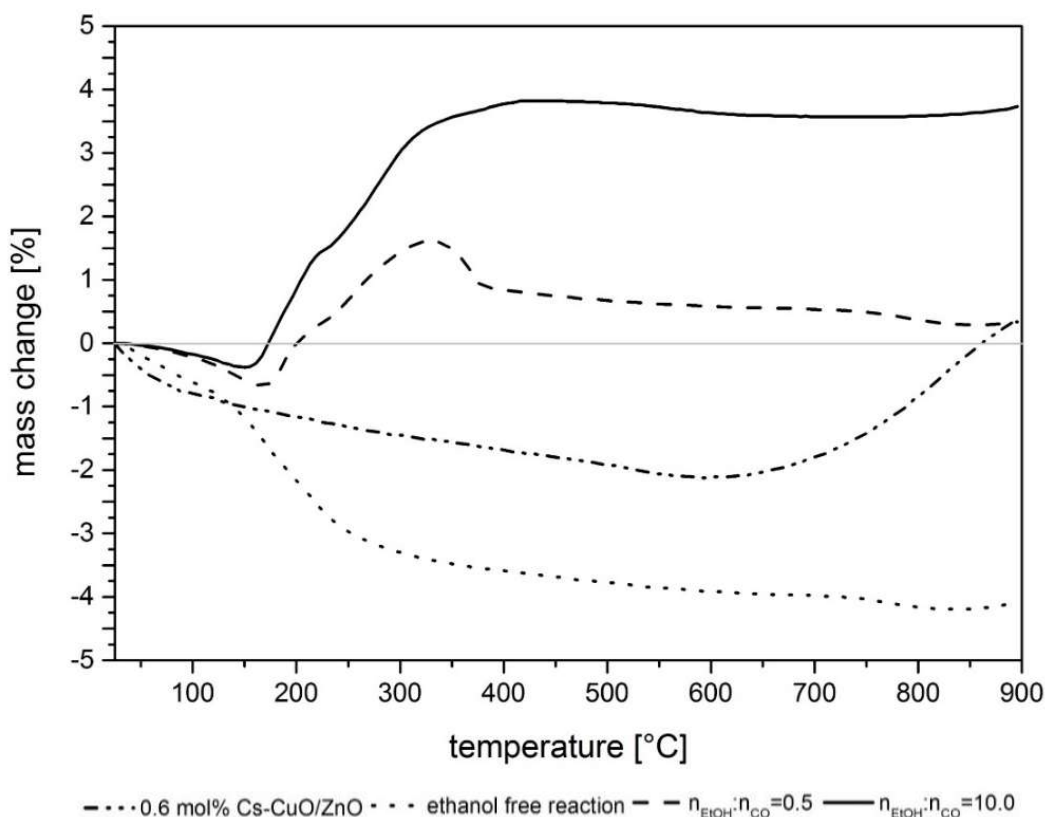


Figure 31: Thermogravimetric analysis of the calcined 0.6 mol.% Cs-CuO/ZnO catalyst and after the different reactions: ethanol free, $n_{\text{EtOH}} : n_{\text{CO}} = 0.5:1$ and $n_{\text{EtOH}} : n_{\text{CO}} = 10.0:1$. Conditions: heating rate= 10 K/min; T_{start} = room temperature $T_{\text{finish}}=1173$ K, under pure O_2 (60 ml/min, STP).

To additionally verify the absence of carbonaceous deposits, ATR-IR spectroscopy was used. The band around 1400 cm^{-1} could be either attributed to the skeleton vibration of CH in CH, CH_2 , or CH_3 in aliphatic groups²⁰² or bicarbonates. However, this band was not very pronounced and carbonate species may have formed after air exposure²⁰³.

In summary, after the reaction a particle growth was observed, as evidenced by TEM and XRD. No significant changes in the catalyst composition were found, but leaching was observed for $n_{\text{EtOH}} : n_{\text{CO}}$ ratio of 10.0:1. No evidence of deactivation due to the presence of carbonaceous deposits was identified.

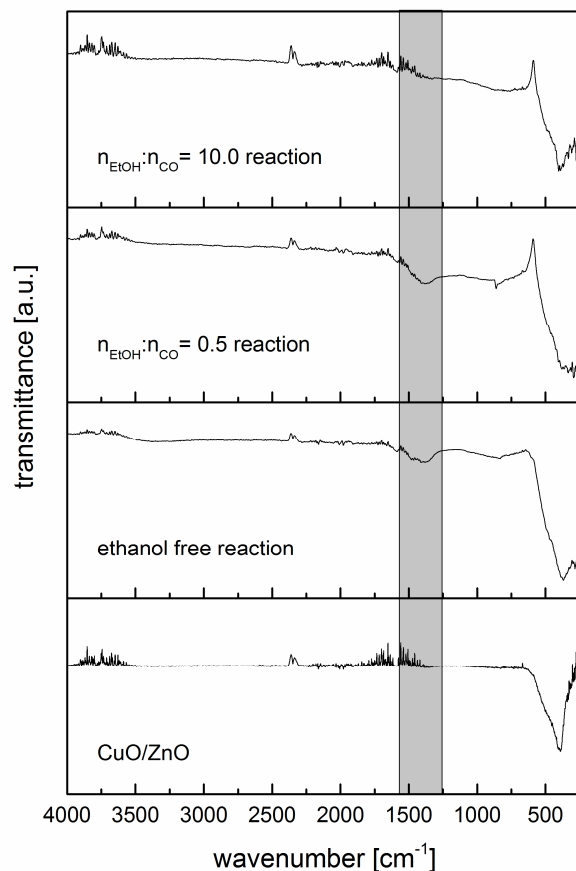


Figure 32: ATR-IR spectra of the calcined 0.6 mol.% Cs-CuO/ZnO catalyst and after the different reactions: ethanol free, $n_{\text{EtOH}} : n_{\text{CO}} = 0.5:1$ and $n_{\text{EtOH}} : n_{\text{CO}} = 10.0:1$.

4.1.5. Conclusions

The addition of ethanol to synthesis gas during the production of higher alcohols was systematically studied in a batch reactor on promoted Cu/ZnO catalysts. Cs promotion led to higher yields and selectivities towards higher alcohols compared to Ru, because the latter favored the formation of alkanes and alkenes via Fischer-Tropsch synthesis. The highest yields and selectivities towards higher alcohols were obtained for Cs doping between 0.3 - 1.0 mol.%. Higher Cs doping hampered the reducibility of the catalyst, as verified by the temperature programmed reduction experiments in section 3.1, affecting the catalyst performance. The addition of ethanol up to an optimum $n_{\text{EtOH}} : n_{\text{CO}}$ ratio of 0.5:1 was beneficial for the synthesis of higher alcohols, as the comparison of the ethanol free and ethanol containing conditions showed. At the optimum ratio the yield of higher alcohols was maximized with the side products being in an acceptable range.

A summary of the conclusions is presented in Figure 33. Compared to the classical synthesis conditions (no ethanol in the feed) the reaction proceeded via a mechanism preferentially involving the ethanol present in the feed for the C-C chain growth. Apparently, for the ethanol free reactions, predominantly aldol-type coupling of methanol derived C_1 intermediates with alcohol intermediates occurred, since the preferred product was 2-methyl-1-propanol. As ethanol was added, in addition to products formed by the reaction of ethanol derivatives with C_1 -intermediates (i.e. 1-propanol), also products formed via the homocoupling reaction of ethanol were also observed (i.e. 2-butanol and 1-butanol). When ethanol was present in an excess, mainly products formed from the homocoupling of ethanol were found. After the reaction with an excess of ethanol at a ratio of $n_{EtOH} : n_{CO} = 10.0 : 1$, sintering of the particles and leaching of Cu and Zn were found. No evidence of carbonaceous deposits was identified.

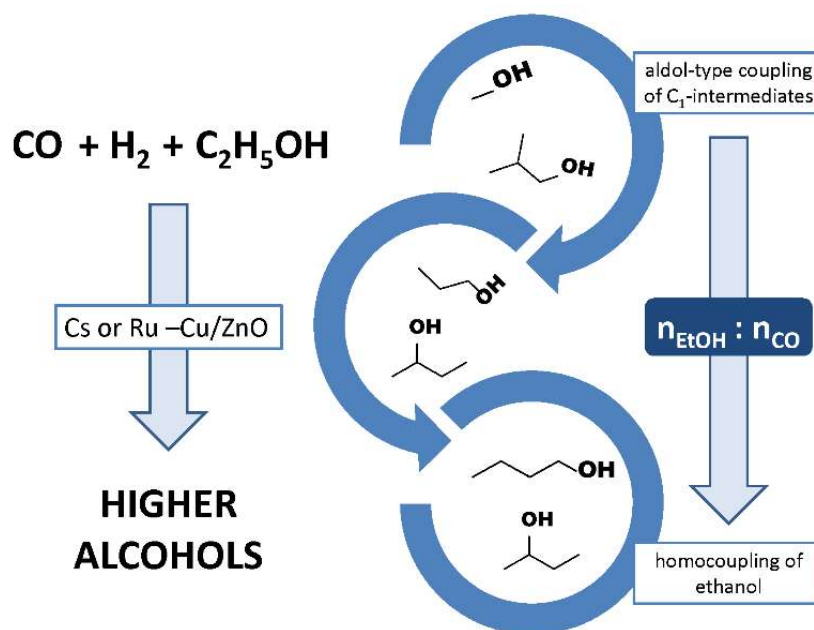


Figure 33: Summary of the changes in reaction path as a function of the $n_{EtOH} : n_{CO}$ in the higher alcohol synthesis in batch reactors over 1 g of Cs-doped CuO/ZnO catalysts at 593 K and 5.0 MPa initial pressure and $H_2 : CO = 1 : 1$.¹⁸²

4.2. Supported catalysts

In this section several parameters were varied to identify the most suitable catalysts in the higher alcohols synthesis for further tests in continuous operation. First the effect of the preparation method for Al_2O_3 supported catalysts is presented, followed by the influence of the loading of active species on the Al_2O_3 support. For the most suitable CuO/ZnO loading several types of supports were tested and their effects on the higher alcohols synthesis are discussed.

Finally, other preparation methods were compared for Cs-doped catalysts. More details on the CO conversion, ethanol conversion, selectivities and yields of the calibrated products are found in the supporting information (Table S 20 to Table S 27 in the supporting information). Some of the data presented in this section were obtained during a joint research project with Marc-André Serrer within the frame of his bachelor thesis.¹⁸⁸

4.2.1. Effect of preparation method

The influence of the catalyst preparation procedure was studied using two CuO/ZnO/Al₂O₃ catalysts. The catalysts were synthesized by wet impregnation and increasing pH precipitation, respectively. For comparison, also a physical mixture with the same proportions of CuO/ZnO and Al₂O₃ was tested. The results are displayed in Figure 34. Additional details are presented in Table S 20 and Table S 24 (supporting information).

The catalyst prepared by wet impregnation seemed to be more active in the higher alcohols synthesis (yield: 6.0 %-C and selectivity: 8.5 %-C) in comparison to the catalyst prepared by increasing pH precipitation or the physical mixture, which produced either small amounts or no alcohols at all. This shows that a proper interaction between Cu, ZnO and the support is required for the synthesis of higher alcohols. For the catalyst prepared by wet impregnation, among the C₃₊ alcohols, the highest yields were found for 1-butanol (2.2 %-C), 2-butanol (1.8 %-C) and 1-propanol (1.4 %-C). Methanol was produced with a similar yield reaching 2.2 %-C. Methanol production was not detected for the catalyst prepared by increasing pH precipitation. For the physical mixture, methanol yield resulted in only 0.1 %-C. CO₂ represented the main side product for all catalysts (yielding between 8.8 and 11.0 %-C). Among the oxygenated products, diethyl ether was produced more selectively (Table S 24), particularly for the catalyst prepared by increasing pH precipitation (6.8 %-C). Diethyl ether was not detected as a byproduct during the synthesis of higher alcohols using undoped catalysts, therefore its formation was probably related to the acid centers contained in the support. Diethyl ether was formed by the dehydration of ethanol on the acidic Al₂O₃ surface.^{204, 205} Probably, for the catalysts prepared by precipitation more acidic sites were available on the Al₂O₃ surface to form diethyl ether. For the physical mixture, high amounts of hydrocarbons, particularly ethane, were identified in comparison to the other catalysts (yield = 6.6 %-C). The differences in the product yields among the catalysts could be attributed to the different preparation methods, which would lead to changes in the exposed catalyst surface. For example, the

formation of dehydration products was related to the exposed Al_2O_3 surface. In the case of catalysts prepared by wet impregnation, CuO/ZnO seemed more evenly distributed on the Al_2O_3 surface leading preferentially to alcohols. For the physical mixture, no direct interaction or coverage of the Al_2O_3 surface occurred, therefore most of the ethanol was dehydrated to ethylene and then hydrogenated to ethane on Cu sites. For catalysts prepared by increasing pH precipitation, products derived from partial dehydration, such as diethyl ether, were preferred. The formation of diethyl ether and ethylene (and ethane after hydrogenation) corresponded to competing reactions, which were influenced by type of adsorption on the Al_2O_3 sites.^{204, 205}

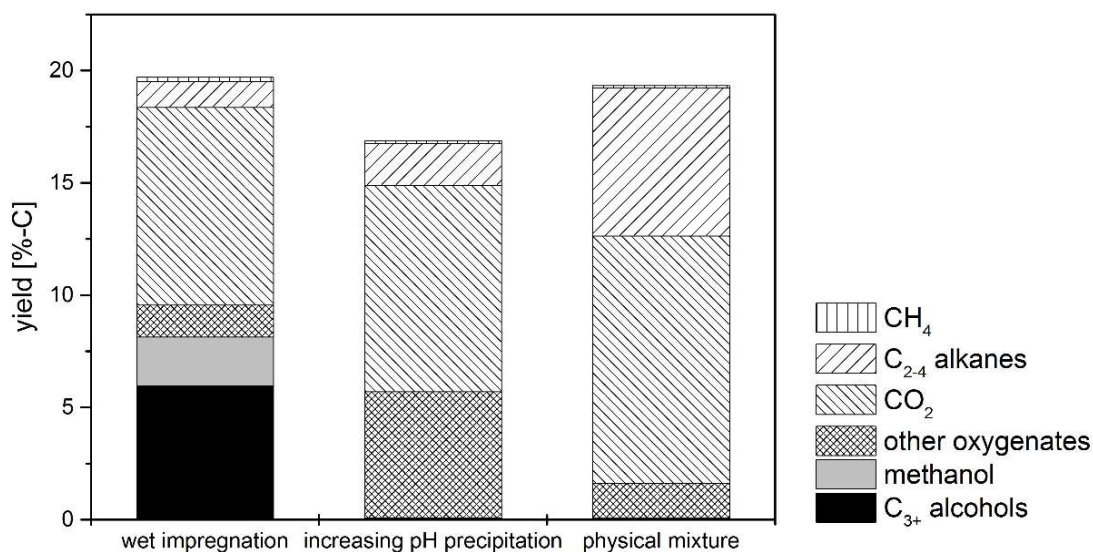


Figure 34: Product yield in the higher alcohols synthesis with $\text{H}_2 : \text{CO}=1:1$ and $n_{\text{EtOH}} : n_{\text{CO}} \sim 0.5:1$ at 593 K, 5.0 MPa initial pressure over 1.7 g of $\text{CuO}/\text{ZnO}/\text{Al}_2\text{O}_3$ prepared by wet impregnation, increasing pH precipitation and a physical mixture. (reaction time=3 h, liquid phase= 47.4 g cyclohexane and 2.6 g ethanol).

4.2.2. CuO/ZnO loading on the support

The effect of the CuO/ZnO loading on the Al_2O_3 support is presented in Figure 35. More details are found in Table S 21 and Table S 25 (supporting information).

The mass of catalyst during the reaction was chosen in a way that the same amount of active phase (CuO/ZnO) was available for each reaction. As the amount of CuO/ZnO on the support was increased, more alcohols and less diethyl ether were formed. Like in the previous section, the number of acidic sites from Al_2O_3 influenced the synthesis of dehydration products. Also the yield and selectivity towards methanol was affected by the amount of CuO/ZnO on the support. The selectivity was reduced from 3.1 %-C to 0.2 %-C as the CuO/ZnO content decreased from 30 wt.% to 10 wt.%. Both byproducts derived from dehydration reactions were

favored with higher exposition of the Al_2O_3 surface. Approximately the same yield and selectivity towards CO_2 was identified for all CuO/ZnO loadings, which might indicate that the water gas shift reaction was preferred over the alcohol synthesis. A catalyst containing 40 wt.% of CuO/ZnO was also prepared but discarded for further testing due to an inhomogeneous distribution on the support. Both CO and ethanol conversion decreased as the CuO/ZnO loading on the support was increased.

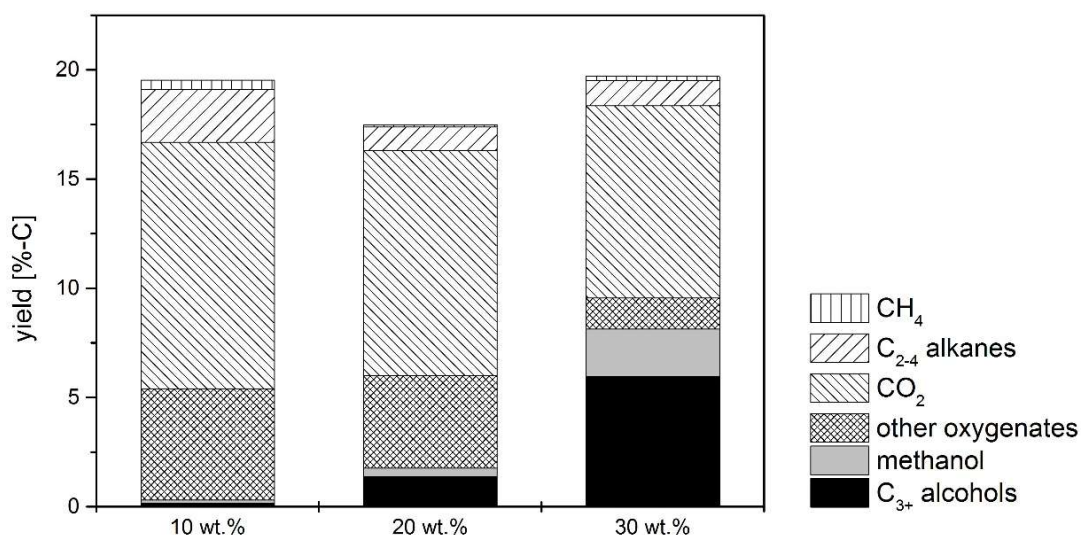


Figure 35: Product yield in the higher alcohols synthesis with $\text{H}_2 : \text{CO}=1:1$ and $n_{\text{EtOH}} : n_{\text{CO}} \sim 0.5:1$ at 593 K, 5.0 MPa initial pressure over: 5.0 g, 2.5 g and 1.7 g of CuO/ZnO/ Al_2O_3 correspondent to 10, 20 and 30 wt.% CuO/ZnO on Al_2O_3 prepared by wet impregnation, respectively. (reaction time=3 h, liquid phase= 47.4 g cyclohexane and 2.6 g ethanol).

4.2.3. Influence of the support material

After identifying the optimal preparation method and CuO/ZnO loading, SiO_2 and activated carbon were tested as alternative supports. The different support materials are compared in Figure 36. Additional information is found in Table S 22 and Table S 26 (supporting information).

Higher CO and ethanol conversions were achieved with Al_2O_3 as support (50 % and 90 %, respectively, supporting information Table S 22). The highest yield towards higher alcohols was obtained for catalysts supported on Al_2O_3 reaching values up to 6.0 %-C. Both SiO_2 and activated carbon as supports resulted in yields to higher alcohols around 1.9 %-C. The preferred higher alcohol products for the Al_2O_3 supported catalyst were 1-butanol, 2-butanol and 1-propanol. For the other support materials mostly 1-butanol and 2-butanol were formed.

Methanol yield was also higher for the Al_2O_3 supported catalyst (2.2 %-C). Hardly any methanol was formed when SiO_2 and activated carbon were used as supports. Both these facts indicated that reactions involving an aldol-type coupling of methanol derivatives took place only on catalysts supported on Al_2O_3 . CuO/ZnO supported on Al_2O_3 seemed more active towards the water gas shift reaction, since the yield to CO_2 was higher in comparison to the other supports. The yield towards C_{2-4} hydrocarbons was higher for catalysts supported on activated carbon (1.7 %-C) probably due to other active species contained on the activated carbon support (see Figure 13). The selectivity towards other oxygenates corresponded to 2.0, 8.7 and 6.6 %-C for catalysts supported on Al_2O_3 , SiO_2 and AC, respectively. For catalysts supported on Al_2O_3 mostly diethyl ether was formed, whereas for SiO_2 and AC both ethyl acetate and diethyl ether were preferred. Esterification reactions were most probably either competing with alcohol synthesis reactions or corresponded to a subsequent reaction of the formed alcohols facilitated by the active sites present on these catalysts.

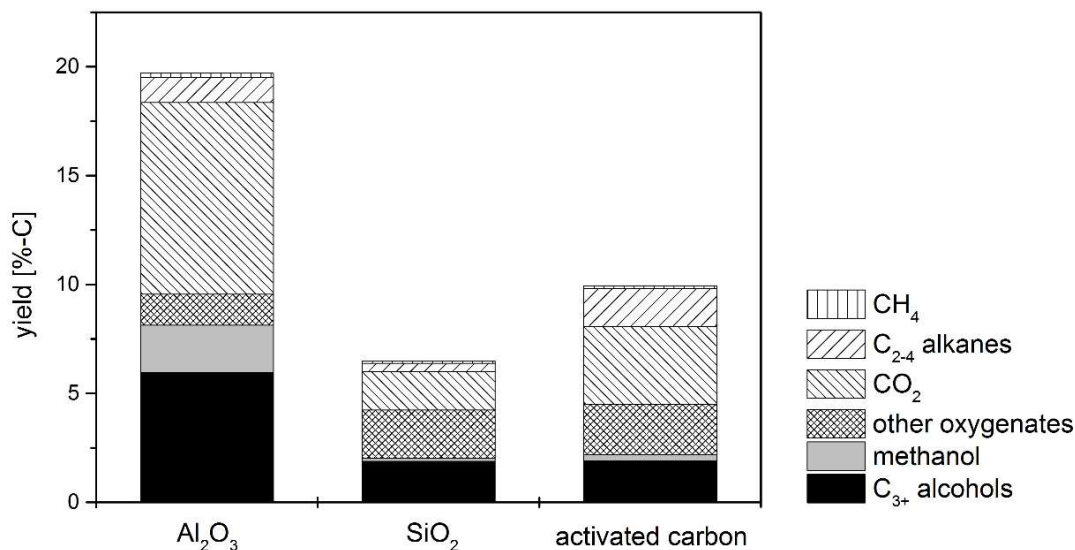


Figure 36: Product yield in the higher alcohol synthesis with $\text{H}_2 : \text{CO}=1:1$ and $n_{\text{EtOH}} : n_{\text{CO}} \sim 0.5:1$ at 593 K, 5.0 MPa initial pressure over 1.7 g of CuO/ZnO on Al_2O_3 , SiO_2 and activated carbon prepared by wet impregnation. (reaction time=3 h, liquid phase= 47.4 g cyclohexane and 2.6 g ethanol).

4.2.4. Influence of the preparation method of Cs-doped catalysts

Additional synthesis methods were tested for a 1 mol% Cs doped catalyst supported on Al_2O_3 . All the prepared $\text{CuO}/\text{ZnO}/\text{Al}_2\text{O}_3$ catalysts were afterwards impregnated with the corresponding amount of Cs to obtain a 1 mol.% Cs doping of the catalyst. A comparison

between wet impregnation, constant pH precipitation, flame spray pyrolysis and a commercial methanol synthesis catalysts is presented in Figure 37 and Figure 38. Each preparation method is described in detail in the experimental (section 2.1). Some additional information regarding the catalytic tests can be found in Table S 23 and Table S 27.

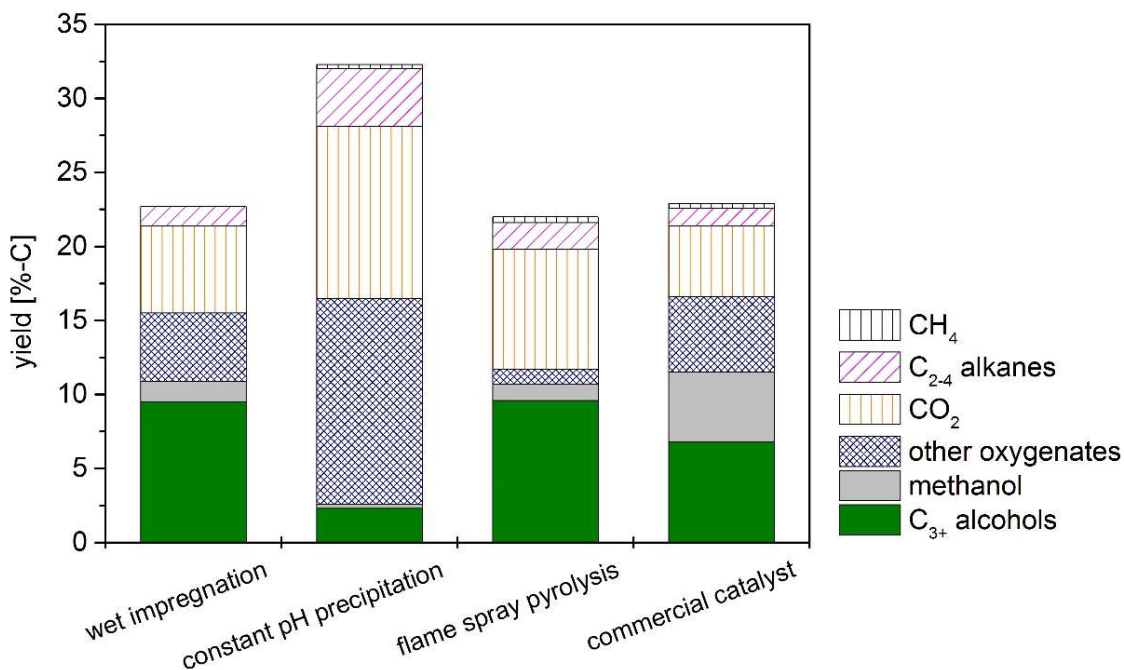


Figure 37: Product yield in the higher alcohol synthesis with $H_2 : CO=1:1$ and $n_{EtOH} : n_{CO} \sim 0.5:1$ at 593 K, 5.0 MPa initial pressure over 1.7 g of 1 mol.% Cs-CuO/ZnO on Al_2O_3 prepared by wet impregnation, constant pH precipitation, flame spray pyrolysis and a 1 mol.% Cs doped commercial catalyst. (reaction time=3 h, liquid phase= 47.4 g cyclohexane and 2.6 g ethanol).

Significant differences in the product yields and alcohol selectivity were found depending on the preparation method, which would suggest different types of sites on each catalyst. Both catalysts prepared by wet impregnation and flame spray pyrolysis showed the largest higher alcohol yields, reaching values up to 9.5 - 9.6 %-C. The catalyst prepared by wet impregnation gave higher selectivities towards higher alcohols in comparison to the catalyst prepared by flame spray pyrolysis (22.0 and 13.0 %-C, respectively). The lowest yield towards higher alcohols was found for the catalyst prepared by constant pH precipitation (2.3 %-C). The commercial catalyst yielded 6.8 %-C of higher alcohols. As expected, methanol was produced with the highest yield (4.7 %-C) and selectivity (9.5 %-C) by the commercial catalyst. The majority of other oxygenates were produced by the constant pH precipitation catalyst (9.6 %-C). Most of the higher oxygenates corresponded to ethers (13.9 %-C), mostly methoxyethane. Most probably the ethers were produced on the Al_2O_3 surface. The commercial catalyst and the

wet impregnated catalyst yielded similar amounts of other oxygenates (5.0 and 4.6 %-C, respectively). The highest selectivities for these catalysts corresponded to ethyl acetate and diethyl ether (Table S 27). The catalyst prepared by flame spray pyrolysis yielded the lowest amount of higher oxygenates (1.0 %-C). CO₂ was produced with higher yields by the constant pH precipitation catalyst (11.6 %-C), whereas for the other catalysts it reached yields between 4.8 and 8.1 %-C. C₂₋₄ alkanes were in general produced to similar extents, except for the catalyst prepared by constant pH precipitation (3.9 %-C). It seemed that either wet impregnation or flame spray pyrolysis represented the most appropriate preparation method.

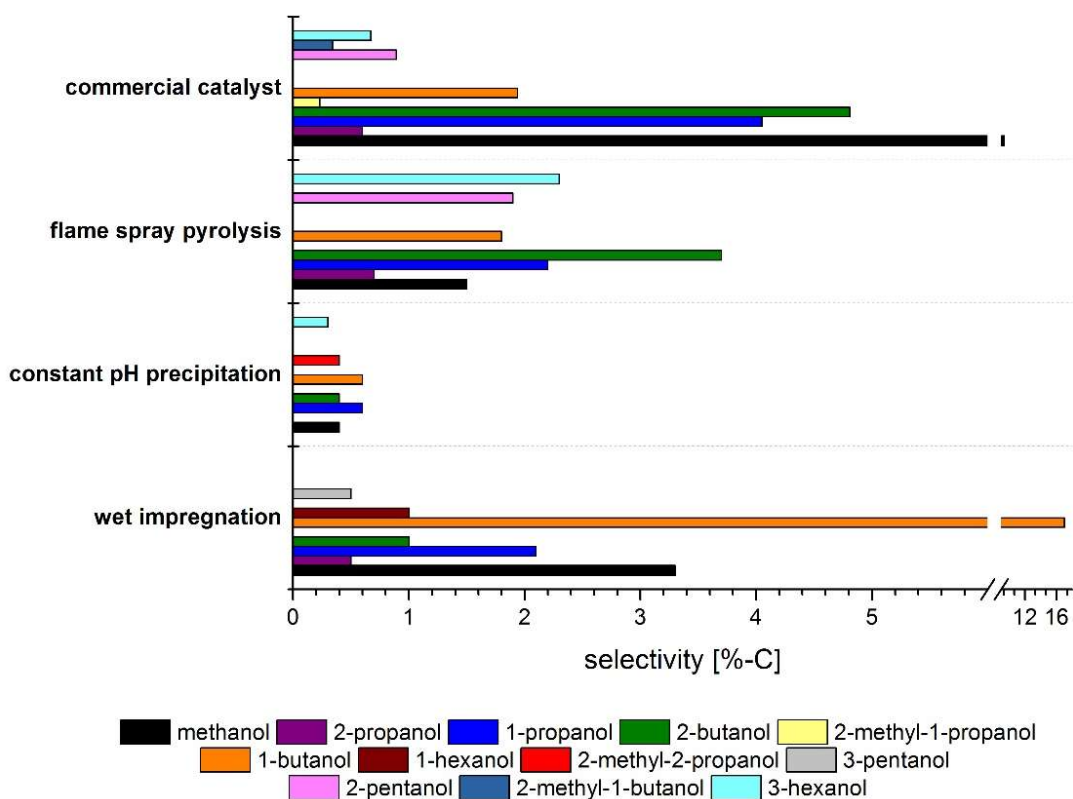


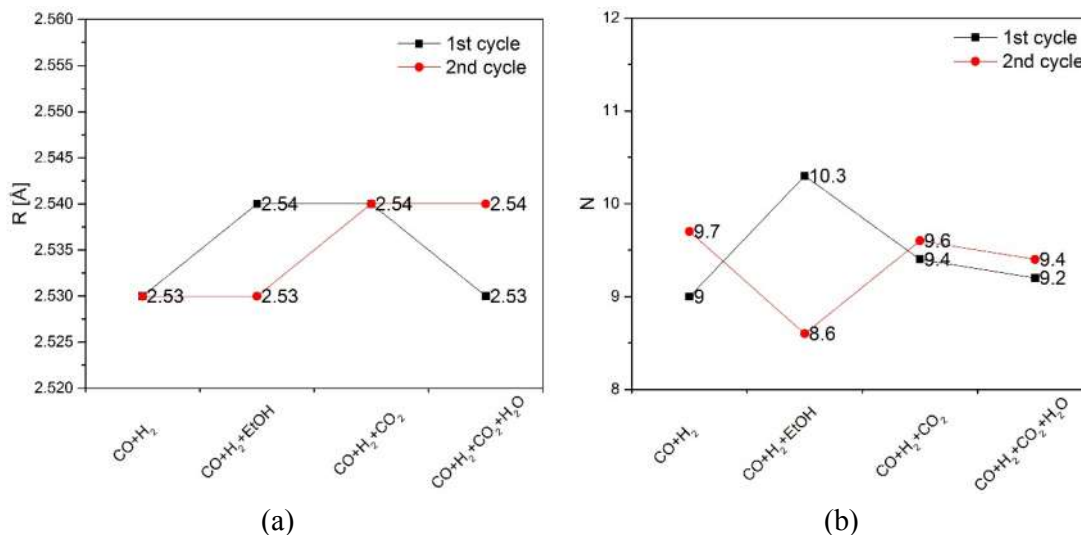
Figure 38: Influence of the preparation method on the alcohol selectivity in the higher alcohol synthesis with H₂ : CO=1:1, 5.0 MPa initial pressure over 1.7 g of 1 mol.% Cs-CuO/ZnO on Al₂O₃ prepared by wet impregnation, constant pH precipitation, flame spray pyrolysis and a commercial catalyst. (reaction time=3 h, liquid phase= 47.4 g cyclohexane and 2.6 g ethanol).

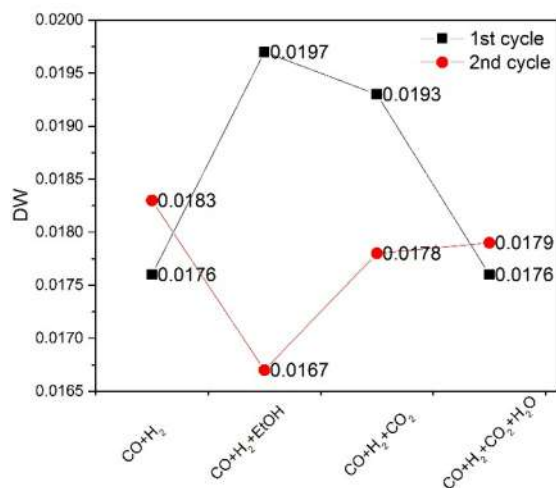
Like in Figure 37, important differences in the alcohols selectivities were observed in **Figure 38**. The preferred higher alcohol product varied with the preparation method. The catalyst prepared by wet impregnation formed mainly 1-butanol, whereas the commercial catalyst favored both 1-propanol and 2-butanol to a similar extent. The catalyst prepared by flame spray pyrolysis was selective to 1-propanol, 2-butanol, 1-butanol, 3-hexanol and 2-pentanol to similar extents.

These observations could suggest differences in the preferred reaction paths at the different sites. In the case of the catalyst prepared by wet impregnation most probably homocoupling of ethanol occurred in which the oxygen from the alcohol was retained occurred. For the commercial catalyst, coupling reactions of either methanol with adsorbed ethanol or homocoupling of ethanol occurred. In this case, the retention of the oxygen from the C₁ or C₂ oxygen-containing intermediate was favored during the coupling reactions. In the case of the catalyst prepared by flame spray pyrolysis, no clear preference by one or the other type of coupling was observed.

4.2.5. Catalysts characterization during and after reaction

The catalysts were characterized by XAS simulating the environment during higher alcohol synthesis at ambient pressure and 593 K. The results of this experiment are presented in Figure 39. The catalyst was first reduced in an analogous way as described for the *in situ* TPR experiments. Afterwards, the reaction environment was changed as described in section 2.2.8. Copper particles remained in a reduced state regardless of the environment that they were exposed to. No changes in the Cu-Cu distance, coordination number and Debye-Waller factor were observed during both experimental cycles. No evidence of sintering of the copper particles was found.





(c)

Figure 39: Effect of different reaction environments on: (a) Variation of Cu-Cu distance (first shell) at different gas conditions, (b) Variation of coordination number (first shell) at different gas conditions, (c) Variation of Debye-Waller factor (first shell) at different gas conditions. Reaction conditions: 593 K, 0.1 MPa, 1 mm capillary, Cu-K edge, reaction environment: CO+H₂, CO+H₂+ethanol, CO+H₂+CO₂ and CO+H₂+CO₂+water.

The supported 1 mol.% Cs-CuO/ZnO prepared by wet impregnation was characterized by XRD after the higher alcohol synthesis. For comparison the same catalyst is also displayed both in its calcined and reduced form. The three diffraction patterns are displayed in Figure 40. The reduction was performed in a reduction oven using 10 % H₂/N₂ at 673 K. Prior to the measurement the reduced catalyst was exposed to air. In both the reduced and post-reaction diffraction patterns, no CuO reflections were identified suggesting a complete reduction of the catalysts. Note that the catalyst after reaction showed clear Cu reflections at 43.3 and 50.5°, whereas the reflection were shifted to 42.9 and 49.9, respectively for the catalyst reduced in the oven. The shift in the copper reflections is a clear sign that the reducing atmosphere played an important role in the activation of the catalyst as discussed in the literature⁷⁶. Most probably the catalyst reduced in the oven led to a reversible interaction between Cu and Zn or the formation of a Cu-Zn alloy.^{74-76, 78} The catalyst after reaction showed broader copper reflections and with lower intensity in comparison with the catalyst reduced in the oven. This indicated that smaller copper particles were formed when the catalyst was reduced during the reaction (in the presence of CO and H₂). This was further verified by estimation of the crystallite size with the Scherrer equation. The Cu (reflection at 42.9°) and ZnO (reflection at 56.7°) crystallite sizes corresponded to 69 and 24 nm, respectively after the reduction in the oven. On the other hand, the Cu (reflection at 43.3°) and ZnO (reflection at 56.6°) crystallite sizes corresponded to 13 and 30 nm, respectively after the higher alcohol synthesis in the batch reactor.

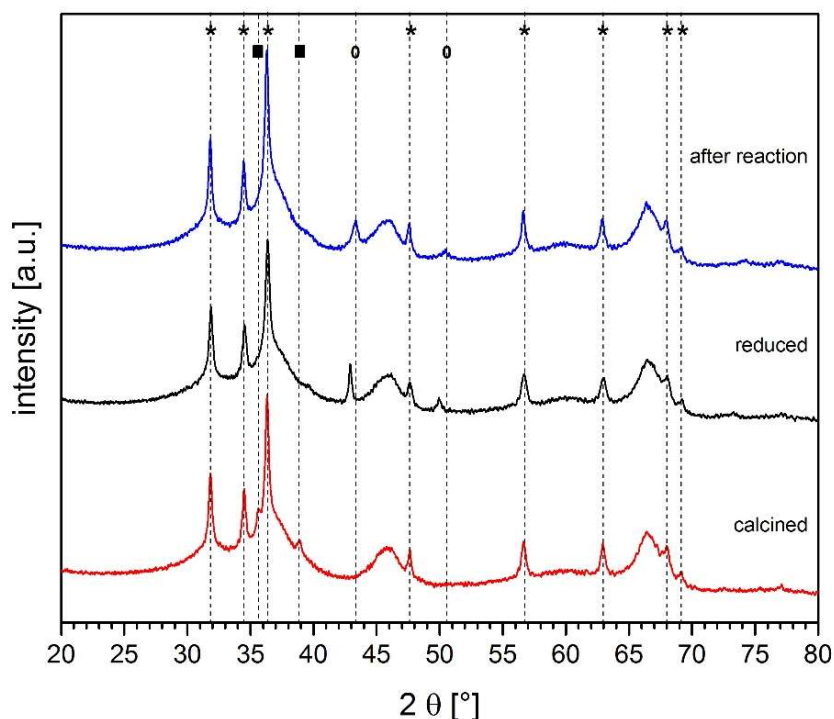


Figure 40: X-ray diffraction patterns for [1 mol.% Cs-CuO/ZnO]/Al₂O₃ catalyst fresh calcined, fresh reduced and after higher alcohol synthesis with H₂ : CO=1:1 and n_{EIOH} : n_{CO} ~ 0.5:1 at 593 K, 5.0 MPa initial pressure. *: ZnO, ■: CuO and °: Cu.

4.2.6. Conclusions

The importance of the catalyst preparation method in the higher alcohol synthesis was investigated in this chapter. Several parameters had to be optimized in order to obtain an active and selective catalyst, but further improvements in this regard are still needed. The suppression of CO₂ production via water gas shift reaction, and reactions, which led to other oxygenates, represent the main challenges in this regard.

Al₂O₃ proved to be the best support in comparison to activated carbon and SiO₂. A 30 wt.% loading with Cu/ZnO gave the highest yields of higher alcohols. Further attempts to deposit higher loadings of Cu/ZnO on the Al₂O₃ support might be necessary to improve the selectivity and yield towards higher alcohols.

In general, catalysts prepared by wet impregnation or flame spray pyrolysis seemed to be more active and selective in the synthesis of higher alcohols. Catalysts prepared by wet impregnation showed higher yields towards oxygenates, whereas the catalyst prepared by flame spray pyrolysis led to higher yields towards CO₂. Additional considerations for future catalyst

optimization might include preparation methods, which might result in better metal dispersion and enable a large scale production of the catalyst for future industrial applications.

Characterization of the catalysts after reaction showed the formation of relatively large metallic Cu particles during the reaction probably due to sintering. During the *in situ* characterization with XAS, the copper particles did not show any changes in their coordination number, Debye-Waller factor and Cu-Cu distances. This is at first contradictory to the results obtained by XRD. Note, however, that the catalysts characterized by XRD were exposed to air. *In situ* characterization should be repeated under more realistic conditions, such as higher pressures.

To complement the results obtained using batch reactor, experiments in a continuous-flow reactor were performed and are presented in chapter 6 of this thesis.

5. Design and construction of a high pressure, continuous-flow reactor

As part of this thesis, a laboratory scale trickle-bed reactor for pressures up to 20 MPa and temperatures up to 773 K was designed and constructed at the Institute of Catalysis Research and Technology (IKFT) at KIT to perform further catalytic tests and parameter evaluation in the synthesis of higher alcohols from synthesis gas and ethanol. The laboratory plant was designed in collaboration with Dr. Martin Schubert and completely built up during this thesis.

This chapter is divided in three sections. Firstly, basic considerations regarding reactor design and construction are discussed. The second section presents the design and construction of the reactor and laboratory plant itself. The third section shows the performance of the reactor during a well-known reaction (methanol synthesis) to prove the functioning of the setup.

5.1. Theoretical background

A trickle-bed reactor consists of a liquid and a gas phase flowing through a fixed-bed of catalyst particles.²⁰⁶ Trickle-flow reactors are not the most suitable for determining reaction kinetics, since fluid dynamics and reaction kinetics are too closely interlinked.^{207, 208} However, they are widely used in industrial applications, particularly in the petroleum industry, since they are of simple construction and operation and allow large reactor sizes.^{206, 209} Advantages of this type of reactor include²⁰⁹:

- A close to plug-flow behavior for liquid and gas phases.
- Allowing changes in the liquid and gas velocities.
- Having a small liquid phase hold up.
- Minimal catalyst loss.
- Permitting operation at high temperatures and pressures.

Liquid hold up describes the effectiveness of contacting between the liquid and solid catalyst and is expressed as a fractional bed volume. To ensure a behavior that approximates to an ideal reactor, several design aspects have to be considered. These considerations enable proper interpretation of the obtained data.

Since trickle-bed reactors are classified as continuous three-phase fixed-bed reactors, they should conform to the design equation of an ideal plug-flow reactor (PFR) for steady state and isothermal conditions. The kinetic data obtained in the reactor should only represent chemical events. Therefore, all gradients must be eliminated. Mederos et al.²¹⁰ defined those gradients in the following:

- Intraparticle: internal gradients within an individual catalyst particle.
- Interphase: gradients between the external surface of the catalyst particles and the adjacent bulk reaction mixture phase to them.
- Interparticle: gradients from catalyst particle to catalyst particle.
- Intrareactor: gradients between the local bulk fluid regions (flow-film-wall).

The design of the reactor should consider criteria to verify mass and heat transfer limitations, wetting efficiency, liquid/gas hold up, non-preferential flow (bed structure), axial and radial dispersion and the homogeneity of the bed.²⁰⁹⁻²¹¹ According to Mary et al.²⁰⁹ the filling method (bed structure); mass, heat and axial dispersion and; heat and mass transfer have a high effect on the PFR equation. Therefore attention should be paid to fulfill those criteria.

Trickle-bed reactors have been analyzed by several authors.^{207-210, 212, 213} A summary of criteria is presented in Table 16.²⁰⁹ Table 17 shows the effect of reactor parameters on the above mentioned phenomena.²⁰⁹

Several of the criteria proposed in Table 16 are not easy to determine experimentally. Therefore, some practical tests are suggested in the literature to verify them. Perego and Peratello²⁰⁸ reviewed experimental methods in catalyst kinetics for several reactor types. Very small particles should be avoided to minimize the pressure drop in the catalyst bed. It is recommended to calculate or determine the pressure drop in the reactor. An isothermal operation should be confirmed to estimate the kinetics of a reaction. Intrareactor temperature gradients could be avoided by a differential operation of the reactor (low conversion level, less than 5 % per pass), but this approach complicates the product analysis. If the reactor is operated in an integral way, difficulties arise while achieving a uniform temperature along the catalyst bed. To reduce temperature gradients three measures could be taken: (i) dilution of the reactants feed with an inert substance (improves the heat removal from the reaction zone), (ii) dilution of the catalyst with inert particles (reduces local hot spots and improves temperature distribution) or (iii) reduction of the reactor diameter, which implies a reduction of the catalyst particle size as well. Therefore an increase in the pressure drop along the bed should be

expected in the latter case. The bed should be diluted with an inert material (proper size) for good fluid distribution to overcome this effect also. To improve interphase temperature gradients, it is recommended to reduce the particle size or increase the flow rate (gas-solid), it is not an important issue for the liquid-solid interphase. An increase in the flow rate is advisable to overcome external concentration gradients. Two tests to prove the absence of such gradients are suggested.²⁰⁸ They are based on the fact that the conversion at any space velocity must be independent of the linear velocity through the bed in the absence of interphase transport limitations.

Test a: The reactant flow rate and the catalyst volume should be increased simultaneously at constant space velocity. The conversion will change if interphase limitations are present, because the mass transfer coefficient will depend on the fluid velocity in the catalyst bed. This test is not suitable if temperature effects also interfere, these might (over) compensate for concentration effects.

Test b: First a run with a catalyst volume V is performed. Followed by a second a run with catalyst volume $5V$. The residence time is changed for each series of tests. A plot comparing both tests of conversion as a function of residence time is plotted. When external diffusion limitations become important, both curves will cease to overlap.

The particle size should be reduced as much as possible to overcome intraphase concentration gradients. Internal limitations can be tested at laboratory scale by changing the particle size at constant space velocity. If conversion varies for a decrease in particle size, intraphase mass transfer is limiting. On the contrary, the reaction is occurring in a kinetically controlled regime if the conversion is constant.

According to Kapteijn and Moulijn²⁰⁷ the relative importance of the gradients for a laboratory scale operation, is:

$$(T - \text{grad})_{\text{bed}} > (T - \text{grad})_{\text{ext}} > (C - \text{grad})_{\text{int}} > (T - \text{grad})_{\text{int}} > (C - \text{grad})_{\text{ext}}$$

with T = temperature, C = concentration, int = internal and ext = external

Table 16: Criteria for ensuring the proper function of a trickle-bed reactor.²⁰⁹

	Conditions					
	Method of packing	Catalyst wetting	Axial mixing	No channeling	Isothermality	Mass transfer vs. kinetics
Criteria	-	$W = \frac{\eta_L U_L}{\rho_L d_p^2 g} \geq 5 \cdot 10^{-6}$ $\eta \phi^2 \geq \frac{\phi \tan \phi}{1 + \frac{\phi \tan \phi}{B_{mi}}}$ $\phi = d_p \sqrt{\frac{\rho_p k}{D_e}}$	$\frac{L}{d_p} \geq 100$ $\frac{D}{d_p} \geq 10$ $\frac{L}{d_p} \geq \frac{20n}{Bo} \ln \left(\frac{C_0}{C_f} \right)$	$\frac{D}{d_p} \geq 25$ $d_{pi} \geq \frac{d_p}{10}$	$\frac{D}{d_p} \geq 100$ $\frac{\Delta_r H r D^2}{k_e T_w} \leq 1.6 \frac{RT_w}{E}$ $\frac{\Delta_r H r d_p}{h_p T_0} \leq 0.30 \frac{RT_0}{E}$ $\frac{\Delta_r H r d_p^2}{\lambda T_0} \leq 0.6 \frac{RT_0}{E}$	$\left(\frac{10 d_p}{C} \right) r (1 - \varepsilon) \leq k_{ext}$ $\frac{r (1 - \varepsilon) \left(\frac{d_p}{2} \right)^2}{D_e C} \leq 1$
Consequence of fulfilled criterion	Perfect packing, no odd phenomena (channeling, hot spots ...) due to catalyst mal distribution	Good catalyst wetting and good contact solid-reactant	No axial dispersion, reactor behavior close to PFR	Non preferential flow and no wall effects in the reactor	Isothermal behavior, no temperature gradients inside the reactor	No mass transfer limitations, kinetics rate limiting

W: dimensionless wetting number. **η_L :** dynamic viscosity of the liquid (Pa·s). **U_L :** liquid velocity (m/s). **ρ_L :** liquid density (kg/m³). **d_p :** diameter of the bed particles (m). **g :** gravity constant (m/s²). **η :** overall effectiveness. **ϕ :** Thiele modulus. **B_{mi} :** Biot number for mass transfer. **ρ_p :** density of the pellet (kg/m³). **k :** rate constant (m³/kg·s). **D_e :** effective diffusivity (m²/s). **L :** length of the bed (m). **D :** diameter of the reactor (m). **n :** reaction order. **Bo :** Bodenstein number. **C_0 :** inlet concentration of reactant (mol/m³). **C_f :** outlet concentration of reactant (mol/m³). **d_{pi} :** diameter of inert particles (m). **$\Delta_r H$:** heat of reaction at a temperature (J/mol). **r :** rate of reaction (mol/s·m³). **k_e :** bed effective radial conductivity (W/m·K). **T_w :** wall temperature (K). **R :** gas constant (J/mol·K). **E :** activation energy for the catalytic reaction (J/mol). **h_p :** particle to fluid heat transfer coefficient (W/m²·K). **T_0 :** temperature of the fluid adjacent to the particles (K). **λ :** effective thermal conductivity of the particle (W/m²·K). **C :** concentration of reactant (mol/m³). **ε :** bed voidage. **k_{ext} :** mass transfer coefficient (m/s).

Table 17: Effects of parameters on the trickle-bed operation.²⁰⁹

Parameters	Conditions					
	Method of packing	Catalyst wetting	Axial mixing neglected	No channeling	Isothermality	Mass transfer vs. kinetics
Length of the bed, L	More difficult to pack a bigger bed	-	Less axial dispersion for a longer bed	-	-	-
Diameter of the reactor, d		-	Less axial dispersion for a larger bed	Better hydrodynamics with bigger diameter	Better behavior at smaller diameter	-
Diameter of the catalyst particle, d_p	-	Better for smaller particle	Particles of small diameters reduce axial mixing	Better hydrodynamics with small particles	Better for small particles	Better for small particles
Diameter of the inert particle, d_{pi}	-			Better hydrodynamics with small particles (not so small)		
Dilution (R_c , catalyst to inert ratio)	Impossible to obtain a uniform bed for a high ratio (more than 1:2)	-	Better hydrodynamics with dilution with small fines	Better hydrodynamics with dilution with small fines	Dilution with conductive inerts helps to provide isothermicity	-
Velocity of the liquid, U_L	-	Better efficiency for a higher velocity	Decreases with an increase in U_L	Decreases with an increase in U_L	-	Higher with high velocity
Velocity of the gas U_G ,	-	Almost no effect	Almost no effect	Decreases with an increase in U_G	-	
Others	Type of packing (dry, wet), pre-wetting methods	Density and viscosity of the liquid, pre-wetting methods	Order of the reaction, hydrodynamics (Peclet, Reynolds, ...), regime (upflow, downflow), phase (gas, liquid)	Distributor, bed uniformity, pre-wetting method	Heat transfer at the wall, heat of reaction, heat resistances, rate of reaction, temperatures inside the reactor	Rate of reaction, mass transfer coefficients, concentration, wetting efficiency, fluid characteristics

5.2. Design and construction considerations

For the design of the high pressure continuous-flow reactor, theoretical calculations were performed to evaluate the parameters presented in section 5.1.

Since trickle-bed reactors are three phase systems, difficulties in ensuring a proper mixing of the phases increase compared to two phase reactors. The flow regime in the reactor will determine how the phases behave. It is important to avoid poor gas and liquid distributions or channeling when low velocities are used. According to different authors^{206, 209, 212, 214}, for downward trickle-bed reactors four different flow regimes exist: (1) trickle-flow, (2) spray-flow; (3) pulse-flow and; (4) bubble-flow. For a trickle-flow, the gas phase corresponds to a continuous phase and the liquid to a dispersed one. A method for determining the type of flow in a non-foaming system was proposed by Mary et al.²⁰⁹ which is presented in Table 18.

Table 18: Flow regimes for a non-foaming trickle-bed reactor.²⁰⁹

Definitions	$\lambda = \sqrt{\frac{\rho_G}{\rho_{air}} \frac{\rho_L}{\rho_{H_2O}}}, \quad \psi = \frac{\sigma_{H_2O}}{\sigma_L} \left(\frac{\mu_L}{\mu_{H_2O}} \right)^{\frac{1}{3}} \left(\frac{\rho_{H_2O}}{\rho_L} \right)^{\frac{1}{3}}, \quad \phi = 4.76 + 0.5 \frac{\rho_G}{\rho_{air}}$
Type of flow	
Trickle-flow	$\frac{R_L}{R_G} \frac{\lambda \psi}{\phi} \leq \left(\frac{R_G}{\lambda} \right)^{-1.3}$ and $0.01 \leq \frac{R_G}{\lambda} \leq 1$
Spray-flow	$\frac{R_L}{R_G} \frac{\lambda \psi}{\phi} \leq \left(\frac{R_G}{\lambda} \right)^{-1.3}$ and $\frac{R_G}{\lambda} \geq 1$
Pulse-flow	$\frac{R_L}{R_G} \frac{\lambda \psi}{\phi} \geq \left(\frac{R_G}{\lambda} \right)^{-1.3}$

For the continuous reactor in this work, no changes in the fluid properties with temperature and pressure were assumed in order to determine the parameters presented in Table 18. According to this, the flow regime for our reactor corresponded to a trickle-flow for all the range of volumetric flows under consideration (Table 19).

The first estimation of the reactor parameters was calculated assuming a gas phase reaction in a fixed-bed reactor as it is the case for the methanol synthesis. As a rule of thumb, the following criteria have to be fulfilled: $L_{min} = 5 \cdot D$ and $d_p = D/20$. From reactor design considerations, the diameter (annular gap) was fixed at $D = 7.4$ mm. According to this first estimation, the bed length should have a length of 37 mm and the particle diameter should be 0.4 mm.

These results were refined considering some of the criteria presented in Table 16. For the calculations, a catalyst sieve fraction between 0.250 and 0.500 mm was used. The equations were solved for the most unfavorable conditions, which were obtained when the largest particle size was considered (Table 20). The axial mixing, the non-preferential flow and the isothermality criteria were not fulfilled under these conditions (marked in red in the Table 20 for these settings). Recalculating these values to fit the criteria gave the parameters presented in Table 21.

Table 19: Verification of the flow regimes for the trickle-bed reactor used during this thesis.

\dot{v}_{EtOH} (ml/min)	R_L (kg/m ² s)	\dot{v}_{gas} (ml/min) (20 % N ₂ , 40 % CO, 40 % H ₂)	R_G (kg/m ² s)	Trickle-bed reactor
0.1	1.64 · 10 ⁻²	100	1.52 · 10 ⁻²	$\lambda = 0.693$
				$\psi = 3.772$
5	8.21 · 10 ⁻²	500	7.58 · 10 ⁻²	$\phi = 5.064$
$\dot{v}_{EtOH,max}$ $\dot{v}_{gas,max}$	$\frac{R_L \lambda \psi}{R_G \phi} = 5.59 \leq \left(\frac{R_G}{\lambda}\right)^{-1.3} = 17.8$ and $0.01 \leq \frac{R_G}{\lambda} = 0.11 \leq 1$		$\dot{v}_{EtOH,max}$ $\dot{v}_{gas,min}$	$\frac{R_L \lambda \psi}{R_G \phi} = 27.96 \leq \left(\frac{R_G}{\lambda}\right)^{-1.3} = 143.9$ and $0.01 \leq \frac{R_G}{\lambda} = 0.02 \leq 1$
$\dot{v}_{EtOH,min}$ $\dot{v}_{gas,max}$	$\frac{R_L \lambda \psi}{R_G \phi} = 0.11 \leq \left(\frac{R_G}{\lambda}\right)^{-1.3} = 17.8$ and $0.01 \leq \frac{R_G}{\lambda} = 0.11 \leq 1$		$\dot{v}_{EtOH,min}$ $\dot{v}_{gas,min}$	$\frac{R_L \lambda \psi}{R_G \phi} = 0.56 \leq \left(\frac{R_G}{\lambda}\right)^{-1.3} = 143.9$ and $0.01 \leq \frac{R_G}{\lambda} = 0.02 \leq 1$

Two additional considerations could contribute to avoid preferential flow along the catalyst bed: (1) either further decreasing the particle diameter or (2) diluting the catalyst bed. Dilution of the catalyst bed was considered to be the most appropriate option since it also contributed to the homogeneity of the catalyst bed. The dilution of the catalyst bed with smaller SiC particles should also improve the isothermality within the catalyst bed and approximate the behavior of the trickle-bed reactor to that of a plug-flow reactor. In this case, since the catalyst should be characterized after the reaction, an inert particle diameter different to that of the catalyst particles was chosen. SiC with a particle size of 210 μm ($d_{pi} = 0.210 \geq \frac{d_p}{10} = 0.025$) was chosen as inert material for the dilution. The dilution ratio corresponded to 1:1.

The reactor bed was packed using a dry packing method, which involved filling a portion of catalyst with the same portion of SiC and then vibrating the reactor to reach a homogeneous distribution.

Filling the bed with inert particles also contributed to improve the wetting efficiency, avoiding channeling and stagnant zones and reducing wall effects. The length of the reactor and the particle diameter have the greatest influence on the axial mixing. Longer reactor beds decrease the probability of axial mixing. The use of smaller inert particles implied that the hydrodynamics of the reactor were dictated by the inert material (SiC) and the kinetics by the catalyst, therefore improving the performance of the reactor. The choice of a downward operation regime contributed also to reduce the axial mixing. A downward flow reactor also facilitated the flow of the reactants and products.

Avoiding a preferential flow within the catalyst bed involves reducing wall effects, bypass, channeling and stagnant zones. These phenomena are a consequence of poor flow distribution and deviations from ideal hydrodynamics and plug-flow model. The presence of preferential flow would lead to poor catalyst performance, faster deactivation and inappropriate thermal behavior. One of the most important considerations in this regard is the incoming flow. To ensure proper mixing of the ethanol and synthesis gas, to reduce channeling effects and to improve the heat transfer within the reactor, the reactor was also filled with SiC (500 μm) up and downstream from the catalytic bed.

The absence of radial and axial thermal gradients have to be ensured to interpret laboratory data in an appropriate way. This problem can be minimized by dilution of the catalytic bed with small inert particles, which dissipate the heat along the bed to the wall, or by reducing the diameter of the reactor. The use of an inert material was chosen in our case. The feed of the reactants was diluted with N_2 (inert substance), which should improve the heat removal of the reaction zone to avoid hot spots formation. N_2 was additionally used for determining the mass balance for the gas phase products.

Table 20: Trickle-bed reactor parameters according to criteria for gas phase reaction in a fixed-bed reactor.

	Conditions				
	Catalyst wetting	Axial mixing	Non-preferential flow	Isothermality	Mass transfer vs. kinetics
Criteria	$W = \frac{\eta_L U_L}{\rho_L d_p^2 g} = 1.29 \cdot 10^{-3} \geq 5 \cdot 10^{-6}$	$\frac{L}{d_{p,max}} = 7.4 \not\geq 100$ $\frac{D}{d_p} = 14.8 \geq 10$	$\frac{D}{d_p} = 14.8 \not\geq 25$	$\frac{D}{d_p} = 14.8 \not\geq 100$	Determined experimentally with the tests presented in the introduction

Table 21: Trickle-bed reactor parameters according to criteria presented in Table 16.

Parameter	Value	Unit	Parameter	Value	Unit
Minimum length (L)	50	[mm]	Diameter (D)	7.415	[mm]
Internal wall diameter	10.59	[mm]	Thermocouple external diameter	3.175	[mm]
Particle diameter (d_p)	0.250-0.500	[mm]	Inert diameter (d_{pi})	0.210	[mm]
Gas flow	100-500	[ml/min]	Liquid flow	0.01-10	[ml/min]
Maximum oven temperature	773	K	Maximum heating cables temperature	723	K
Maximum pressure	20.0	MPa			

5.3. Details of the laboratory plant

Details on the reactor construction and catalyst packing are given in the next paragraphs. Specific details on the reaction conditions used during the higher alcohols synthesis are given in chapter 2, section 2.3.2.

During the design and construction process, attention was paid to avoid product accumulation downstream of the reactor. During the construction phase some modifications were made to the original plan to optimize collection and quantification of the products. The reactor was designed to operate up to pressures and temperatures of 20.0 MPa and 773 K, respectively. Several pressure and temperature sensors were implemented to monitor the reactant and product streams along the reactor (PTR, PI and TR). Check valves (CV) were located in the reactant streams to avoid backflow. Relief valves (RV) were placed to avoid overpressure during the reaction.

The piping and instrumentation diagram (PID) is presented in (Figure 41). The reactor was fed with gases (CO, H₂ and N₂), which were compressed to the required operation pressure in a compressor station with 3 single acting, single air drive head and single stage compressors (Gas Booster DLE 30-1, Maximator, maximum 60.0 MPa, pressure ratio 1 : 30, compression ratio 1 : 20, displacement volume: 60 cm³). The gas flows were controlled by independent mass flow controllers (Wagner Mess und Regeltechnik, 0.04 - 2 l/min, 1.0 - 21.0 MPa inlet pressure, 0 - 20.0 MPa outlet pressure). The gases were mixed after the MFCs. The liquid phase (ethanol) was dosed with a HPLC pump WADOSE-10-SS-U (Wagner Mess und Regeltechnik, 10 ml/min, maximal 40.0 MPa). The flow of the pump was adjusted between 0.01 and 10 ml/min. Both the liquid and gas pipes were preheated with heating cables before entering the reactor to achieve a more stable temperature at the reactor. Both phases were mixed at the reactor entrance. The reactor was heated with an electrical oven with one isothermal zone (HTM Reetz GmbH), controlled with a PID controller (Eurotherm 2416). After the reactor, the temperature of the product stream was reduced in a heat exchanger operated at 258 K. The product stream passed through a filter to avoid contamination of the following reactor parts with catalyst particles. The reactor pressure was adjusted by a back-pressure regulator (Tescom Serie 26-1700) controlled manually (PC-1).

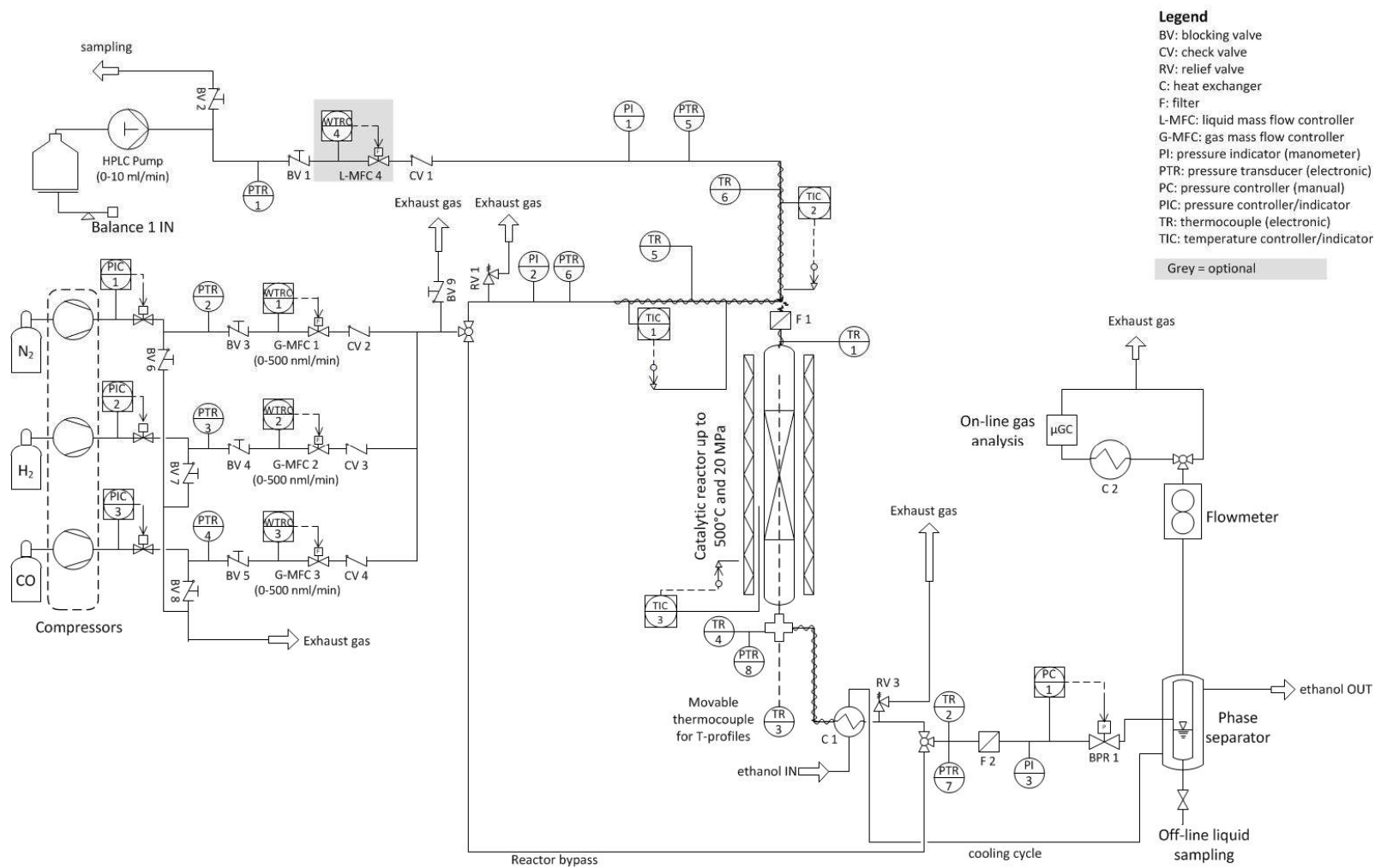


Figure 41: Piping and instrumentation diagram for the trickle-bed reactor set up.

The liquid and gas streams were separated in a condenser cooled with ethanol at 258 K. The volumetric flow of the product gas stream was measured with a flowmeter Serie G2 (Swagelok, 0.1-1 l/min air). The gas stream composition was determined online with a micro GC described in more detail in section 2.4.1. The gas was passed through a trap cooled with a dry ice/acetone mixture to exclude contamination with condensable products in the micro GC. As mentioned before, N₂ was used as an internal standard for the gas phase quantification. The liquid phase was collected for a certain amount of time in the phase separator. The mass and volume of the collected liquid products were used for quantification of this phase. The liquid was analyzed using a GC described in more detail in section 2.4.2. The data from the electronic sensors was recorded using Labview software.

In Figure 42 the reactor dimensions and packing are presented. The reactor consists of a stainless steel tube with a diameter of ½ inch (wall thickness: 0.083 inch) and a length of 46 cm. A movable Type K thermocouple (1 in Figure 42) was located inside the reactor. This thermocouple enables temperature measurements along the catalyst bed.

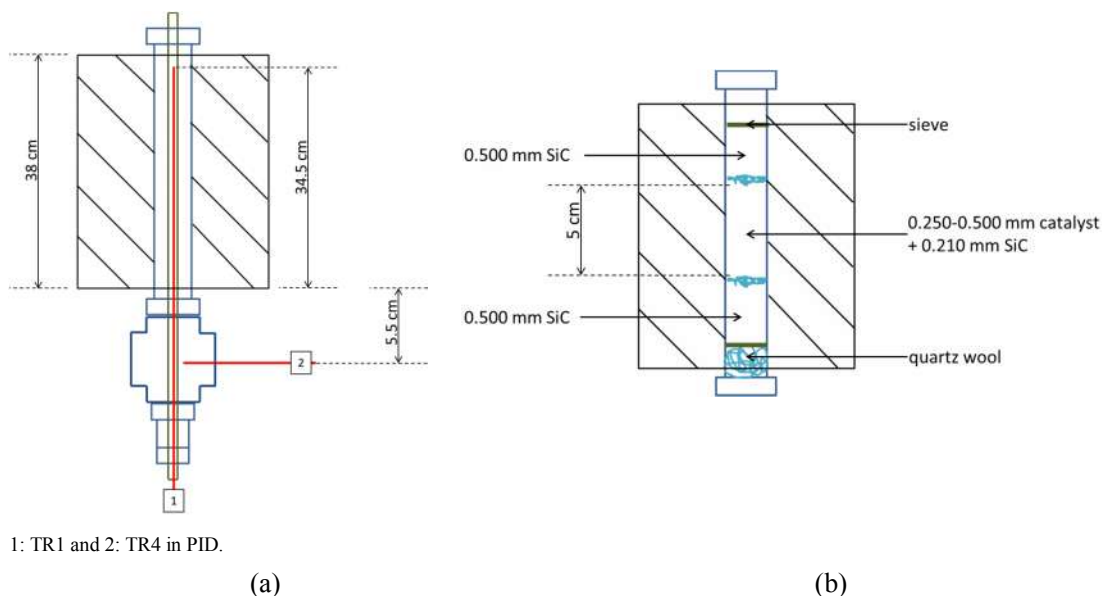


Figure 42: (a) Trickle-bed reactor dimensions. (b) Suggested reactor packing to avoid mass and heat transfer limitations.

The catalyst bed of 5 cm height was placed in the isothermal zone of the reactor. The catalyst bed was diluted with 210 μm SiC particles (VWR Chemicals, technical). Up and downstream from the catalyst bed, the reactor was filled with 500 μm particles of SiC (VWR Chemicals, technical) to ensure a better distribution of the reactants and better heat transfer properties.

Different sieve fractions were used to enable the separation of the catalyst after the reaction. Each layer was separated with quartz wool.

The temperature profiles of the empty reactor and the reactor filled with SiC (500 μm) are displayed in Figure 43. The profiles were measured at atmospheric pressure, with a total flow of 50, 100, 300 and 500 ml/min of nitrogen. The temperature of the oven was set at 648 K and the preheating at 424 K. As the volumetric flow increased, the isothermal zone shifted towards the outlet of the reactor. An isothermal zone of 5 cm was achieved within ± 2 K.

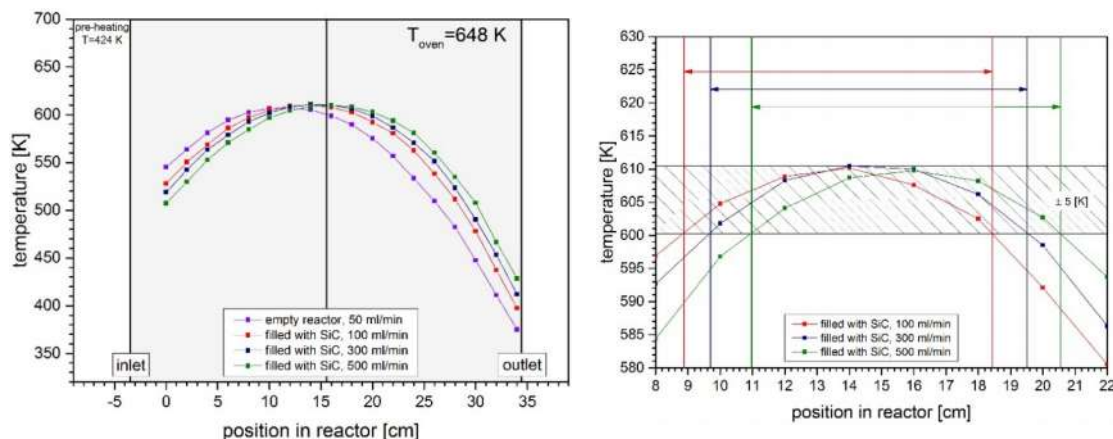


Figure 43: Axial temperature profile of the trickle-bed reactor.

5.4. Proof of concept: methanol synthesis reaction

A commercial methanol catalyst was packed into the reactor and methanol synthesis was performed using a gas mixture containing 16 % CO / 63 % H₂ / 8 % CO₂ / 13 % N₂ at a pressure of 5 MPa and a temperature of 543 K. The total flow corresponded to 500 ml/min. The catalyst was activated by reduction in 10 % H₂/N₂ for 2 h (500 ml/min, 5 K/min to 563 K, 0.1 MPa). According to (Eq. 14, section 1.3), the parameter S was equal to 2.2 in this case. The elemental composition of the catalyst is presented in chapter 3, section 3.2, Table 6. The specific area of the catalyst corresponded to 90 m²/g. The copper surface area corresponded to 36 m²/g_{cat}, which gave a copper particle dispersion of 11 %.

The results of this catalytic test are shown in Table 22, Table 23 and Figure 44. Table 22 presents data for two sampling points measured within an interval of 60 min. The reactor showed a high dead volume, because the first drops of liquid were collected 90 min after the reactor reached steady reaction conditions. The standard deviation of the data points was

between 0.1 and 0.2 %, except for the methanol space time yield which corresponded to 18 %. Nevertheless, the mass balance could be improved.

Table 23 shows the averaged results obtained for the complete reaction time. It includes product collected in the liquid trap (dry ice / acetone mixture) and product which was collected in the phase separator after the end of the reaction. A total of 3.73 g and 1.95 g of liquid products were collected in the liquid trap and the phase separator respectively, from a total of 5.04 g collected during the samplings. Even though the mass balance reached 90 % with these considerations, it was impossible to collect some of the liquids. They were identified as a shifting peak at high retention times in channel 1 of the micro GC. It is important to notice that half of the mass of the collected liquids was not collected during sampling. Therefore an online GC analysis for both the liquid and gas products should be considered for further improvements of the reactor system. The advantage of online analysis for comparable set ups has been already discussed in literature.²¹⁵

Figure 44 presents both the selectivity (green) and the yield (blue) towards the main reaction products. Traces of other oxygenates were also found, but not in considerable amounts. As for the parameters presented in Table 22, a very good reproducibility of different data points was found. The methanol selectivity and yield corresponded to 83 and 21 %-C, respectively. Methane yield was below 0.04 %-C and its selectivity below 0.2 %-C. Ethanol yielded 0.2 %-C with a selectivity of 0.6 %-C.

Table 22: CO conversion, CO₂ conversion, total mass balance, carbon balance and methanol space-time yield in the methanol synthesis for two data points (543 K, 5 MPa, GHSV= 10 kg/kg_{cat} h, 16 % CO / 63 % H₂ / 8 % CO₂ / 13 % N₂).

		#1	#2	Average	Standard deviation
CO conversion	[%-C]	36.6	36.8	36.7	0.1
CO₂ conversion	[%-C]	3.7	3.7	3.7	0
C balance	[%]	95.6	96.0	95.8	0.2
Mass balance	[%]	86.7	87.1	86.9	0.2
Methanol space-time yield	[g/ kg _{cat} h]	1185	1211	1198	18.4

Table 23 shows the turnover frequency for the methanol synthesis reaction calculated in two different ways. The methanol space-time yield found in the present study (Table 22) agreed well with results presented by Studt et al.¹³⁶ using a catalyst with similar elemental

composition, even though the pressure, space velocity and H₂ : CO ratio differ and, in the present study CO₂ and N₂ were present. The authors¹³⁶ calculated methanol space-time yields of 842, 1315 and 2666 g/kg_{cat} h for temperatures of 523, 548 and 573 K, respectively. The reaction conditions used by these authors corresponded to 10.0 MPa, H₂ : CO ratio of 1:1 vol.%.

Table 23: CO conversion, CO₂ conversion, total mass balance, carbon balance, turnover number and turnover frequency in the methanol synthesis averaged for the complete reaction time including liquid trap and liquid collected in the condenser (543 K, 5 MPa, GHSV= 10 kg/kg_{cat} h, 16 % CO / 63 % H₂ / 8 % CO₂ / 13 % N₂).

		Average
CO conversion	[%-C]	36.7
CO ₂ conversion	[%-C]	4.1
C balance	[%]	96.8
Mass balance	[%]	90.0
TOF	[1/s]	0.01
TOF	[mol _{MeOH} /m ² _{cat} s]	3.1·10 ⁻⁷

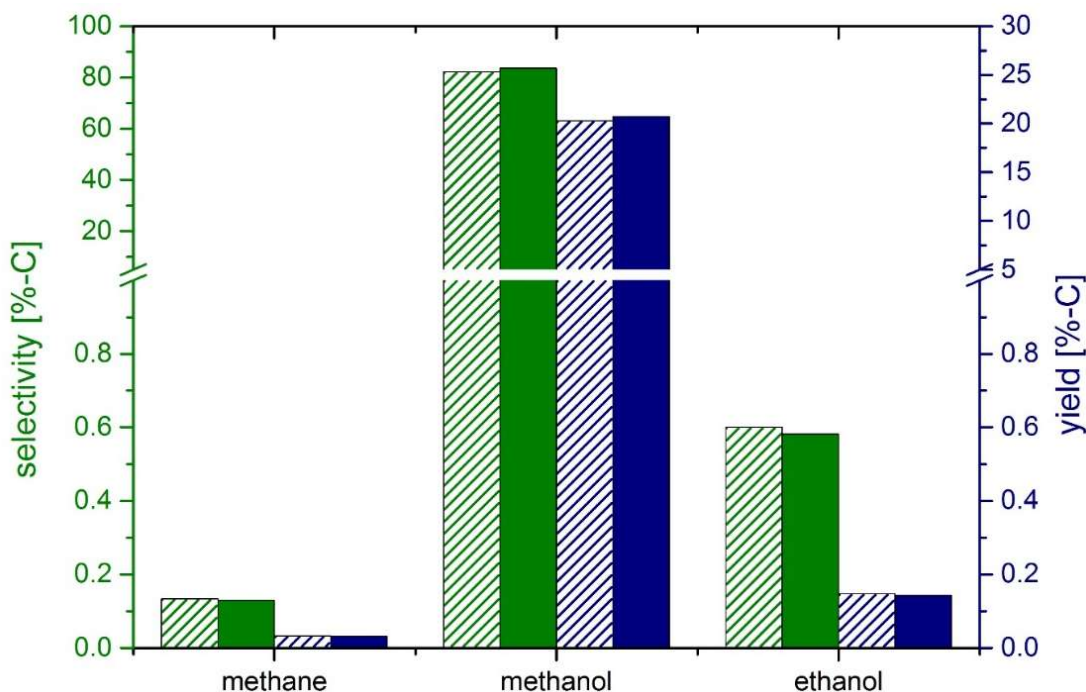


Figure 44: Selectivity (green) and yield (blue) to methane, methanol and ethanol in the methanol synthesis for two data points (543 K, 5 MPa, GHSV= 10 kg/kg_{cat} h, 16 % CO / 63 % H₂ / 8 % CO₂ / 13 % N₂).

5.5. Conclusions

For the appropriate design of the reactor, several parameters were derived by theoretical calculations and following empirical recommendations to ensure appropriate catalyst wetting and the isothermality of the catalyst bed as well as to avoid axial mixing, preferential flow, and mass and heat transfer limitations. Following literature recommendations to hinder the above mentioned phenomena, it was decided to dilute the catalysts bed with SiC as inert material. The particle diameter of the SiC corresponded to 210 μm , which did not contradict the criteria presented during this chapter and allowed the physical separation of the catalyst for characterization after reaction. Additionally, the reactor was packed with SiC (500 μm) up and downstream from the catalyst bed to ensure an appropriate flow and facilitate heat transfer to the reactants. N_2 was used as internal standard to quantify the gaseous phase and to improve heat transfer within the catalyst bed. From theoretical calculations the minimal length of the catalyst bed corresponded to 5 cm. For the considered reactants flow a trickle-flow regime was theoretically ensured.

For the construction phase of the downward, three-phase continuous-flow reactor, theoretical parameters calculated in this chapter were considered. This was accounted in the piping and instrumentation diagram of the reactor system and the suggested catalyst packing of the reactor. The reactor itself consists of a stainless steel tube reactor (external diameter $\frac{1}{2}$ inch) and a length of 46 cm. Inside the reactor a moveable thermocouple was installed to monitor the temperature along the catalyst bed.

As a proof of concept, a well-known reaction (methanol synthesis) was performed using the reactor constructed during this thesis. A good reproducibility of different data points was achieved. A methanol selectivity and yield of approximate 80 and 20 %-C were achieved, respectively. Only small quantities of byproducts, such as methane and ethanol, were identified. Even though the synthesis was successfully performed, improvements are still required mostly regarding the liquid products quantification. The use of online analytics for all reaction products is suggested to improve carbon and mass balances.

6. Synthesis of higher alcohols: continuous-flow reactor

After screening the catalysts and operation conditions in batch reactors, the [1 mol.% Cs-CuO/ZnO] / Al₂O₃ catalyst was tested in a continuous-flow reactor as suggested by the results in section 4.2. Several tests were performed as follows:

- Effect of space velocity
- Influence of the reaction temperature
- Influence of n_{EtOH} : n_{CO} ratio

As in chapter 4, the different tests are divided in sections to facilitate the analysis. Additional details are found in the supporting information (Table S 28 to Table S 30). In general, both C balance and mass balance were improved in comparison to the batch reactor tests.

6.1. Effect of space velocity

The effect of space velocity on a chemical reaction is very important since it influences the contact time of the reactants with the catalyst bed. For this study, three different space velocities were applied: 7400, 15100 and 19400 L(STP) / kg_{cat} · h and their effect on the yield and selectivities towards higher alcohols was evaluated.

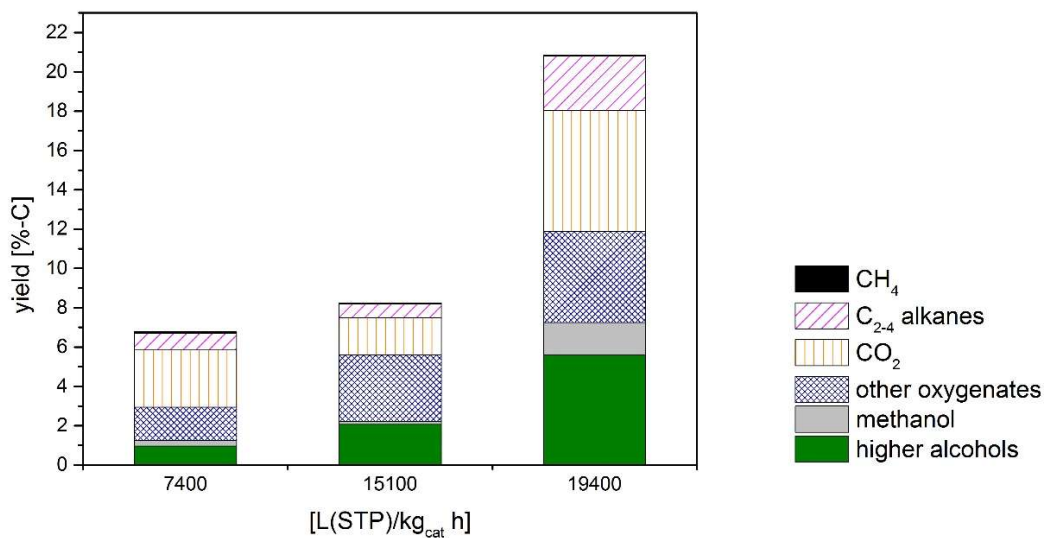
Table 24 and Figure 45 present the results obtained for experiments with different space velocities. CO conversion increased with space velocity (Table 24). It is likely that higher flow increased the turbulence in the reactor (higher Reynolds number), resulting in more efficient diffusion of CO to the active sites. Ethanol conversion showed a minimum at medium space velocities (32.1 %). The higher alcohol yield increased with increasing space velocity from 1.0 to 5.6 %-C. Since higher alcohol synthesis is a chain growth reaction, it was expected that longer residence times would have favored their production. Most probably if the space velocity would be increased even further, the higher alcohol yield might reach a maximum. In general, the yields towards all products increased with higher space velocities. Figure 45 (b) presents the selectivity towards different reaction products. Higher space velocities also improved selectivity towards higher alcohols (16.2 %-C) and methanol (4.8 %-C). The increase in methanol selectivity could be related to the higher CO conversion. CO₂ formation increased with the space velocity, which would suggest that the water gas shift reaction occurred fast. Additionally, higher selectivities towards alkanes were observed at higher space velocities

reaching up to 8.0 %-C. Interestingly, medium space velocities led to a higher selectivity towards other oxygenates, which suggested that higher oxygenates formation was slower than alcohol formation, particularly for esters and ethers as observed in Figure 46 (b).

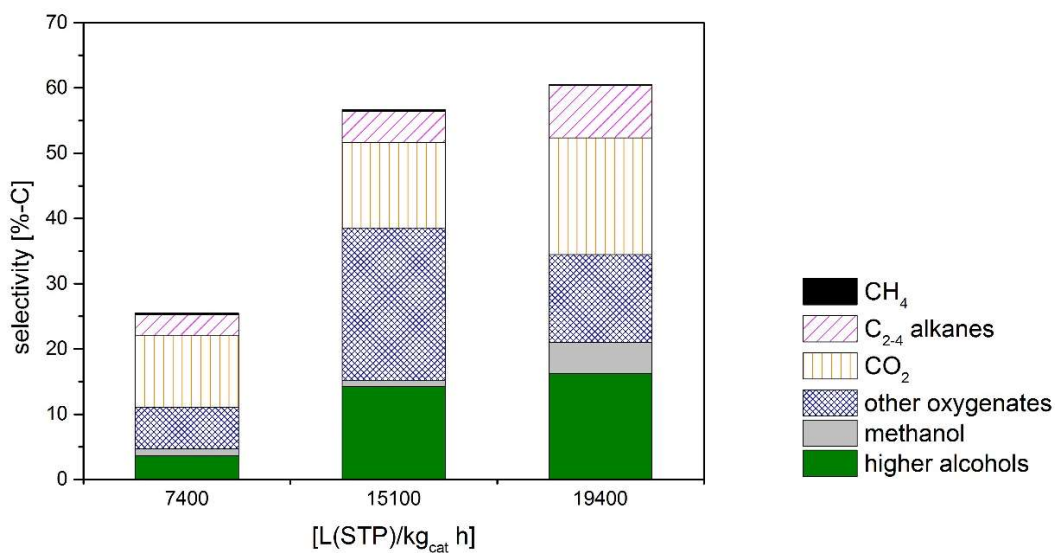
Table 24: Effect of space velocity on the CO conversion, ethanol conversion and carbon and mass balances in the higher alcohols synthesis over a CuO/ZnO (30 wt.%) supported on Al₂O₃ catalyst ($n_{\text{EtOH}} : n_{\text{CO}} = 0.3:1$; 593 K, 80 bar).

Space velocity	Units	7400	15100	19400
[L(STP)/kg _{cat} h]				
Total mass balance	%	85.0	95.1	90.7
C-balance	%	80.2	93.7	86.3
CO conversion	%-C	6.0	3.7	15.2
Ethanol conversion	%-C	62.5	32.1	66.6

The alcohol and product selectivities are presented in Figure 46 (a) and (b), respectively. The selectivity to 1-butanol showed a maximum at medium space velocities as was the case for the selectivity to esters. The selectivity towards 2-butanol increased with the space velocity. At 19400 L(STP) / kg_{cat} h the selectivities to methanol, 1-butanol, 2-butanol and C₅₊ alcohols reached the same values (~ 4.5 - 4.9 %-C). The production of 2-methyl-1-propanol was only observed at higher space velocities. As mentioned in the previous chapters, this product is the termination product in the higher alcohol synthesis over Cs-doped Cu/ZnO catalysts.¹⁵³ From Figure 46 (b) it can be seen that all product selectivities, except ethers and esters, increased with higher space velocity.

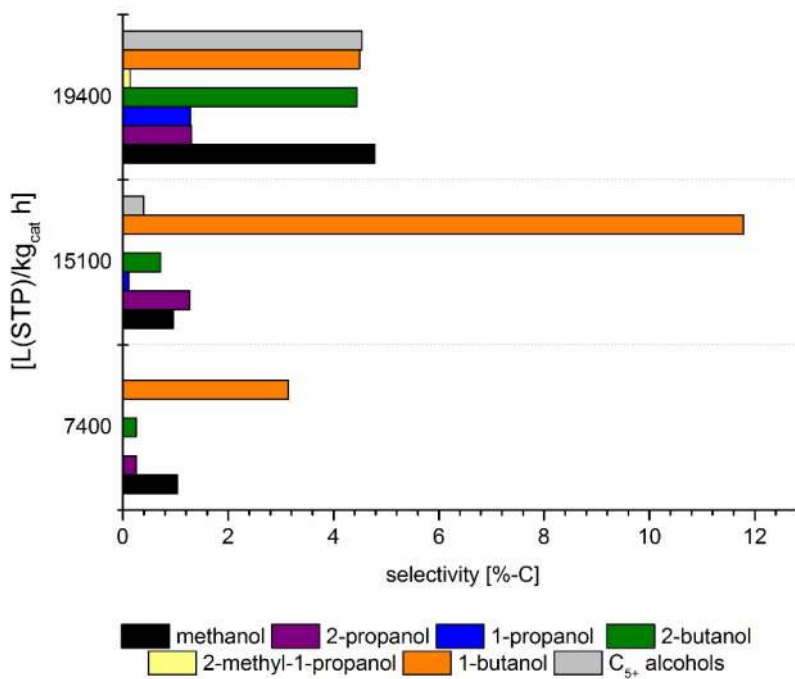


(a)



(b)

Figure 45: Effect of space velocity on: (a) product yield and (b) selectivity in the higher alcohol synthesis with $H_2 : CO=1:1$ and $n_{EtOH} : n_{CO} \sim 0.3:1$ at 593 K, 8.0 MPa over 1.54 g of [1 mol.% Cs-CuO/ZnO]/Al₂O₃ diluted with 1.56 g of 210 μm SiC. Conditions with increasing SV: ethanol flow: 0.05, 0.12 and 0.15 ml/min; total flow: 190, 390 and 500 ml/min.



(a)

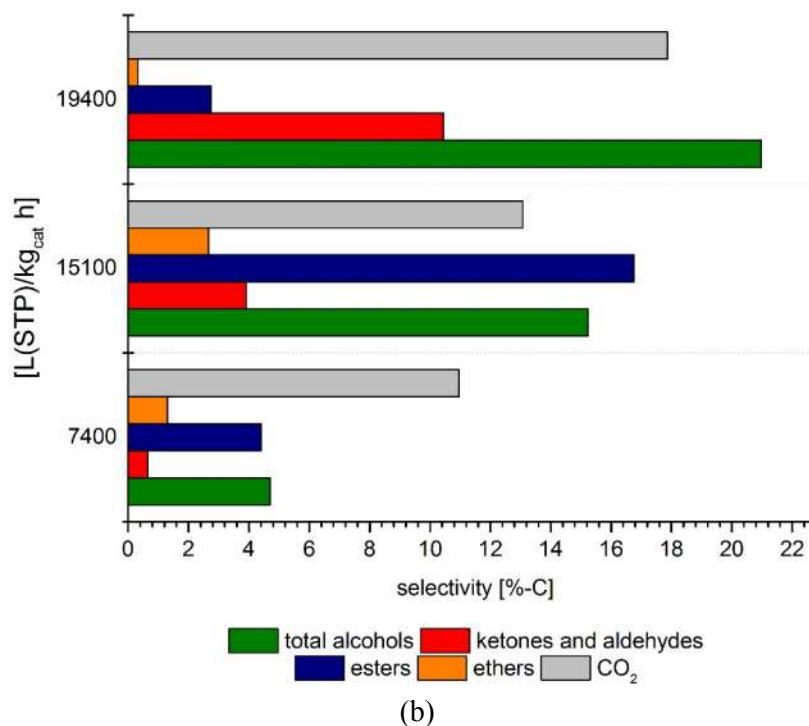


Figure 46: Influence of space velocity on the: (a) alcohol selectivity and (b) product selectivity in the higher alcohol synthesis with $H_2 : CO=1:1$ and $n_{EtOH} : n_{CO} \sim 0.3:1$ at 593 K, 8.0 MPa over 1.54 g of [1 mol.% Cs-CuO/ZnO]/Al₂O₃ diluted with 1.56 g of 210 μm SiC. Conditions with increasing SV: ethanol flow: 0.05, 0.12 and 0.15 ml/min; total flow: 190, 390 and 500 ml/min.

6.2. Influence of the reaction temperature

Temperature does not only affect the reactivity of the catalyst, but it also plays a key role in its stability. It is well known that copper tends to sinter at high temperatures leading to a deactivation of the catalyst. Therefore an in depth investigation of the catalyst stability at these temperatures would be required for a conclusive statement. However, due to time reasons this could not be performed.

The influence of temperature in the higher alcohol synthesis is presented in Table 25, Figure 47 and Figure 48. The yield towards all reaction products, except methanol and other oxygenates, increased with temperature (Figure 47 (a)). Probably, methanol further reacted to higher alcohols or other products at higher temperatures. Even though higher temperatures favored higher alcohol synthesis, also yields and selectivities of the other products, such as CO₂ and alkanes, increased.

The selectivity and yield towards higher oxygenates did not seem to be affected by temperature (except at 543 K). A selectivity and yield around 13.0 and 5.0 %-C, respectively, was

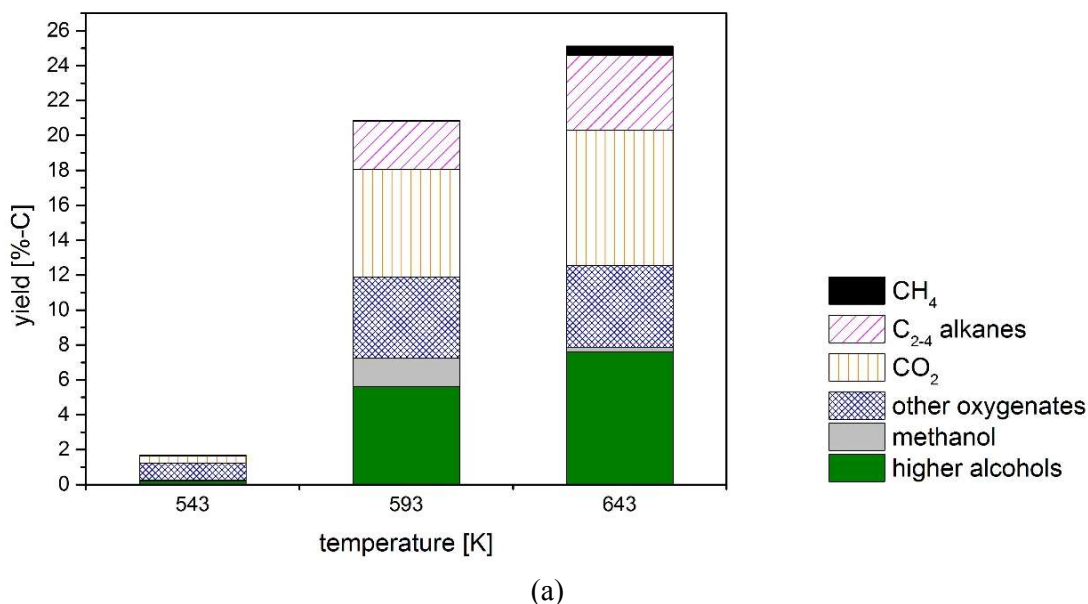
maintained for the higher temperatures. Even though the ethanol conversion increased with temperature, only a slight increase in liquid products derived from ethanol was observed. This would suggest that some of the ethanol further reacted to form C₂₋₄ alkanes or CH₄ was formed.

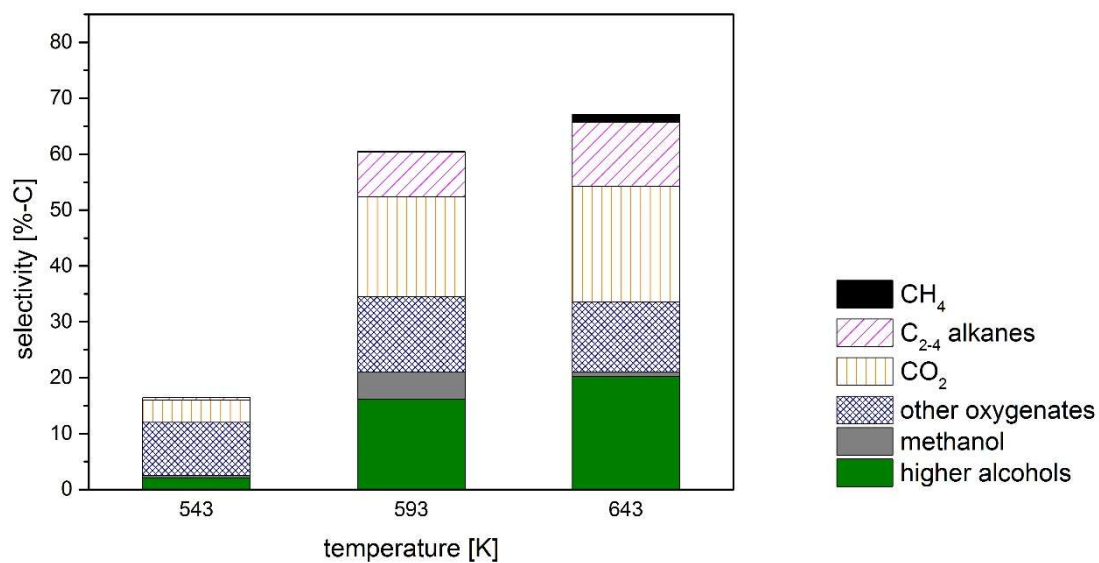
Table 25: Effect of temperature on the CO conversion, ethanol conversion and carbon and mass balances in the higher alcohols synthesis over a CuO/ZnO (30 wt.%) supported on Al₂O₃ catalyst (n_{EtOH} : n_{CO} = 0.3:1; 80 bar; ~19400 L(STP)/kg_{cat} h).

Temperature [K]	Units	543	593	643
Total mass balance	%	96.1	90.7	89.8
C-balance	%	91.5	86.3	87.6
CO conversion	%-C	0.2	15.2	12.6
Ethanol conversion	%-C	26.4	66.6	77.8

The influence of temperature on the product selectivities is presented in Figure 48. Higher temperatures favored the formation of 1-butanol among the alcohols. A slight increase in C₅₊ alcohols was observed with higher temperatures. This suggested that 1-butanol desorbed quickly from the catalyst surface, preventing any further chain growth after its formation.

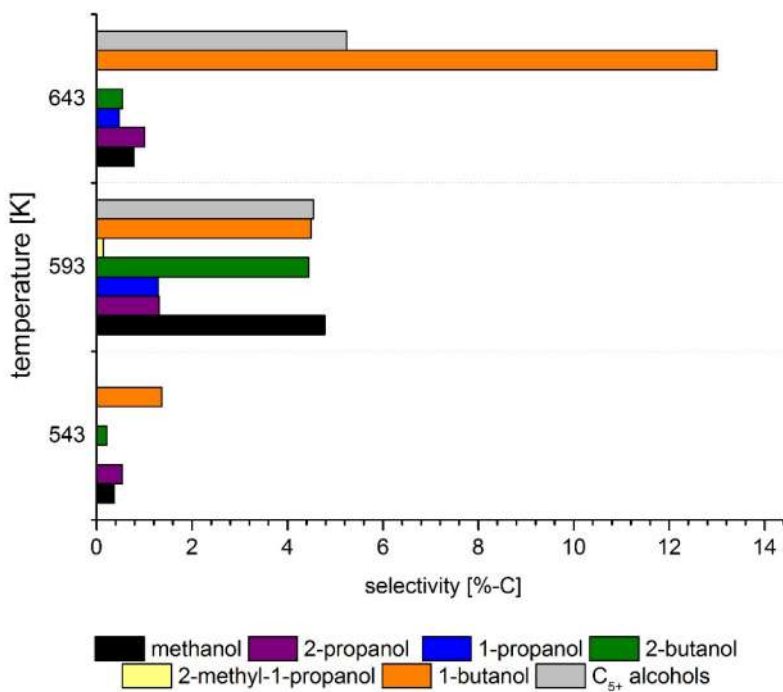
Esters were formed with higher selectivities at lower temperatures (6.9 %-C). The selectivity towards ethers increased with temperature reaching 3.3 %-C. Ketones and aldehydes showed a maximum at intermediate temperatures (10.4 %-C).





(b)

Figure 47: Effect of temperature on: (a) product yield and (b) selectivity in the higher alcohol synthesis with H_2 : $CO=1:1$ and $n_{EtOH} : n_{CO} \sim 0.3:1$ at 593 K, 8.0 MPa over 1.54 g of [1 mol.% Cs-CuO/ZnO]/ Al_2O_3 diluted with 1.56 g of 210 μm SiC. Conditions: ethanol flow: 0.15 ml/min; total flow ~ 500 ml/min.



(a)

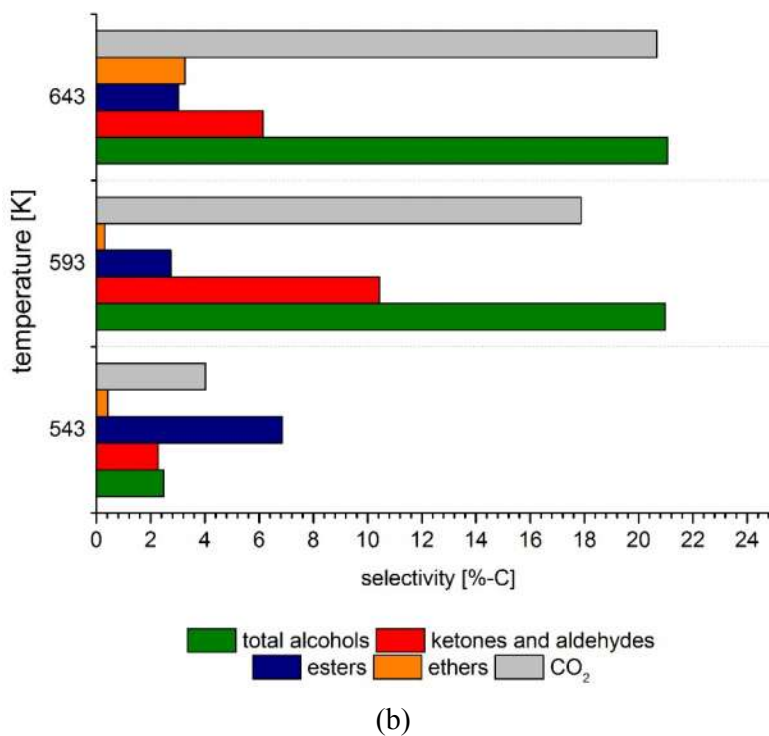


Figure 48: Effect of temperature on: (a) alcohol selectivity and (b) product selectivity in the higher alcohol synthesis with $H_2 : CO = 1:1$ and $n_{EtOH} : n_{CO} \sim 0.3:1$ at 593 K, 8.0 MPa over 1.54 g of [1 mol.% Cs-CuO/ZnO]/Al₂O₃ diluted with 1.56 g of 210 μ m SiC. Conditions: ethanol flow: 0.15 ml/min; total flow \sim 500 ml/min.

6.3. Influence of $n_{EtOH} : n_{CO}$ ratio

As in the experiments in a batch reactor, the effect of the $n_{EtOH} : n_{CO}$ ratio on the higher alcohol synthesis was analyzed. Four different ethanol to CO ratios were studied and the results are presented in Table 26, Figure 49 and Figure 50.

In general, as for the tests in a batch reactor, a maximum in the higher alcohol yield and selectivity was observed for a medium $n_{EtOH} : n_{CO}$ ratio of 0.3:1. Lower ratios favored mostly the formation of gaseous products such as alkanes and CO₂. Increasing the $n_{EtOH} : n_{CO}$ ratio led to an abrupt rise in yield and selectivity of other oxygenates, partially at the expense of alcohol production. Similar results were observed during the batch screening, where an increase from 0.5:1 to 0.9:1 in the $n_{EtOH} : n_{CO}$ provoked a marked increase in the formation of other oxygenates. The maximum yield and selectivity during the continuous reaction corresponded to 5.6 and 16.2 %-C respectively, whereas the maximum for the batch reactor tests were: (a) 12.5 and 22.6 %-C for the 1.0 mol.% Cs-CuO/ZnO catalyst and (b) 9.5 and 21.7 %-C for the [1.0 mol.% Cs-CuO/ZnO] / Al₂O₃, respectively (both with a $n_{EtOH} : n_{CO}$ of 0.5:1). Therefore

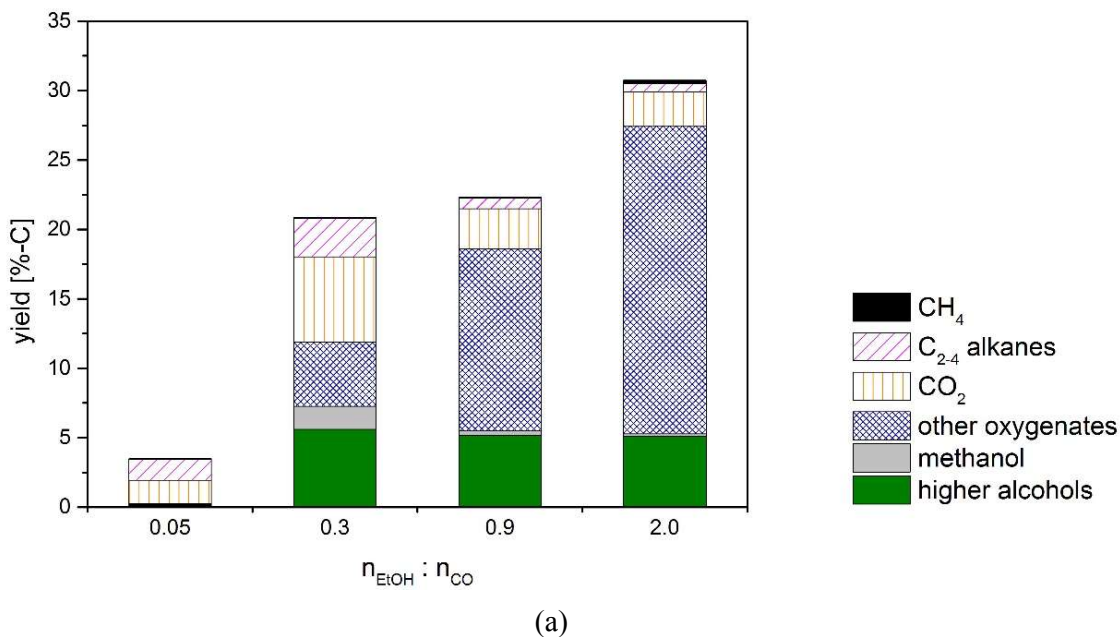
further improvements in higher alcohol yield and selectivity could be expected if the ratio is increased to 0.5:1.

Methanol synthesis also showed a maximum at the same $n_{\text{EtOH}} : n_{\text{CO}}$ ratios, which suggested that higher alcohols and methanol were both formed at similar active sites. Interestingly, also the selectivity to gaseous products decreased with increasing $n_{\text{EtOH}} : n_{\text{CO}}$ ratio.

CO and ethanol conversions showed a maximum for the optimum $n_{\text{EtOH}} : n_{\text{CO}}$ of 0.3:1. As the $n_{\text{EtOH}} : n_{\text{CO}}$ increased, different tendencies regarding the conversion were observed. CO conversion decreased with higher ratios, whereas ethanol conversion showed no clear tendency.

Table 26: Effect of $n_{\text{EtOH}} : n_{\text{CO}}$ on the CO conversion, ethanol conversion and carbon and mass balances in the higher alcohols synthesis over a CuO/ZnO (30 wt.%) supported on Al₂O₃ catalyst (593 K; 80 bar; ~19400 L(STP)/kg_{cat} h).

$n_{\text{EtOH}} : n_{\text{CO}}$	Units	0.05	0.3	0.9	2.0
Total mass balance	%	94.4	90.7	91.6	93.1
C-balance	%	96.4	86.3	91.3	86.2
CO conversion	%-C	4.0	15.2	4.4	0.0
Ethanol conversion	%-C	47.2	66.6	46.8	56.8



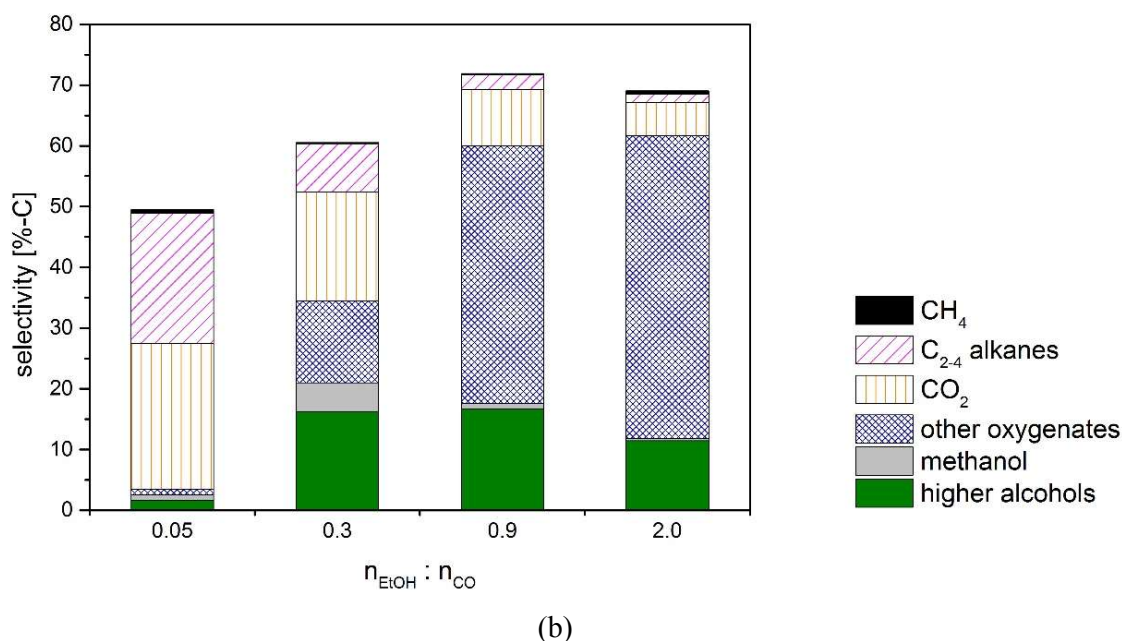
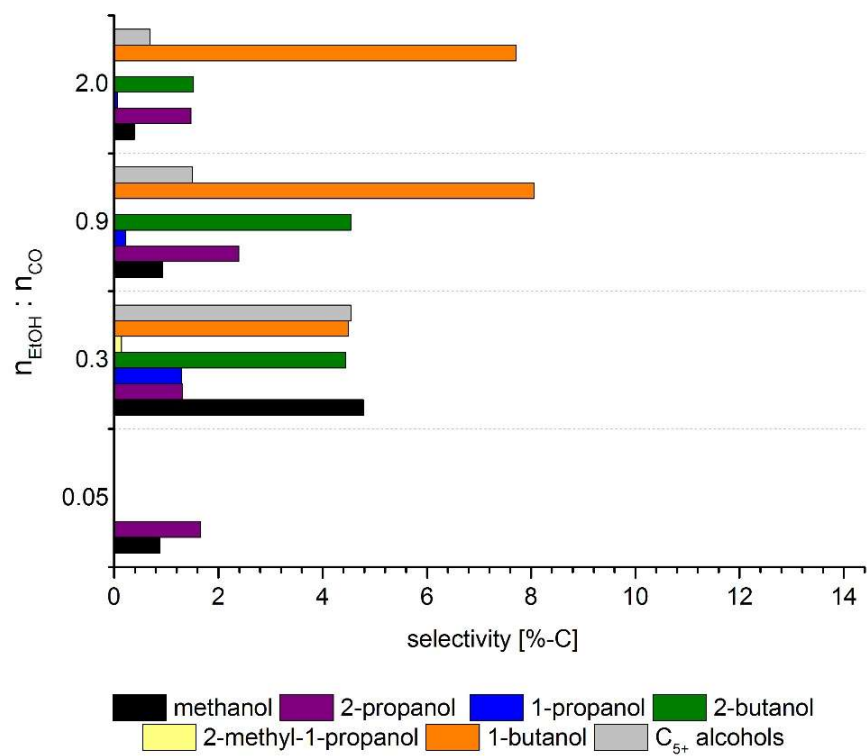


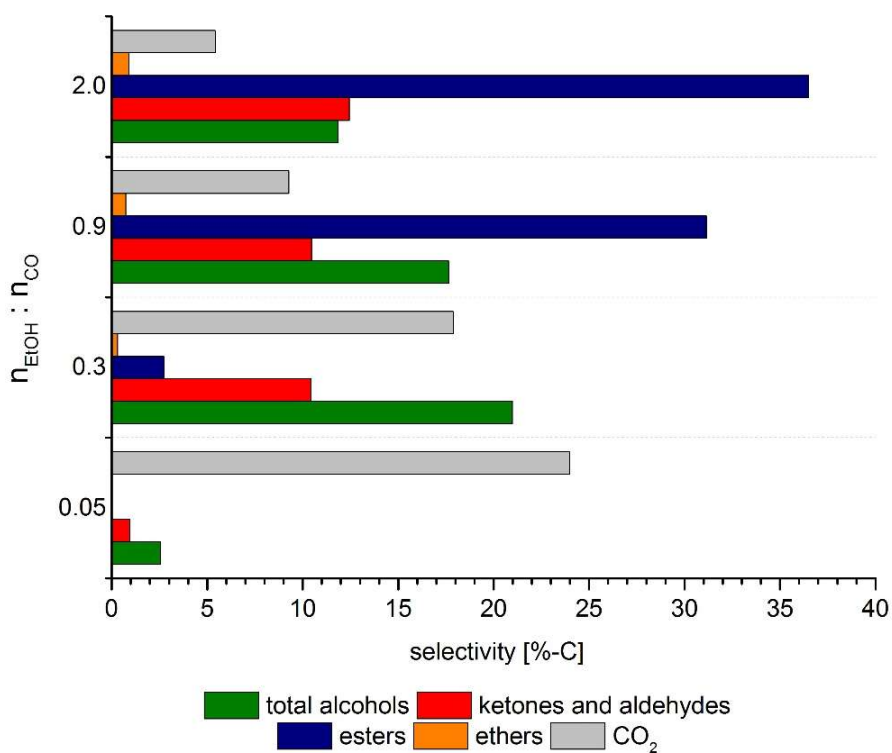
Figure 49: Effect of ethanol to CO ratio on: (a) product yield and (b) selectivity in the higher alcohol synthesis with $\text{H}_2 : \text{CO} = 1:1$ at 593 K, 8.0 MPa over 1.54 g of [1 mol.% Cs-CuO/ZnO]/ Al_2O_3 diluted with 1.56 g of 210 μm SiC. Conditions: ethanol flow with increasing $n_{\text{EtOH}} : n_{\text{CO}}$: 0.02, 0.15, 0.42 and 0.96 ml/min; total flow \sim 500 ml/min.

Figure 50 shows the effect of $n_{\text{EtOH}} : n_{\text{CO}}$ on the product selectivities. A shift in the alcohol selectivity was observed when increasing the $n_{\text{EtOH}} : n_{\text{CO}}$ ratio (Figure 50 (a)). At $n_{\text{EtOH}} : n_{\text{CO}}$ ratio of 0.05:1 mostly methanol and 2-propanol were found, which suggested a direct synthesis of methanol from CO/H_2 and the hydrogenation of acetone to produce 2-propanol. Acetone could be produced directly from ethanol as suggested by Gines and Iglesia.¹⁹³ At $n_{\text{EtOH}} : n_{\text{CO}}$ ratio of 0.3:1 the preferred alcohol products were methanol, 2-butanol, 1-butanol and C_{5+} alcohols. Also 2-propanol, 1-propanol and 2-methyl-1-propanol were identified. This alcohol distribution suggested that aldol-type coupling of both oxygen containing C_1 and C_2 intermediates was occurring. Both 1-butanol and 2-butanol were formed from ethanol homocoupling. Methanol and 2-propanol were formed in an analogous way as mentioned for $n_{\text{EtOH}} : n_{\text{CO}}$ ratio of 0.05:1. 1-propanol and 2-methyl 1-propanol were formed by aldol-type coupling of C_1 intermediates with ethanol and 1-propanol, respectively, as suggested by Nunan et al.¹⁵³ A further increase in the ratio led to higher selectivity of 1-butanol at the expense of other alcohols. The maximum in the 1-butanol selectivity corresponded to 8.1 %-C at $n_{\text{EtOH}} : n_{\text{CO}}$ ratio of 0.9:1.

From these observations it can be derived that increasing ethanol content during higher alcohols synthesis changed the reaction environment in favor of the synthesis of 1-butanol.



(a)



(b)

Figure 50: Effect of ethanol to CO ratio on: (a) alcohol selectivity and (b) product selectivity in the higher alcohol synthesis with $\text{H}_2 : \text{CO}=1:1$ at 593 K, 8.0 MPa over 1.54 g of [1 mol.% Cs-CuO/ZnO]/Al₂O₃ diluted with 1.56 g of 210 μm SiC. Conditions: ethanol flow with increasing $n_{\text{EtOH}}:n_{\text{CO}}$: 0.02, 0.15, 0.42 and 0.96 ml/min; total flow \sim 500 ml/min.

In general, the formation of all ketones/aldehydes followed most probably the same path: (1) dehydration to the alkene, followed by (2) hydrogenation to the ketone or the aldehyde. No clear evidence could be found with the experiments performed so far in regard to this aspect. One possibility could be that higher contents of ethanol increased the amount of ethanol derivatives adsorbed on the surface changing the basicity/acidity of the catalyst surface, which could lead to the preferred formation of one or the other intermediate. From the discussion in the previous chapters, presence of Cs in the catalyst led to a more basic environment, which would favor the faster C₁-aldol type coupling with retention of the oxygen of the C₁ intermediate as suggested by Nunan et al.¹⁵³ In the case that adsorbed ethanol would block the more basic surface sites, this path would be less favored leading also to an aldol-type coupling, but with retention of the oxygen of the alcohol derivative (Scheme 3, III). Applied to our case with C₂ intermediates, this would lead to the formation of more 1-butanol (Scheme 3, III) instead of 2-butanol (Scheme 3, II), which is formed presumably at more basic sites. The presence of more basic sites influenced the type of adsorption of the intermediate. In the presence of Cs, the alkyl oxygen is adsorbed at Cs⁺ cations, leading to a complete hydrogenation of the free -CHO group to -CH₃.¹⁹³ Another possibility considered a blocking of the Cu sites by adsorbed ethanol which, according to Gines and Iglesia¹⁹³, enhanced the hydrogen transfer step required to interconvert the aldol into the keto form. This would lead to a smaller number of keto species on the surface, which can be further transformed into 2-butanol.

In Figure 50 (b) the selectivity towards other reactions products is presented. Higher n_{EIOH} : n_{CO} ratios led to a decrease in the selectivities towards CO₂ for all ratios and alcohols except for n_{EIOH} : n_{CO} ratio of 0.05:1 to 0.3:1. The formation of ketones and aldehydes was maintained in the same level (10.4 to 12.4 %-C), except for n_{EIOH} : n_{CO} ratio of 0.05:1. Both the selectivities towards esters and ethers increased with higher n_{EIOH} : n_{CO} ratios. The maximum selectivity to esters was obtained at a n_{EIOH} : n_{CO} of 2.0:1 (36.5 %-C). These results suggest that ketones and aldehydes might represent intermediates in the formation of both esters and alcohols. The adsorption of more ethanol derivatives on the catalyst surface might have partially blocked the copper hydrogenation sites, which enabled the further hydrogenation of the aldehydes and ketones to alcohols. More available ethanol on the surface would most probably have favored the reaction of acetaldehyde with adsorbed ethanol leading to ethyl acetate in particular or esters in general. Elliot and Penella¹⁹⁴ suggested the formation of esters through the Tischenko reaction mechanism with the reaction of an aldehyde with a surface alkoxide. Acetaldehyde

selectivity also increased with the ethanol to CO ratio (see further supporting information, Table S 28 and Table S 30). It could be possible that copper sites favored dehydrogenation reactions instead of hydrogenations, leading to more acetaldehyde.

Most of the identified products could be formed either by: (1) the homocoupling of ethanol (or ethanol derivatives) or (2) from the coupling of butanols with ethanol (or both of its derivatives). Similar results have been also suggested by Elliot and Penella.¹⁹⁴ The authors suggested that the main products for C_n alcohols reactions were: n aldehydes, 2n esters, 2n ketones and 2n-1 ketones. Under inert atmosphere (N₂) the main products were the n aldehyde and 2n esters, whereas in a CO containing environment the 2n ketones were predominant. The authors suggested that CO was oxidized to CO₂ by lattice oxygen forming oxygen vacancies. Since the catalyst was reduced, its basicity increased, which should favor the formation of 2n ketones by aldol condensation reactions. On the contrary, in the present study, hydrogen was present in the reaction atmosphere additional to CO. Therefore, the ketones were probably hydrogenated to the corresponding alcohols. In the cases of n_{EtOH} : n_{CO} ratio of 0.9:1 and 2.0:1, most of the catalyst surface was probably occupied by adsorbed ethanol or comparable species. The adsorption of ethanol (or acetaldehyde) might have hindered the lattice oxygen removal by CO oxidation. Since no oxygen vacancies would be available, as was the case under inert atmosphere in the study of Elliot and Penella¹⁹⁴, the formation of 2n ketones and, consequently 2n alcohols through aldol condensation would be suppressed. As a result of this, the preferred products would be esters. For the catalyst system used in the present thesis, the most abundant ester corresponded to ethyl acetate (Scheme 3, IV).

6.4. Characterization after reaction

The catalyst used in the previous experiments was taken from the reactor, sieved to separate it from the SiC particles and then analyzed by XRD (Figure 51). Additionally, its composition was determined by elemental analysis (Table 27) and its specific surface was obtained area by N₂ physisorption.

Before measuring the XRD pattern after the higher alcohol synthesis in the continuous reactor, the catalyst was exposed to air, therefore some CuO reflections could be expected. The reduced catalyst was maintained in an inert atmosphere until the XRD pattern was measured. After the reaction, Cu (reflection at 43.2°) and ZnO (reflection at 56.6°) reflections were identified with a crystallite size of 29 and 23 nm, respectively. In comparison to the catalyst after the batch

experiment (Figure 40), the copper reflections after the reaction in the continuous reactor had higher intensities and were narrower. This indicated that the copper crystallites were larger after the tests in the continuous reactor, as shown also by the crystallite size determined by the Scherrer equation. It is important to notice that during the reaction in the continuous reactor the catalyst was exposed to different reactions conditions, including higher temperatures, while the catalyst after the batch experiments was only used for a single reaction. The Cu (reflection at 43.2°) and ZnO (reflection at 56.6°) crystallite sizes for the catalyst reduced in hydrogen corresponded to 55 and 23 nm, respectively. The Cu crystallite size after the reduction in hydrogen was larger in comparison to the size after the synthesis of higher alcohols, whereas the ZnO crystallite size was the same.

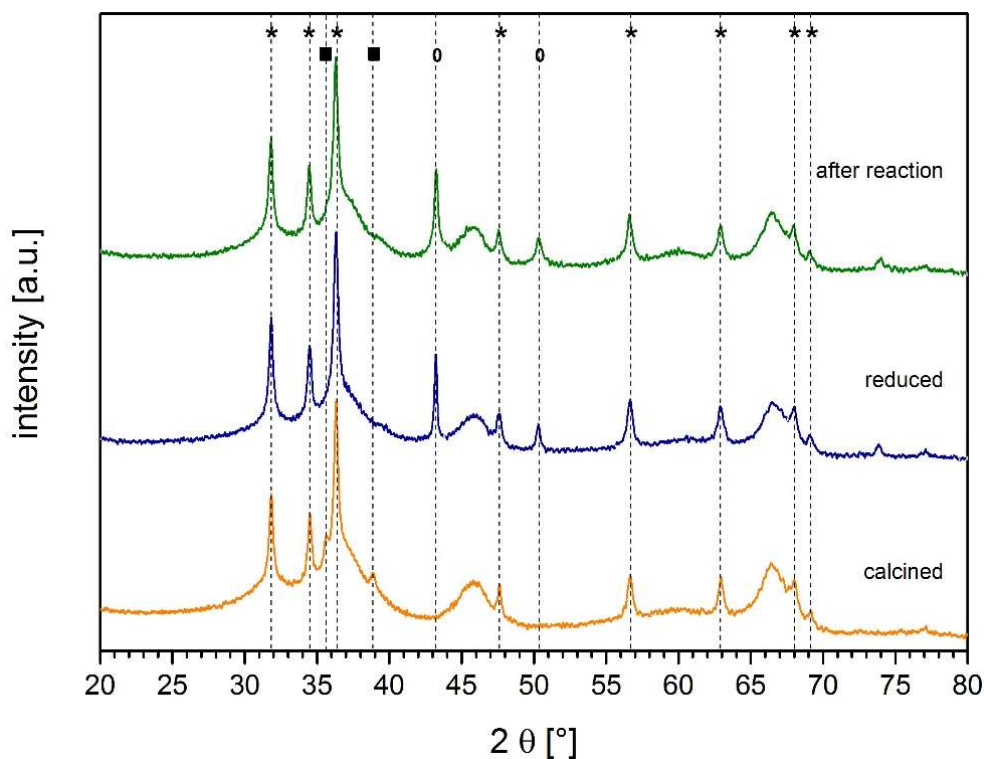


Figure 51: X-ray diffraction patterns for [1 mol.% Cs-CuO/ZnO]/Al₂O₃ catalyst freshly calcined, freshly reduced and after higher alcohol synthesis with H₂ : CO=1:1 for all experiments presented in chapter 6. *: ZnO, °: CuO and °: Cu.

The specific surface area of the catalyst after reaction corresponded to 140 m²/g which is 13 % lower in comparison to the freshly prepared catalyst which corresponded to 160 m²/g (section 3.2, Table 8). The catalyst after reaction was analyzed by ICP-OES to determine its elemental composition (Table 27). In comparison with the composition of the catalyst before the reaction (section 3, Table 6), some of the copper originally present on the catalyst leached since the

percentage of Cu decreased from 7.2 to 5.7 wt.% causing an increased value for the other metal components.

Table 27: Elemental composition of the [1.0 mol.%Cs-CuO/ZnO]/Al₂O₃ catalyst after reaction in the higher alcohol synthesis in the continuous-flow reactor.

Catalyst	Measured [wt.%]			
	Al/Si	Cu	Zn	Cs
CuO/ZnO/Al ₂ O ₃ _wi	33.2	5.7	18.1	0.4

6.5. Conclusions

Reactions using a continuous-flow reactor allow the variation of parameters which could not be controlled during batch experiments. Therefore it is very important to compare both types of experiments to obtain the most possible information about the target reaction.

For this study, the catalytic synthesis of higher alcohols starting from synthesis gas and ethanol was tested in a trickle-bed reactor using a [1.0 mol.% Cs-CuO/ZnO] supported on Al₂O₃ catalyst. The effects of space velocity, temperature and ethanol to CO ratio were analyzed.

A space velocity of approximate 19400 L(STP) / kg_{cat} h showed the highest yield and selectivity towards higher alcohols, with the lowest selectivity towards by-products such as other oxygenates. These conditions also enhanced the production of C₅₊ alcohols.

Moderate temperatures (593 K) seemed more appropriate for the catalytic synthesis of higher alcohols under the reaction conditions studied. Even though a temperature of 643 K increased the yield and selectivity towards higher alcohols, at the same time it enhanced the production of undesired gaseous products such as alkanes and CO₂. Additionally, according to literature studies higher temperatures promote the sintering of copper particles. The production of liquid byproducts such as other oxygenates was not influenced by further increasing the temperature after 593 K. The selectivity to ketones and aldehydes showed a maximum at 593 K, whereas lower temperatures (543 K) were preferred for esters.

An optimum n_{EIOH} : n_{CO} ratio of 0.3:1 was found for the production of higher alcohols. This ratio promoted higher alcohol yields without enhancing the formation of other oxygenates, particularly esters. The ethanol to CO ratio played an important role in the product distribution. Especially in the alcohol distribution, higher ethanol to CO ratios led to the preferential

formation of 1-butanol. Lower ratios favored the formation of methanol, 2-butanol, 1-butanol and C₅₊ alcohols. This suggested a change in the preferred reaction path. The change in the reaction path could be a consequence of a reactant inhibition, since ethanol adsorbed on the copper sites could hinder the hydrogen adsorption or the removal of lattice oxygen through CO oxidation.

7. Final remarks and outlook

The present work represents a first approach in the synthesis of higher alcohols starting from synthesis gas and ethanol using CuO/ZnO supported catalysts. The addition of ethanol intended to circumvent the slow coupling step from C₁ to C₂ species. Several steps were performed to optimize the catalyst and reaction conditions. First, a modified CuO/ZnO system was tested in the higher alcohol synthesis using a batch reactor. The effect of two different dopants on the catalyst was tested and optimized. Variations in the ethanol to carbon monoxide ratio strongly influenced the reaction path. The optimal ethanol to CO ratio was found to be 0.5:1 and the study was extended to a supported catalyst system. Various catalysts obtained by different preparation methods were tested in a larger batch reactor as well as variations in the reaction temperature for a selected catalyst. In parallel, a high pressure, continuous-flow reactor was designed and built. Before the reactor was used for the target reaction, a traditional methanol synthesis was performed as a proof of concept of the reactor. Finally, the catalyst that was best performing in the batch reactor screening was tested in the continuous setup for the synthesis of higher alcohols. The effect of space velocity, temperature and ethanol to CO ratio were studied. Similarly to the synthesis of higher alcohols in batch reactors, a correlation between the amount of ethanol dosed to the reactor and the production distribution was observed.

The type of dopant on the CuO/ZnO catalyst had an important influence on the product distribution and conversion. Cs doping resulted in a better performance in the higher alcohols synthesis in comparison to Ru. The presence of Cs favored the synthesis of alcohols, whereas Ru doping shifted the products towards alkanes and alkenes. The content of Cs on the CuO/ZnO catalyst changed the yield and selectivities towards higher alcohols. An optimum Cs content was found between 0.6 and 1.0 mol.%. This effect was observed regardless of the ethanol to CO ratio used for the reaction. The absence of Cs favored the production of CH₄, alkanes and CO₂ whereas it shifted the alcohol selectivity towards methanol. An excess of Cs led to a blockage of the hydrogenation sites which inhibited the higher alcohols synthesis.

The ethanol to CO ratio played a key role in the product distribution of the liquid phase. The presence or absence of ethanol shifted the preferred reaction path. In the absence of ethanol, the main alcohol products were methanol, 1-propanol and 2-methyl-1-propanol, in accordance with literature reports. In the presence of solely ethanol and synthesis gas (cyclohexane free reactions), the alcohol selectivity was shifted towards 1-butanol and 2-butanol. For

intermediate ratios, a mixture of both pathways was observed indicated by a shift in the preferred reaction path as a function of the ethanol content in the reactor. In the absence of ethanol, an aldol-type condensation of oxygen containing C₁ intermediates with adsorbed alcohols (or intermediates) was observed. As the ethanol concentration in the reaction mixture increased, also an aldol type condensation occurred, but the homocoupling of ethanol was preferred instead of the coupling of C₁ intermediates. Additionally, an excess of ethanol led to an increase in the formation of byproducts, mostly ethyl acetate, and to leaching of the active species. Most probably an inhibition of the surface reactions by adsorbed ethanol derived intermediates was occurring.

Higher temperatures shifted the reaction towards higher alcohols, but attention is required regarding the sintering of copper particles. The preparation method had an influence on the production of higher alcohol. Most probably the different methods led to different arrangements between the Cu and ZnO particles. As proposed by the literature, the activity of the catalyst depended on the type of interaction between Cu particles and ZnO.

A continuous-flow reactor was successfully design and built as demonstrated by the methanol synthesis experiment. The optimal operation parameters were calculated assuming worst case scenarios to ensure the proper performance of the reactor. According to the calculations no mass or heat transfer limitations were present as well as preferential flow effects. Additional experimental verification of the absence of mass and heat transfer limitations is still required. To improve the performance of the reactor, changes in the product quantification methods are advisable. The use of an online gas chromatography system for all products would improve the mass and carbon balances and avoid errors due to evaporation of the products. This can be helpful to overcome problems concerning product condensation and quantification.

The target reaction was successfully performed in the continuous-flow reactor. Despite of the need of condensation of the reaction products, clear tendencies in the product distribution were observed as the reactions parameters were varied. Increasing the space velocity (shorter residence time) led to an increase in the yield and selectivity towards higher alcohols. Apparently, longer residence times allowed the side reactions to progress, leading to an increase in the formation of other oxygenates (esters and ketones). It is suggested that ketones and aldehydes are the intermediates of both the alcohol and esters formation. Therefore, longer residence times shifted the reaction towards esters, since the reactants were adsorbed at the surface for a longer time allowing the side reactions to occur. Like for the batch reactions

increasing the reaction temperature led to an increase in the production of alcohols. Nevertheless, the production and selectivity of gaseous products, such as alkanes and CO₂, increased as well. Higher temperatures shifted the alcohol selectivity to 1-butanol. No evidence of temperature effects influencing the production of esters was observed.

As for the batch reactions, the ethanol to CO ratio played an important role in the alcohol distribution. The optimum ethanol to CO ratio was found to be 0.3:1. Increasing the ethanol content in the reaction led to an abrupt jump in the production and selectivity towards other oxygenates. The results derived from this section suggested that aldehydes and ketones were intermediates to the formation of either alcohols or esters. Increasing ethanol availability led to a shift towards the formation of esters. This shift towards esters might be a consequence of partially blocked hydrogenation sites by adsorbed ethanol derivatives hampering the further hydrogenation of the aldehydes and ketones to alcohols. On the other hand, more ethanol on the surface would most probably favor the reaction of acetaldehyde with adsorbed ethanol leading to ethyl acetate. The preferential formation of either primary or secondary alcohols was a consequence of an equilibrium reaction between the aldol and keto form from the coupling product of two acetaldehydes. The equilibrium was clearly affected by the presence of ethanol in the reaction medium. Two possibilities were suggested to explain this phenomenon: (1) higher contents of ethanol increased the amount of ethanol derivatives adsorbed on the surface, changing the basicity/acidity of the catalyst surface or (2) the adsorbed ethanol blocked the Cu sites, which allowed the hydrogen transfer step required to interconvert the aldol into the keto form.

In general, during this thesis it was proven that the addition of an appropriate amount of ethanol to the synthesis gas improved the production of higher alcohols. Nevertheless, the system remains challenging and needs further improvements before fulfilling the requirements for industrial applications. Therefore, still several modifications to the catalyst have to be done to improve its selectivity and yield towards higher alcohols. It would be reasonable to test other dopants and supports as well as further variations in reaction parameters (temperature, $n_{\text{EtOH}} : n_{\text{CO}}$ ratio and space velocity), since they play a key role in the synthesis of higher alcohols. Further experiments regarding the influence of pressure, long term behavior and surface modifications are still required. The number of parameters that can be tuned is rather large and further efforts should be done to combine theoretical and experimental findings. Catalysts containing Cu and Co appear to be interesting for further studies. Another catalyst system that has been widely studied due to its attractive characteristics, as mentioned in section 1.4.1.2,

corresponds to Mo-based catalysts. Another interesting aspect regarding higher alcohol synthesis, once an appropriate catalyst is found, is analyzing the catalyst behavior during transient reaction conditions by X-ray absorption spectroscopy. This type of analysis would indicate, for example, changes in the catalyst during the reaction or understanding in the precise effect of adsorbed ethanol on the catalyst. Further analysis to understand how the surface of catalyst changes with the reaction conditions are required. *In operando* or *in situ* IR or Raman studies, enable the characterization of the catalyst or adsorbed substrates, intermediates and products to gain valuable mechanistic information. An interesting approach would involve understanding the precise role of the promoter (XPS, XAS or IR experiments). Knowledge at this length scale would contribute to elucidate how the catalyst works giving an input to theoretical calculations in order to derive a reaction mechanism. An appropriate *in situ* cell has to be developed, which would enable studies at high temperatures (> 423 K) and high pressures (> 4.0 MPa), to perform this type of analysis. Additionally, a long term stability test of the catalyst is indispensable before any further scaling up considerations.

References

1. IEA, *World Energy Outlook 2015*. OECD Publishing: 2015; ISBN: 9789264243668
2. IEA, *Key World Energy Statistics 2015*. OECD Publishing: 2015; ISBN: 9789264266544
3. van Swaaij, W. P. M.; Kersten, S. R. A.; Palz, W., *Biomass Power for the World*. Pan Stanford Publishing: 2015; ISBN: 9789814613897
4. Rostrup-Nielsen, J. R., Fuels and Energy for the Future: The Role of Catalysis. *Catal. Rev.* **2004**, *46*, 247-270.
5. Abbasi, T.; Abbasi, S. A., Biomass energy and the environmental impacts associated with its production and utilization. *Renew. Sust. Energ. Rev.* **2010**, *14*, 919-937.
6. Kumar, A.; Jones, D.; Hanna, M., Thermochemical Biomass Gasification: A Review of the Current Status of the Technology. *Energies* **2009**, *2*, 556-581.
7. Alonso, D. M.; Bond, J. Q.; Dumesic, J. A., Catalytic conversion of biomass to biofuels. *Green Chem.* **2010**, *12*, 1493-1513.
8. Chheda, J. N.; Huber, G. W.; Dumesic, J. A., Liquid-Phase Catalytic Processing of Biomass-Derived Oxygenated Hydrocarbons to Fuels and Chemicals. *ChemInform* **2007**, *38*, 7164-7183.
9. Serrano-Ruiz, J. C.; Luque, R.; Sepulveda-Escribano, A., Transformations of biomass-derived platform molecules: from high added-value chemicals to fuels via aqueous-phase processing. *Chem. Soc. Rev.* **2011**, *40*, 5266-5281.
10. Demirbaş, A., Biomass resource facilities and biomass conversion processing for fuels and chemicals. *Energy Convers. Manage.* **2001**, *42*, 1357-1378.
11. Huber, G. W.; Iborra, S.; Corma, A., Synthesis of Transportation Fuels from Biomass: Chemistry, Catalysts, and Engineering. *Chem. Rev.* **2006**, *106*, 4044-4098.
12. Kaltschmitt, M., Biomass biomass as Renewable Source of Energy biomass as renewable source of energy , Possible Conversion Routes. In *Encyclopedia of Sustainability Science and Technology*, Meyers, R., Ed. Springer New York: 2012; 1198-1231.
13. Küçük, M. M.; Demirbaş, A., Biomass conversion processes. *Energy Convers. Manage.* **1997**, *38*, 151-165.
14. Pant, K. K.; Mohanty, P., Biomass, Conversion Routes and Products – An Overview. In *Transformation of Biomass*, John Wiley & Sons, Ltd: 2014; 1-30.
15. Isahak, W. N. R. W.; Hisham, M. W. M.; Yarmo, M. A.; Yun Hin, T.-y., A review on bio-oil production from biomass by using pyrolysis method. *Renew. Sust. Energ. Rev.* **2012**, *16*, 5910-5923.
16. Kirubakaran, V.; Sivaramakrishnan, V.; Nalini, R.; Sekar, T.; Premalatha, M.; Subramanian, P., A review on gasification of biomass. *Renew. Sust. Energ. Rev.* **2009**, *13*, 179-186.
17. Dahmen, N.; Dinjus, E.; Kolb, T.; Arnold, U.; Leibold, H.; Stahl, R., State of the art of the bioliq® process for synthetic biofuels production. *Environmental Progress & Sustainable Energy* **2012**, *31*, 176-181.

18. Abuelnuor, A. A. A.; Wahid, M. A.; Hosseini, S. E.; Saat, A.; Saqr, K. M.; Sait, H. H.; Osman, M., Characteristics of biomass in flameless combustion: A review. *Renew. Sust. Energ. Rev.* **2014**, *33*, 363-370.
19. Boscagli, C.; Raffelt, K.; Zevaco, T. A.; Olbrich, W.; Otto, T. N.; Sauer, J.; Grunwaldt, J.-D., Mild hydrotreatment of the light fraction of fast-pyrolysis oil produced from straw over nickel-based catalysts. *Biomass Bioenergy* **2015**, *83*, 525-538.
20. Mortensen, P. M.; Grunwaldt, J. D.; Jensen, P. A.; Knudsen, K. G.; Jensen, A. D., A review of catalytic upgrading of bio-oil to engine fuels. *Appl. Catal., A* **2011**, *407*, 1-19.
21. Wender, I., Synthesis Gas as a Source of Fuels and Chemicals: C-1 Chemistry. *Annual Review of Energy* **1986**, *11*, 295-314.
22. Spath, P. L.; Dayton, D. C.; (U.S.), N. R. E. L. Preliminary Screening-Technical and Economic Assessment of Synthesis Gas to Fuels and Chemicals with Emphasis on the Potential for Biomass-derived Syngas; *NREL/TP-510-34929*; 2003.
23. Ni, M.; Leung, D. Y. C.; Leung, M. K. H.; Sumathy, K., An overview of hydrogen production from biomass. *Fuel Process. Technol.* **2006**, *87*, 461-472.
24. Chorkendorff, I.; Niemantsverdriet, J. W., Heterogeneous Catalysis in Practice: Hydrogen. In *Concepts of Modern Catalysis and Kinetics*, Wiley-VCH Verlag GmbH & Co. KGaA: 2005; 301-348.
25. Schlögl, R., *Chemical Energy Storage*. De Gruyter: 2012; 978-3-11-026632-0
26. Henstra, A. M.; Sipma, J.; Rinzema, A.; Stams, A. J. M., Microbiology of synthesis gas fermentation for biofuel production. *Curr. Opin. Biotechnol.* **2007**, *18*, 200-206.
27. Khaodee, W.; Tangchupong, N.; Jongsomjit, B.; Praserttham, P.; Assabumrungrat, S., A study on isosynthesis via CO hydrogenation over ZrO₂-CeO₂ mixed oxide catalysts. *Catal. Commun.* **2009**, *10*, 494-501.
28. Shah, Y. T.; Perrotta, A. J., Catalysts for Fischer-Tropsch and Isosynthesis. *Product R&D* **1976**, *15*, 123-131.
29. Caili, S.; Dehua, H.; Junrong, L.; Zhenxing, C.; Qiming, Z., Influences of preparation parameters on the structural and catalytic performance of zirconia in isosynthesis. *J. Mol. Catal. A: Chem.* **2000**, *153*, 139-146.
30. Erkey, C.; Wang, J.; Postula, W.; Feng, Z.; Phillip, C. V.; Akgerman, A.; Anthony, R. G., Isobutylene Production from Synthesis Gas over Zirconia in a Slurry Reactor. *Ind. Eng. Chem. Res.* **1995**, *34*, 1021-1026.
31. Li, Y.; He, D.; Zhu, Q.; Zhang, X.; Xu, B., Effects of redox properties and acid-base properties on isosynthesis over ZrO₂-based catalysts. *J. Catal.* **2004**, *221*, 584-593.
32. Agbossou, F.; Carpentier, J.-F.; Mortreux, A., Asymmetric Hydroformylation. *Chem. Rev.* **1995**, *95*, 2485-2506.
33. Franke, R.; Selent, D.; Börner, A., Applied Hydroformylation. *Chem. Rev.* **2012**, *112*, 5675-5732.
34. Dry, M. E., The Fischer-Tropsch process: 1950-2000. *Catal. Today* **2002**, *71*, 227-241.
35. Jahangiri, H.; Bennett, J.; Mahjoubi, P.; Wilson, K.; Gu, S., A review of advanced catalyst development for Fischer-Tropsch synthesis of hydrocarbons from biomass derived syn-gas. *Catal. Sci. Technol.* **2014**, *4*, 2210-2229.

36. Mills, G. A.; Steffgen, F. W., Catalytic Methanation. *Catal. Rev.* **1974**, 8, 159-210.
37. Sehested, J.; Dahl, S.; Jacobsen, J.; Rostrup-Nielsen, J. R., Methanation of CO over Nickel: Mechanism and Kinetics at High H₂/CO Ratios. *The Journal of Physical Chemistry B* **2005**, 109, 2432-2438.
38. Kambolis, A.; Schildhauer, T. J.; Kröcher, O., CO Methanation for Synthetic Natural Gas Production. *CHIMIA International Journal for Chemistry* **2015**, 69, 608-613.
39. Rönsch, S.; Schneider, J.; Matthischke, S.; Schlüter, M.; Götz, M.; Lefebvre, J.; Prabhakaran, P.; Bajohr, S., Review on methanation – From fundamentals to current projects. *Fuel* **2016**, 166, 276-296.
40. Fang, K.; Li, D.; Lin, M.; Xiang, M.; Wei, W.; Sun, Y., A short review of heterogeneous catalytic process for mixed alcohols synthesis via syngas. *Catal. Today* **2009**, 147, 133-138.
41. Gupta, M.; Smith, M. L.; Spivey, J. J., Heterogeneous Catalytic Conversion of Dry Syngas to Ethanol and Higher Alcohols on Cu-Based Catalysts. *ACS Catal.* **2011**, 1, 641-656.
42. Herman, R. G., Advances in catalytic synthesis and utilization of higher alcohols. *Catal. Today* **2000**, 55, 233-245.
43. Surisetty, V. R.; Dalai, A. K.; Kozinski, J., Alcohols as alternative fuels: An overview. *Appl. Catal., A* **2011**, 404, 1-11.
44. Zaman, S.; Smith, K. J., A Review of Molybdenum Catalysts for Synthesis Gas Conversion to Alcohols: Catalysts, Mechanisms and Kinetics. *Catal. Rev.* **2012**, 54, 41-132.
45. Hedrick, S. A.; Chuang, S. S. C.; Pant, A.; Dastidar, A. G., Activity and selectivity of Group VIII, alkali-promoted Mn-Ni, and Mo-based catalysts for C₂₊ oxygenate synthesis from the CO hydrogenation and CO/H₂/C₂H₄ reactions. *Catal. Today* **2000**, 55, 247-257.
46. Mawson, S.; McCutchen, M. S.; Lim, P. K.; Roberts, G. W., Thermodynamics of higher alcohol synthesis. *Energ. Fuel.* **1993**, 7, 257-267.
47. Mazanec, T. J., On the mechanism of higher alcohol formation over metal oxide catalysts: I. A rationale for branching in the synthesis of higher alcohols from syngas. *J. Catal.* **1986**, 98, 115-125.
48. Medford, A.; Lausche, A.; Abild-Pedersen, F.; Temel, B.; Schjødt, N.; Nørskov, J.; Studt, F., Activity and Selectivity Trends in Synthesis Gas Conversion to Higher Alcohols. *Top. Catal.* **2014**, 57, 135-142.
49. Spivey, J. J.; Egbebi, A., Heterogeneous catalytic synthesis of ethanol from biomass-derived syngas. *Chem. Soc. Rev.* **2007**, 36, 1514-1528.
50. Subramani, V.; Gangwal, S. K., A Review of Recent Literature to Search for an Efficient Catalytic Process for the Conversion of Syngas to Ethanol. *Energ. Fuel.* **2008**, 22, 814-839.
51. Christensen, J. M.; Mortensen, P. M.; Trane, R.; Jensen, P. A.; Jensen, A. D., Effects of H₂S and process conditions in the synthesis of mixed alcohols from syngas over alkali promoted cobalt-molybdenum sulfide. *Appl. Catal., A* **2009**, 366, 29-43.
52. Surisetty, V. R.; Eswaramoorthi, I.; Dalai, A. K., Comparative study of higher alcohols synthesis over alumina and activated carbon-supported alkali-modified MoS₂ catalysts promoted with group VIII metals. *Fuel* **2012**, 96, 77-84.
53. Morgan, C. R.; Warner, J. P.; Yurchak, S., Gasoline from alcohols. *Industrial & Engineering Chemistry Product Research and Development* **1981**, 20, 185-190.

54. Bertau, M. e.; Offermanns, H. e.; Plass, L. e.; Schmidt, F. e.; Wernicke, H.-J. e., *Methanol: The Basic Chemical and Energy Feedstock of the Future Asinger's Vision Today*. 2014;
55. Olah, G.; Goepfert, A.; Surya Prakash, G., *Beyond Oil and Gas: The Methanol Economy*. Wiley-VCH: Weinheim, Germany: 2006; 3-527-31275-7
56. Chen, H.; Yang, L.; Zhang, P.-h.; Harrison, A., The controversial fuel methanol strategy in China and its evaluation. *Energy Strategy Reviews* **2014**, 4, 28-33.
57. Corporation, M. Methanex Investor Presentation. <https://www.methanex.com/sites/default/files/investor/MEOH%20Methanex%20Presentation%20-%20Dec%202015.pdf> (14.02.2016)
58. Ahmad, R.; Arnold, U.; Deutsch, D.; Döring, M.; Sauer, J., Passivation and reactivation of catalyst systems for the single step synthesis of dimethyl ether from CO-rich synthesis gas. *J. Mol. Catal. A: Chem.* **2016**, 422, 207-215.
59. Gentzen, M.; Habicht, W.; Doronkin, D. E.; Grunwaldt, J. D.; Sauer, J.; Behrens, S., Bifunctional hybrid catalysts derived from Cu/Zn-based nanoparticles for single-step dimethyl ether synthesis. *Catal. Sci. Technol.* **2016**, 6, 1054-1063.
60. Stiefel, M.; Ahmad, R.; Arnold, U.; Döring, M., Direct synthesis of dimethyl ether from carbon-monoxide-rich synthesis gas: Influence of dehydration catalysts and operating conditions. *Fuel Process. Technol.* **2011**, 92, 1466-1474.
61. Behrens, M.; Schlögl, R., How to Prepare a Good Cu/ZnO Catalyst or the Role of Solid State Chemistry for the Synthesis of Nanostructured Catalysts. *Z. Anorg. Allg. Chem.* **2013**, 639, 2683-2695.
62. Ott, J.; Gronemann, V.; Pontzen, F.; Fiedler, E.; Grossmann, G.; Kersebohm, D. B.; Weiss, G.; Witte, C., Methanol. In *Ullmann's Encyclopedia of Industrial Chemistry*, Wiley-VCH Verlag GmbH & Co. KGaA: 2000.
63. Hansen, J. B.; Højlund Nielsen, P. E., Methanol Synthesis. In *Handbook of Heterogeneous Catalysis*, Wiley-VCH Verlag GmbH & Co. KGaA: 2008.
64. Fichtl, M. B.; Schlereth, D.; Jacobsen, N.; Kasatkin, I.; Schumann, J.; Behrens, M.; Schlögl, R.; Hinrichsen, O., Kinetics of deactivation on Cu/ZnO/Al₂O₃ methanol synthesis catalysts. *Appl. Catal., A* **2015**, 502, 262-270.
65. Beale, A. M.; Gibson, E. K.; O'Brien, M. G.; Jacques, S. D. M.; Cernik, R. J.; Michiel, M. D.; Cobden, P. D.; Pirgon-Galin, Ö.; Water, L. v. d.; Watson, M. J.; Weckhuysen, B. M., Chemical imaging of the sulfur-induced deactivation of Cu/ZnO catalyst bodies. *J. Catal.* **2014**, 314, 94-100.
66. Twigg, M. V.; Spencer, M. S., Deactivation of Copper Metal Catalysts for Methanol Decomposition, Methanol Steam Reforming and Methanol Synthesis. *Top. Catal.* **2003**, 22, 191-203.
67. Kurtz, M.; Wilmer, H.; Genger, T.; Hinrichsen, O.; Muhler, M., Deactivation of Supported Copper Catalysts for Methanol Synthesis. *Catal. Lett.* **86**, 77-80.
68. Baltes, C.; Vukojević, S.; Schüth, F., Correlations between synthesis, precursor, and catalyst structure and activity of a large set of CuO/ZnO/Al₂O₃ catalysts for methanol synthesis. *J. Catal.* **2008**, 258, 334-344.

69. Fujita, S.-i.; Moribe, S.; Kanamori, Y.; Takezawa, N., Effects of the Calcination and Reduction Conditions on a Cu/ZnO Methanol Synthesis Catalyst. *React. Kinet. Catal. Lett.* **2000**, *70*, 11-16.
70. Irandoukht, A.; Sohrabi, M.; Mandegarian, R., Effect of Preparation Parameters on the Activity of Methanol Synthesis Catalysts: A Laboratory Scale Study. *React. Kinet. Catal. Lett.* **2000**, *70*, 259-264.
71. Kniep, B. L.; Girgsdies, F.; Ressler, T., Effect of precipitate aging on the microstructural characteristics of Cu/ZnO catalysts for methanol steam reforming. *J. Catal.* **2005**, *236*, 34-44.
72. Muhamad, E. N.; Irmawati, R.; Taufiq-Yap, Y. H.; Abdullah, A. H.; Kniep, B. L.; Girgsdies, F.; Ressler, T., Comparative study of Cu/ZnO catalysts derived from different precursors as a function of aging. *Catal. Today* **2008**, *131*, 118-124.
73. Ning, W.; Shen, H.; Liu, H., Study of the effect of preparation method on CuO-ZnO-Al₂O₃ catalyst. *Appl. Catal., A* **2001**, *211*, 153-157.
74. Kuld, S.; Conradsen, C.; Moses, P. G.; Chorkendorff, I.; Sehested, J., Quantification of Zinc Atoms in a Surface Alloy on Copper in an Industrial-Type Methanol Synthesis Catalyst. *Angewandte Chemie International Edition* **2014**, *53*, 5941-5945.
75. Derrouiche, S.; Lauron-Pernot, H.; Louis, C., Synthesis and Treatment Parameters for Controlling Metal Particle Size and Composition in Cu/ZnO Materials—First Evidence of Cu₃Zn Alloy Formation. *Chemistry of Materials* **2012**, *24*, 2282-2291.
76. Clausen, B. S.; Schiøtz, J.; Gråbæk, L.; Ovesen, C. V.; Jacobsen, K. W.; Nørskov, J. K.; Topsøe, H., Wetting/ non-wetting phenomena during catalysis: Evidence from in situ on-line EXAFS studies of Cu-based catalysts. *Top. Catal.* **1994**, *1*, 367-376.
77. Burch, R.; Golunski, S. E.; Spencer, M. S., The role of copper and zinc oxide in methanol synthesis catalysts. *J. Chem. Soc., Faraday Trans.* **1990**, *86*, 2683-2691.
78. Grunwaldt, J. D.; Molenbroek, A. M.; Topsøe, N. Y.; Topsøe, H.; Clausen, B. S., In Situ Investigations of Structural Changes in Cu/ZnO Catalysts. *J. Catal.* **2000**, *194*, 452-460.
79. Wilmer, H.; Hinrichsen, O., Dynamical Changes in Cu/ZnO/Al₂O₃ Catalysts. *Catal. Lett.* **2002**, *82*, 117-122.
80. Hansen, P. L.; Wagner, J. B.; Helveg, S.; Rostrup-Nielsen, J. R.; Clausen, B. S.; Topsøe, H., Atom-Resolved Imaging of Dynamic Shape Changes in Supported Copper Nanocrystals. *Science* **2002**, *295*, 2053-2055.
81. Klier, K.; Chatikavanij, V.; Herman, R. G.; Simmons, G. W., Catalytic synthesis of methanol from COH₂: IV. The effects of carbon dioxide. *J. Catal.* **1982**, *74*, 343-360.
82. Chinchin, G. C.; Denny, P. J.; Parker, D. G.; Spencer, M. S.; Whan, D. A., Mechanism of methanol synthesis from CO₂/CO/H₂ mixtures over copper/zinc oxide/alumina catalysts: use of ¹⁴C-labelled reactants. *Appl. Catal.* **1987**, *30*, 333-338.
83. Grabow, L. C.; Mavrikakis, M., Mechanism of Methanol Synthesis on Cu through CO₂ and CO Hydrogenation. *ACS Catal.* **2011**, *1*, 365-384.
84. Zuo, Z.-J.; Han, P.-D.; Li, Z.; Hu, J.-S.; Huang, W., Can methanol be synthesized from CO by direct hydrogenation over Cu/ZnO catalysts? *Appl. Surf. Sci.* **2012**, *261*, 640-646.

85. Kunkes, E. L.; Studt, F.; Abild-Pedersen, F.; Schlögl, R.; Behrens, M., Hydrogenation of CO₂ to methanol and CO on Cu/ZnO/Al₂O₃: Is there a common intermediate or not? *J. Catal.* **2015**, 328, 43-48.
86. Park, N.; Park, M.-J.; Lee, Y.-J.; Ha, K.-S.; Jun, K.-W., Kinetic modeling of methanol synthesis over commercial catalysts based on three-site adsorption. *Fuel Process. Technol.* **2014**, 125, 139-147.
87. Studt, F.; Behrens, M.; Kunkes, E. L.; Thomas, N.; Zander, S.; Tarasov, A.; Schumann, J.; Frei, E.; Varley, J. B.; Abild-Pedersen, F.; Nørskov, J. K.; Schlögl, R., The Mechanism of CO and CO₂ Hydrogenation to Methanol over Cu-Based Catalysts. *ChemCatChem* **2015**, 7, 1105-1111.
88. Green, G. J.; Yan, T. Y., Water tolerance of gasoline-methanol blends. *Ind. Eng. Chem. Res.* **1990**, 29, 1630-1635.
89. Hansen, A. C.; Zhang, Q.; Lyne, P. W. L., Ethanol–diesel fuel blends — a review. *Bioresour. Technol.* **2005**, 96, 277-285.
90. Kumar, S.; Cho, J. H.; Park, J.; Moon, I., Advances in diesel–alcohol blends and their effects on the performance and emissions of diesel engines. *Renew. Sust. Energ. Rev.* **2013**, 22, 46-72.
91. Smith, J. L.; Workman, J. P., Alcohol for Motor Fuels. In 2004.
92. Lapuerta, M. n.; García-Contreras, R.; Campos-Fernández, J.; Dorado, M. P., Stability, Lubricity, Viscosity, and Cold-Flow Properties of Alcohol–Diesel Blends. *Energ. Fuel.* **2010**, 24, 4497-4502.
93. Umsicht, F.-I. f. U.-S.-u. E. Jahres Bericht 2010/11. <http://www.umsicht.fraunhofer.de/content/dam/umsicht/de/dokumente/jahresberichte/2010-jahresbericht.pdf> (04.03.2016)
94. Chen, M. J.; Feder, H. M.; Rathke, J. W., A general homogeneous catalytic method for the homologation of methanol to ethanol. *J. Am. Chem. Soc.* **1982**, 104, 7346-7347.
95. Francoisse, P. B.; Thyron, F. C., Methanol to ethanol by homologation: kinetic approach. *Industrial & Engineering Chemistry Product Research and Development* **1983**, 22, 542-548.
96. Halttunen, M. E.; Niemelä, M. K.; Krause, A. O. I.; Vuori, A. I., Liquid phase methanol hydrocarbonylation with homogeneous and heterogeneous Rh and Ru catalysts. *J. Mol. Catal. A: Chem.* **1996**, 109, 209-217.
97. Guglielminotti, E.; Pinna, F.; Rigoni, M.; Strukul, G.; Zanderighi, L., The effect of iron on the activity and the selectivity of Rh/ZrO₂ catalysts in the CO hydrogenation. *Journal of Molecular Catalysis. A, Chemical* **1995**, 103, 105-116.
98. Guglielminotti, E.; Giamello, E.; Pinna, F.; Strukul, G.; Martinengo, S.; Zanderighi, L., Elementary Steps in CO Hydrogenation on Rh Catalysts Supported on ZrO₂ and Mo/ZrO₂. *J. Catal.* **1994**, 146, 422-436.
99. Wang, Y.; Li, J.; Mi, W., Probing study of Rh catalysts on different supports in CO hydrogenation. *React. Kinet. Catal. Lett.* **2002**, 76, 141-150.
100. Luo, H. Y.; Zhang, W.; Zhou, H. W.; Huang, S. Y.; Lin, P. Z.; Ding, Y. J.; Lin, L. W., A study of Rh-Sm-V/SiO₂ catalysts for the preparation of C₂-oxygenates from syngas. *Appl. Catal., A* **2001**, 214, 161-166.

101. Haider, M. A.; Gogate, M. R.; Davis, R. J., Fe-promotion of supported Rh catalysts for direct conversion of syngas to ethanol. *J. Catal.* **2009**, 261, 9-16.
102. Jiang, D.; Ding, Y.; Pan, Z.; Chen, W.; Luo, H., CO Hydrogenation to C₂-oxygenates over Rh–Mn–Li/SiO₂; Catalyst: Effects of Support Pretreatment with nC₁–C₅ Alcohols. *Catal. Lett.* **2008**, 121, 241-246.
103. Hu, J.; Wang, Y.; Cao, C.; Elliott, D. C.; Stevens, D. J.; White, J. F., Conversion of biomass-derived syngas to alcohols and C₂ oxygenates using supported Rh catalysts in a microchannel reactor. *Catal. Today* **2007**, 120, 90-95.
104. Gogate, M. R.; Davis, R. J., Comparative study of CO and CO₂ hydrogenation over supported Rh–Fe catalysts. *Catal. Commun.* **2010**, 11, 901-906.
105. Surisetty, V. R.; Dalai, A. K.; Kozinski, J., Effect of Rh promoter on MWCNT-supported alkali-modified MoS₂ catalysts for higher alcohols synthesis from CO hydrogenation. *Appl. Catal., A* **2010**, 381, 282-288.
106. Liu, Z.; Li, X.; Close, M. R.; Kugler, E. L.; Petersen, J. L.; Dadyburjor, D. B., Screening of Alkali-Promoted Vapor-Phase-Synthesized Molybdenum Sulfide Catalysts for the Production of Alcohols from Synthesis Gas. *Ind. Eng. Chem. Res.* **1997**, 36, 3085-3093.
107. Wu, Q.; Christensen, J. M.; Chiarello, G. L.; Duchstein, L. D. L.; Wagner, J. B.; Temel, B.; Grunwaldt, J.-D.; Jensen, A. D., Supported molybdenum carbide for higher alcohol synthesis from syngas. *Catal. Today* **2013**, 215, 162-168.
108. Iranmahboob, J.; Toghiani, H.; Hill, D. O., Dispersion of alkali on the surface of Co–MoS₂/clay catalyst: a comparison of K and Cs as a promoter for synthesis of alcohol. *Appl. Catal., A* **2003**, 247, 207-218.
109. Li, D.; Yang, C.; Qi, H.; Zhang, H.; Li, W.; Sun, Y.; Zhong, B., Higher alcohol synthesis over a La promoted Ni/K₂CO₃/MoS₂ catalyst. *Catal. Commun.* **2004**, 5, 605-609.
110. Li, Z.-r.; Fu, Y.-l.; Jiang, M., Structures and performance of Rh–Mo–K/Al₂O₃ catalysts used for mixed alcohol synthesis from synthesis gas. *Appl. Catal., A* **1999**, 187, 187-198.
111. Li, Z.-r.; Fu, Y.-l.; Jiang, M.; Meng, M.; Xie, Y.-n.; Hu, T.-d.; Liu, T., Structures and performance of Pd–Mo–K/Al₂O₃ catalysts used for mixed alcohol synthesis from synthesis gas. *Catal. Lett.* **2000**, 65, 43-48.
112. Bian, G. Z.; Fu, Y. L.; Ma, Y. S., Structure of Co–K–Mo/γ–Al₂O₃ catalysts and their catalytic activity for mixed alcohols synthesis. *Catal. Today* **1999**, 51, 187-193.
113. Christensen, J. M.; Duchstein, L. D. L.; Wagner, J. B.; Jensen, P. A.; Temel, B.; Jensen, A. D., Catalytic Conversion of Syngas into Higher Alcohols over Carbide Catalysts. *Ind. Eng. Chem. Res.* **2012**, 51, 4161-4172.
114. Mahdavi, V.; Peyrovi, M. H., Synthesis of C₁–C₆ alcohols over copper/cobalt catalysts. Investigation of the influence of preparative procedures on the activity and selectivity of Cu–Co₂O₃/ZnO, Al₂O₃ catalyst. *Catal. Commun.* **2006**, 7, 542-549.
115. Deng, S.; Chu, W.; Xu, H.; Shi, L.; Huang, L., Effects of impregnation sequence on the microstructure and performances of Cu–Co based catalysts for the synthesis of higher alcohols. *Journal of Natural Gas Chemistry* **2008**, 17, 369-373.
116. Ding, M.; Qiu, M.; Wang, T.; Ma, L.; Wu, C.; Liu, J., Effect of iron promoter on structure and performance of CuMnZnO catalyst for higher alcohols synthesis. *Appl. Energ.* **2012**, 97, 543-547.

117. Xu, R.; Yang, C.; Wei, W.; Li, W. H.; Sun, Y. H.; Hu, T. D., Fe-modified CuMnZrO₂ catalysts for higher alcohols synthesis from syngas. *J. Mol. Catal. A: Chem.* **2004**, 221, 51-58.
118. Ding, M.; Qiu, M.; Liu, J.; Li, Y.; Wang, T.; Ma, L.; Wu, C., Influence of manganese promoter on co-precipitated Fe–Cu based catalysts for higher alcohols synthesis. *Fuel* **2013**, 109, 21-27.
119. Lin, M.; Fang, K.; Li, D.; Sun, Y., CO hydrogenation to mixed alcohols over co-precipitated Cu–Fe catalysts. *Catal. Commun.* **2008**, 9, 1869-1873.
120. Chu, W.; Kieffer, R.; Kiennemann, A.; Hindermann, J. P., Conversion of syngas to C₁-C₆ alcohol mixtures on promoted CuLa₂Zr₂O₇ catalysts. *Appl. Catal., A* **1995**, 121, 95-111.
121. Tien-Thao, N.; Zahedi-Niaki, M. H.; Alamdari, H.; Kaliaguine, S., Conversion of syngas to higher alcohols over nanosized LaCo_{0.7}Cu_{0.3}O₃ perovskite precursors. *Appl. Catal., A* **2007**, 326, 152-163.
122. Cao, R.; Pan, W. X.; Griffin, G. L., Direct synthesis of higher alcohols using bimetallic copper/cobalt catalysts. *Langmuir* **1988**, 4, 1108-1112.
123. Bailliard-Letournel, R. M.; Gomez Cobo, A. J.; Mirodatos, C.; Primet, M.; Dalmon, J. A., About the nature of the Co-Cu interaction in Co-based catalysts for higher alcohols synthesis. *Catal. Lett.* **1989**, 2, 149-156.
124. Kiennemann, A.; Diagne, C.; Hindermann, J. P.; Chaumette, P.; Courty, P., Higher alcohols synthesis from CO+2H₂ on cobalt–copper catalyst: Use of probe molecules and chemical trapping in the study of the reaction mechanism. *Appl. Catal.* **1989**, 53, 197-216.
125. Fierro, G.; Lo Jacono, M.; Inversi, M.; Dragone, R.; Porta, P., TPR and XPS study of cobalt–copper mixed oxide catalysts: evidence of a strong Co–Cu interaction. *Top. Catal.* **2000**, 10, 39-48.
126. Volkova, G. G.; Yurieva, T. M.; Plyasova, L. M.; Naumova, M. I.; Zaikovskii, V. I., Role of the Cu–Co alloy and cobalt carbide in higher alcohol synthesis. *J. Mol. Catal. A: Chem.* **2000**, 158, 389-393.
127. Tavares Figueiredo, R.; López Granados, M.; Fierro, J. L. G.; Vigas, L.; Ramírez de la Piscina, P.; Homs, N., Preparation of alumina-supported CuCo catalysts from cyanide complexes and their performance in CO hydrogenation. *Appl. Catal., A* **1998**, 170, 145-157.
128. Wang, J.; Chernavskii, P. A.; Khodakov, A. Y.; Wang, Y., Structure and catalytic performance of alumina-supported copper–cobalt catalysts for carbon monoxide hydrogenation. *J. Catal.* **2012**, 286, 51-61.
129. Prieto, G.; Beijer, S.; Smith, M. L.; He, M.; Au, Y.; Wang, Z.; Bruce, D. A.; de Jong, K. P.; Spivey, J. J.; de Jongh, P. E., Design and Synthesis of Copper–Cobalt Catalysts for the Selective Conversion of Synthesis Gas to Ethanol and Higher Alcohols. *Angewandte Chemie International Edition* **2014**, 53, 6397-6401.
130. Cobo, A. G.; Mouaddib, N.; Dalmqn, J. A.; Mirodatos, C.; Perrichon, V.; Primet, M.; Chaumette, P.; Courty, P., Evidence and Role of Carbonyl Adspecies in Higher Alcohols Synthesis on Heterogeneous Cobalt-Copper Catalysts. In *Stud. Surf. Sci. Catal.*, A. Holmen, K. J. J.; Kolboe, S., Eds. Elsevier: 1991; Vol. Volume 61, 257-263.
131. Boz, I., Higher alcohol synthesis over a K-promoted Co₂O₃/CuO/ZnO/Al₂O₃ catalyst. *Catal. Lett.* **2003**, 87, 187-194.

132. Cosultchi, A.; Pérez-Luna, M.; Morales-Serna, J.; Salmón, M., Characterization of Modified Fischer–Tropsch Catalysts Promoted with Alkaline Metals for Higher Alcohol Synthesis. *Catal. Lett.* **2012**, 142, 368-377.
133. Ishida, T.; Yanagihara, T.; Liu, X.; Ohashi, H.; Hamasaki, A.; Honma, T.; Oji, H.; Yokoyama, T.; Tokunaga, M., Synthesis of higher alcohols by Fischer–Tropsch synthesis over alkali metal-modified cobalt catalysts. *Appl. Catal., A* **2013**, 458, 145-154.
134. Wang, J.; Chernavskii, P. A.; Wang, Y.; Khodakov, A. Y., Influence of the support and promotion on the structure and catalytic performance of copper–cobalt catalysts for carbon monoxide hydrogenation. *Fuel* **2013**, 103, 1111-1122.
135. Medford, A. J.; Vojvodic, A.; Hummelshøj, J. S.; Voss, J.; Abild-Pedersen, F.; Studt, F.; Bligaard, T.; Nilsson, A.; Nørskov, J. K., From the Sabatier principle to a predictive theory of transition-metal heterogeneous catalysis. *J. Catal.* **2015**, 328, 36-42.
136. Studt, F.; Abild-Pedersen, F.; Wu, Q.; Jensen, A. D.; Temel, B.; Grunwaldt, J.-D.; Nørskov, J. K., CO hydrogenation to methanol on Cu–Ni catalysts: Theory and experiment. *J. Catal.* **2012**, 293, 51-60.
137. Wang, J.; Kawazoe, Y.; Sun, Q.; Chan, S.; Su, H., The selectivity and activity of catalyst for CO hydrogenation to methanol and hydrocarbon: A comparative study on Cu, Co and Ni surfaces. *Surf. Sci.* **2016**, 645, 30-40.
138. Yang, L.; Liu, P., Ethanol Synthesis from Syngas on Transition Metal-Doped Rh(111) Surfaces: A Density Functional Kinetic Monte Carlo Study. *Top. Catal.* **2014**, 57, 125-134.
139. Beretta, A.; Sun, Q.; Herman, R. G.; Klier, K., Synthesis of 2-methylpropan-1-ol-methanol mixtures from H₂-CO synthesis gas over double-bed Cs/Cu/ZnO/Cr₂O₃ and Cs/ZnO/Cr₂O₃ catalysts. *J. Chem. Soc., Chem. Commun.* **1995**, 2525-2526.
140. Epling, W. S.; B. Hoflund, G.; Minahan, D. M., Higher alcohol synthesis reaction study VI: effect of Cr replacement by Mn on the performance of Cs- and Cs, Pd-promoted Zn/Cr spinel catalysts. *Appl. Catal., A* **1999**, 183, 335-343.
141. Epling, W. S.; Hoflund, G. B.; Hart, W. M.; Minahan, D. M., Reaction and surface characterization study of higher alcohol synthesis catalysts: I. K-promoted commercial Zn/Cr spinel. *J. Catal.* **1997**, 169, 438-446.
142. Epling, W. S.; Hoflund, G. B.; Hart, W. M.; Minahan, D. M., Reaction and surface characterization study of higher alcohol synthesis catalysts: II. Cs-promoted commercial Zn/Cr spinel. *J. Catal.* **1997**, 172, 13-23.
143. Epling, W. S.; Hoflund, G. B.; Minahan, D. M., Reaction and Surface Characterization Study of Higher Alcohol Synthesis Catalysts: VII. Cs- and Pd-Promoted 1:1 Zn/Cr Spinel. *J. Catal.* **1998**, 175, 175-184.
144. Minahan, D.; Epling, W.; Hoflund, G., An efficient catalyst for the production of isobutanol and methanol from syngas. VIII: Cs- and Pd-promoted Zn/Cr spinel (excess ZnO). *Catal. Lett.* **1998**, 50, 199-203.
145. Tronconi, E.; Ferlazzo, N.; Forzatti, P.; Pasquon, I., Synthesis of alcohols from carbon oxides and hydrogen. 4. Lumped kinetics for the higher alcohol synthesis over a zinc-chromium-potassium oxide catalyst. *Ind. Eng. Chem. Res.* **1987**, 26, 2122-2129.
146. Hoflund, G. B.; Epling, W. S.; Minahan, D. M., Higher alcohol synthesis reaction study using K- promoted ZnO catalysts. III. *Catal. Lett.* **1997**, 45, 135-138.

147. Minahan, D. M.; Epling, W. S.; Hoflund, G. B., Higher-alcohol synthesis reaction study V. Effect of excess ZnO on catalyst performance. *Appl. Catal., A* **1998**, 166, 375-385.
148. Hoflund, G. B.; Epling, W. S.; Minahan, D. M., Reaction and surface characterization study of higher-alcohol synthesis catalysts XII: K- and Pd-promoted Zn/Cr/Mn spinel. *Catal. Today* **1999**, 52, 99-109.
149. Minahan, D. M.; Epling, W. S.; Hoflund, G. B., Reaction and Surface Characterization Study of Higher Alcohol Synthesis Catalysts: IX. Pd- and Alkali-Promoted Zn/Cr-Based Spinel Containing Excess ZnO. *J. Catal.* **1998**, 179, 241-257.
150. Verkerk, K. A. N.; Jaeger, B.; Finkeldei, C.-H.; Keim, W., Recent developments in isobutanol synthesis from synthesis gas. *Appl. Catal., A* **1999**, 186, 407-431.
151. Spivey, J. J.; Egbibi, A., Heterogeneous Catalytic Synthesis of Ethanol from Biomass-Derived Syngas. *ChemInform* **2007**, 38, 1514-1528.
152. Nunan, J.; Klier, K.; Young, C.-W.; Himelfarb, P. B.; Herman, R. G., Promotion of methanol synthesis over Cu/ZnO catalysts by doping with caesium. *J. Chem. Soc., Chem. Commun.* **1986**, 193-195.
153. Nunan, J. G.; Bogdan, C. E.; Klier, K.; Smith, K. J.; Young, C.-W.; Herman, R. G., Higher alcohol and oxygenate synthesis over cesium-doped CuZnO catalysts. *J. Catal.* **1989**, 116, 195-221.
154. Nunan, J. G.; Herman, R. G.; Klier, K., Higher alcohol and oxygenate synthesis over Cs/Cu/ZnO/M₂O₃ (M /Al, Cr) catalysts. *J. Catal.* **1989**, 116, 222-229.
155. Berndt, H.; Briehn, V.; Evert, S.; Gutschick, D.; Kotowski, W., Relation between preparation, porosity and selectivity of CuO-ZnO-MeOx catalysts in the synthesis of alcohol mixtures. *Catal. Lett.* **1992**, 14, 185-195.
156. Boz, I.; Sahibzada, M.; Metcalfe, I. S., Kinetics of the Higher Alcohol Synthesis over a K-promoted CuO/ZnO/Al₂O₃ Catalyst. *Ind. Eng. Chem. Res.* **1994**, 33, 2021-2028.
157. Klier, K.; Beretta, A.; Sun, Q.; Feeley, O. C.; Herman, R. G., Catalytic synthesis of methanol, higher alcohols and ethers. *Catal. Today* **1997**, 36, 3-14.
158. Hilmen, A.-M.; Xu, M.; Gines, M. J. L.; Iglesia, E., Synthesis of higher alcohols on copper catalysts supported on alkali-promoted basic oxides. *Appl. Catal., A* **1998**, 169, 355-372.
159. Beretta, A.; Sun, Q.; Herman, R. G.; Klier, K., Production of Methanol and Isobutyl Alcohol Mixtures over Double-Bed Cesium-Promoted Cu/ZnO/Cr₂O₃ and ZnO/Cr₂O₃ Catalysts. *Ind. Eng. Chem. Res.* **1996**, 35, 1534-1542.
160. Burcham, M. M.; Herman, R. G.; Klier, K., Higher Alcohol Synthesis over Double Bed Cs-Cu/ZnO/Cr₂O₃ Catalysts: Optimizing the Yields of 2-Methyl-1-propanol (Isobutanol). *Ind. Eng. Chem. Res.* **1998**, 37, 4657-4668.
161. Campos-Martín, J. M.; Fierro, J. L. G.; Guerrero-Ruiz, A.; Herman, R. G.; Klier, K., Promoter effect of cesium on C-C bond formation during alcohol synthesis from CO/H₂ over Cu/ZnO/Cr₂O₃ catalysts. *J. Catal.* **1996**, 163, 418-428.
162. Nunan, J.; Bogdan, C.; Herman, R.; Klier, K., Efficient carbon-carbon bond formation in ethanol homologation by CO/H₂ with specific C₁ oxygen retention over Cs/Cu/ZnO catalysts. *Catal. Lett.* **1989**, 2, 49-55.

163. Nunan, J. G.; Bogdan, C. E.; Klier, K.; Smith, K. J.; Young, C.-W.; Herman, R. G., Methanol and C₂ oxygenate synthesis over cesium doped CuZnO and Cu/ZnO/Al₂O₃ catalysts: A study of selectivity and ¹³C incorporation patterns. *J. Catal.* **1988**, 113, 410-433.
164. Beretta, A.; Lietti, L.; Tronconi, E.; Forzatti, P.; Pasquon, I., Development of a Mechanistic Kinetic Model of the Higher Alcohol Synthesis over a Cs-Doped Zn/Cr/O Catalyst. 2. Analysis of Chemical Enrichment Experiments. *Ind. Eng. Chem. Res.* **1996**, 35, 2154-2160.
165. Goodarznia, S.; Smith, K. J., Properties of alkali-promoted Cu–MgO catalysts and their activity for methanol decomposition and C₂-oxygenate formation. *J. Mol. Catal. A: Chem.* **2010**, 320, 1-13.
166. Beretta, A.; Tronconi, E.; Forzatti, P.; Pasquon, I.; Micheli, E.; Tagliabue, L.; Antonelli, G. B., Development of a Mechanistic Kinetic Model of the Higher Alcohol Synthesis over a Cs-Doped Zn/Cr/O Catalyst. 1. Model Derivation and Data Fitting. *Ind. Eng. Chem. Res.* **1996**, 35, 2144-2153.
167. Kiennemann, A.; Idriss, H.; Kieffer, R.; Chaumette, P.; Durand, D., Study of the mechanism of higher alcohol synthesis on copper-zinc oxide-aluminum oxide catalysts by catalytic tests, probe molecules, and temperature programmed desorption studies. *Ind. Eng. Chem. Res.* **1991**, 30, 1130-1138.
168. Slaa, J. C.; van Ommen, J. G.; Ross, J. R. H., The synthesis of higher alcohols using modified Cu/ZnO/Al₂O₃ catalysts. *Catal. Today* **1992**, 15, 129-148.
169. Smith, K. J.; Young, C. W.; Herman, R. G.; Klier, K., Development of a kinetic model for alcohol synthesis over a cesium-promoted copper/zinc oxide catalyst. *Ind. Eng. Chem. Res.* **1991**, 30, 61-71.
170. Xu, M.; Iglesia, E., Carbon–Carbon Bond Formation Pathways in CO Hydrogenation to Higher Alcohols. *J. Catal.* **1999**, 188, 125-131.
171. Vedage G, A.; Himelfarb P, B.; Simmons G, W.; Klier, K., Alkali-Promoted Copper-Zinc Oxide Catalysts for Low Alcohol Synthesis. In *Solid State Chemistry in Catalysis*, American Chemical Society: 1985; Vol. 279, 295-312.
172. Herman, R. G.; Klier, K.; Simmons, G. W.; Finn, B. P.; Bulko, J. B.; Kobylinski, T. P., Catalytic synthesis of methanol from COH₂: I. Phase composition, electronic properties, and activities of the Cu/ZnO/M₂O₃ catalysts. *J. Catal.* **1979**, 56, 407-429.
173. Teoh, W. Y.; Amal, R.; Madler, L., Flame spray pyrolysis: An enabling technology for nanoparticles design and fabrication. *Nanoscale* **2010**, 2, 1324-1347.
174. Høj, M.; Pham, D. K.; Brorson, M.; Mädler, L.; Jensen, A. D.; Grunwaldt, J.-D., Two-Nozzle Flame Spray Pyrolysis (FSP) Synthesis of CoMo/Al₂O₃ Hydrotreating Catalysts. *Catal. Lett.* **2013**, 143, 386-394.
175. Strobel, R.; Mädler, L.; Piacentini, M.; Maciejewski, M.; Baiker, A.; Pratsinis, S. E., Two-Nozzle Flame Synthesis of Pt/Ba/Al₂O₃ for NO_x Storage. *Chemistry of Materials* **2006**, 18, 2532-2537.
176. Schuh, K.; Kleist, W.; Høj, M.; Trouillet, V.; Jensen, A. D.; Grunwaldt, J. D., One-step synthesis of bismuth molybdate catalysts via flame spray pyrolysis for the selective oxidation of propylene to acrolein. *Chem. Commun.* **2014**, 50, 15404-15406.
177. Tepluchin, M.; Pham, D. K.; Casapu, M.; Madler, L.; Kureti, S.; Grunwaldt, J.-D., Influence of single- and double-flame spray pyrolysis on the structure of MnO_x/[gamma]-Al₂O₃

and FeO_x/[gamma]-Al₂O₃ catalysts and their behaviour in CO removal under lean exhaust gas conditions. *Catal. Sci. Technol.* **2015**, 5, 455-464.

178. Scherrer, P., Bestimmung der inneren Struktur und der Größe von Kolloidteilchen mittels Röntgenstrahlen. In *Kolloidchemie Ein Lehrbuch*, Springer Berlin Heidelberg: Berlin, Heidelberg, 1912; 387-409.

179. Allen, F., The Cambridge Structural Database: a quarter of a million crystal structures and rising. *Acta Crystallographica Section B* **2002**, 58, 380-388.

180. Augustine, R. L., *Heterogeneous catalysis for the synthetic chemist*. Dekker: New York [u.a.], 1996; ISBN: 0824790219 9780824790219

181. Scanlon, J. T.; Willis, D. E., Calculation of Flame Ionization Detector Relative Response Factors Using the Effective Carbon Number Concept. *J. Chromatogr. Sci.* **1985**, 23, 333-340.

182. Walter, K. M.; Schubert, M.; Kleist, W.; Grunwaldt, J.-D., Effect of the Addition of Ethanol to Synthesis Gas on the Production of Higher Alcohols over Cs and Ru Modified Cu/ZnO Catalysts. *Ind. Eng. Chem. Res.* **2015**, 54, 1452-1463.

183. Fierro, G.; Lo Jacono, M.; Inversi, M.; Porta, P.; Cioci, F.; Lavecchia, R., Study of the reducibility of copper in CuO/ZnO catalysts by temperature-programmed reduction. *Appl. Catal., A* **1996**, 137, 327-348.

184. Kiener, C.; Kurtz, M.; Wilmer, H.; Hoffmann, C.; Schmidt, H. W.; Grunwaldt, J. D.; Muhler, M.; Schüth, F., High-throughput screening under demanding conditions: Cu/ZnO catalysts in high pressure methanol synthesis as an example. *J. Catal.* **2003**, 216, 110-119.

185. Grunwaldt, J.-D.; Kiener, C.; Schüth, F.; Baiker, A., X-ray absorption spectroscopy on Cu/ZnO catalysts selected by high-throughput experimentation techniques. *Phys. Scr.* **2005**, 2005, 819.

186. Pasha, N.; Lingaiah, N.; Reddy, P. S.; Prasad, P. S. S., Direct Decomposition of N₂O over Cesium-doped CuO Catalysts. *Catal. Lett.* **2009**, 127, 101-106.

187. Pike, J.; Chan, S.-W.; Zhang, F.; Wang, X.; Hanson, J., Formation of stable Cu₂O from reduction of CuO nanoparticles. *Appl. Catal., A* **2006**, 303, 273-277.

188. Serrer, M.-A. Untersuchungen zur heterogen katalysierten Synthese höherer Alkohole an Cu/ZnO - basierten Katalysatoren. Bachelor thesis, Karlsruhe Institut für Technologie (KIT), Karlsruhe, 2014.

189. Linstrom, P. J.; Mallard Eds., W. G., NIST Chemistry WebBook NIST Standard Reference Database Number 69. In *NIST Standard Reference Database Number 69*, National Institute of Standards and Technology: Gaithersburg MD, 20899, <http://webbook.nist.gov>, (retrieved July 18, 2014).

190. Gines, M. J. L.; Oh, H.-S.; Xu, M.; Hilmen, A.-M.; Iglesia, E., Isobutanol and methanol synthesis on copper supported on alkali- modified MgO and ZnO supports. In *Stud. Surf. Sci. Catal.*, A. Parmaliana, D. S. F. F. A. V.; F, A., Eds. Elsevier: 1998; Vol. Volume 119, 509-514.

191. Stiles, A. B.; Chen, F.; Harrison, J. B.; Hu, X.; Storm, D. A.; Yang, H. X., Catalytic conversion of synthesis gas to methanol and other oxygenated products. *Ind. Eng. Chem. Res.* **1991**, 30, 811-821.

192. Klier, K.; Young, C. W.; Nunan, J. G., Promotion of the water gas shift reaction by cesium surface doping of the model binary copper/zinc oxide catalyst. *Industrial & Engineering Chemistry Fundamentals* **1986**, *25*, 36-42.
193. Gines, M. J. L.; Iglesia, E., Bifunctional Condensation Reactions of Alcohols on Basic Oxides Modified by Copper and Potassium. *J. Catal.* **1998**, *176*, 155-172.
194. Elliott, D. J.; Pennella, F., The formation of ketones in the presence of carbon monoxide over CuO/ZnO/Al₂O₃. *J. Catal.* **1989**, *119*, 359-367.
195. Lorenzut, B.; Montini, T.; De Rogatis, L.; Canton, P.; Benedetti, A.; Fornasiero, P., Hydrogen production through alcohol steam reforming on Cu/ZnO-based catalysts. *Appl. Catal., B* **2011**, *101*, 397-408.
196. Cavallaro, S.; Freni, S., Ethanol steam reforming in a molten carbonate fuel cell. A preliminary kinetic investigation. *Int. J. Hydrogen Energy* **1996**, *21*, 465-469.
197. Santacesaria, E.; Carotenuto, G.; Tesser, R.; Di Serio, M., Ethanol dehydrogenation to ethyl acetate by using copper and copper chromite catalysts. *Chem. Eng. J.* **2012**, *179*, 209-220.
198. Riittonen, T.; Toukoniitty, E.; Madnani, D. K.; Leino, A.-R.; Kordas, K.; Szabo, M.; Sapi, A.; Arve, K.; Wärnå, J.; Mikkola, J.-P., One-Pot Liquid-Phase Catalytic Conversion of Ethanol to 1-Butanol over Aluminium Oxide—The Effect of the Active Metal on the Selectivity. *Catalysts* **2012**, *2*, 68-84.
199. Toukoniitty, E.; Madnani, D. K.; Kordas, K.; Mikkola, J.-P., Conversion of Bioethanol to 1-Butanol – A Step Towards Sustainable Transportation Fuels. *Conference abstract* **2009**.
200. Twigg, M.; Spencer, M., Deactivation of Copper Metal Catalysts for Methanol Decomposition, Methanol Steam Reforming and Methanol Synthesis. *Top. Catal.* **2003**, *22*, 191-203.
201. Trimm, D. L., The regeneration or disposal of deactivated heterogeneous catalysts. *Appl. Catal., A* **2001**, *212*, 153-160.
202. Zhang, H.; Shao, S.; Xiao, R.; Shen, D.; Zeng, J., Characterization of Coke Deposition in the Catalytic Fast Pyrolysis of Biomass Derivates. *Energ. Fuel.* **2013**, *28*, 52-57.
203. Millar, G. J.; Rochester, C. H.; Bailey, S.; Waugh, K. C., Combined temperature-programmed desorption and fourier-transform infrared spectroscopy study of CO₂, CO and H₂ interactions with model ZnO/SiO₂, Cu/SiO₂ and Cu/ZnO/SiO₂ methanol synthesis catalysts. *J. Chem. Soc., Faraday Trans.* **1993**, *89*, 1109-1115.
204. Christiansen, M. A.; Mpourmpakis, G.; Vlachos, D. G., Density Functional Theory-Computed Mechanisms of Ethylene and Diethyl Ether Formation from Ethanol on γ -Al₂O₃(100). *ACS Catal.* **2013**, *3*, 1965-1975.
205. DeWilde, J. F.; Chiang, H.; Hickman, D. A.; Ho, C. R.; Bhan, A., Kinetics and Mechanism of Ethanol Dehydration on γ -Al₂O₃: The Critical Role of Dimer Inhibition. *ACS Catal.* **2013**, *3*, 798-807.
206. Satterfield, C. N., Trickle-bed reactors. *AIChE J.* **1975**, *21*, 209-228.
207. Kapteijn, F.; Moulijn, J. A., Laboratory Catalytic Reactors: Aspects of Catalyst Testing. In *Handbook of Heterogeneous Catalysis*, Wiley-VCH Verlag GmbH & Co. KGaA: 2008.
208. Perego, C.; Peratello, S., Experimental methods in catalytic kinetics. *Catal. Today* **1999**, *52*, 133-145.

209. Mary, G.; Chaouki, J.; Luck, F., Trickle-Bed Laboratory Reactors for Kinetic Studies. In *International Journal of Chemical Reactor Engineering*, 2009; Vol. 7.
210. Mederos, F. S.; Ancheyta, J.; Chen, J., Review on criteria to ensure ideal behaviors in trickle-bed reactors. *Appl. Catal., A* **2009**, 355, 1-19.
211. Lange, R.; Schubert, M.; Dietrich, W.; Grünewald, M., Unsteady-state operation of trickle-bed reactors. *Chem. Eng. Sci.* **2004**, 59, 5355-5361.
212. Biardi, G.; Baldi, G., Three-phase catalytic reactors. *Catal. Today* **1999**, 52, 223-234.
213. Woods, D. R., Reactors. In *Rules of Thumb in Engineering Practice*, Wiley-VCH Verlag GmbH & Co. KGaA: 2007; 185-279.
214. Charpentier, J.-C.; Favier, M., Some liquid holdup experimental data in trickle-bed reactors for foaming and nonfoaming hydrocarbons. *AIChE J.* **1975**, 21, 1213-1218.
215. Andersson, R.; Boutonnet, M.; Järås, S., On-line gas chromatographic analysis of higher alcohol synthesis products from syngas. *J. Chromatogr. A* **2012**, 1247, 134-145.

Supporting information

1) Unsupported catalysts

a) Complete reaction data

Table S 1: CO-conversion, total mass balance and carbon balance in the higher alcohols synthesis (ethanol free).

Catalyst	Units	CuO/ZnO	0.3 mol.% Cs-CuO/ZnO	0.6 mol.% Cs-CuO/ZnO	1.0 mol.% Cs-CuO/ZnO	3.0 mol.% Cs-CuO/ZnO	0.5 mol.% Ru-CuO/ZnO	1.0 mol.% Ru-CuO/ZnO
Total mass balance	%	96.5	96.2	93.5	95.1	95.6	95.8	93.7
C-balance	%	82.1	54.4	51.5	62.8	76.1	43.7	52.0
CO-conversion	%-C	28.9	56.7	58.9	46.6	28.6	58.1	49.4

Conditions: T=593 K, $p_{\text{start}}=5.0$ MPa, 1 g catalyst, H₂:CO=1:1, reaction time = 3 h, liquid phase= 30 g cyclohexane.

Table S 2: CO-conversion, ethanol conversion, total conversion, total mass balance and carbon balance in the higher alcohols synthesis ($n_{\text{EtOH}} : n_{\text{CO}}=0.5:1$).

Catalyst	Units	CuO/ZnO	0.3 mol.% Cs-CuO/ZnO	0.6 mol.% Cs-CuO/ZnO	1.0 mol.% Cs-CuO/ZnO	3.0 mol.% Cs-CuO/ZnO	0.5 mol.% Ru-CuO/ZnO	1.0 mol.% Ru-CuO/ZnO
Total mass balance	%	96.4	99.8	97.3	97.4	97.9	96.6	95.1
C-balance	%	57.0	56.7	65.6	68.4	69.7	58.1	59.0
Total conversion	%-C	62.1	66.6	57.6	55.1	45.6	45.8	46.7
CO conversion	%-C	35.2	38.2	34.4	31.8	23.8	5.8	4.6
Ethanol conversion	%-C	90.5	96.1	81.5	79.3	68.3	87.6	90.5

Conditions: T=593 K, $p_{\text{start}}=5.0$ MPa, 1 g catalyst, H₂:CO=1:1, reaction time = 3 h, liquid phase= ~28.6 g cyclohexane and ~1.4 g ethanol.

Table S 3: CO-conversion, ethanol conversion, total conversion, total mass balance and carbon balance in the higher alcohols synthesis ($n_{\text{EtOH}} : n_{\text{CO}}=0.9:1$).

Catalyst	Units	CuO/ZnO	0.3 mol.% Cs-CuO/ZnO
Total mass balance	%	95.0	95.4
C-balance	%	57.0	71.3
Total conversion	%-C	64.7	55.6
CO conversion	%-C	37.5	34.8
Ethanol conversion	%-C	79.5	67.2

Conditions: T=593 K, $p_{\text{start}}= 5.0$ MPa, 1 g catalyst, $\text{H}_2:\text{CO}=1:1$, reaction time = 3 h, liquid phase= ~27.5 g cyclohexane and ~2.5 g ethanol .

Table S 4: CO-conversion, ethanol conversion, total conversion, total mass balance and carbon balance in the higher alcohols synthesis ($n_{\text{EtOH}} : n_{\text{CO}}=10.0:1$).

Catalyst	Units	CuO/ZnO	0.3 mol.% Cs-CuO/ZnO	0.6 mol.% Cs-CuO/ZnO
Total mass balance	%	95.4	98.6	97.6
C-balance	%	84.1	97.6	89.6
Total conversion	%-C	37.5	25.3	30.4
CO conversion	%-C	36.2	48.2	49.5
Ethanol conversion	%-C	37.6	24.1	29.4

Conditions: T=593 K, $p_{\text{start}}= 5.0$ MPa, 1 g catalyst, $\text{H}_2:\text{CO}=1:1$, reaction time = 3 h, liquid phase= 30 g ethanol.

Table S 5: Ethanol conversion, total mass balance and carbon balance in the higher alcohols synthesis (CO and H_2 free).

Catalyst	Units	CuO/ZnO
Total mass balance	%	97.7
C-balance	%	81.7
Ethanol conversion	%-C	42.2

Conditions: T=593 K, $p_{\text{start}}= 5.0$ MPa, 1 g catalyst, Ar, reaction time = 3 h, liquid phase= 30 g ethanol.

Table S 6: Product selectivities in the higher alcohols synthesis as a function of the doping of the catalysts (ethanol free) [%-C].

Catalyst	CuO/ZnO	0.3 mol.% Cs-	0.6 mol.% Cs-	1.0 mol.% Cs-	3.0 mol.% Cs-	0.5 mol.% Ru-	1.0 mol.% Ru-
		CuO/ZnO	CuO/ZnO	CuO/ZnO	CuO/ZnO	CuO/ZnO	CuO/ZnO
CO ₂	27.0	11.0	10.1	12.9	12.5	0.2	0.2
ethane	1.8	0.4	0.2	0.2	0.0	0.1	0.5
propane	0.3	0.1	0.0	0.1	0.0	0.0	0.1
butane	0.0	0.0	0.0	0.0	0.0	0.0	0.0
H ₂	0.0	0.0	0.0	0.0	0.0	0.0	0.0
N ₂	0.0	0.0	0.0	0.0	0.0	0.0	0.0
CH ₄	3.7	0.8	0.9	1.3	0.8	0.9	2.5
CO	-	-	-	-	-	-	-
methanol	3.1	2.5	1.6	0.7	1.5	0.0	0.0
ethanol	0.5	0.6	0.5	0.3	0.3	0.9	0.0
diethyl ether	0.0	0.0	0.0	0.0	0.0	0.1	0.0
2-propanol	0.0	0.0	0.0	0.0	0.0	0.0	0.0
1-propanol	0.1	1.0	1.0	0.8	0.2	0.5	0.0
butanal	0.0	0.0	0.0	0.0	0.0	0.1	0.0
ethyl acetate	0.0	0.0	0.0	0.0	0.0	0.0	0.0
2-butanone	0.1	0.1	0.1	0.1	0.4	0.1	0.2
2-butanol	0.0	0.1	0.4	0.5	0.0	0.0	0.0
2-methyl-1-propanol	1.2	2.3	2.3	2.8	0.4	0.0	0.1
1-butanol	0.1	0.2	0.3	0.2	0.1	0.1	0.0
1,1-diethoxy ethane	0.0	0.0	0.0	0.0	0.0	0.0	0.0
1-pentanol	0.0	0.3	0.3	0.3	0.1	0.1	0.0
ethyl butyrate	0.0	0.0	0.0	0.0	0.0	0.0	0.0
butyl acetate	0.0	0.0	0.1	0.0	0.0	0.0	0.0
1-hexanol	0.0	0.0	0.0	0.0	0.0	0.0	0.0

Conditions: T=593 K, p_{start}= 5.0 MPa, 1 g catalyst, H₂:CO=1:1, reaction time = 3 h, liquid phase= 30 g cyclohexane.

Table S 7: Product yields in the higher alcohols synthesis as a function of the doping of the catalysts (ethanol free) [%-C].

Catalyst	CuO/ZnO	0.3 mol.% Cs- CuO/ZnO	0.6 mol.% Cs- CuO/ZnO	1.0 mol.% Cs- CuO/ZnO	3.0 mol.% Cs- CuO/ZnO	0.5 mol.% Ru- CuO/ZnO	1.0 mol.% Ru- CuO/ZnO
CO ₂	7.8	6.2	5.9	6.0	3.6	0.1	0.1
ethane	0.5	0.2	0.1	0.1	0.0	0.1	0.2
propane	0.1	0.0	0.0	0.0	0.0	0.0	0.0
butane	0.0	0.0	0.0	0.0	0.0	0.0	0.0
H ₂	0.0	0.0	0.0	0.0	0.0	0.0	0.0
N ₂	0.0	0.0	0.0	0.0	0.0	0.0	0.0
CH ₄	1.1	0.5	0.5	0.6	0.2	0.6	1.0
CO	-	-	-	-	-	-	-
methanol	0.9	1.1	0.9	0.3	0.4	0.0	0.0
ethanol	0.2	0.3	0.3	0.2	0.1	0.5	0.0
diethyl ether	0.0	0.0	0.0	0.0	0.0	0.1	0.0
2-propanol	0.0	0.0	0.0	0.0	0.0	0.0	0.0
1-propanol	0.0	0.6	0.6	0.4	0.1	0.3	0.0
butanal	0.0	0.0	0.0	0.0	0.0	0.1	0.0
ethyl acetate	0.0	0.0	0.0	0.0	0.0	0.0	0.0
2-butanone	0.0	0.0	0.0	0.1	0.1	0.1	0.1
2-butanol	0.0	0.0	0.2	0.2	0.0	0.0	0.0
2-methyl-1-propanol	0.3	1.3	1.3	1.3	0.1	0.0	0.1
1-butanol	0.0	0.1	0.2	0.1	0.0	0.1	0.0
1,1-diethoxy ethane	0.0	0.0	0.0	0.0	0.0	0.0	0.0
1-pentanol	0.0	0.2	0.2	0.1	0.0	0.0	0.0
ethyl butyrate	0.0	0.0	0.0	0.0	0.0	0.0	0.0
butyl acetate	0.0	0.0	0.0	0.0	0.0	0.0	0.0
1-hexanol	0.0	0.0	0.0	0.0	0.0	0.0	0.0

Conditions: T=593 K, p_{start} = 5.0 MPa, 1 g catalyst, H₂:CO=1:1, reaction time = 3 h, liquid phase= 30 g cyclohexane.

Table S 8: Product selectivities in the higher alcohols synthesis as a function of the doping of the catalysts ($n_{\text{EtOH}} : n_{\text{CO}} = 0.5:1$) [%-C].

Catalyst	CuO/ZnO	0.3 mol.% Cs-	0.6 mol.% Cs-	1.0 mol.% Cs-	3.0 mol.% Cs-	0.5 mol.% Ru-	1.0 mol.% Ru-
		CuO/ZnO	CuO/ZnO	CuO/ZnO	CuO/ZnO	CuO/ZnO	CuO/ZnO
CO ₂	11.9	11.5	10.0	11.1	8.9	1.0	1.6
ethane	2.5	1.9	0.6	0.5	0.1	4.1	6.9
propane	0.1	0.2	0.0	0.0	0.0	0.2	0.2
butane	0.0	0.0	0.0	0.0	0.0	0.0	0.0
H ₂	0.0	0.0	0.0	0.0	0.0	0.0	0.0
N ₂	0.0	0.0	0.0	0.0	0.0	0.0	0.0
CH ₄	0.6	1.6	1.3	1.0	0.2	1.5	1.7
CO	-	-	-	-	-	-	-
methanol	1.8	0.8	2.5	3.3	2.9	0.0	0.0
ethanol	-	-	-	-	-	-	-
diethyl ether	0.0	0.0	0.0	0.0	0.0	0.0	0.0
2-propanol	0.6	1.0	1.2	1.3	0.8	0.0	0.0
1-propanol	2.2	5.8	12.0	11.4	10.8	0.2	0.3
butanal	0.0	0.0	0.0	0.0	0.1	0.0	0.1
ethyl acetate	0.3	0.1	1.7	2.1	2.4	1.2	0.8
2-butanone	2.2	1.2	1.8	1.3	0.8	0.0	0.6
2-butanol	5.7	6.5	5.2	5.9	1.2	0.0	0.0
2-methyl-1-propanol	0.6	1.5	1.4	1.2	0.0	0.0	0.0
1-butanol	1.3	1.3	1.9	2.4	4.6	0.5	0.0
1,1-diethoxy ethane	0.0	0.0	0.0	0.1	0.1	0.0	0.0
1-pentanol	0.6	0.8	0.5	0.5	0.3	0.0	0.0
ethyl butyrate	0.0	0.0	0.0	0.2	0.2	0.0	0.0
butyl acetate	0.6	0.6	0.2	0.4	0.2	0.0	0.0
1-hexanol	0.0	0.0	0.0	0.0	0.0	0.0	0.0

Conditions: T=593 K, $p_{\text{start}} = 5.0$ MPa, 1 g catalyst, H₂:CO=1:1, reaction time = 3 h, liquid phase= ~28.6 g cyclohexane and ~1.4 g ethanol.

Table S 9: Product yields in the higher alcohols synthesis as a function of the doping of the catalysts ($n_{\text{EtOH}} : n_{\text{CO}} = 0.5:1$) [%-C].

Catalyst	CuO/ZnO	0.3 mol.% Cs- CuO/ZnO	0.6 mol.% Cs- CuO/ZnO	1.0 mol.% Cs- CuO/ZnO	3.0 mol.% Cs- CuO/ZnO	0.5 mol.% Ru- CuO/ZnO	1.0 mol.% Ru- CuO/ZnO
CO ₂	7.4	7.7	5.8	6.1	4.1	0.5	0.7
ethane	1.6	1.3	0.4	0.3	0.1	1.9	3.2
propane	0.0	0.1	0.0	0.0	0.0	0.1	0.1
butane	0.0	0.0	0.0	0.0	0.0	0.0	0.0
H ₂	0.0	0.0	0.0	0.0	0.0	0.0	0.0
N ₂	0.0	0.0	0.0	0.0	0.0	0.0	0.0
CH ₄	0.4	1.1	0.7	0.6	0.1	0.7	0.8
CO	-	-	-	-	-	-	-
methanol	1.1	0.5	1.4	1.8	1.3	0.0	0.0
ethanol	-	-	-	-	-	-	-
diethyl ether	0.0	0.0	0.0	0.0	0.0	0.0	0.0
2-propanol	0.4	0.7	0.7	0.7	0.4	0.0	0.0
1-propanol	1.4	3.9	6.9	6.3	4.9	0.1	0.1
butanal	0.0	0.0	0.0	0.0	0.0	0.0	0.0
ethyl acetate	0.2	0.1	1.0	1.2	1.1	0.5	0.4
2-butanone	1.3	0.8	1.1	0.7	0.3	0.0	0.3
2-butanol	3.5	4.4	3.0	3.2	0.6	0.0	0.0
2-methyl-1- propanol	0.4	1.0	0.8	0.7	0.0	0.0	0.0
1-butanol	0.8	0.89	1.1	1.3	2.1	0.2	0.0
1,1-diethoxy ethane	0.0	0.0	0.0	0.1	0.0	0.0	0.0
1-pentanol	0.3	0.6	0.3	0.3	0.2	0.0	0.0
ethyl butyrate	0.0	0.0	0.0	0.1	0.1	0.0	0.0
butyl acetate	0.4	0.4	0.1	0.2	0.1	0.0	0.0
1-hexanol	0.0	0.0	0.0	0.0	0.0	0.0	0.0

Conditions: T=593 K, $p_{\text{start}} = 5.0$ MPa, 1 g catalyst, H₂:CO=1:1, reaction time = 3 h, liquid phase= ~28.6 g cyclohexane and ~1.4 g ethanol.

Table S 10: Product selectivities in the higher alcohols synthesis as a function of the doping of the catalysts ($n_{\text{EtOH}} : n_{\text{CO}} = 0.9:1$) [%-C].

Catalyst	Selectivity		Yield	
	CuO/ZnO	0.3 mol.% Cs-CuO/ZnO	CuO/ZnO	0.3 mol.% Cs-CuO/ZnO
CO ₂	8.9	8.5	5.8	4.7
ethane	2.2	1.2	1.4	0.7
propane	0.0	0.0	0.0	0.0
butane	0.0	0.0	0.0	0.0
H ₂	0.0	0.0	0.0	0.0
N ₂	0.0	0.0	0.0	0.0
CH ₄	0.5	1.0	0.3	0.6
CO	-	-	-	-
methanol	1.5	2.1	0.9	1.2
ethanol	-	-	-	-
diethyl ether	0.0	0.0	0.0	0.0
2-propanol	0.8	0.9	0.5	0.5
1-propanol	1.9	7.7	1.2	4.3
butanal	0.0	0.0	0.0	0.0
ethyl acetate	1.7	11.5	1.1	6.4
2-butanone	1.9	2.4	1.2	1.3
2-butanol	11.4	10.1	7.4	5.6
2-methyl-1-propanol	0.2	0.5	0.2	0.3
1-butanol	1.5	1.6	0.9	0.9
1,1-diethoxy ethane	0.0	0.0	0.0	0.0
1-pentanol	0.3	0.2	0.2	0.1
ethyl butyrate	0.0	0.3	0.0	0.2
butyl acetate	0.9	0.4	0.6	0.2
1-hexanol	0.0	0.0	0.0	0.0

Conditions: T=593 K, $p_{\text{start}} = 5.0$ MPa, 1 g catalyst, H₂:CO=1:1, reaction time = 3 h, liquid phase= ~27.5 g cyclohexane and ~2.5 g ethanol.

Table S 11: Product selectivities and yields in the higher alcohols synthesis as a function of the doping of the catalysts ($n_{\text{EtOH}} : n_{\text{CO}} = 10.0:1$) [%-C].

Catalyst	Selectivity			Yield		
	CuO/ZnO	0.3 mol.% Cs-CuO/ZnO	0.6 mol.% Cs-CuO/ZnO	CuO/ZnO	0.3 mol.% Cs-CuO/ZnO	0.6 mol.% Cs-CuO/ZnO
CO ₂	1.0	1.3	1.4	0.4	0.3	0.4
ethane	1.0	1.1	1.0	0.4	0.3	0.3
propane	0.0	0.0	0.0	0.0	0.0	0.0
butane	0.0	0.0	0.0	0.0	0.0	0.0
H ₂	0.0	0.0	0.0	0.0	0.0	0.0
N ₂	0.0	0.0	0.0	0.0	0.0	0.0
CH ₄	0.1	0.1	0.1	0.0	0.0	0.0
CO	-	-	-	-	-	-
methanol	0.8	3.7	2.7	0.3	0.9	0.8
ethanol	-	-	-	-	-	-
diethyl ether	0.3	0.4	0.0	0.1	0.1	0.0
2-propanol	0.2	1.1	0.9	0.1	0.3	0.3
1-propanol	0.1	0.5	0.4	0.0	0.1	0.1
butanal	0.0	0.0	0.0	0.0	0.0	0.0
ethyl acetate	45.0	65.5	43.7	16.9	16.5	13.3
2-butanone	1.1	1.4	0.8	0.4	0.4	0.2
2-butanol	5.3	8.8	5.8	2.0	2.2	1.8
2-methyl-1-propanol	0.9	1.6	0.8	0.3	0.4	0.3
1-butanol	1.5	4.1	6.2	0.6	1.0	1.9
1,1-diethoxy ethane	0.1	0.2	0.2	0.0	0.1	0.1
1-pentanol	0.0	0.0	0.0	0.0	0.0	0.0
ethyl butyrate	0.2	0.4	0.7	0.1	0.1	0.2
butyl acetate	0.2	0.4	1.2	0.1	0.1	0.3
1-hexanol	0.0	0.0	0.0	0.0	0.0	0.0

Conditions: T=593 K, $p_{\text{start}} = 5.0$ MPa, 1 g catalyst, H₂:CO=1:1, reaction time = 3 h, liquid phase= 30 g ethanol.

Table S 12: Product selectivities and yields in the higher alcohols synthesis over a CuO/ZnO catalyst (CO and H₂ free).

Catalyst	Selectivity	Yield
	CuO/ZnO	CuO/ZnO
CO ₂	0.1	0.0
ethane	1.4	0.6
propane	0.0	0.0
butane	0.0	0.0
H ₂	0.0	0.0
N ₂	0.0	0.0
CH ₄	0.1	0.1
CO	0.1	0.0
methanol	0.0	0.0
ethanol	-	-
diethyl ether	0.3	0.1
2-propanol	0.2	0.1
1-propanol	0.1	0.0
butanal	0.0	0.0
ethyl acetate	40.1	16.9
2-butanone	0.6	0.2
2-butanol	6.5	2.8
2-methyl-1-propanol	5.2	2.2
1-butanol	1.1	0.5
1,1-diethoxy ethane	0.0	0.0
1-pentanol	0.5	0.2
ethyl butyrate	0.1	0.1
butyl acetate	0.1	0.1
1-hexanol	0.0	0.0

Conditions: T=593 K, p_{start}= 5.0 MPa, 1 g catalyst, Ar, reaction time = 3 h, liquid phase= 30 g ethanol.

Table S 13: Effect of the reaction temperature on product selectivities and yields in the higher alcohols synthesis over a 1.0 mol.% CuO/ZnO catalyst ($n_{\text{EtOH}} : n_{\text{CO}} = 0.5:1$) [%-C].

Temperature [K]	Selectivity			Yield		
	533	563	593	533	563	593
CO ₂	0.0	6.0	8.3	0.9	0.0	3.9
ethane	0.0	0.0	0.5	0.0	0.0	0.3
propane	0.0	0.0	0.0	0.0	0.0	0.0
butane	0.1	0.4	0.4	0.1	0.0	0.1
H ₂	0.0	0.0	0.0	0.0	0.0	0.0
N ₂	0.0	0.0	0.0	0.0	0.0	0.0
CH ₄	0.0	0.5	0.5	0.1	0.0	0.1
CO	-	-	-	-	-	-
methanol	9.9	8.6	7.5	1.5	2.7	3.5
ethanol	-	-	-	-	-	-
diethyl ether	0.0	0.1	0.0	0.0	0.0	0.0
2-propanol	0.0	0.8	1.6	0.0	0.3	0.7
1-propanol	2.1	4.7	8.8	0.3	1.5	4.1
butanal	0.0	0.0	0.0	0.0	0.0	0.0
ethyl acetate	2.5	3.1	2.9	0.4	1.0	1.4
2-butanone	0.0	0.0	0.9	0.0	0.0	0.4
2-butanol	0.0	0.8	1.6	0.0	0.3	0.7
2-methyl-1-propanol	0.5	0.0	1.5	0.1	0.0	0.7
1-butanol	0.0	0.9	2.5	0.0	0.3	1.2
1,1-diethoxy ethane	0.0	0.0	0.0	0.0	0.0	0.0
1-pentanol	0.0	0.0	0.2	0.0	0.0	0.1
ethyl butyrate	0.0	0.0	0.2	0.0	0.0	0.1
butyl acetate	0.0	0.0	0.2	0.0	0.0	0.1
1-hexanol	0.0	0.0	0.0	0.0	0.0	0.0

Table S 14: GC-MS identified products in the higher alcohols synthesis (ethanol free).

Compound	CuO/ZnO	0.3 mol.% Cs- CuO/ZnO	0.6 mol.% Cs- CuO/ZnO	1.0 mol.% Cs- CuO/ZnO	3.0 mol.% Cs- CuO/ZnO	0.5 mol.% Ru- CuO/ZnO	1.0 mol.% Ru- CuO/ZnO
hydroxyacetic acid	x						
propene							x
hydroxyacetaldehyde	x						
butane	x						
2-methyl-butane	x	x	x	x			x
Pentane	x	x		x		x	x
2-methyl-pentane	x	x			x		
3-methyl-pentane	x						
1-hexene							x
hexane	x				x	x	x
sec-butyl formate		x					
heptane	x				x	x	x
2-heptene						x	x
methyl-cyclohexane	x	x	x	x	x	x	x
2-methyl-heptane	x						
3-methyl-1-butanol		x	x	x			
2-methyl-1-butanol	x	x	x	x			
toluene	x						
3-methyl-heptane	x						
2-methyl-3-pentanol		x	x	x			
3-hexanol		x	x	x			
2-hexanol			x				
octane	x			x	x	x	x
2,3-dimethyl-1-butanol				x			
2-methyl-1-pentanol	x	x	x	x			
3-heptanol		x	x	x			
nonane						x	x
1-heptanol			x				
decane	x					x	

Table S 15: GC-MS identified products in the higher alcohols synthesis ($n_{\text{EtOH}} : n_{\text{CO}} = 0.5:1$).

Compound	CuO/ZnO	0.3 mol.% Cs- CuO/ZnO	0.6 mol.% Cs- CuO/ZnO	1.0 mol.% Cs- CuO/ZnO	3.0 mol.% Cs- CuO/ZnO	0.5 mol.% Ru- CuO/ZnO	1.0 mol.% Ru- CuO/ZnO
propene						x	x
butane	x	x					
2-methyl-butane	x	x					
1,2-diethoxy ethane						x	
ethyl ether							x
methyl acetate	x		x	x	x		
2-methyl-pentane							
3-methyl-pentane	x	x					
1-hexene						x	x
hexane						x	x
methyl propionate					x		
cyclohexene						x	
3-methyl-2-butanol	x	x	x	x			
2-pentanone			x	x	x		
3-pentanone		x	x	x	x		
3-methyl-2-heptanol	x						
2-pentanol		x	x	x	x		
heptane						x	x
2-heptene						x	
ethyl propanoate		x	x	x	x	x	x
n-propyl acetate			x	x	x		
methyl-cyclohexane	x	x		x	x	x	x
2-methyl-heptane							
3-methyl-1-butanol							
2-methyl-1-butanol	x	x	x	x	x		
3-methyl-heptane	x						
2-methyl-3-pentanol		x					
3-hexanone	x	x	x	x	x		
3-methyl-2-pentanol	x	x					
3-hexanol	x	x	x				
2-hexanol	x	x					
octane						x	
n-propyl propionate		x	x	x	x		
2-methyl-1-pentanol		x					

Table S 15: GC-MS identified products in the higher alcohols synthesis ($n_{\text{EtOH}} : n_{\text{CO}} = 0.5:1$). (cont.)

Compound	CuO/ZnO	0.3 mol.% Cs- CuO/ZnO	0.6 mol.% Cs- CuO/ZnO	1.0 mol.% Cs- CuO/ZnO	3.0 mol.% Cs- CuO/ZnO	0.5 mol.% Ru- CuO/ZnO	1.0 mol.% Ru- CuO/ZnO
2-methyl-3-hexanol	x	x					
4-heptanone		x					
3-heptanone		x					
4-heptanol	x	x					
3-heptanol	x	x					
nonane						x	
2-heptanol		x					
3-methyl-4-heptanone	x						
3-methyl-4-heptanol	x						
1-heptanol							
4-octanol	x	x					
3-octanol		x					
decane						x	

Table S 16: GC-MS identified products in the higher alcohols synthesis ($n_{\text{EtOH}} : n_{\text{CO}} = 10.0:1$).

Compound	CuO/ZnO	0.3 mol.% Cs-CuO/ZnO	0.6 mol.% Cs-CuO/ZnO
hydroxyacetaldehyde	x		
methyl acetate	x	x	x
2-pentanone	x		
2-pentanol	x	x	x
ethyl propanoate	x	x	x
n-propyl acetate	x	x	x
3-methyl-1-butanol		x	
sec-butyl acetate	x	x	x
3-hexanone	x	x	x
3-methyl-2-pentanol	x	x	x
3-Hexanol	x	x	x

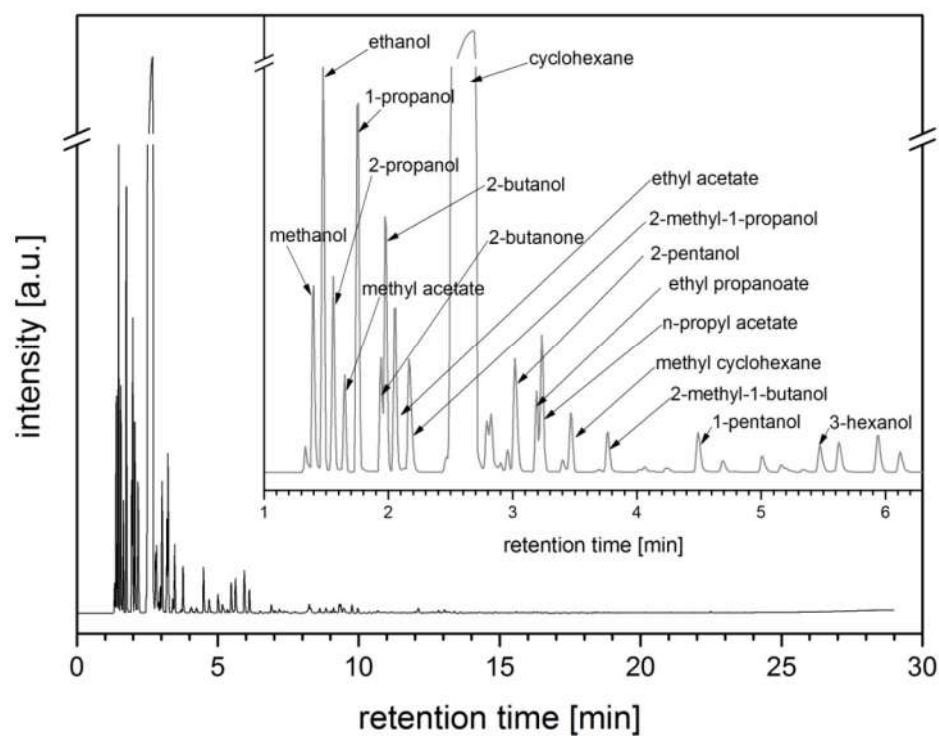


Figure S 1: GC-MS chromatogram of the 0.6 mol.% Cs-CuO/ZnO after the $n_{\text{EtOH}} : n_{\text{CO}} = 0.5:1$ reaction.

Table S 17: Residual activity of the reactor.

Gas	Gas phase composition		
	Experiment 1	Experiment 2	Experiment 3
	[mol.%]	[mol.%]	[mol.%]
CO ₂	0.2	0.2	0.3
ethane	0.1	0.4	0.1
propane	0.0	0.0	0.0
butane	0.0	0.0	0.0
CH ₄	0.1	0.1	0.1

Conditions: T=593 K, p_{start}= 5.0 MPa, not catalyzed, H₂:CO=1:1, reaction time = 3 h, liquid phase= 30 g ethanol.

b) Reproducibility batch experiments. Example CuO/ZnO catalyst.

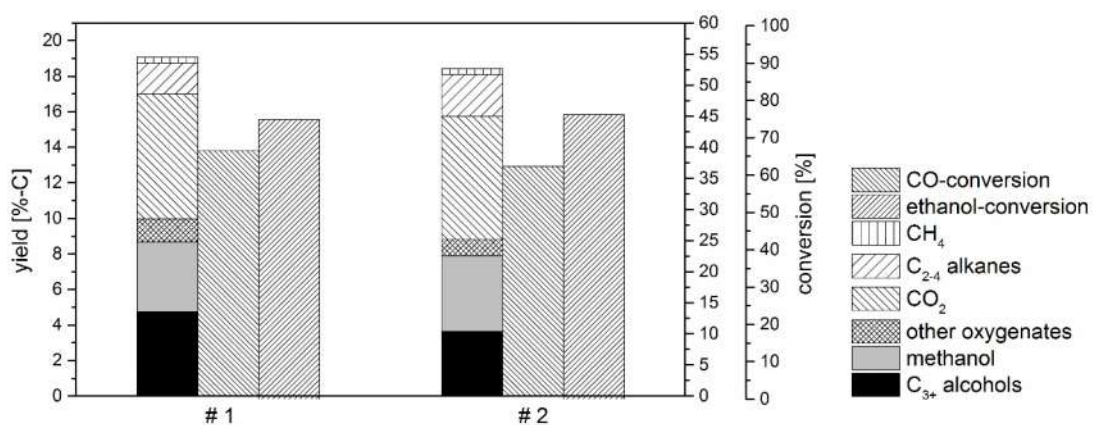


Figure S 2: Reproducibility test of the synthesis of higher alcohols over a CuO/ZnO catalyst (reaction time = 3 h, liquid phase= 47.4 g cyclohexane and 2.6 g ethanol).

Table S 18: Reproducibility of the experiments. Effect on the CO-conversion, ethanol conversion and carbon balance in the higher alcohols synthesis over a CuO/ZnO catalyst ($n_{\text{EtOH}} : n_{\text{CO}} = 0.5:1$).

Experiment number	Units	#1	#2
C-balance	%	62.8	62.3
CO conversion	%-C	39.5	36.9
Ethanol conversion	%-C	74.8	76.2

Table S 19: Reproducibility of the experiments. Effect on product selectivities and yields in the higher alcohols synthesis over a CuO/ZnO catalyst ($n_{\text{EtOH}} : n_{\text{CO}} = 0.5:1$).

Experiment number	Selectivity		Yield	
	#1	#2	#1	#2
CO ₂	12.4	12.4	7.0	6.9
ethane	3.1	3.4	1.7	1.9
propane	0.0	0.1	0.0	0.0
butane	0.0	0.7	0.0	0.4
H ₂	0.0	0.0	0.0	0.0
N ₂	0.0	0.0	0.0	0.0
CH ₄	0.6	0.6	0.3	0.3
CO			31.7	32.3
methanol	7.0	7.6	3.9	4.2
ethanol			12.0	11.6
diethyl ether	0.0	0.0	0.0	0.0
2-propanol	0.0	0.0	0.0	0.0
1-propanol	1.8	2.1	1.0	1.2
butanal	0.0	0.0	0.0	0.0
ethyl acetate	1.5	1.1	0.8	0.6
2-butanone	0.4	0.0	0.2	0.0
2-butanol	4.4	2.1	2.5	1.2
2-methyl-1-propanol	0.5	0.6	0.3	0.3
1-butanol	1.3	1.3	0.7	0.8
1,1-diethoxy ethane	0.0	0.0	0.0	0.0
1-pentanol	0.3	0.4	0.2	0.2
ethyl butyrate	0.0	0.0	0.0	0.0
butyl acetate	0.5	0.5	0.3	0.3
1-hexanol	0.0	0.0	0.0	0.0

2) Supported catalysts

a) Complete reaction data batch reactions

Table S 20: Effect of the preparation method on the CO conversion, ethanol conversion and carbon balance in the higher alcohols synthesis over a CuO/ZnO (30 wt.%) supported on Al₂O₃ catalyst ($n_{\text{EtOH}} : n_{\text{CO}} = 0.5:1$).

Preparation method	Units	wi	inc_pH	pm
C-balance	%	49.8	34.8	38.7
CO conversion	%-C	51.4	75.5	63.0
Ethanol conversion	%-C	91.5	88.7	99.1

wi: wet impregnation; inc_pH: increasing pH precipitation and pm: physical mixture.

Table S 21: Effect of the CuO/ZnO loading on the Al₂O₃ support prepared by wet impregnation in the CO conversion, ethanol conversion and carbon balance in the higher alcohols synthesis ($n_{\text{EtOH}} : n_{\text{CO}} = 0.5:1$).

CuO/ZnO content	Units	20	10
[wt.%]			
C-balance	%	36.3	36.9
CO conversion	%-C	63.8	66.6
Ethanol conversion	%-C	100.0	98.5

Table S 22: Effect of the support material (wet impregnation) on the CO conversion, ethanol conversion and carbon balance in the higher alcohols synthesis ($n_{\text{EtOH}} : n_{\text{CO}} = 0.5:1$).

Support	Units	SiO ₂	AC
C-balance	%	81.1	74.8
CO conversion	%-C	27.9	20.9
Ethanol conversion	%-C	81.1	74.8

AC: activated carbon.

Table S 23: Effect of the preparation method on the CO conversion, ethanol conversion and carbon balance in the higher alcohols synthesis over a 1.0 mol.% CuO/ZnO (30 wt.%) supported on Al₂O₃ catalyst, except commercial catalyst ($n_{\text{EtOH}} : n_{\text{CO}} = 0.5:1$).

Preparation method	Units	wi	const_pH	fsp	com
C-balance	%	78.8	50.8	47.8	72.7
CO conversion	%-C	17.3	69.0	59.7	37.4
Ethanol conversion	%-C	69.0	95.6	89.2	62.9

wi: wet impregnation, const_pH: constant pH precipitation; fsp: flame spray pyrolysis and com: commercial catalyst.

Table S 24: Effect of the preparation method on the product selectivities and yields in the higher alcohols synthesis over a CuO/ZnO (30 wt.%) supported on Al₂O₃ catalyst ($n_{\text{EtOH}} : n_{\text{CO}} = 0.5:1$).

Preparation method	Selectivity			Yield		
	wi	inc_pH	pm	wi	inc_pH	pm
CO ₂	12.6	11.2	13.7	8.8	9.2	11.0
ethane	1.2	2.0	8.1	0.9	1.6	6.5
propane	0.1	0.1	0.1	0.0	0.1	0.0
butane	0.3	0.2	0.0	0.2	0.2	0.0
H ₂	0.0	0.0	0.0	0.0	0.0	0.0
N ₂	0.0	0.0	0.0	0.0	0.0	0.0
CH ₄	0.3	0.2	0.1	0.2	0.1	0.1
CO	-	-	-	-	-	-
methanol	3.1	0.0	0.1	2.2	0.0	0.1
ethanol	-	-	-	-	-	-
diethyl ether	1.4	6.8	1.9	1.0	5.5	1.5
2-propanol	0.2	0.0	0.0	0.2	0.0	0.0
1-propanol	2.0	0.0	0.0	1.4	0.0	0.0
butanal	0.0	0.0	0.0	0.0	0.0	0.0
ethyl acetate	0.5	0.1	0.0	0.4	0.1	0.0
2-butanone	0.0	0.0	0.0	0.0	0.0	0.0
2-butanol	2.6	0.0	0.0	1.8	0.0	0.0
2-methyl-1-propanol	0.0	0.0	0.0	0.0	0.0	0.0
1-butanol	3.1	0.1	0.0	2.2	0.1	0.0
1,1-diethoxy ethane	0.0	0.0	0.0	0.0	0.0	0.0
1-pentanol	0.3	0.0	0.0	0.2	0.0	0.0
ethyl butyrate	0.0	0.0	0.0	0.0	0.0	0.0
butyl acetate	0.1	0.0	0.0	0.1	0.0	0.0
1-hexanol	0.3	0.0	0.0	0.2	0.0	0.0

wi: wet impregnation; inc_pH: increasing pH precipitation and pm: physical mixture.

Table S 25: Effect of the CuO/ZnO loading on the Al₂O₃ support prepared by wet impregnation in the product selectivities and yields in the higher alcohols synthesis ($n_{\text{EtOH}} : n_{\text{CO}} = 0.5:1$).

CuO/ZnO content [wt.%]	Selectivity		Yield	
	20	10	20	10
CO ₂	12.7	13.7	10.3	11.3
ethane	1.0	2.8	0.8	2.3
propane	0.1	0.1	0.1	0.1
butane	0.2	0.1	0.2	0.0
H ₂	0.0	0.0	0.0	0.0
N ₂	0.0	0.0	0.0	0.0
CH ₄	0.1	0.5	0.1	0.4
CO	-	-	-	-
methanol	0.4	0.2	0.4	0.1
ethanol	-	-	-	-
diethyl ether	5.0	6.0	4.0	5.0
2-propanol	0.0	0.0	0.0	0.0
1-propanol	0.9	0.2	0.7	0.2
butanal	0.0	0.0	0.0	0.0
ethyl acetate	0.1	0.1	0.1	0.1
2-butanone	0.0	0.0	0.0	0.0
2-butanol	0.0	0.0	0.0	0.0
2-methyl-1-propanol	0.0	0.0	0.0	0.0
1-butanol	0.7	0.0	0.6	0.0
1,1-diethoxy ethane	0.0	0.0	0.0	0.0
1-pentanol	0.0	0.0	0.0	0.0
ethyl butyrate	0.0	0.0	0.0	0.0
butyl acetate	0.2	0.0	0.1	0.0
1-hexanol	0.1	0.0	0.1	0.0

Table S 26: Effect of the support material (wet impregnation) on the product selectivities and yields in the higher alcohols synthesis ($n_{\text{EtOH}} : n_{\text{CO}} = 0.5:1$).

Support	Selectivity		Yield	
	SiO ₂	AC	SiO ₂	AC
CO ₂	6.9	10.2	1.8	3.6
ethane	1.3	4.7	0.3	1.7
propane	0.0	0.0	0.0	0.0
butane	0.3	0.2	0.1	0.1
H ₂	0.0	0.0	0.0	0.0
N ₂	0.0	0.0	0.0	0.0
CH ₄	0.4	0.4	0.1	0.1
CO	6.9	10.2	50.9	48.5
methanol	0.6	0.8	0.1	0.3
ethanol			23.7	16.4
diethyl ether	1.9	2.6	0.5	0.9
2-propanol	0.0	0.0	0.0	0.0
1-propanol	0.0	0.3	0.0	0.1
butanal	0.0	0.0	0.0	0.0
ethyl acetate	5.2	3.2	1.3	1.1
2-butanone	0.4	0.0	0.1	0.0
2-butanol	1.0	0.8	0.3	0.3
2-methyl-1-propanol	0.0	0.0	0.0	0.0
1-butanol	6.4	4.4	1.6	1.5
1,1-diethoxy ethane	0.0	0.0	0.0	0.0
1-pentanol	0.0	0.0	0.0	0.0
ethyl butyrate	0.7	0.5	0.2	0.2
butyl acetate	0.5	0.3	0.1	0.1
1-hexanol	0.0	0.0	0.0	0.0

AC: activated carbon.

Table S 27: Effect of the preparation method on product selectivities and yields in the higher alcohols synthesis over a 1.0 mol.% CuO/ZnO (30 wt.%) supported on Al₂O₃ catalyst, except commercial catalyst ($n_{\text{EtOH}} : n_{\text{CO}} = 0.5:1$).

Preparation method	Selectivity				Yield			
	wi	const_pH	fsp	com	wi	const_pH	fsp	com
CO ₂	13.7	14.2	10.9	9.5	5.9	11.6	8.1	4.8
ethane	2.6	1.8	1.9	2.0	1.1	1.5	1.4	1.0
propane	0.0	0.1	0.1	0.0	0.0	0.1	0.1	0.0
butane	0.5	0.2	0.0	0.4	0.2	0.2	0.0	0.2
H ₂	0.0	0.0	0.0	0.0	0.0	0.0	0.0	0.0
N ₂	0.0	0.0	0.0	0.0	0.0	0.0	0.0	0.0
CH ₄	0.0	0.4	0.5	0.7	0.0	0.3	0.4	0.3
CO	-	-	-	-	-	-	-	-
methanol	3.3	0.4	1.5	9.5	1.4	0.3	1.1	4.7

Table S 27 (cont.): Effect of the preparation method on product selectivities and yields in the higher alcohols synthesis over a 1.0 mol.% CuO/ZnO (30 wt.%) supported on Al₂O₃ catalyst, except commercial catalyst ($n_{\text{EtOH}} : n_{\text{CO}} = 0.5:1$).

Preparation method	Selectivity				Yield			
	wi	const_pH	fsp	com	wi	const_pH	fsp	com
ethanol	-	-	-	-	-	-	-	-
diethyl ether	3.2	6.1	0.4	0.4	1.4	4.9	0.3	0.2
2-propanol	0.5	0.0	0.7	0.6	0.2	0.0	0.5	0.3
1-propanol	2.1	0.6	2.2	4.0	0.9	0.5	1.6	2.0
butanal	0.0	0.0	0.0	0.0	0.0	0.0	0.0	0.0
ethyl acetate	2.8	0.0	0.0	5.7	1.2	0.0	0.0	2.9
2-butanone	0.3	0.0	0.0	1.7	0.1	0.0	0.0	0.8
2-butanol	1.0	0.4	3.7	4.8	0.4	0.3	2.7	2.4
2-methyl-1-propanol	0.0	0.0	0.0	0.2	0.0	0.0	0.0	0.1
1-butanol	17.0	0.6	1.8	1.9	7.3	0.5	1.4	1.0
1,1-diethoxy ethane	0.0	0.0	0.0	0.0	0.0	0.0	0.0	0.0
1-pentanol	0.0	0.0	0.0	0.0	0.0	0.0	0.0	0.0
ethyl butyrate	1.0	0.0	0.0	0.0	0.4	0.0	0.0	0.0
butyl acetate	0.8	0.0	0.0	0.0	0.3	0.0	0.0	0.0
1-hexanol	1.0	0.0	0.0	0.0	0.4	0.0	0.0	0.0
dimethyl ether	0.0	1.1	0.1	0.0	0.0	0.9	0.1	0.0
butane	0.0	1.2	0.5	0.0	0.0	1.0	0.3	0.0
ethyl methyl ether	1.6	7.6	0.7	0.7	0.7	6.2	0.5	0.4
pentane	0.0	0.3	0.0	0.0	0.0	0.2	0.0	0.0
methyl propyl ether	0.0	0.4	0.0	0.0	0.0	0.3	0.0	0.0
hexane	0.0	0.9	0.0	0.0	0.0	0.8	0.0	0.0
2-methyl-2-propanol	0.0	0.4	0.0	0.0	0.0	0.3	0.0	0.0
ethyl propyl ether	0.0	0.3	0.0	0.0	0.0	0.3	0.0	0.0
butyl methyl ether	0.0	0.8	0.0	0.0	0.0	0.6	0.0	0.0
sec-butyl ethyl ether	0.0	0.4	0.0	0.0	0.0	0.3	0.0	0.0
1-ethoxy-2-propanol	0.0	0.6	0.0	0.0	0.0	0.5	0.0	0.0
3-hexanol	0.0	0.3	2.3	0.7	0.0	0.2	1.7	0.3
3-methyl-hexane	0.0	0.2	0.0	0.0	0.0	0.2	0.0	0.0
butyl ethyl ether	0.0	0.3	0.0	0.0	0.0	0.3	0.0	0.0
3-pentanol	0.5	0.0	0.0	0.0	0.2	0.0	0.0	0.0
vinyl butyrate	0.9	0.0	0.0	0.0	0.4	0.0	0.0	0.0
2-pentanone	0.0	0.0	0.0	0.7	0.0	0.0	0.0	0.4
3-pentanone	0.0	0.0	0.0	0.7	0.0	0.0	0.0	0.3
2-pentanol	0.0	0.0	1.9	0.9	0.0	0.0	1.4	0.4
2-methyl-1-butanol	0.0	0.0	0.0	0.3	0.0	0.0	0.0	0.2
3-hexanone	0.0	0.0	0.0	0.2	0.0	0.0	0.0	0.1
4-heptanol	0.0	0.0	0.4		0.0	0.0	0.3	

wi: wet impregnation, const_pH: constant pH precipitation, fsp: flame spray pyrolysis and com: commercial catalyst.

b) Complete reaction data continuous-flow reactions

Table S 28: Effect of the space velocity on the product selectivities and yields in the higher alcohols synthesis over a CuO/ZnO (30 wt.%) supported on Al₂O₃ catalyst (n_{EIOH} : n_{CO} = 0.3:1; 593 K, 80 bar).

Space velocity [L(STP)/kg _{cat} h]	Selectivity			Yield			Space velocity [L(STP)/kg _{cat} h]	Selectivity			Yield		
	7400	15100	19400	7400	15100	19400		7400	15100	19400	7400	15100	19400
CO ₂	11.0	13.1	17.9	2.9	1.9	6.2	3-hexanone	0.0	0.0	2.0	0.0	0.0	0.7
ethane	3.0	4.6	7.9	0.8	0.7	2.7	3-hexanol	0.0	0.0	1.4	0.0	0.0	0.5
propane	0.2	0.2	0.1	0.0	0.0	0.0	2-heptanol	0.0	0.0	0.0	0.0	0.0	0.0
butane	0.0	0.0	0.0	0.0	0.0	0.0	3-methyl-2-pentanone	0.0	0.0	0.7	0.0	0.0	0.2
H ₂	0.0	0.0	0.0	0.0	0.0	0.0	ethyl hexyl ether	0.0	0.0	0.0	0.0	0.0	0.0
N ₂	0.0	0.0	0.0	0.0	0.0	0.0	butyl butyrate	0.0	0.0	0.0	0.0	0.0	0.0
CH ₄	0.3	0.3	0.2	0.1	0.0	0.1	2-hexanone	0.0	0.0	0.3	0.0	0.0	0.2
CO	-	-	-	-	-	-	2-hexanol	0.0	0.0	0.2	0.0	0.0	0.1
methanol	1.0	1.0	4.8	0.3	0.1	1.7	3-methyl-2-butanone	0.0	0.0	0.2	0.0	0.0	0.1
ethanol	-	-	-	-	-	-	butyl ethyl ether	0.4	0.5	0.1	0.1	0.1	0.0
diethyl ether	0.9	2.2	0.2	0.2	0.3	0.1	3-pentanone	0.0	0.0	0.2	0.0	0.0	0.1
2-propanol	0.3	1.3	1.3	0.1	0.2	0.4	2-methyl-1-butanol	0.0	0.0	0.4	0.0	0.0	0.1
1-propanol	0.0	0.1	1.3	0.0	0.0	0.4	3-methyl-2-pentanol	0.0	0.0	0.3	0.0	0.0	0.1
Butanal	0.1	0.4	0.2	0.0	0.1	0.1	2-ethyl-1-butanol	0.0	0.0	0.0	0.0	0.0	0.0
ethyl acetate	3.3	13.5	1.8	0.9	2.0	0.6	3-methyl-1-pentanol	0.0	0.0	0.0	0.0	0.0	0.0
2-butanone	0.2	0.9	3.0	0.0	0.1	1.0	4-heptanone	0.0	0.0	0.5	0.0	0.0	0.2
2-butanol	0.3	0.7	4.4	0.1	0.1	1.5	4-heptanol	0.0	0.0	0.4	0.0	0.0	0.1
2-methyl-1-propanol	0.0	0.0	0.1	0.0	0.0	0.0	3-methyl-4-heptanone	0.0	0.0	0.6	0.0	0.0	0.2
1-butanol	3.1	11.8	4.5	0.8	1.7	1.5	4-octanone	0.0	0.0	0.4	0.0	0.0	0.1
1,1-diethoxy ethane	0.0	0.0	0.0	0.0	0.0	0.0	butyl isobutyrate	0.0	0.0	0.0	0.0	0.0	0.0
1-pentanol	0.0	0.0	0.2	0.0	0.0	0.1	3-octanone	0.0	0.0	0.1	0.0	0.0	0.0
ethyl butyrate	0.7	2.1	0.3	0.2	0.3	0.1	4-octanol	0.0	0.0	0.2	0.0	0.0	0.1
butyl acetate	0.5	1.2	0.3	0.1	0.2	0.1	3-octanol	0.0	0.0	0.2	0.0	0.0	0.1
1-hexanol	0.0	0.4	0.2	0.0	0.1	0.1	4-nonane	0.0	0.0	0.0	0.0	0.0	0.0
acetaldehyde	0.4	2.5	0.7	0.1	0.4	0.3	4-nonanol	0.0	0.0	0.0	0.0	0.0	0.0
acetone	0.1	0.1	0.3	0.0	0.0	0.1	3-methyl-4-heptanol	0.0	0.0	0.2	0.0	0.0	0.1
2-heptanone	0.0	0.0	0.0	0.0	0.0	0.0	n-hexyl acetate	0.0	0.0	0.0	0.0	0.0	0.0
3-pentanol	0.0	0.0	0.0	0.0	0.0	0.0	2-ethyl-1-hexanol	0.0	0.0	0.0	0.0	0.0	0.0
2-pentanone	0.0	0.0	1.2	0.0	0.0	0.4	ethyl methyl ether	0.0	0.0	0.0	0.0	0.0	0.0
2-pentanol	0.0	0.0	1.1	0.0	0.0	0.4	methyl butyrate	0.0	0.0	0.1	0.0	0.0	0.0
sec butyl acetate	0.0	0.0	0.2	0.0	0.0	0.1							

Table S 29: Effect of the reaction temperature on the product selectivities and yields in the higher alcohols synthesis over a CuO/ZnO (30 wt.%) supported on Al₂O₃ catalyst ($n_{\text{EtOH}} : n_{\text{CO}} = 0.3:1$; 80 bar; ~19400 L(STP)/kg_{cat} h).

Temperature [K]	Selectivity		Yield		Temperature [K]	Selectivity		Yield	
	543	643	543	643		543	643	543	643
CO ₂	4.0	20.7	0.4	7.7	3-hexanone	0.0	0.5	0.0	0.2
ethane	0.4	9.7	0.0	3.6	3-hexanol	0.0	0.5	0.0	0.2
propane	0.0	1.8	0.0	0.7	2-heptanol	0.0	0.1	0.0	0.0
butane	0.0	0.0	0.0	0.0	3-methyl-2-pentanone	0.0	0.1	0.0	0.0
H ₂	0.0	0.0	0.0	0.0	ethyl hexyl ether	0.0	0.5	0.0	0.2
N ₂	0.0	0.0	0.0	0.0	butyl butyrate	0.0	0.6	0.0	0.2
CH ₄	0.0	1.4	0.0	0.5	2-hexanone	0.0	0.0	0.0	0.0
CO	-	-	-	-	2-hexanol	0.0	0.0	0.0	0.0
methanol	0.4	0.8	0.0	0.3	3-methyl-2-butanone	0.0	0.0	0.0	0.0
ethanol	-	-	-	-	butyl ethyl ether	0.0	1.6	0.0	0.6
diethyl ether	0.4	1.1	0.0	0.4	3-pentanone	0.0	0.0	0.0	0.0
2-propanol	0.5	1.0	0.1	0.4	2-methyl-1-butanol	0.0	0.2	0.0	0.1
1-propanol	0.0	0.5	0.0	0.2	3-methyl-2-pentanol	0.0	0.0	0.0	0.0
Butanal	0.0	1.2	0.0	0.5	2-ethyl-1-butanol	0.0	0.6	0.0	0.2
ethyl acetate	6.9	0.7	0.7	0.3	3-methyl-1-pentanol	0.0	0.0	0.0	0.0
2-butanone	0.4	0.8	0.0	0.3	4-heptanone	0.0	0.5	0.0	0.2
2-butanol	0.2	0.5	0.0	0.2	4-heptanol	0.0	0.6	0.0	0.2
2-methyl-1-propanol	0.0	0.0	0.0	0.0	3-methyl-4-heptanone	0.0	0.0	0.0	0.0
1-butanol	1.4	13.0	0.1	4.9	4-octanone	0.0	0.0	0.0	0.0
1,1-diethoxy ethane	0.0	0.0	0.0	0.0	butyl isobutyrate	0.0	0.0	0.0	0.0
1-pentanol	0.0	0.1	0.0	0.0	3-octanone	0.0	0.1	0.0	0.0
ethyl butyrate	0.0	0.7	0.0	0.3	4-octanol	0.0	0.0	0.0	0.0
butyl acetate	0.0	0.7	0.0	0.3	3-octanol	0.0	0.0	0.0	0.0
1-hexanol	0.0	1.9	0.0	0.7	4-nonane	0.0	0.0	0.0	0.0
acetaldehyde	1.1	0.6	0.1	0.2	4-nonanol	0.0	0.0	0.0	0.0
acetone	0.8	0.4	0.1	0.1	3-methyl-4-heptanol	0.0	0.0	0.0	0.0
2-heptanone	0.0	0.2	0.0	0.1	n-hexyl acetate	0.0	0.2	0.0	0.1
3-pentanol	0.0	0.1	0.0	0.0	2-ethyl-1-hexanol	0.0	0.2	0.0	0.1
2-pentanone	0.0	1.6	0.0	0.6	ethyl methyl ether	0.0	0.0	0.0	0.0
2-pentanol	0.0	0.9	0.0	0.3	methyl butyrate	0.0	0.1	0.0	0.0
sec butyl acetate	0.0	0.1	0.0	0.0					

Table S 30 Effect of the $n_{\text{EtOH}} : n_{\text{CO}}$ on the product selectivities and yields in the higher alcohols synthesis over a CuO/ZnO (30 wt.%) supported on Al₂O₃ catalyst (593 K; 80 bar; ~19400 L(STP)/kg_{cat} h).

$n_{\text{EtOH}} : n_{\text{CO}}$	Selectivity			Yield			$n_{\text{EtOH}} : n_{\text{CO}}$	Selectivity			Yield		
	0.04	0.86	1.97	0.04	0.86	1.97		0.04	0.86	1.97	0.04	0.86	1.97
CO ₂	24.0	9.3	5.4	1.7	2.9	2.4	3-hexanone	0.0	0.7	0.3	0.0	0.2	0.1
ethane	21.4	2.4	1.3	1.5	0.8	0.6	3-hexanol	0.0	0.5	0.1	0.0	0.2	0.1
propane	0.0	0.1	0.1	0.0	0.0	0.0	2-heptanol	0.0	0.0	0.0	0.0	0.0	0.0
butane	0.0	0.0	0.0	0.0	0.0	0.0	3-methyl-2-pentanone	0.0	0.1	0.1	0.0	0.0	0.0
H ₂	0.0	0.0	0.0	0.0	0.0	0.0	ethyl hexyl ether	0.0	0.0	0.0	0.0	0.0	0.0
N ₂	0.0	0.0	0.0	0.0	0.0	0.0	butyl butyrate	0.0	0.0	0.0	0.0	0.0	0.0
CH ₄	0.6	0.2	0.6	0.0	0.1	0.2	2-hexanone	0.0	0.1	0.0	0.0	0.0	0.0
CO	-	-	-	-	-	-	2-hexanol	0.0	0.0	0.0	0.0	0.0	0.0
methanol	0.9	0.9	0.4	0.1	0.3	0.2	3-methyl-2-butanone	0.0	0.0	0.0	0.0	0.0	0.0
ethanol	-	-	-	-	-	-	butyl ethyl ether	0.0	0.1	0.1	0.0	0.0	0.0
diethyl ether	0.0	0.6	0.8	0.0	0.2	0.4	3-pentanone	0.0	0.0	0.0	0.0	0.0	0.0
2-propanol	1.7	2.4	1.5	0.1	0.7	0.7	2-methyl-1-butanol	0.0	0.0	0.0	0.0	0.0	0.0
1-propanol	0.0	0.2	0.1	0.0	0.1	0.0	3-methyl-2-pentanol	0.0	0.1	0.0	0.0	0.0	0.0
Butanal	0.0	0.5	1.1	0.0	0.2	0.5	2-ethyl-1-butanol	0.0	0.0	0.0	0.0	0.0	0.0
ethyl acetate	0.0	27.2	30.9	0.0	8.4	13.8	3-methyl-1-pentanol	0.0	0.0	0.0	0.0	0.0	0.0
2-butanone	0.9	4.5	2.8	0.1	1.4	1.2	4-heptanone	0.0	0.1	0.0	0.0	0.0	0.0
2-butanol	0.0	4.5	1.5	0.0	1.4	0.7	4-heptanol	0.0	0.0	0.0	0.0	0.0	0.0
2-methyl-1-propanol	0.0	0.0	0.0	0.0	0.0	0.0	3-methyl-4-heptanone	0.0	0.0	0.0	0.0	0.0	0.0
1-butanol	0.0	8.1	7.7	0.0	2.5	3.4	4-octanone	0.0	0.0	0.0	0.0	0.0	0.0
1,1-diethoxy ethane	0.0	0.0	0.0	0.0	0.0	0.0	butyl isobutyrate	0.0	0.0	0.0	0.0	0.0	0.0
1-pentanol	0.0	0.0	0.0	0.0	0.0	0.0	3-octanone	0.0	0.0	0.0	0.0	0.0	0.0
ethyl butyrate	0.0	2.0	3.4	0.0	0.6	1.5	4-octanol	0.0	0.0	0.0	0.0	0.0	0.0
butyl acetate	0.0	1.7	2.0	0.0	0.5	0.9	3-octanol	0.0	0.0	0.0	0.0	0.0	0.0
1-hexanol	0.0	0.2	0.2	0.0	0.0	0.1	4-nonane	0.0	0.0	0.0	0.0	0.0	0.0
acetaldehyde	0.0	2.8	5.7	0.0	0.9	2.5	4-nonanol	0.0	0.0	0.0	0.0	0.0	0.0
acetone	0.0	0.8	1.6	0.0	0.3	0.7	3-methyl-4-heptanol	0.0	0.0	0.0	0.0	0.0	0.0
2-heptanone	0.0	0.0	0.0	0.0	0.0	0.0	n-hexyl acetate	0.0	0.0	0.0	0.0	0.0	0.0
3-pentanol	0.0	0.0	0.0	0.0	0.0	0.0	2-ethyl-1-hexanol	0.0	0.0	0.0	0.0	0.0	0.0
2-pentanone	0.0	0.8	0.8	0.0	0.3	0.4	ethyl methyl ether	0.0	0.0	0.0	0.0	0.0	0.0
2-pentanol	0.0	0.7	0.4	0.0	0.2	0.2	methyl butyrate	0.0	0.0	0.0	0.0	0.0	0.0
sec butyl acetate	0.0	0.2	0.1	0.0	0.1	0.0							

3) Calculation examples for the design and construction of a high pressure, continuous-flow reactor

Type of flow

The flow regime through the catalyst bed was determined according to the criteria presented in Table 18. A calculation example of the parameters for the minimum gas and liquid flows is presented in the following:

$$\lambda = \frac{\sqrt{\rho_G \rho_L}}{\sqrt{\rho_{air} \rho_{H_2O}}} = \frac{\sqrt{0.73 \left(\frac{kg}{m^3}\right) \cdot 790 \left(\frac{kg}{m^3}\right)}}{\sqrt{1.2 \left(\frac{kg}{m^3}\right) \cdot 1000 \left(\frac{kg}{m^3}\right)}} = 0.693$$

$$\psi = \frac{\sigma_{H_2O}}{\sigma_L} \left(\frac{\mu_L}{\mu_{H_2O}}\right)^{\frac{1}{3}} \left(\frac{\rho_{H_2O}}{\rho_L}\right)^{\frac{1}{3}} = \frac{7.4 \cdot 10^{-2} (N \cdot m)}{0.0226 (N \cdot m)} \left(\frac{1.2 \cdot 10^{-3} (Pa \cdot s)}{1.0 \cdot 10^{-3} (Pa \cdot s)}\right)^{\frac{1}{3}} \left(\frac{1000 \left(\frac{kg}{m^3}\right)}{790 \left(\frac{kg}{m^3}\right)}\right)^{\frac{1}{3}} = 3.772$$

$$\phi = 4.76 + 0.5 \frac{\rho_G}{\rho_{air}} = 4.76 + 0.5 \cdot \frac{0.73 \left(\frac{kg}{m^3}\right)}{1.2 \left(\frac{kg}{m^3}\right)} = 5.064$$

$$R_{L,min} = \frac{1.32 \cdot 10^{-7}}{8.04 \cdot 10^{-5}} = 1.64 \cdot 10^{-3} \left(\frac{kg}{m^2 \cdot s}\right)$$

$$R_{G,min} = \frac{1.21 \cdot 10^{-6}}{8.04 \cdot 10^{-5}} = 1.52 \cdot 10^{-2} \left(\frac{kg}{m^2 \cdot s}\right)$$

For a trickle flow regime:

$$\frac{R_L \lambda \psi}{R_G \phi} = \frac{1.64 \cdot 10^{-3} \left(\frac{kg}{m^2 \cdot s}\right)}{1.52 \cdot 10^{-2} \left(\frac{kg}{m^2 \cdot s}\right)} \cdot \frac{0.693 \cdot 3.772}{5.064} = 0.06 \leq \left(\frac{R_G}{\lambda}\right)^{-1.3} = \left(\frac{1.52 \cdot 10^{-2} \left(\frac{kg}{m^2 \cdot s}\right)}{0.693}\right)^{-1.3} = 143.9$$

and

$$0.01 \leq \frac{R_G}{\lambda} = \frac{1.52 \cdot 10^{-2} \left(\frac{kg}{m^2 \cdot s}\right)}{0.693} = 0.02 \leq 1$$

Catalyst wetting, axial mixing, non-preferential flow and isothermality

The catalyst wetting, axial mixing, non-preferential flow and isothermality criteria were evaluated with the criteria presented in Table 16. Calculation examples for all the applied criteria are presented in the following.

Catalyst wetting

$$W = \frac{\eta_L U_L}{\rho_L d_p^2 g} = \frac{1.2 \cdot 10^{-3} (\text{Pa} \cdot \text{s}) \cdot 0.002 \left(\frac{\text{m}}{\text{s}}\right)}{790 \left(\frac{\text{kg}}{\text{m}^3}\right) \cdot (5 \cdot 10^{-4})^2 \cdot 9.81 \left(\frac{\text{m}}{\text{s}^2}\right)} = 1.29 \cdot 10^{-3} \geq 5 \cdot 10^{-6}$$

Axial mixing

$$\frac{L_{\min}}{d_{p,\max}} = \frac{L_{\min}}{0.5(\text{mm})} \geq 100$$

$$L_{\min} = 50(\text{mm})$$

$$\frac{D}{d_p} = \frac{7.415 (\text{mm})}{0.5(\text{mm})} = 14.8 \geq 10$$

Non-preferential flow

$$\frac{D}{d_p} = \frac{7.415 (\text{mm})}{0.5(\text{mm})} = 14.8 \not\geq 25$$

Dilution with inerts was required.

$$d_{pi} = 0.21(\text{mm}) \geq \frac{d_p}{10} = \frac{0.5(\text{mm})}{10} = 0.05(\text{mm})$$

Isothermality

$$\frac{D}{d_p} = \frac{7.415 (\text{mm})}{0.5(\text{mm})} = 14.8 \not\geq 100$$

List of abbreviations

μ GC	: Micro Gas Chromatograph
AAS	: Atomic Absorption Spectroscopy
AC	: Activated Carbon
ANKA	: Angströmquelle Karlsruhe
ATR-IR	: Attenuated Total Reflection – Infrared spectroscopy
BET	: Brunauer-Emmet-Teller model
CDS	: Cambridge Structural Database
com	: Commercial Methanol Catalyst
const_pH	: Constant pH precipitation
DME	: Dimethyl ether
DMFC	: Direct Methanol Fuel Cell
EDX	: Energy Dispersive X-ray Spectroscopy
EXAFS	: Extended X-ray Absorption Fine Structure
FID	: Flame Ionization Detector
fsp	: Flame Spray Pyrolysis
FT	: Fischer-Tropsch
FT-IR	: Fourier Transformed Infrared spectroscopy
GC	: Gas Chromatography
grad	: Gradient
HA	: Higher alcohols
H ₂ -TA	: Hydrogen Transient Adsorption
H ₂ -TPD	: Temperature Programmed Desorption with Hydrogen
H ₂ -TPR	: Hydrogen Temperature Programmed Reduction
HPLC	: High Performance Liquid Chromatography
HRTEM	: High Resolution Transmission Electron Microscopy
ICI	: Imperial Chemical Industries
ICP-OES	: Inductively Coupled Plasma – Optical Emission Spectroscopy
IEA	: International Energy Agency
IKFT	: Institute of Catalysis Research and Technology

inc_pH	: Increasing pH precipitation
ITCP	: Institute for Chemical Technology and Polymer Chemistry
MFC	: Mass Flow Controllers
mol.%	: Mole percentage
MS	: Mass Spectrometry
MTA	: Methanol to Aromatics
MTBE	: Methyl tert-butyl ether
MTG	: Methanol to Gasoline
MTO	: Methanol to Olefins
MTP	: Methanol to Propylene
MWCNT	: Multiwall Carbon Nanotubes
n.d.	: Not determined
N ₂ O-RFC	: N ₂ O Reactive Frontal Chromatography
PC	: Backpressure regulator
PFR	: Plug Flow Reactor
PI	: Pressure Indicator
PID	: Piping and Instrumentation Diagram
POM	: Polyoxymethylene
PTR	: Pressure Transducer
rWGS	: Reverse Water Gas Shift
S.V.	: Space Velocity
SNG	: Synthetic Natural Gas
TCD	: Thermal Conductivity Detector
TEM	: Transmission Electron Microscopy
TGA	: Thermogravimetric Analysis
TR	: Thermocouple
TR-XRD	: Time Resolved X-ray Diffraction
TOF	: Turnover frequency
WGS	: Water Gas Shift
wi	: Wet impregnation
wt.%	: Weight percentage

XANES : X-ray Absorption Near Edge Structure
XAS : X-ray Absorption Spectroscopy
XPS : X-ray Photoelectron Spectroscopy
XRD : X-ray Diffraction

List of symbols

$\Delta_r H$: Heat of reaction at a temperature
μ_i	: Viscosity of component i
Area _i	: Integration area of component i
B_{mi}	: Biot number of mass transfer
Bo_i	: Bodenstein number for the phase i
C	: Concentration of reactant
C_f	: Outlet concentration of reactant
C_0	: Inlet concentration of reactant
conc _{2-butanol}	: Concentration of the standard 2-butanol in GC sample
D	: Internal reactor diameter
D_e	: Effective Diffusivity
d_p	: Particle diameter
d_{pi}	: Inert particle diameter
E	: Activation energy for the catalytic reaction
ECN _i	: Effective carbon number of component i
g	: Gravity constant
h_p	: Particle to fluid heat transfer coefficient
k	: Rate constant
K	: crystallite shape factor
k_e	: Bed effective radial conductivity
k_{ext}	: External mass transfer coefficient
L	: Length of the catalytic bed
L_{min}	: Minimal length of reactor
m_{cat}	: Mass of catalyst
m_{gas}	: Mass of gas
m_{liquid}	: Mass of liquid
MW_i	: Molecular weight of component i
n	: Reaction order
n_{CO}	: Number of moles of CO

n_{H_2}	:	Number of moles of hydrogen
n_{CO_2}	:	Number of moles of CO_2
n_{EtOH}	:	Number of moles of ethanol
n_i	:	Number of moles of component i
r	:	Rate of reaction
R	:	Gas constant
R_G	:	Specific mass flow rate of gas
R_L	:	Specific mass flow rate of liquid
S	:	Quotient between the difference of moles of H_2 and CO_2 and the summation of moles of CO_2 and CO
S_i	:	Selectivity of component i
T	:	Temperature
T_0	:	Temperature of the fluid adjacent to the particles
T_w	:	Temperature of the wall
U_G	:	Velocity of the gas
U_L	:	Velocity of the liquid
\dot{V}_{gas}	:	Volumetric flow of gas
\dot{V}_{liquid}	:	Volumetric flow of liquid
W	:	Dimensionless wetting number
X	:	Conversion
X_{CO}	:	CO conversion
X_{EtOH}	:	Ethanol conversion
Y_i	:	Yield of component i
β	:	full width at half maximum of the X-ray reflection
$\beta(N)$:	Aldol coupling with retention of the keto oxygen
$\beta(R)$:	Aldol coupling with retention of the alcoxide oxygen
δ	:	Partial charge
ε	:	Bed voidage
η	:	Overall effectiveness
η_G	:	Dynamic viscosity of the gas
η_L	:	Dynamic viscosity of the liquid
θ	:	Bragg angle

λ	:	Effective thermal conductivity of the particle
λ	:	Wavelength of the X-rays
ρ_i	:	Density of component i
ρ_G	:	Density of the gas
ρ_L	:	Density of the liquid
ρ_p	:	Density of the pellet
σ_i	:	Surface tension of component i
σ_L	:	Surface tension of the liquid
$u_{c,i}$:	Number of carbons of component i
φ	:	Thiele modulus

Curriculum Vitae

Personal Details

Name Karin Marcela Walter Bahamondes

Education

Since 05/2012 PhD Student
Karlsruhe Institute of Technology (KIT), Institute for Chemical Technology and Polymer Chemistry

03/2011 – 03/2005 Chemical Engineering Studies
Universidad de Concepción, Chile
Degree: Graduate in Chemical Engineering “*Ingeniero Civil Químico*” (March 2011)
Thesis: “Quimisorción Selectiva de Gases en Catalizadores de Metales Soportados”

03/2004 - 12/2003 Exchange Student
Hainberg-Gymnasium Göttingen, Germany

12/2004 – 03/1990 Primary and Secondary School Education: Deutsche Schule Concepción (DSC), Chile

Professional experience

11/2011 –04/2011 Project Engineer in Research Area
Universidad de Concepción, Chile
Grant: Fondef-CONICYT: “Implementación de Procesos de Co-combustión de Carbón y Biomasa en Chile. Estudio de Factibilidad Técnica-económica”

07/2011 - 03/2011 Teaching assistantship
Course: Mass and Energy Balance

12/2010 – 08/2010 Teaching assistantship
Course: Numerical Analysis in Chemical Engineering

12/2009 Internship
Bío-Bío S.A. (Fish meal producers)

Accomplishments

03/2016 – 10/2012 DAAD Scholarship: Direct Fellowship DAAD, awarded by Deutscher Akademischer Austauschdienst

- 2011 “Premio Marcos Orrego Puelma”. Granted by the Institute of Engineers from Chile.
- 2011 “Premio Lan”. Granted by the University of Concepción.
- 2011 “Premio Facultad de Ingeniería” granted by the Engineering Faculty of the University of Concepción
- 2011 “Premio Universidad de Concepción”. Granted by University of Concepción.
- 2004 “Premio mejor alumno de la promoción”. Granted by Deutsche Schule Concepción.

List of publications, poster/oral presentations and co-supervised theses

Publications in this thesis

K. M. Walter, M. Schubert, W. Kleist, J.-D. Grunwaldt

Effect of the addition of ethanol to synthesis gas on the production of higher alcohols over Cs and Ru modified CuO/ZnO catalysts

Industrial and Engineering Chemistry Research, 54 (2015), pp. 1452 – 1463.

Chapter 3, section 3.1 and chapter 4, section 4.1 of this thesis.

Other publications

M. Roeckel, E. Aspé, K. M. Walter

Analysis of Nitrogen and Carbon Removal from Organic Loaded Effluents using Reactors in Series and Integrated Reactors

Chapter 3, In *Advances in Environmental Research Vol.5 “Water treatment: Processes, Uses and Ecological Impact”*, Nova Science Publishers, Inc., 2010; pp 113 - 137.

Oral presentations

K. M. Walter, M. Schubert, W. Kleist, J.-D. Grunwaldt

Effect of ethanol addition to synthesis gas for the production of higher alcohols over Cs-CuO/ZnO catalysts

24th North American Meeting of the North American Catalysis Society, 14th – 19th of June 2015, Pittsburgh, United States of America

K. M. Walter, M. Schubert, W. Kleist, J.-D. Grunwaldt

Cs-modified Cu/ZnO catalysts for the production of higher alcohols from ethanol and synthesis gas

ProcessNet- Jahrestagung 2014 und der 31. Jahrestagung der Biotechnologen, 30th of September – 2nd of October 2014, Aachen, Germany

Poster presentations

K. M. Walter, K. F. Kalz, M. Schubert, W. Kleist, J.-D. Grunwaldt

Catalytic synthesis of higher alcohols from synthesis gas and ethanol

49. Jahrestreffen Deutscher Katalytiker, 16th – 18th of March 2016, Weimar, Germany

K. M. Walter, M. Schubert, G. Cavusoglu, W. Kleist, J.-D. Grunwaldt

Catalytic synthesis of higher alcohols from short-chain alcohols

46. Jahrestreffen Deutscher Katalytiker, 13th – 15th of March 2013, Weimar, Germany

M. Schubert, G. Cavusoglu, K. M. Walter, W. Kleist, J.-D. Grunwaldt

Investigations on the homologation of short-chain alcohols with synthesis gas over heterogeneous catalysts

2nd International Conference on Materials for Energy EnMat II, 12th – 16th of March 2013, Karlsruhe, Germany

M. Schubert, G. Cavusoglu, K. M. Walter, W. Kleist, J.-D. Grunwaldt

Höhere Alkohole durch heterogen katalysierte Homologisierung kurzkettiger Alkohole mit Synthesegas

Workshop der AG Chemie und energie der GDCh, 15th – 16th of November 2012, Karlsruhe, Germany

Bachelor theses in the framework of this thesis

Philipp Avon

„Die Untersuchung modifizierter Fischer-Tropsch Katalysatoren zur Synthese höherer Alkohole“, (12.06.2014 - 12.09.2014).

Marc-André Serrer

„Untersuchungen zur heterogen katalysierten Synthese höherer Alkohole and Cu/ZnO – basierten Katalysatoren“, (03.03.2016 - 03.06.2014).

Eidesstattliche Erklärung

Hiermit versichere ich, die vorliegende Doktorarbeit selbständig angefertigt und keine anderen als die von mir angegebenen Quellen und Hilfsmittel verwendet, sowie wörtliche und sinngemäße Zitate als solche gekennzeichnet zu haben. Weiterhin habe ich die Satzung des Karlsruher Instituts für Technologie (KIT) zur Sicherung guter wissenschaftlicher Praxis in der gültigen Fassung beachtet. Die Arbeit wurde in gleicher oder anderer Form keiner anderen Prüfungsbehörde zur Erlangung eines akademischen Grades vorgelegt. Die elektronische Version der Arbeit stimmt mit der schriftlichen überein und die Primärdaten sind beim Institut gesichert.

Karlsruhe, den _____

Datum und Unterschrift